Enhancing the robustness of *Clostridium saccharoperbutylacetonicum* N1-4 for butanol production through metabolic engineering and cell immobilization strategies

by

Pablo Jimenez-Bonilla

A dissertation submitted to the Graduate Faculty of
Auburn University
in partial fulfillment of the
requirements for the Degree of
Doctor of Philosophy

Auburn, Alabama
December 14, 2019

Keywords: Clostridium, butanol, fermentation, metabolic engineering, cell immobilization

by Pablo Jimenez-Bonilla

Approved by

Yi Wang, Chair, Assistant Professor, Department of Biosystems Engineering
David Blersch, Associate Professor, Department of Biosystems Engineering
Yifen Wang, Professor, Department of Biosystems Engineering
Luz-Estela Gonzalez de Bashan, Affiliate Associate Professor, Department of Entomology and Plant Pathology

Abstract

n-Butanol (butanol hereafter) has many advantages over ethanol to be used as a biofuel. However, one of the significant drawbacks in bacterial production of butanol is the low productivity and titer due to the low butanol tolerance in the host strain. Lignocellulosic materials are considered as cheap and renewable feedstock for biofuel production through microbial fermentation. Nevertheless, there are by-products generated during the conversion of biomass into sugar-rich hydrolysates that could inhibit bacterial growth and lead to unsatisfying fermentation performance. In this study, combinatory strategies have been investigated for improving the tolerance of strains used for butanol production, particularly focused on *Clostridium saccharoperbutylacetonicum* N1-4, a hyper-butanol producing strain. Firstly, the effects of two genetic engineering strategies, including the overexpression of the *srp* efflux pump system from *Pseudomonas putida* and the identification and deletion of autolysin genes, were investigated. The efflux pump could extrude toxic compounds out of the cells, and increase the maximum levels of furfural and ferulic acid (two representative lignocellulosic inhibitors) in which *C. saccharoperbutylacetonicum* N1-4 can survive. The deletion of four autolysin genes led to enhanced cell growth and butanol production, and meanwhile increased the plasmid DNA transformation efficiency for the mutant strain. The results also provided a better understanding about the role of the endogenous megaplasmid within *C. saccharoperbutylacetonicum* N1-4, and supported other recent findings. Finally, a cell immobilization strategy was evaluated for the effects of butanol fermentation, based on the cationic surfaces such as insoluble chitosan and

cationized celluloses. Results indicated that chitosan promoted microgranulation, increased the amount of cell biomass present in the liquid phase, elevated the butanol productivity in C. saccharoperbutylacetonicum N1-4, and also improved the butanol titer in another prominent butanol-producing strain *C. beijerinckii* 8052.

Overall, the results of this study provided insights towards the enhancement of biobutanol production from lignocellulosic feedstocks through integrated strain development and bioprocess development strategies.

Graphical abstract

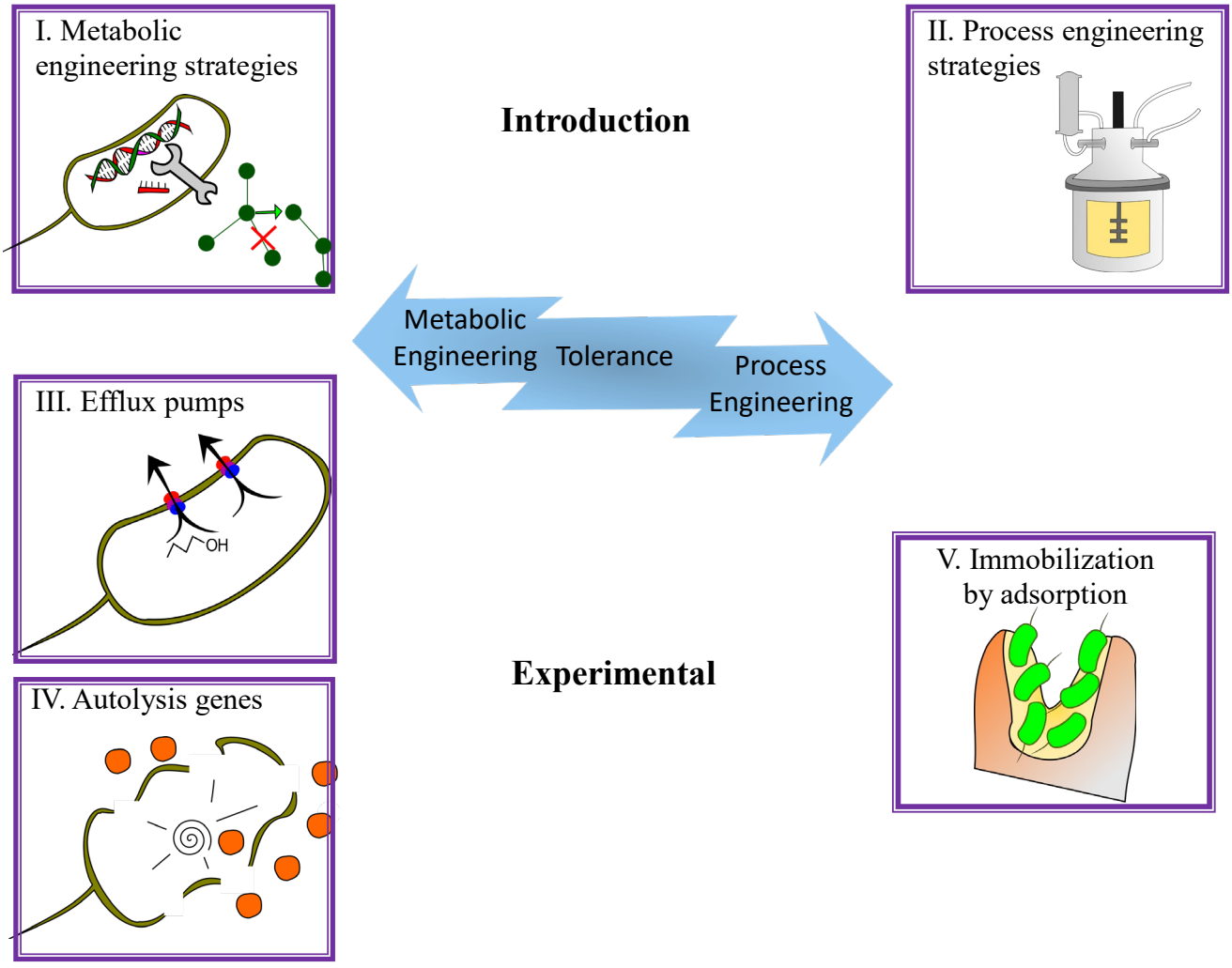

Dedication

I dedicate this dissertation to my lovely wife Johanna.

Thanks for leaving your whole life just to be my partner in this adventure. This achievement also belongs to you.

Acknowledgements

I thank God for giving me life and many opportunities on it, including the one of realizing this project and meeting the people who made it possible.

I thank my family: my wife and my children: Mariana, Natalia & Samuel. You guys were my unconditional support, and I am glad we shared many adventures, during this five years. Hope you guys enjoyed the way as much as I did. To my parents, who in all my life have been supporting me, and came to Alabama many times to assist me when I needed it.

I want to thank my advisor, Dr. Yi Wang for all the things I have learned during these years. For showing me how to work with intensity, passion, and excellence, and for being an understanding friend. Also, all my committee members for their multiple recommendations and improvements to this work. Dr. Yoav and Dr. Luz Bashan for your unselfish support, even when they experiment very during difficult times. I also want to thank Dr. Yifen Wang and Dr. David Blersch for their support and understanding.

I need to thank the two generations of lab-mates. The lab members of the first generation: Dr. Jie Zhang, and Dr. Jun Feng, Dr. Shaohua Wang, Dr. Wei Hong, M.Sc. Nemo Zhang, Dr. Peter Wang, Dr. Xiaofei Wang, Sheng Dong and M.Sc. Shangjun Wang. And also the second generation: Dr. Zhu Chen, Dr. Junping Zhou, Dr. Yuechao Ma, Xianshuang Cao, Tingbi Xu, Ian Schlosser, Dr. Haijiao Wang, Na Guo and Liana Liang. Beside all the help with the experimentation, you guys showed me your Chinese culture and you invaluable friendship.

I had no words to say thanks to many people who support me and my family and me in different ways. CC and Evan Cox, Emily, Arthur and Mayra Muniz, Amanda Reaves, Lizzie Baumbach, Michelle and Matt Schultz, Silvia and Perry Rissler, Kayline Pudner, Bernal Sibaja, Ricardo Ballestero, Gabriel Proano, Francisca Burgos, Javier Santillan, Gisella Martinez and Abel Paladines. I am sure that I would not be able to finish this adventure, without your support and friendship. I know, you guys are the part of this experience that I am going to miss badly.

I thank the financial support for my Ph.D. studies from the National University of Costa Rica (Universidad Nacional (UNA), Heredia Costa Rica), as part of the "Plan for strengthening and stabilization of the faculty members". I thank all faculty and administrative personnel of the Chemistry School of UNA: my colleagues, mentors and friends. Thanks for giving me the confidence of executing this project, and thanks for believing in my work. I want to give a special acknowledgement to Dr. Roy Soto, and M.Sc. Jose Pablo Sibaja. Also, I thank the Board of Scholarships, the administration of the World Bank Program (from UNA), and all the people contributing in the administration of my scholarship.

Table of Contents

Abstract ii

Graphical abstract iv

Dedication v

Acknowledgements vi

Table of Contents viii

List of Tables xv

List of Figures xvii

List of Abbreviations xxi

Introduction 1

Background 1

Objectives 2

References 4

Chapter I. Literature Review. State of the art and prospective on solvent and chemical tolerance of selected biotechnologically significant *Clostridium* strains, focusing on butanol production ... 1

Abstract 1

1.1 Introduction 2

1.2 Fermentation Inhibitions 3

1.2.1 Fermentation end-product inhibition 3

1.2.2 Inhibition from the biomass processing derived inhibitors 7

1.2.3 Oxygen inhibition 11

1.3 Strategies for tolerance improvement 12
1.3.1 Evolutionary engineering and random mutagenesis 13
1.3.2 Metabolic engineering 14
1.4 Genes and mechanisms related to inhibition 18
1.4.1 Extracellular polymeric substances (EPS) 19
1.4.2 Metabolic switch 20
1.4.3 Heat shock proteins and chaperones 20
1.4.4 Efflux pumps 22
1.4.5 Cell envelope 23
1.4.6 Autolysins 25
1.4.7 Enzymatic detoxification 26
1.4.8 Stress response 26
1.5 Conclusions and prospective 27
References 29
Chapter II. Literature Review. *In situ* biobutanol recovery from clostridial fermentations: a critical review 41
Abstract 41
2.1 Introduction 42
2.2 Extraction-based techniques 44
2.2.1 Liquid–liquid extraction 44
2.2.2 Perstraction 50
2.2.3 Reactive extraction 53
2.3 Adsorption-based techniques 55
2.4 Evaporation-based techniques 60
2.4.1 Pervaporation 60

2.4.2 Vacuum and flash fermentation 63

2.4.3 Gas stripping 64

2.5 Comparison of performance and energy requirement 65

2.6 Conclusions and prospects 67

2.7 Disclosure statement 68

2.8 ORCID 68

References 69

Chapter III. Tolerance enhancement of *Clostridium saccharoperbutylacetonicum* N1-4 against lignocellulosic-biomass-derived inhibitors by overexpressing of efflux pumps genes from *Pseudomonas putida*. 78

Abstract 78

3.1 Introduction 79

3.2 Materials and methods 81

3.2.1 Reagents, bacterial strains and cultivation 81

3.2.2 Genetic manipulation 82

3.2.3 DNA transformation 82

3.2.4 Effects of the overexpression of efflux pump genes on the strain tolerance to butanol and lignocellulosic inhibitors 83

3.2.5 Fermentation procedures 84

3.2.6 Analytic procedures 85

3.3 Results and discussion 85

3.3.1 Tolerance test 85

3.3.2 Effects of the overexpression of efflux pump genes on the strain tolerance to furan aldehyde inhibitors 88

3.3.3 Effects of the overexpression of efflux pump genes on the strain tolerance to phenolic inhibitors 91

3.3.4 Model fit of the profile of fermentation with inhibitors 93

3.4 Conclusions 97

3.5 Acknowledgments 97

References 98

Chapter IV. Identification and deletion of the autolysin genes in *Clostridium saccharoperbutylacetonicum* N1-4 101

Abstract 101

4.1 Introduction 102

4.2 Materials and methods 104

4.2.1 Reagents and strains 104

4.2.2 Overexpression of putative autolysin 105

4.2.3 Autolysin gene identification 106

4.2.4 Gene deletion 107

4.2.5 Serum bottle fermentation 108

4.2.6 Bioreactor fermentation 108

4.3 Results 109

4.3.1 Identification of autolysin genes 109

4.3.2 Phenotype of the autolysin deficient mutants 111

4.3.3 Transformation efficiency 116

4.4 Conclusions 117

4.5 Acknowledgements 117

References 118

Chapter V. Polycationic surfaces promote whole cell immobilization and induce micro-granulation of *C. saccharoperbutylacetonicum* N1-4 for enhanced biobutanol productivity 120

Abstract 120

5.1 Introduction 121
5.2 Materials and methods 125
5.2.1 Strain cultivation 125
5.2.2 Preparation and characterization of carrier material for immobilization 125
5.2.3 Investigation of Maillard reaction's effects 126
5.2.4 Serum bottle fermentations 127
5.2.5 Analysis of metabolites 127
5.2.6 Biomass analysis 127
5.2.7 Surface area analysis 129
5.2.8 Cationic charge density determination 129
5.2.9 Cell zeta potential 130
5.2.10 Bacterial potentiometric titration 130
5.2.11 Microscopy 131
5.3 Results and analysis 131
5.3.1 Performance of the fermentation containing chitosan (insoluble) as the carrier material 131
5.3.2 Effect of the Maillard reaction on surface of chitosan-glucose carrier 134
5.3.3 Adsorption, microgranulation, and proposed mechanism 137
5.3.4 Effect of cellulosic materials prepared through two different cationization approaches by amination or ammonization 140
5.3.5 Effect of electrostatic interactions 143
5.3.6 Effects of functional group 145
5.4 Conclusions 146
5.5 Acknowledgements 147
References 148

Summary and perspective 152

References 156

Appendix I. General procedures 157

General equipment 157

Anaerobic chamber (Globes box) 157

Culture media 157

Liquid culture media 157

Solid culture media 158

Antibiotic supplementation 158

Fermentations 158

Serum bottles 159

Analytic determination of glucose, butanol, acetone, ethanol, butyric and acetic acid by HPLC 159

Electrotransformation on *C. saccharoperbutylacetonicum* N1-4 161

PCR procedures 163

Appendix II. Supplementary information for Chapter II. *In situ* biobutanol recovery from clostridial fermentation: a critical review 165

References 175

Appendix III. Supplementary information for chapter III. Tolerance improvement of *Clostridium saccharoperbutylacetonicum* N1-4 against biomass-derived phenolics and furan aldehydes inhibitors by overexpression of efflux pumps srpABC from *Pseudomonas putida* S12. 180

Methods 180

Tolerance test 180

Results 181

Homology comparison using NCBI Blast 181

srpB Blast 181

Appendix IV. Supplementary information chapter IV. Identification, deletion, and study of new autolysins on *Clostridium saccharoperbutylacetonicum* N1-4 183

Genetic manipulations 183

Statistics 185

References 186

Appendix V. Supplementary information chapter V. Polycationic surfaces promote whole cell immobilization and induced micro-granulation on *C. saccharoperbutylacetonicum* N1-4 fermentation, for increased biobutanol productivity. 187

Methods 187

Adsorption support preparation and characterization 187

Surface area determination 187

Cation density and fluorescein determination 191

Protein analysis for biomass analysis 193

Elemental analysis raw data 195

Additional fermentation data 198

List of Tables

Table 2.1 The butanol partition coefficient and selectivity of selected extractants during liquid-liquid extraction with ABE fermentation broth or model solutions. 47

Table 2.2 Summary of performance of perstraction for butanol recovery in various batch fermentations for butanol production..... 51

Table 3.1 List of primers, plasmids and strains used in this study..... 82

Table 3.2 Summary of parameter values in the simulation models based on the fermentation results at different concentrations of inhibitors..... 95

Table 4.1 Fifteen putative autolysin genes in *C. saccharoperbutylacetonicum* N1-4 110

Table 4.2 Transformation efficiency..... 117

Table 5.1 Materials for adsorption of *Clostridium*..... 122

Table 5.2 Serum bottle fermentation performance of *C. saccharoperbutylacetonicum* N1-4 and *C. beijerinckii* NCIMB 8052 immobilized with chitosan as the carrier material..... 132

Table S1.1 Glucose and solvents standard curve preparation..... 159

Table S1.2 Acid standard curve preparation 160

Table S1. 3 Glucose and solvents standard curve HPLC measurement..... 160

Table S1.4 Acid standard curve HPLC measurement..... 160

Table S1.5. Q5 reaction components 163

Table S1.6 Termocycling conditions for Q5..... 163

Table S2.1 Toxicity on cells of selected extractant candidates tested in the literature for butanol recovery..... 165

Table S2.2 The butanol partition coefficient and selectivity of various extractants during liquid-liquid extraction for butanol recovery in ABE fermentation broth or model solutions..... 167

Table S2.3 Summary of partition coefficients and loading capacities of the adsorbants used for biobutanol recovery from the literature. 171

Table S2.4 The parameters and adsorbent characteristics in Langmuir model for butanol adsorption. 172

Table S2.5 Freundlich constants for butanol adsorption with different adsorbents 173

Table S3.1 Ammounts of inhibitors used in tolerance tests 180

Table S3.2 Homologous of *P. putida* S12 *srp*ABC efflux pump in *C. saccharoperbutylacetonicum* N1-4 181

Table S4.1 List of primers used in this study 183

Table S4.2 List of plasmids used in this study 184

Table S4.3 Yields, maximum titers and Tukey's HSD analysis 185

Table S4.4 Statistical analysis on OD_{600} difference for bottle fermentations 185

Table S5.1 Cationization 187

Table S5.2 Methylene blue calibration curve preparation 188

Table S5.3 Fluoresceine calibration curve preparation 192

Table S5.4 Conditions for fluorescence analysis 192

Table S5.5 Bradford standard preparation 193

Table S5.6 Elemental analysis data 195

List of Figures

Figure 1.1 The effect of inhibitors on ABE fermentation with solventogenic clostridia 6

Figure 1.2 Mechanism of acid reactions from polysaccharides to inhibitors. (A) Cellulose hydrolysis and conversion into glucose. (B) Glucose transformation into HMF and then into levulinic acid and formic acid..... 7

Figure 1.3 Lignin, precursors and derivatives. (a) R1=R2=-H: coumaric acid; R1=-OCH3, R2=H: ferulic acid; R1=R2=-OCH3: sinapic acid. (b) R1=R2=-H: 4-hydroxyacetophenone; R1=-OCH3, R2=H: acetovanillone. (c) R1=R2=H: 4-hydroxybenzaldehyde; R1=-OCH3, R2=H: vanillin; R1=R2=-OCH3: syringaldehyde. (d) cinnamic acid. (e) 4-hydroxybenzoic acid. (f) salicylic acid. 9

Figure 1.4 Genetic tools that have been developed and applied in *Clostridium*. (A) Single crossover plasmid integration. (B) Antisense RNA for down-regulating gene expression. (C) Group II Intron for gene disruption. (D) Double crossover homologous recombination. (E) ds-blunt ended DNA breakage by Cas9. (F) ds-sticky ended DNA breakage by Cpf1. (G) ss DNA breakage by nCas9. (H) nuclease deficient Cas binds DNA for gene expression interfering. (I) endogenous CRISPR-Cas system. 17

Figure 1.5 The main components of cell membrane and cell wall for Gram-positive (left) and Gram-negative bacteria (right), respectively 24

Figure 2.1 Schematic of various recovery systems (a) Regular solvent extraction through direct contact between the extractant and the broth; (b) “Tube”-type perstraction: extractant is pumped through the fermentation flask without direct contact with the broth; butanol migrates from the broth (in contact with the external of the hose) to the extractant (inside of the hose); (c) Fiber filter perstraction: broth is pumped through the shell and returned back to the bioreactor; the extractant is driven inside of the hollow; (d) Membrane filter perstraction: a circular filter separates the compartment of the broth and the extractant; butanol exchange takes place through the filter; (e) vacuum evaporation; (f) flash fermentation; and (g) gas stripping..... 45

Figure 2.2 Comparison of several primary recovery techniques. (a) highest productivity, concentration and selectivity (PE selectivity not reported) (b) estimated energy consumption range. GS: Gas stripping, PV: Pervaporation, LL: liquid-liquid extraction with oleyl alcohol, A: adsorption, PE: perstraction. ND: No data..... 66

Figure 3.1 Relative growth of PJB3 (A,C and E) and PJB5 (B,D and E), compared to the control strain (C. saccharoperbutylacetonicum N1-4 containing pJZ100) when these strains were challenged with butanol (A, B), furfural (C, D) and ferulic acid (E,F). 86

Figure 3.2 (1) HAE-1 efflux pumps in Gram-negative bacteria, and (2) cell member of Gram-positive bacteria 88

Figure 3.3 Fermentation profile comparison of strain expressing srpB (pPJB3) and control strain (pJZ100) with 0 g/L, 3 g/L, 3.5 g/L and 4 g/L of furfural. 90

Figure 3.4 Comparison of fermentation profiles of strain expressing srpB (pPJB3) and control strain (pJZ100) with 0.8 g/L, 1.0 g/L, 1.2 g/L, and 1.4 g/L ferulic acid. 92

Figure 3.5 Trends of modeling variables against inhibition concentration, for butanol fermentations. Continuous lines represent the models simulation, and the individual points represent the experimental data. 96

Figure 4.1 Autolysin groups by hydrolytic activity 103

Figure 4.2 Growth curves of six strains overexpressing the putative autolysin gene. P-value for repeated measures ANOVA comparison during stationary/death phase (36 h-72 h) is included on the top of each profile. The error bars represents the standard error at 95% interval of confidence. 112

Figure 4.3 A)-F): Agarose gel electropherogram showed the PCR results confirming the gene deletion in the mutant strain (St) versus control (Ctrl), which are 4166 vs 2186, and 3070 vs 2125 for genes 26 and 30, respectively. Length of genes 1980 (gene 26) and 945 bp (gene 30). G) Scheme of gene deletion using the CRISPR-Cas9 system. 113

Figure 4.4 Profiles of serum bottle fermentation of the single deletion mutant of Gene 26 and Gene 30 compared to the mother strains (*C. saccharoperbutylacetonicum* N1-4, Δ1234, and Δ12345). The error bar represents the standard error at 95% interval of confidence. 114

Figure 4.5 Profiles of batch fermentation in bioreactors with pH controlled for Δ1234Δ26 compared to Δ1234 and wild type. The error bar represents the standard error at 95% interval of confidence. 115

Figure 5.1 Reaction of cellulosic materials (cotton and microcrystalline cellulose) with CHTPA (top) and DEAEC (bottom) for partial cationization of the surface 126

Figure 5.2 Chitosan Millard reaction effects on the fermentations with immobilized C. saccharoperbutylacetonicum N1-4, containing Chitosan-Maillard adducts with different reaction times: R0 = 0 min, R45 = 45 min, R60 = 60 min, and R85 = 85 min. (A) Effects of Maillard reaction on different properties of the material: surface area, cation density, growth rate, and estimated substitution degree. (B) Maillard – Amadori reaction scheme. (C), (D), (E), and (F) illustrate the immobilized cell biomass (expressed as protein concentration) in R0, R45, R60 and R85, respectively. 135

Figure 5.3 Adsorption and induced-microgranulation process of *C. saccharoperbutylacetonicum* N1-4 with chitosan. (A-H) SEM micrographs ((A-D) 2500X, (E-H) 10000X, at different times). (I-L) scheme of adsorption immobilization and microgranulation process. (M-O) Optical micrograph of cell culture at 24 h stained with crystal violet, for planktonic cells, a small piece of

chitosan suspended and attached to a microgranule, and a high cell-density microgranule. (P) The cell biomass profiles, L: liquid, S: solid, T: total 138

Figure 5.4 Profiles of fermentations with cellulosic materials modified with CHTPA as the immobilization carrier, with the properties of the carrier were illustrated as well. (A) & (D) Cell biomass profiles, (B) & (E) Butanol production profiles, and (C) & (F) total ABE production, (G) & (H) the properties for cotton and MCC respectively. Increasing numbers from 1-7 and 8-14 represent decreasing molar rates used for the derivatization. 142

Figure 5.5 Cell envelope, potentiometric titration and electrophoretic motility. (A) ζ potential and potentiometric titration of cell envelope. (B) Cell envelope diagram. (C) Particle analogue. EPS: Extracellular polymeric substances, LB: loose bonded, TB: tight bonded 144

Figure 5.6 Structure of different carriers for adsorption immobilization in this study 146

Figure S1.1 Standard curves for ABE metabolites 161

Figure S2.1 Structure and morphology of selected adsorbents for butanol recovery. (a) Silicalite and zeolite ZSM-5, (b) Silicon oxide functionalized with calixarenes, (c) Carbon (graphite), (d) Poly(styrene-co-divinylbenzene). 174

Figure S2.2 Butanol extractive esterification equilibria 175

Figure S2.3 Selected butanol derivatives that can be potentially produced by in situ reactive extraction. 1 represents butyl linear esters, m=0, 2 for acetic and butyric and m=0-22 for linear saturated derivatives; 2 represents butyl acrylic esters: butyl acrylate when R=H and butyl methacrylate when R= CH_3; 3 is butylamine; 4 represents butyl glycol ethers: n has typical values 1-3; 5 is butyraldehyde: [Ox] means oxidation. Details about catalysts, coproducts and conditions are not specified. 175

Figure S5.1 Methylene blue calibration curve 188

Figure S5.2 Langmuir isotherm linearization for raw and modified samples of chitosan, microcrystalline cellulose and cotton 189

Figure S5.3 Fluorescein calibration curve 192

Figure S5.4 Bradford calibration curve 194

Figure S5.5 Protein vs OD_{600} equivalence 195

Figure S5.6 Elemental percent composition and structure 195

Figure S5.7 Fermentation profiles for bottles fermentation containing chitosan 198

Figure S5.8 Biomass in the carrier at the end of fermentation. (A) CHPTA, (B) DEAE 199

Figure S5.9 Fermentation profiles containing cellulosic materials modified with DEAE as immobilization carrier, as well as the properties of carriers. 199

List of Abbreviations

ABE: Acetone-Butanol-Ethanol

adh: alcohol dehydrogenase

BET: Brunauer, Emmett and Teller isotherm

Cas: CRISPR associated protein

nCas9: nickase Cas9

dCas9: dead Cas9

Cla: Clarithromycin

CHTPA: 9-chloro-2-hydroxypropyl trimethyl ammonium chloride

CNT: carbon nanotube

CRISPR: clustered regularly interspaced short palindromic repeats

CRISPRi: CRISPR interference

DEAEC: N,N-diethylaminoethyl chloride

DMF: Dimethylformamide

DNA: deoxyribonucleic acid

EPS: extracellular polymeric substances

HMF: hydroxymethylfurfural

LB: Luria-Bertani culture media

MCC: Microcrystalline cellulose

MOF: metal-organic framework

NAD^+: Nicotinamide adenine dinucleotide (oxidized)

NADH: Nicotinamide adenine dinucleotide (reduced)

OD_{600}: optical density at 600 nm

PCR: polymerase chain reaction

cPCR: colony PCR

PDMS: silicone (Poly(dimethylsiloxane))

PE: polyethylene

PEBA: Polyether-block-amide

POMS: poly(octhylmethyl siloxane)

PP: polypropylene

PTFE: polytetrafluoroethylene

PTMSP: poly(1-trimethylsilyl-1-propyne)

PVDF: Poly(vinylidene fluoride)

gRNA: guide RNA

ss (DNA breakage): single stranded

ds (DNA breakage): double stranded

TGY: Tryptone-Glucose-Yeast extract medium

Introduction

Background

The Intergovernmental Panel on Climate Change has been advising on the potential irreversible effect if the average temperature on the earth increases by 1.5 °C and the global warming continues (Tollefson, 2018). There is a global concern about this issue, which drives many researchers to work on the renewable fuel research.

Renewable energy in transportation accounts for 5% with a major contribution from the liquid biofuels (bioethanol and biodiesel). E85 fuel (85% ethanol) is currently available at many gas stations, and the price is in average 10% lower than E0 or E10 gasoline (US Department of Energy, 2019). On the other hand, estimation on lignocellulosic ethanol production cost indicated in the best scenario a price similar as gasoline (van Rin, *et al*. 2018). This can be improved by developing more efficient enzymes for biomass hydrolysis, and more robust strains able to perform an efficient consolidated bioprocessing (CBP).

Some other liquid biofuels include Fischer–Tropsch liquids, methanol/dimethylether, butanol, alcohol mixtures and pyrolytic oils. Among them, butanol (particularly, *n*-butanol) is considered as a very promising one, according to the current development condition (McCormick, 2006). Butanol can be produced through the clostridial acetone-butanol-ethanol (ABE) fermentation from renewable resources such as lignocellulosic biomass. However, currently biobutanol production has two major limitations: low production/productivity and high

energy/cost required for the recovery. Current genetic engineering work is trying to improve productivity and production, and different recovery techniques have been evaluated.

As we described in this dissertation, there are reviving interests in fermentative production of butanol due to the fossil fuel crisis and the associated environmental problems. Various genetic engineering efforts as well as process engineering have been conducted in order to improve the economy for the production of biobutanol. In this study, we aim to improve the tolerance of the host strain, which is one of the primary bottlenecks, using genetic engineering and cell immobilization strategies.

Objectives

For the first objective, I propose to improve the tolerance of the host strain *Clostridium saccharoperbutylacetonicum* N1-4 to furan aldehydes and phenolic inhibitors present in the biomass hydrolysates by overexpressing exogenous efflux pump encoding genes. The efflux pumps utilized for this purpose are from *Pseudomonas putida* S12, a strain with an exceptional tolerance to butanol.

The second objective was the improvement on the stability of *C. saccharoperbutylacetonicum* N1-4. In order to achieve this objective we identified new autolysin genes, deleted them from the genome using the CRISPR-Cas9 genome editing tools, and studied the phenotype of the mutants.

The third objective was the development of a cell immobilization system. We explored chitosan and cationized cellulose as carrier materials for immobilization. We also studied the

mechanism involved and the relationship between the chemical properties of the carriers and the fermentation performance of the strain.

References

US Department of Energy (2019). Alternative Fuel Price Report, July 2019. Consulted online: https://afdc.energy.gov/fuels/prices.html

McCormick, R. (2006) Liquid Fuels from Biomass. Consulted online: https://www.energy.gov/sites/prod/files/2014/03/f9/2006_deer_mccormick.pdf

Tollefson, J. 2018. IPCC says limiting global warming to 1.5°C will require drastic action. Nature 562: 172-173

Van Rijn, Rick, Ismael Nieves, KT Shanmugam, Lonnie Ingram, Wilfred Vermerris. 2018. Techno-Economic Evaluation of Cellulosic Ethanol Production Based on Pilot Biorefinery Data: a Case Study of Sweet Sorghum Bagasse Processed via L+SScF. BioEnergy research 11 (2):414-425

Chapter I. Literature Review.

State of the art and prospective on solvent and chemical tolerance of selected biotechnologically significant *Clostridium* strains, focusing on butanol production

Abstract

Non-pathogenic *Clostridium* strains are major natural biobutanol producers and good platforms for the production of many other biofuels and biochemicals. During the fermentation, *Clostridium* strains are subjected to various inhibitory stresses, including oxygen (solventogenic clostridia are strict anaerobes), and inhibition from self-products (alcohols, other solvents, organic acids). Additionally, some heterologous inhibitors, such as furan aldehydes and phenolics, are present in the fermentation. These inhibitors are derived from the process in which lignocellulosic biomass is transformed into monosaccharides (biomass hydrolysates), in order to be used as fermentation substrate. Lignocellulosic biomass is abundant, inexpensive, and does not compete with food production, and thus is considered as promising feedstock for biofuel production. Recent development in genetic engineering tools for solventogenic clostridia has enabled various strategies for enhancing the tolerance of the strain to endproducts and other inhibitors and thus ultimately establishing *Clostridium* as desirable platform for biofuel and biochemical production. This review summarizes various genetic mechanisms related to tolerance, such as extracellular polysaccharides, metabolic switch, heat shock proteins, the membrane composition, autolysins, enzymatic detoxification, and the general stress response genes.

Keywords: butanol tolerance, fermentation inhibitors, metabolic engineering, *Clostridium*

1.1 Introduction

Various valuable industrial chemicals can be produced by *Clostridium* strains such as butanol, ethanol, acetone, acetic acid, butyric acid, caproic acid, isopropanol, 1,3-propanediol, 1,2-propanediol, acetol, 2,3-butanediol and others. Biobutanol is especially interesting because it is one of the most promising alternatives to ethanol as biofuel blendstock for transportation. Intrinsic physical-chemical properties make butanol more suitable than ethanol for use in motor engines, because it is more energetic, miscible with gasoline, safer to manage, and less corrosive. In addition, butanol and its derivative compounds (e.g. esters, amines, polymers) can be used as chemical feedstocks for various industries.

Conventionally, butanol is produced through the petrochemical routes, which is generally efficient but meanwhile generates various secondary pollutants. Butanol can also be produced biologically through the clostridial acetone-butanol-ethanol (ABE) fermentation (Figure 1.1), although the efficiency is usually low. Recently, the development in genetic engineering tools has made it possible to address various limitations and enhance butanol production in solventogenic clostridia. The production of butanol and other solvents is limited by the microbe tolerance to butanol itself and the combined effect with other solvents and chemicals. The tolerance to inhibitors contained in biomass hydrolysates is especially important when considering the context of large-scale biorefinery.

Some recent review papers summarized the strategies and advancements for butanol tolerance in *Clostridium* strains, but mostly focused on the single effect of butanol (Fu, Chen, and Zhang 2016; Liu, Qureshi, and Hughes 2017; Patakova et al. 2018; Peabody and Kao 2016; Wang, Sun, and Yuan 2018), or only on the factors affecting butanol production from biomass (Amiri and

Karimi 2018; Gottumukkala, Haigh, and Görgens 2017; Kim 2018). This manuscript provides a broader perspective of butanol tolerance related to the general chemical stress, contemplating the relationships between the different compounds involved in the general tolerance and productivity, with especial focus on butanol and metabolic engineering approaches. We also summarize the state-of-art and state from our own prospective about the recent advances in the chemical tolerance, including the biomass-derived inhibitors on *Clostridium* and other butanol-producing microorganisms.

1.2 Fermentation Inhibitions

1.2.1 Fermentation end-product inhibition

ABE fermentation has two stages. During the first stage, acidogenesis phase, the substrates (such as simple sugars), are quickly converted into acetic and butyric acids along with fast cell growth. High concentrations of acids can suppress cell metabolism and stop fermentation early if pH is not controlled and drops lower than 5.0. Acid conditions denaturalize membrane proteins, neutralize cell surface potential and compromises the membrane integrity. This phenomenon is called "acid crash" (Maddox et al. 2000). During the second stage, or solventogenesis phase, fatty acids are re-assimilated and converted into acetone, butanol and ethanol (Reed et al. 1987; Wang 2018). This phase is a mechanism used by the cells to eliminate the acid stress, but incongruously, it creates another stress, generated by the solvents. Figure 1 contains the main metabolic pathways for ABE production in solventogenic *Clostridium* species, such as *C. acetobutylicum*, *C. beijerinckii* & *C. saccharoperbutylacetonicum.* The tolerance to fatty acids and butanol shares similar mechanisms. For example, *C. tyrobutyricum,* a hyper-butyrate strain, naturally producing >40g/L butyrate (Zhu and Yang 2003), has been recently engineered to produce butanol, with a titer of 26.2 g/L, the highest amount produced in simple batch fermentation (Zhang, Zong, et al.

2018). Butyrate is the direct subtract for *adhE* on butanol production, but this particular high titer also suggests a relationship between both chemical stresses.

Wu (2016) has observed an increase in formic, acetic and butyric acid tolerance after the addition of zinc in *C. acetobutylicum*. This results in a higher peak butyric acid production, and then higher butanol titer. Formic acid and lactic acid production is usually low in most solventogenic clostridial strains. Acetic acid production and tolerance has been studied in acetogenic clostridia, such as *C. ljungdahlii, C. autoethanogenum, C. ragsdalei, C. coskatii* (Bengelsdorf et al. 2016), *C. thermoaceticum, C. thermoautotrophicum* (Reed et al. 1987; Schwartz and Keller 1982), *C. drakei*, *C. scatologenes*, & *C. carboxidivorans* (Gößner et al. 2008). Acetogenic *Clostridium* utilizes the Wood–Ljungdahl pathway with ethanol and 2,3-butanediol as the endproducts. The commercial importance of these strains is their applicability on syngas fermentation (Bengelsdorf et al. 2016).

A high concentration of acetone can also limit butanol production. Conversion of acetone into isopropanol by inclusion of a bifunctional *adhE* into an ABE strain usually produce a slight reduction in butanol and total solvent, due on the limited reductive power of the cells (NADH) rather than the toxicity (Bankar et al. 2015; Dai et al. 2012; Lee, Jang, et al. 2012). Acetone production is a necessary intermediate or byproduct for acid reassimilation in most strains. *C. pasteurianum* is one of the most noticeable exceptions. However, butanol production from glycerol fermentation using *C. pasteurianum* contains 1,3-propanodiol as the product (Ahn, Sang, and Um 2011; Biebl 2001). The limiting factor in acetone production seems to be NAD^+ recycling rather than tolerance. Acetone production (and H_2 production) was almost inactivated in *C. acetobutylicum* by the inclusion of 2,3-butanodiol pathway (Liu, Yang, Wang, et al. 2018), but alcohol production was not enhanced. The production of other acids as by-products, such as lactic

and formic, could be related to NAD^+/NADH balance as well. The engineered *C. tyrobutyricum* for butanol production is acetone free, because the metabolic pathway does not contain the *ctfA/B* complex (Zhang, Zong, et al. 2018).

Butanol, isopropanol and ethanol are all aliphatic alcohols; they have similar interactions with cells, with butanol being the most toxic. Isopropanol is less toxic than butanol, not just because of its shorter aliphatic chain, but because it is branched. Therefore, it is harder to intercalate into the cell membrane components (Jiménez-Bonilla and Wang 2018). Some work has reported improvements in isopropanol tolerance by means of chemical mutagenesis and selection (De Gérando et al. 2016) or new isolation of tolerant strains (Youn et al. 2016). Ethanol is significantly less toxic than butanol, and ethanol tolerance is not considered a key factor in ABE strains in general, although ethanol stress is very important in ethanologenic strains. A metabolomics and proteomics study on *C. thermocellum* revealed a reduction in glutamic acid, accumulation of sugar phosphates and inhibition of glycolysis when the cells are "challenged" by adding a high ethanol concentration (Yang et al. 2012). Some *C. thermocellum* and *C. phytofermentans* tolerant strains have been developed by evolutionary engineering (Tolonen et al. 2015; Zhu and Yang 2003).

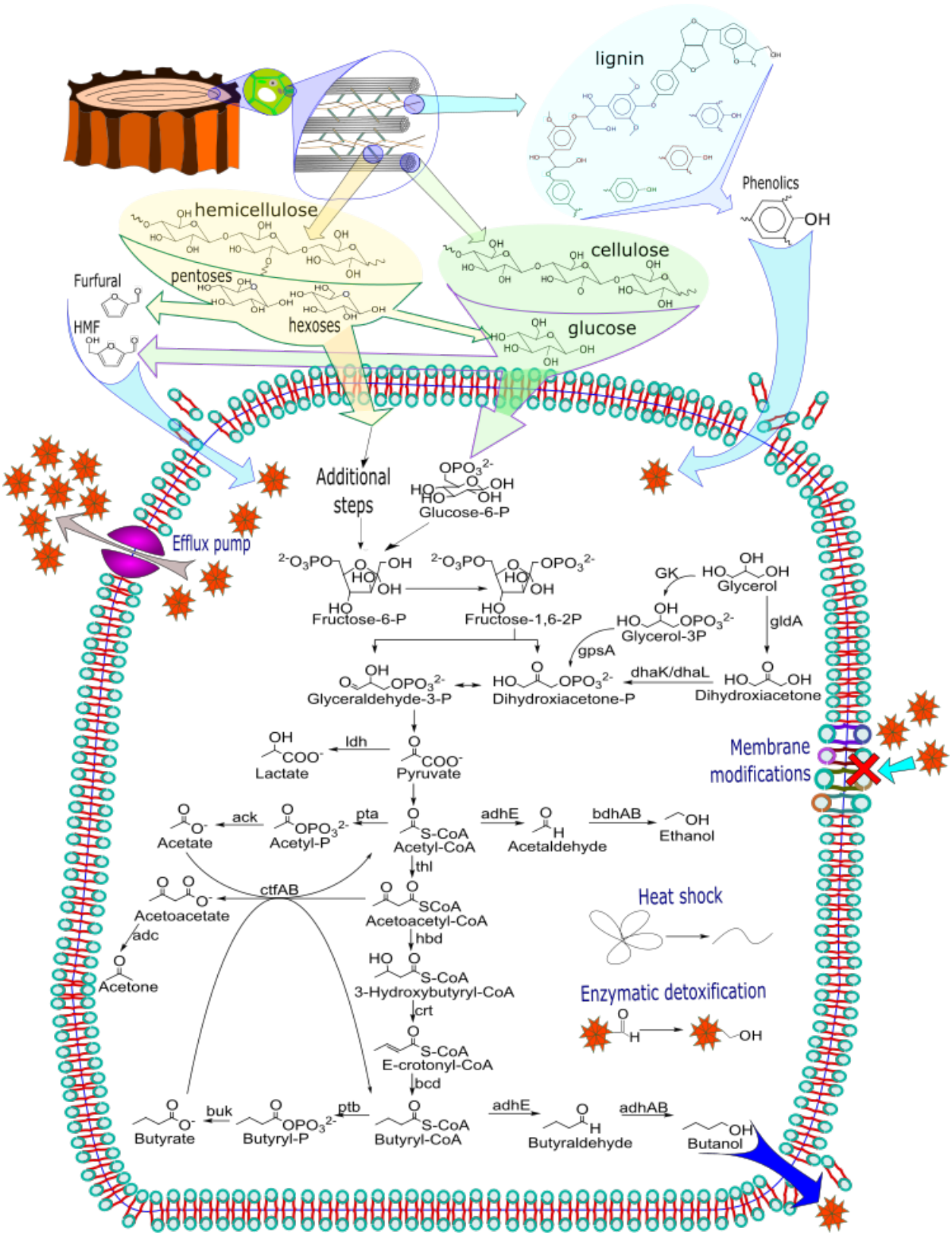

Figure 1.1 The effect of inhibitors on ABE fermentation with solventogenic clostridia

1.2.2 Inhibition from the biomass processing derived inhibitors

Cellulose is the most abundant polysaccharide on earth. Natural function of cellulose is structural and not energetic, and most organisms cannot use it as carbon source. Lignocellulosic wastes are considered valuable feedstock because they are cheap, do not compete with food production, and are widely available from forestry and agricultural production.

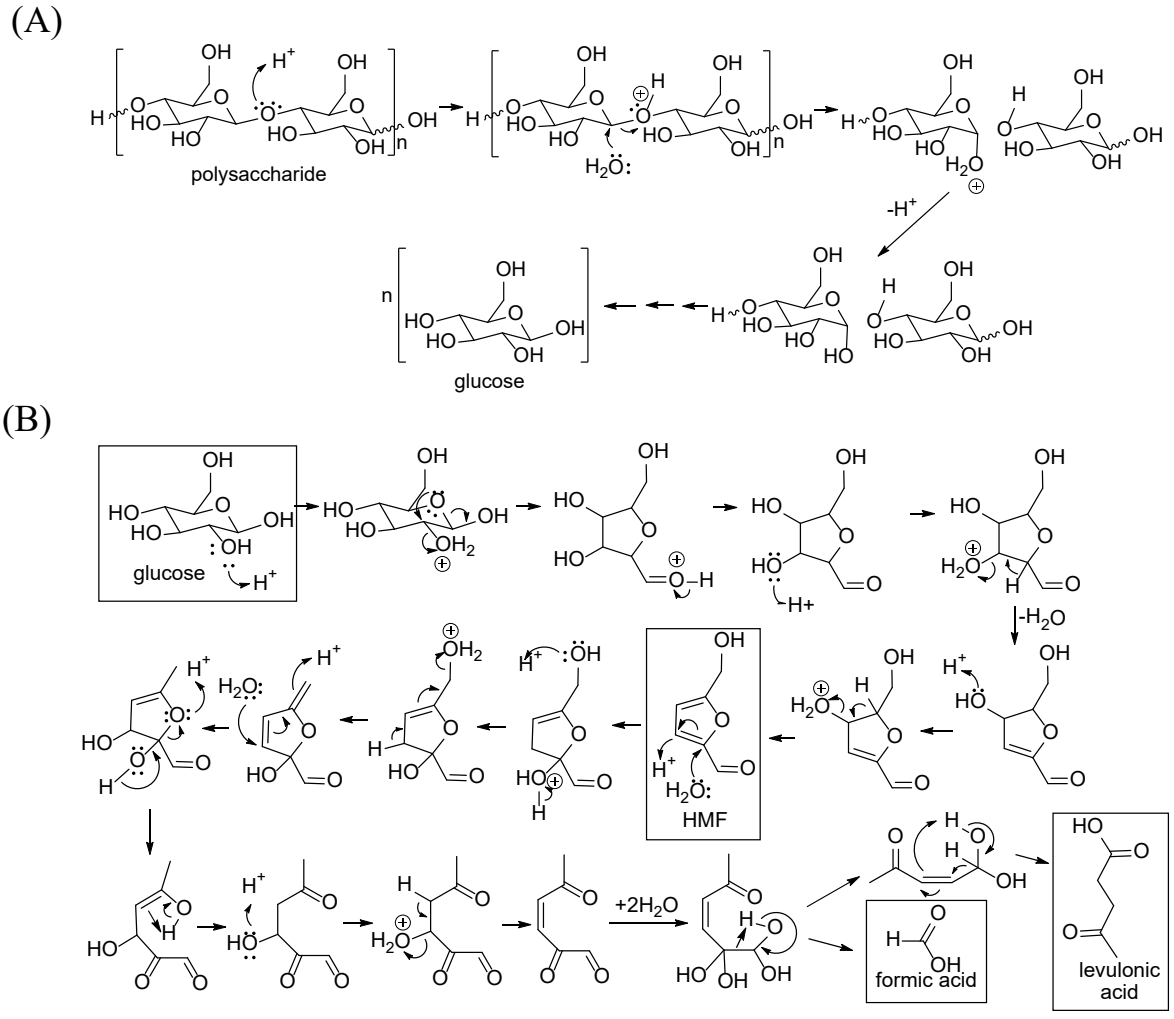

Figure 1.2 Mechanism of acid reactions from polysaccharides to inhibitors. (A) Cellulose hydrolysis and conversion into glucose. (B) Glucose transformation into HMF and then into levulinic acid and formic acid

Generally, there is no natural butanol pathway in *Clostridium* cellulolytic strains. There are a few exceptions but usually the degradation of cellulose or the solvent production is not very efficient (Li et al. 2018; Virunanon et al. 2008). Some cellulolytic strains have been engineered to produced butanol (*C. cellulovorans*) (Wen et al. 2019) or *iso*-butanol (*C. thermocellum* and *C. cellulolyticum*) (Lin et al. 2015; Higashide et al. 2011). The butanol production was achieved with introduction of *adhE1* from *C. acetobutylicum,* and *ctfAB-adc* for enhancement of acid reassimilation. The *iso*-butanol production was achieved by the introduction of the hybrid keto acid pathway: *alsS/ahaS, kari, dhaD, kivD adh*. Those strains have a big potential for consolidated bioprocessing, although they are currently still far from being commercially competitive. *T. thermosaccharolyticum* TG57 (Li et al. 2018) is the only natural cellulolytic butanologenic bacterium, but butanol production only reached 1.93 g/L in a regular batch fermentation.

Since Consolidated Bioprocessing is still not viable for butanol production, another alternative is the conversion of biomass into sugars by chemical or enzymatic hydrolysis, followed by fermentation. For this purpose, lignocellulosic material requires a pretreatment stage, to remove lignin and make the cellulose accessible for chemicals/enzymes, a second stage of hydrolysis, and a third stage of fermentation, involving acid, alkali, oxidant, solvent and/or ionic liquids utilization.

The acid-mediated pretreatment and/or hydrolysis is the most studied and industrially successful process. The acid treatment is optimized to prepare material (during pretreatment) or hydrolysate glyosidic bonds (during hydrolysis). However, a small fraction of the carbohydrates and the lignin decomposed into inhibitors at the same time. These compounds, even in small concentration, impact negatively the growth of solventogenic clostridia and reduce butanol production (Liao et al. 2019). Figure 1.2(A) shows the mechanism of hydrolysis of polysaccharides into simple sugars. Figure 1.2(B) explains the mechanism of conversion of glucose into

hydroxymethylfurfural (HMF) and then into formic acid and levulinic acid. Pentoses can also be transformed into furfural, analogous to the first step as shown above.

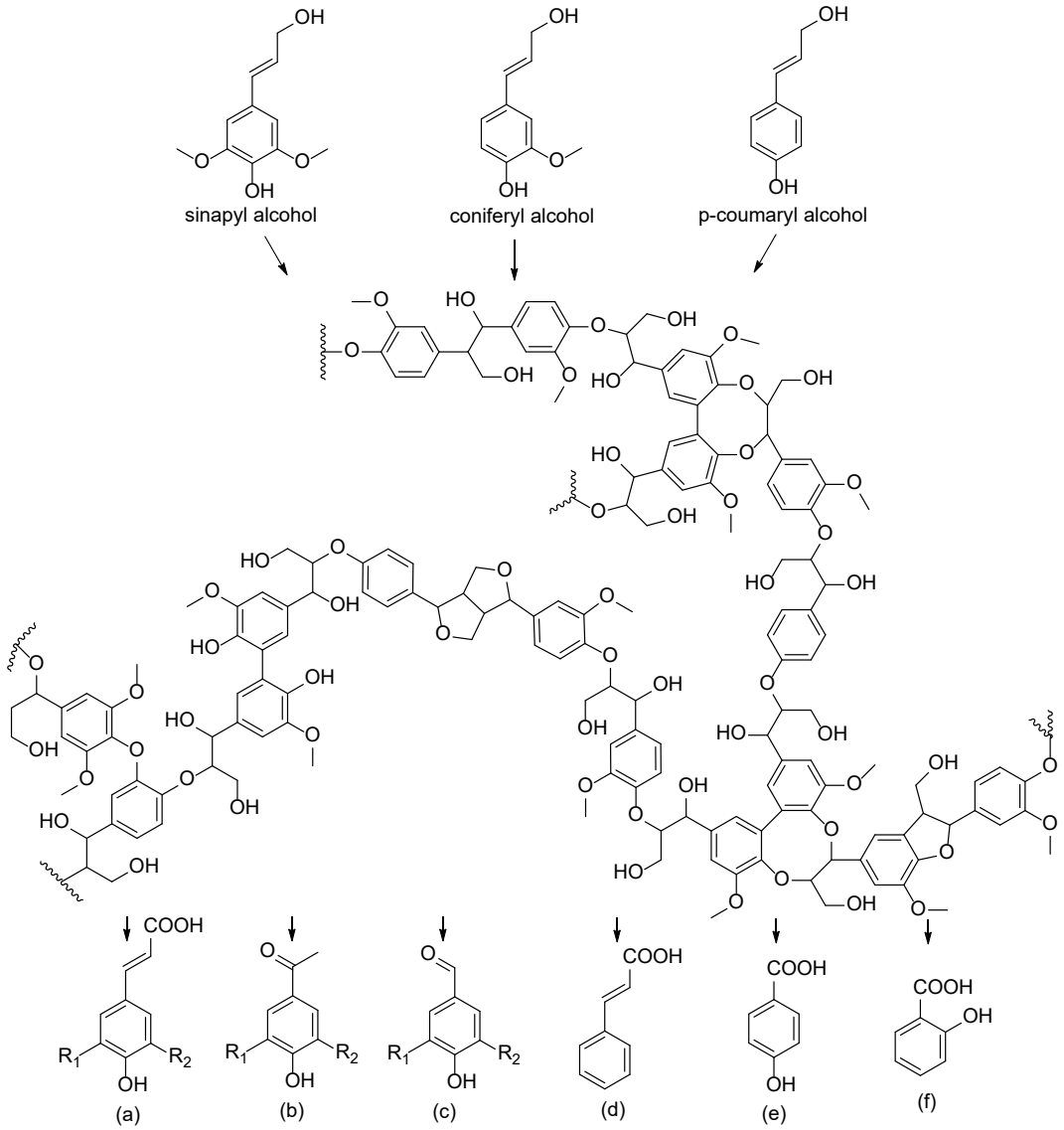

Figure 1.3 Lignin, precursors and derivatives. (a) R1=R2=-H: coumaric acid; R1=-OCH3, R2=H: ferulic acid; R1=R2=-OCH3: sinapic acid. (b) R1=R2=-H: 4-hydroxyacetophenone; R1=-OCH3, R2=H: acetovanillone. (c) R1=R2=H: 4-hydroxybenzaldehyde; R1=-OCH3, R2=H: vanillin; R1=R2=-OCH3: syringaldehyde. (d) cinnamic acid. (e) 4-hydroxybenzoic acid. (f) salicylic acid.

Furan aldehydes (furfural and HMF), like other aldehydes, react with amines including DNA bases. Allopurinol has shown an increased furan aldehydes tolerance in *C. beijerinckii* NCIMB 8052 (Ujor, Agu, Gopalan, & Ezeji, 2015), suggesting that the increased purine salvage and DNA repairing is probably the key mechanism. Furan aldehyde tolerance is around 3 g/L in *C. beijerinckii* BA101 and in *C. saccharoperbutylacetonicum* N1-4 (Ezeji, Qureshi, & Blaschek, 2007; Yao et al., 2017).

Lignin structure is a complex polyphenolic polymer crosslinked with structural polysaccharides. Lignin is synthesized from sinapyl, coniferyl, and p-coumaryl alcohols. Figure 1.3 shows the precursors, a fragment of the polymeric structure, and some water-soluble by-products of the acid or alkali pretreatment. Some of these compounds include *trans*-ferulic acid, acetovanillon, vanillin, syringaldehyde, 4-hydroxyacetophenone, p-coumaric acid, sinapic acid, cinnamic acid, 4- hydroxybenzoic acid and salicylic acid (Liu, Lin, et al. 2018).In general, phenolic compounds inhibit clostridial fermentation more severely than furan aldehydes. In *C. beijerinckii,* the inhibition severity is *p*-coumaric acid > ferulic acid > *p*-hydroxybenzoic acid > vanillic acid > syringaldehyde > vanillin (Cho et al. 2009), while in *C. saccharoperbutylacetonicum* N1-4, *p*-coumaric acid is the most inhibitory followed by syringaldehyde and then ferulic acid (Yao et al. 2017). Considering the chemical structure of the inhibitors: the methoxy group absence in *p*-coumaric acid, compared to ferulic acid, is an element that makes inhibitors more severe, suggesting that electron inducer groups on the aromatic ring reduces inhibition. Studies over the electricity transmitted with methyl viologen over the cell membrane, and the measurement of the concentration of NAD/NADH cofactors suggested the electron transfer chain disruption as the main mechanism for phenolic inhibitors (Liu, Liu, et al. 2018). This also explained the decreased

activities observed before on NADH dependent (or associated) enzymes including acetyl-CoA acetyltransferase, β-hydroxybutyryl-CoA dehydrogenase, 3-hydroxybutyryl-CoA dehydratase, butyryl-CoA dehydrogenase, butyraldehyde dehydrogenase, and butanol dehydrogenase (Chen and Zeng 2018), and also explained the decrease in toxicity by elements on lignin fragment structure that reduces electron capture ability.

1.2.3 Oxygen inhibition

Clostridium strains are strict anaerobic organisms. In the butanol production pathway, the hydrogenation of crotonyl-CoA to butyryl-CoA catalyzed by the butyryl-CoA dehydrogenase/electron transferring flavoprotein (*bcd/etfAB*) complex is difficult to express in recombinant systems (presumably oxygen sensitive) (Lan and Liao 2012). In addition, oxidative conditions have a negative effect over the reduction power, which is essential for alcohol reduction. For example, redox-responsive repressor (*rex*) regulates oxidative stress and also affects the $NADH/NAD^+$ ratio (and butanol production) (Zhang et al. 2014), and NAD kinase (*nadK*), which synthesize $NADP^+$ from NAD^+, also plays an important role in the oxidative stress (Wang et al. 2018; Wu et al. 2017). For example, both *dnaK* from extremophile *Deinococcus wulumuqiensis* R12 and native *dnaK* can increase oxidative tolerance (also related with furfural inhibition) and butanol production in *C. acetobutylicum* ATCC824 (Liao et al. 2017).

Introduction of trehalose pathway into *C. tyrobutyricum* CCTCC W428 reduced acid and oxidative stress (Wu et al. 2017), and the introduction of transglutaminase *mtg* reduces oxidative stress and increases solvent production (Tao et al. 2015). The introduction of *rprA2, dsr*, and rubredoxin (Rd) in a recombinant *nroR* operon increased oxidative tolerance in *C. acetobutylicum* (Kawasaki et al. 2009).

C. acetobutylicum YM1 is a naturally oxygen tolerant strain, with various enzymes that are responsible for oxygen scavenging, such as superoxide dismutase (SOD), catalase and NADH/NADPH oxidases (Al-Shorgani et al. 2015). Other endogenous genes related to oxygen tolerance include desulfoferrodoxin (*dfx*), peroxide repressor (*PerR*)-homologous and *rbr3A* and *rbr3B* (Hillmann et al. 2008).

Different hydrolysates aldehydes, such as vanillin and syringaldehyde are also related with oxidative stress (Liu, Yao, et al. 2017). Aldehydes have an unclear relationship with reactive oxygen species, and also can act as mild oxidant agents (Kang and Nielsen 2017). Glutathione pathway (recombinant *gshA* or *gshB* genes) expressed in *C. acetobutylicum* increased not just oxygen tolerance but butanol tolerance and solvent production (Zhu et al. 2011). This fact could be related with the aldehydes intermediate compounds on solvent production, such as acetaldehyde and butyraldehyde.

Some co-cultures have demonstrated improved oxygen tolerance and butanol production, such as *C. acetobutylicum* TSH1/*Bacillus cereus* TSH2 (Lin et al. 2017; Wu, Wang, et al. 2016), *C. beijerinckii* NCIMB 8052/*B. cereus* CGMCC 1.895 (Mai et al. 2017), and *C. acetobutylicum/Saccharomyces cerevisiae* (Luo et al. 2015). Co-culturing can increase production or confer some features by utilization of the combination of the metabolic pathways of the individual strains, for example, starch utilization, (Mai et al. 2017), or provision of some nutrients such as amino acids (Luo et al. 2015). Also, glucose competition increases the intracellular NADH production (Luo et al. 2015). Finally, a facultative anaerobic partner can consume some levels of oxygen remaining in the medium, and help to keep anaerobic conditions.

1.3 Strategies for tolerance improvement

1.3.1 Evolutionary engineering and random mutagenesis

Evolutionary engineering mimics the natural evolutionary process but occurs in a much shorter time frame. It can be employed to increase the tolerance of strains to different compounds by means of gradual adaptation of the strain to live in the solution containing high levels of toxic compounds (Lee, Na, et al. 2012), or to increase the capability of consumption of a carbon source such as xylose or cellulose (Liu et al. 2010). Usually, adaptive sub-culturing in media containing increasing concentrations of the desired target can generate mutations in genes related with tolerance. Then, mutants with faster growth are selected. Comparison between the genomic mutations between the mutants and the parental strain can provide information about genes related to tolerance (Sandoval-Espinola et al. 2013).

This technique has been employed to increase the tolerance and solvent production in various *Clostridium* strains. *C. acetobutylicum* JB200 is able to produce 21 g/L of butanol, a 68% increase, compared to the parental strain after an evolutionary adaption (Yang and Zhao 2013). In another study, Royce *et al*. (2015) have seen an increase on butanol and isobutanol tolerance when the strain is evolutionarily adapted in a medium containing octanoic acid.

Evolutionary engineering is a great and versatile technique, but there are still some disadvantages: outcomes are unpredictable, protocols are focused on a single compound, and this technique could fail to improve production although the tolerance of the strain is enhanced. Finally, since evolutionary engineering frequently leads to thicker and/or harder cell envelope, the resulting strain is often harder to be further genetically engineered.

For random mutagenesis, a physical or chemical treatment is used to generate mutations. N-methyl-N-nitro-N-nitrosoguanidine (NTG) is the most commonly used. Then screening of

putatively improved strains is done by cultivating the mutants to toxic levels of inhibitory chemicals or by screening for their tolerance improvement (De Gérando et al. 2016). For example, ethanol production is increased by 8-fold during syngas fermentation with a *C. ragsdalei* strain generated through NTG mutagenesis (Patankar et al. 2018).

1.3.2 Metabolic engineering

Clostridium is a genus hard to engineer because it is Gram-positive, spore forming and anaerobic. Recent development in genetic engineering tools makes it possible the understanding and the improvement of mechanisms involved in tolerance and robustness in solventogenic clostridia (Figure 1.4). Genetic engineering is relatively new for *Clostridium*. In 1992, the first plasmid was cloned into *C. acetobutylicum* ATCC824 (Mermelstein et al. 1992), and Campbell-like integration (single crossover homologous recombination) mutants were developed in the same decade (Moon et al. 2016). Campbell integration were used to disrupt genes (Figure 1.4(D)), with very limited applicability. In the 2000s, antisense RNA was used to interrupt the gene expression (Figure 1.4(B), and counter-selection markers were used for double crossover homologous recombination. Later, the group II intron technologies such as Targetron® (Sigma-Aldrich) were introduced (Moon et al. 2016). The group II intron represents an important progress compared to the other techniques in terms of effectiveness and efficiency. However, since this technique disrupts the gene by introducing some DNA fragment (Figure 1.4C), it is possible that the gene still has some residual activity.

Recently, alternative strategies have been reported for efficient, selective, markerless and clean gene editing, inactivation, or repression using the “Clusters of Regularly Interspaced Short

Palindromic Repeats" (CRISPR) system. CRISPR contains nucleases that can effectively be programmed to cut specific DNA sequences. Figure 4 summarizes the systems.

The CRISPR-Cas9 system from *Streptococcus pyogenes* (spCRISPR-Cas9) is the first CRISPR system that has been employed for genome editing and still the mostly utilized. The Cas9 nuclease generates a double stranded (ds) breakage on the DNA, which is lethal in most bacteria (Figure 1.4 (E)). Cas9 could be expressed under an inducible promoter to avoid lethality during transformation. DNA template containing homology arms to the target locus can lead to desirable homologous recombination, and then the cas9 is used as selection tool, killing the unedited background cells (Wang et al. 2016). In this way, the positive mutant can be selected with very high efficiency. Nickase-Cas9 (nCas9) can also be employed for genome editing purpose. The nickase version of Cas9 protein is able to generate a single stranded (ss) breakage (Figure 1.4(G)), which could be repaired using a homologous recombination template (Xu, Li, et al. 2015). nCas9 is less toxic than spCRISPR-Cas9, since ss breakage is less toxic, but the selection power is also weaker for the same reason. In addition, gene inactivation can be achieved by the interconversion of "CG" into "TA" and vice versa based on the fusion of cytidine deaminase, nickase-Cas9^{D10A} and uracil DNA glycosylase inhibitor. This method is not ideal for the deletion of large gene fragment. But since no homologous template is needed, small plasmids can be constructed and employed for genome editing in strains that are difficult to transform (Li et al. 2019).

CRISPR-Cpf1 (Cpf1 is also known as Cas12a) is a similar system as spCRISPR-Cas9, but with some differences: Cpf1 alone is responsible for the maturation of pre-crRNA, can be guided by the ss mature crRNA, cleaves the target DNA to a 5-nt staggered cut distal (Figure 1.4(F)), and the protospacer-adjacent motif (PAM) sequence is "TTTN" (instead of "NGG"; "N" represents

any base) which offers advantages for AT-rich microorganisms such as *Clostridium* (Zhang, Hong, et al. 2018). The cut distal generates a sticky end that decrease the toxicity.

In CRISPR interference (CRISPRi), the nuclease has been deactivated, and works analogue to a broken scissors, which are unable to cut either ss or ds DNA but can bind to the target sequence, blocking the gene expression (Figure 1.4(H)) (Wang et al. 2016). The most common example is dead Cas9 (dCas9), a nuclease deficient version of spCas9. This system has been employed in *C. beijerinckii, C. acetobutylicum* and *C. ljungdahlii* (Woolston et al. 2018). CRISPRi is tunable if it is expressed under an inducible promoter and thus it can be used as an alternative for downregulating essential genes that cannot be deleted (Liu, Gallay, et al. 2017). CRISPRa (activation) also contains a nuclease deficient Cas protein, but fused with an activation domain for upregulation of gene expression (La Russa and Qi 2015). This has not been reported to be used in *Clostridium* yet, but it could be a great alternative to the plasmid-based gene overexpression.

Currently, the expression of exogenous CRISPR systems, such as the described above, has not been universally applied in all *Clostridium* strains. Low plasmid stability, very low transformation efficiencies or not possible transformation/conjugation are some of the most common problems. Recent literature proposed an improvement in the regulation of the expression of the Cas proteins, replacing the inducible promoter by a riboswitch (Cañadas et al. 2019). The "RiboCas" lowered the Cas expression during transformation, and raised it during selection, optimizing both processes.

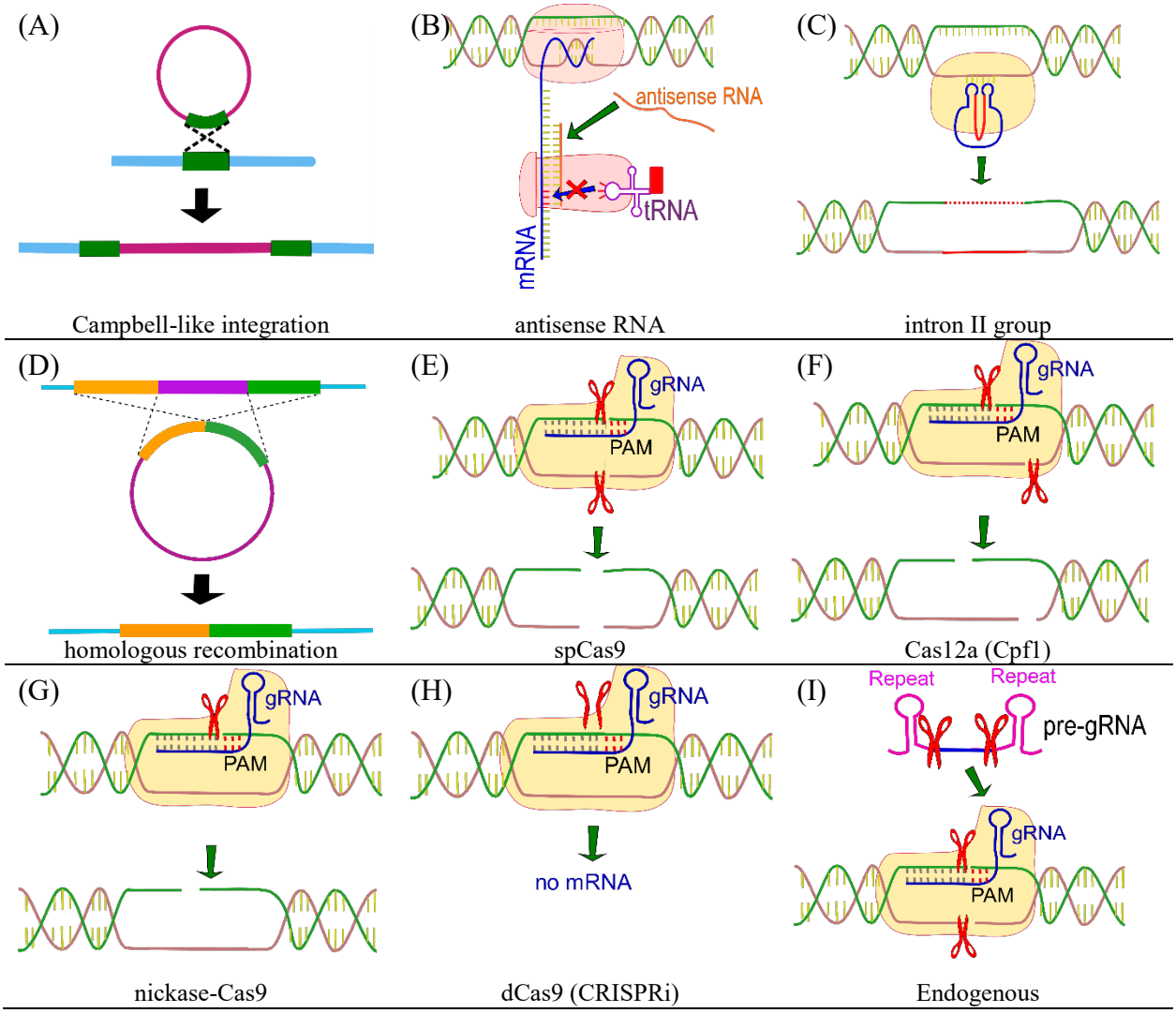

Figure 1.4 Genetic tools that have been developed and applied in *Clostridium*. (A) Single crossover plasmid integration. (B) Antisense RNA for down-regulating gene expression. (C) Group II Intron for gene disruption. (D) Double crossover homologous recombination. (E) ds-blunt ended DNA breakage by Cas9. (F) ds-sticky ended DNA breakage by Cpf1. (G) ss DNA breakage by nCas9. (H) nuclease deficient Cas binds DNA for gene expression interfering. (I) endogenous CRISPR-Cas system.

In some strains, it is possible to use the endogenous CRISPR system. In *Clostridium*, this system has been employed in *C. pasteurianum* and *C. tyrobutyricum* (Pyne et al. 2016; Zhang,

Zong, et al. 2018). They are especially important in strains difficult to transform. Transformation efficiency is significantly higher because of the lack of Cas protein in the plasmids, which induces some toxicity and occupies plasmid loci. To utilize the endogenous CRISPR system, guide RNA sequence is placed between two repeat sequences, and bacterial machinery convert it into mature guide RNA (Figure 1.4(I)). Then, the following genome editing process is based on the CRISPR-Cas-based selection of positive mutant against the background unedited cells, which is very similar to the case using CRISPR-Cas9 or CRISPR-Cpf1.

Argonaute has been reported as a candidate for next generation of genome engineering. Most well characterized nucleolytic argonautes have significant activity at very high temperature (>65°C), so they cannot be easily applied for engineering mesophilic strains. There is a current interest in finding analogues active at mesophilic conditions. Although, there is still not any genetic tool based on it reported, besides the unreproducible retracted article about *Natronobacterium gregoryi* argonaute (NgAgo) (Gao et al. 2016), there is still a potential. In a recent report, *Clostridium butyricum* Argonaute (CbAgo) had been found with nucleolytic activity at 37°C; using small interfering DNA guides (siDNA), and it can be reprogrammed to break ss and ds DNA (Hegge et al. 2019).

1.4 Genes and mechanisms related to inhibition

There are many genes encoding proteins related to chemical tolerance with different mechanisms. Here we classify them, according to the mechanism, into gene categories related to: extracellular polymeric substances (EPS), metabolic switch, chaperones or heat shock proteins, efflux pumps, cell envelope, autolysins, enzymatic detoxification and stress response. Figure 1.1 shows some of the known mechanisms used by the cell to deal with chemical stresses.

1.4.1 Extracellular polymeric substances (EPS)

Biofilm is a natural mechanism that provides protection to the cells. It is composed of the EPS, such as polysaccharides, proteins, lipids, nucleic acids and other macromolecules. The EPS protect cell against the environment, and it is probably one of the most robust strategies to increase tolerance.

Biofilm plays an important role during cell immobilization. Biofilm reactors use a support material to let the cells grow on it and produce biofilm. Then, the EPS create a microenvironment with lower concentration of inhibitors. Different materials such as tygon rings (Raganati et al. 2016), brick pieces (Qureshi et al. 2004), activated carbon, silk, cotton, polyester (Liu et al. 2014), and bagasse (Zhou et al. 2018) have been tested, increasing productivity between 4-7 times compared with planktonic cells (Liu et al. 2014).

In batch fermentations, biofilm formation is important during immobilization by adsorption. Some materials such as cotton, cotton towels, linen, bamboo fiber, silk, and modifications with polyethylenimide and stearic acids (Zhuang et al. 2017; Zhuang et al. 2016) have been employed for this purpose. Some materials can reduce the motility of the polymeric substances and cells, increasing attachment. For example, higher surface area (smaller particles), and cationization of the surface promotes the biofilm formation (Zhuang et al. 2017; Zhuang et al. 2016).

The composition of the biofilm also has an effect on the tolerance. The main components of EPS are polysaccharides. Polysaccharides in EPS are neutral or negatively charged (net charge) and help to preserve the surface charge. Proteins are present in a smaller amount but some of them display high potential, in order to deal with chemical stress. Some cytoplasmic proteins, such as chaperones are retained into the EPS, after partial lysis (Liu, Yang, Chen, et al. 2018). In addition,

the tolerance of the strain can be enhanced by overexpressing some specific extracellular heterologous proteins. For example, tilapia metallothionein (*OmpC-TMT*) increases butanol production and oxidative tolerance in an *E. coli*, harboring *Clostridium* pathway (Chin et al. 2017). Metallothioneins are cysteine rich and heavy metal binding proteins with known activity against oxidative stress (Ruttkay-Nedecky et al. 2013). Other sulfur compounds can also protect against oxidative stress. Proteins can also help to increase acid resistance.

1.4.2 Metabolic switch

Genes related to the control and regulation of solventogenesis, acidogenesis and sporulation are very important for *Clostridium*. Several genes involved in the metabolic shift are related to tolerance. In *C. acetobutylicum* (ATCC 824), *spo0A* is a master regulator of the expression of many genes including the sporulation genes and the genes responsible for the switch from acidogenesis to solventogenesis (Liao et al. 2015), such as *adc,* and the *sol* operon (*adhE*, *ctfA* & *ctfB*) (Fischer, Helms, and Dürre 1993). Other genes related to this process include *solR* (*sol* repressor) (Lee et al. 2008), and multiple sigma factors (complex regulation over phosphorylation of *spo*0A) (Liao et al. 2015).

Some histidine kinases genes related to *spo0A* have an effect on butanol tolerance. The inactivation of *cac3319* gene using Clostron (group II intron) in *C. acetobutylicum* ATCC 55025 increased butanol production and tolerance (Xu, Zhao, et al. 2015), and the overexpression of SMB_G1518-1519 reduced the tolerance (Jia, Zhang, and Li 2012).

1.4.3 Heat shock proteins and chaperones

The heat shock proteins and other molecular chaperones are enzymes that fight against the protein denaturalization generated by chemical or thermal stresses. During stress conditions, other

proteins are folded, then inactivated and degraded. This can also be accompanied by the breakage of protein homeostasis and in protein aggregation (Żwirowski et al. 2017). Heat shock proteins and molecular chaperons unfold proteins, keeping them active.

The *groESL* is a widely spread system in bacteria. It is composed of *groEL*, and *groES* within the same operon. The *groEL* subunit is a cylinder composed of three domains, and the *groES* subunit is a single seven-membered ring which extends a hydrophobic loop structure forming a molecular "lid" for the central cavity (Horwich, Farr, and Fenton 2006). The overexpression of native *groESL* in *C. acetobutylicum* increased butanol tolerance by 45% (Mann et al. 2012). Some exogenous analogues are functional as well. The overexpression of *groESL* from *Deinococcus wulumuqiensis* R12 in *C. acetobutylicum* ATCC824 increased the tolerance of the strain to butanol, furfural, oxidative and acid stress (Liao et al. 2017). Expression of *groESL* from *Thermoanaerobacter tengcongensis* in *C. acetobutylicum* resulted in enhanced cell growth by 4-fold in a medium containing 25% of corn cob hydrolysates (Luan et al. 2014). The overexpression of *groESL* from *Pseudomonas putida* failed to improve tolerance in *C. acetobutylicum*, but improved the thermal tolerance in *E. coli* (Luan et al. 2014). Overexpression of two identical tandem genes *rbr3A* and *rbr3B* encoding the heat shock protein Hsp21 increased tolerance to cold shock, sodium stress, acid stress, oxidative stress and butanol stress in *C. acetobutylicum* (Hillmann, Fischer, and Bahl 2006); while the overexpression of *grpE* and *htpG* increased butanol tolerance by 25 and 56%, respectively (Mann et al. 2012). Transcriptomic analysis showed upregulation of *grpE*, *dnaK*, *dnaJ*, *groESL*, and *htpG* in *C. acetobutylicum* under butanol and butyrate stresses (Wang et al. 2013), and in *C. tyrobutyricum* under butyrate stress. Overexpression of *groESL* and *htpG* significantly improved the tolerance of *C. tyrobutyricum* to butyric acid, while overexpression of *dnaK* and *dnaJ* showed negative effects (Suo et al. 2017).

1.4.4 Efflux pumps

Efflux pumps are membrane proteins for active transportation of chemicals, traditionally known for their role in the antibiotic resistance. These systems pump out the toxic compounds, reducing the intracellular concentration. Recently, members of the subfamily hydrophobic-amphiphilic efflux (HAE-1) from Resistance-Nodulation-Division (RND) superfamily, in Gram-negative bacteria, were studied for their role as active pumps of small molecules (Anes et al. 2015; Nikaido 2018). RND pumps consist of three components: an inner membrane protein which is the extrusion element, an outer pore, and an accessory lipoprotein for stabilization attached to the peptidoglycan (Ramos et al. 2015; Nikaido and Takatsuka 2009). Extrusion is powered by a proton flux from the intermembrane space.

Several efflux pumps gene including *mexEF-oprN* and *ttgABC* from *P. putida*, YP_692684 (and other subunits) from *Alcanivorax borkumensis*, *acrAB-tolC* from *E. coli*, and *srpABC* from *P. putida* (Dunlop et al. 2011) are potentially active against butanol, small alcohols and other small organic chemicals. The *acrABC* gene is the model pump gene, which has been mostly studied. The extruder element *acrB* has been engineered to improve specificity to butanol, by means of selection from a random mutagenesis library (Fisher et al. 2013).

Efflux pumps are complex systems, with different levels of specificity against substrates, and are subjected to complex regulation. Since they are in the membrane, a very high expression level could induce toxicity, probably due to the limitation in the expression of other membrane proteins or because of the modification of the membrane composition. There is a trade-off point where the level of expression minimizes the toxicity of the inhibition and the pump efficiency (Turner and Dunlop 2014).

Some *P. putida* strains have particularly high tolerance against butanol, which could be due to their robust efflux pumps systems. The expression level of the *srpABC* system has been increased when several organic solvents were present. These solvents include aromatic, aliphatic and alcohols. 3mM of butanol led to the increased expression by 6.6 times (Kieboom et al. 1998). Moreover, the overexpression of efflux pumps *srpABC* and the subunit *srpB* alone in *E. coli* could increase the butanol tolerance by 20-35%, when butanol concentration was 0.5-1% (Bui et al. 2015). In addition, an *E. coli* strain demonstrated enhanced butanol tolerance after *ttgABC* was integrated into the chromosome and adaptive evolutionary engineering was conducted (Basler et al. 2018).

1.4.5 Cell envelope

Composition and toughness of cell membrane, cell wall, and EPS are probably the most directly element related to solvent tolerance. A tougher and thicker membrane increases robustness, but makes the strain harder to engineer. The composition of the membrane affects membrane fluidity, and permeability. All different elements on the components of the cell membrane and wall showed an effect on tolerance. For example, thickness peptidoglycans, elements of phospholipids such as some phosphatidic heads and tail characteristics such as saturation, *cis/trans*-unsaturation, length carbon chains, and cyclic structures (Figure 1.5). Genes responsible for synthesis of the different elements of the cell envelope, have an effect on tolerance. The *cis-trans* isomerase (*cti*) from *P. aeruginosa* increased tolerance in *E. coli* (Tan et al. 2016). Also, cyclopropane fatty acid (*cfa*) from different strains, including *C. acetobutylicum*, are related to tolerance (Sandoval and Papoutsakis 2016). Actually, *C. beijerinckii* completely abolished unsaturated fatty acids under alcohol stress (Huffer et al. 2011), and *C. thermocellum* produced longer fatty acids (Timmons et al. 2009). This is because higher Van der Waals forces increase

with the molecular surface area and with linear and rigid structures. *Cis* bonds created a disruption in chain alignment that increases free volume, making a weaker membrane.

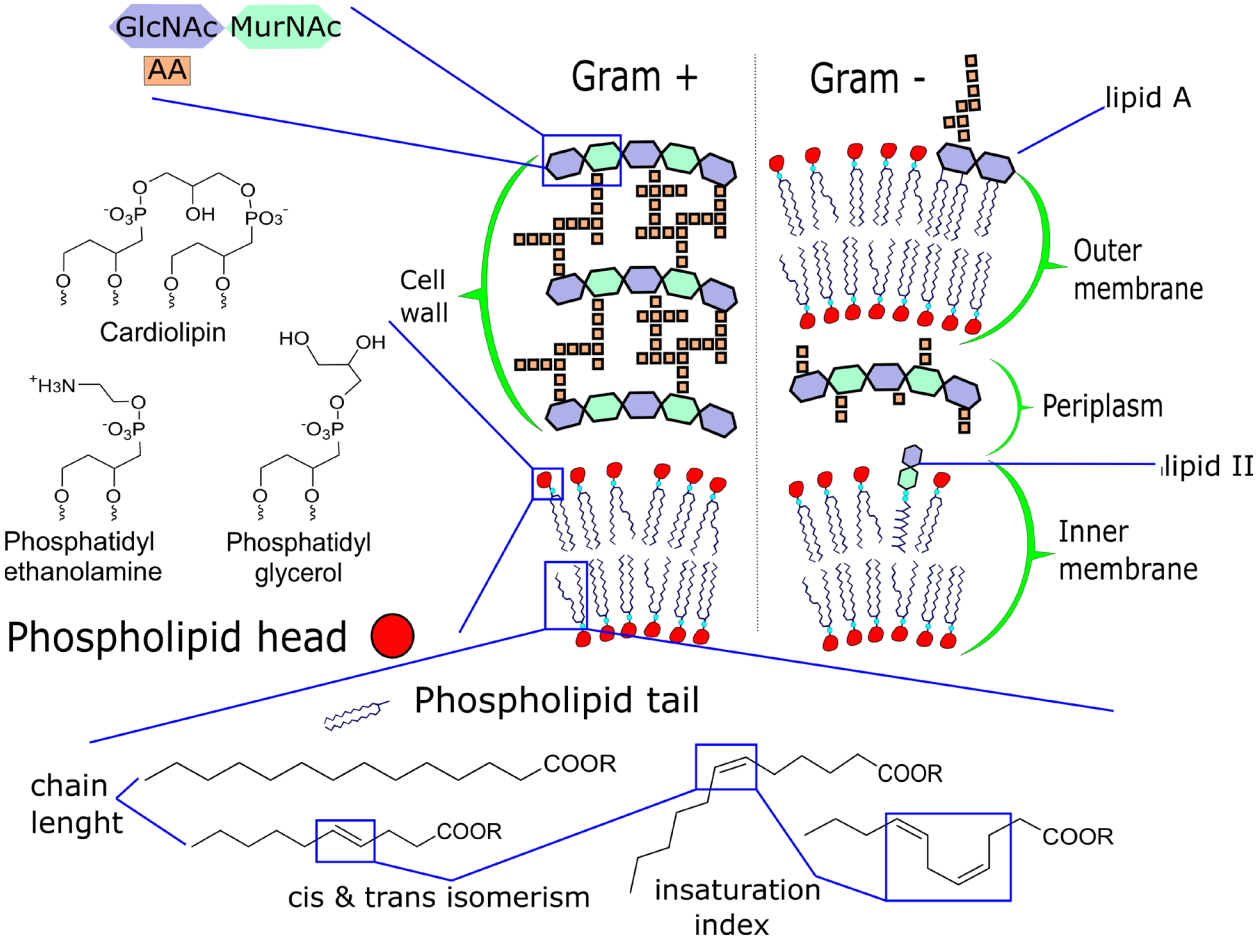

Figure 1.5 The main components of cell membrane and cell wall for Gram-positive (left) and Gram-negative bacteria (right), respectively

Clostridium also produces plasmalogen (lipids with a vinyl ether linking in the opposite side to the ester) (Figure 1.4) (Sandoval and Papoutsakis 2016). In *E. coli*, the overexpression of several genes related to fatty acid composition improved biofuel tolerance. Among the genes of *fabA, fabB, fabD* (and mutated versions), *fabF, fabG, fabH, fabI, fabZ*, and *feoA*, only *fabA, fabD* (construct-variants), and *fabH* increased the alcohol tolerance (Bui et al. 2015).

In *C. acetobutylicum* cardiolipin and the glycerol acetals of plasmenylethanolamine and plasmenyl-N-monomethylethanolamine increased and phosphatidylglycerol and the sum of phosphatidylethanolamine, phosphatidyl-N-monomethylethanolamine decreased (Tian, Guan, and Goldfine 2013). This phenomenon seems to be linked with the change from unsaturated to saturated fatty acids. *C. pasteurianum* also increased cardiolipin and corresponding plasmalogen under similar conditions (Kolek et al. 2015).

The genes related to peptidoglycan biosynthesis like *glmM, murE, murF, amiB, ftsW, ddlB*, and *ftsQ* in some strains are relevant to the tolerance (Sandoval and Papoutsakis 2016). Also, proline addition and proline biosynthesis enhancement (*proABC* overexpression) has an effect on stabilizing protein structures, maintaining cell membrane functions, sweeping away intracellular reactive oxygen substances and lowering DNA melting point, resulting in an improvement of tolerance to lignocellulosic inhibitors (Liao et al. 2019).

1.4.6 Autolysins

Autolysis is a common process in *Clostridium*. This phenomenon contributes to the sporulation process, as a strategy to survive under stress conditions (Liu et al. 2015). However, autolysis decreases the number of cells during the fermentation, and this generates a negative impact on the butanol production. Also autolysis generates an instability of the strain during continuous fermentation processes.

First reports of autolysins isolated in *Clostridium* dated from 1974-1992, from *C. acetobutylicum* P262 (Van Der Westhuizen, Jones, and Woods 1982; Webster et al. 1981; Allcock et al. 1981), in *C. acetobutylicum* ATCC 824 (Croux et al. 1992), and in *C. saccharoperbutylacetonicum* (Yoshino, Ogata, and Hayashida 1982; Ogata and Hongo 1974). A

lit-1 deficient strain from *C. acetobutylicum* P262 was prepared using ethylmethanesulfonate random mutagenesis and isolated by selecting colonies with reduced autolysis (Van Der Westhuizen, Jones, and Woods 1982; Webster et al. 1981; Allcock et al. 1981) The mutant had improved tolerance. More recently, identification and deletion of three genes (SMB_G2359, SMB_G3117 (Yang et al. 2013) and CA_C0554 (Liu et al. 2015)) in *C. acetobutylicum* ATCC 824 improved cell growth, stability, and butanol production titer.

1.4.7 Enzymatic detoxification

Several toxic compounds can be assimilated by the cells or transformed into less toxic ones. Butanol or the desired product cannot be detoxified by means of these kind of mechanisms, because it would be counterproductive but this strategy is important in the detoxification of several other exogenous compounds, such as the biomass inhibitors.

C. beijerinckii and *C. saccharoperbutylacetonicum* can transform furan aldehydes (furfural and HMF) into the corresponding alcohols (Zhang 2013; Yao et al. 2017). *C. beijerinckii* can also degrade 4-hydroxybenzaldehyde and *p*-coumaric acid with an unknown mechanism (Zhang 2013).

C. formicoaceticum has the ability to oxidize aromatic aldehydes like 4-hydroxybenzaldehyde to 4-hydroxybenzoate by constitutive aldehyde oxidoreductase (Frank et al. 1998), and other *Clostridium* can degrade *p*-coumaric acid to *p*-hydroxyhydrocinnamic acid by reduction or to 4-vinylphenol and then 4-ethylphenol by decarboxylation and reduction (Chamkha, Garcia, and Labat 2001).

1.4.8 Stress response

There are several genes and enzymes with unknown or limited understood function and/or mechanisms. Bioinformatics approaches can be used to predict the function of similar genes. Basic Local Alignment Search Tool (BLAST) is an algorithm that compares DNA and amino acid sequences and suggests putative genes or proteins listed by sequence homologies (Schmid and Schmidt-Dannert 2016). Other strategies involved -omics technologies, and are primarily aimed at the universal detection of genes (genomics), mRNA (transcriptomics), proteins (proteomics) and metabolites (metabolomics) (Horgan and Kenny 2011).

Proteomic and transcriptomic analyses of up and down regulation of genes under different kind of stress and/or at different growth and metabolic stages is a powerful strategy to identify new genes related to tolerance. For example, in *C. acetobutylicum*, 29 genes were identified as up-regulated in response to butanol and butyrate stresses, related to protein folding, riboflavin biosynthesis, histidine biosynthesis, ferredoxin hydrogenase, pentose & glucoronate interconvert, fatty acid metabolism, and purine metabolism, and 7 genes were downregulated (Wang et al. 2013). 9 genes are upregulated by butanol, acetate and butyrate, including *lonA, hrcA-grpE-dnaK, groESL, ctsR-yacHI-clpC, hsp90, hsp18, htrA*, CAP0102 and *aad-ctfAB*, most of which are chaperons (Alsaker, Paredes, and Papoutsakis 2010).

1.5 Conclusions and prospective

Conventional tolerance improvement methods such as evolutionary engineering and mutagenesis have several limitations, and recent genetically engineered strains have easily overpassed the production limits defined by conventional approaches. Improvement on genetic tools could not just let us apply the current knowledge about genes related to tolerance, but also improve our understanding on the topic. Since more tolerant strains usually contain tougher

membranes, and higher stability, the development of the genetic tools cannot be considered static, so new challenges could emerge with new development.

There are correlations among different types of chemical stresses. Mechanisms concerning general robustness could be considered a best option rather than those concerning a single stress. But also, an approach completely focused on tolerance can fail in achieving higher production which is usually the ultimate goal. Tolerance mechanisms usually consume cell resources, because they require reducing power, energy, biomass synthesis, membrane space or others. So, it often requires to consider possible trade-offs between the tolerance mechanisms and production.

Tolerance is just a part of the complexity of the cell functions. For those genes related to production and tolerance, their effects related to other cell functions need to be carefully evaluated as well in order to create a solid strategy to achieve the ultimate goal of increasing solvent production.

References

Ahn, Jae-Hyung, Byoung-In Sang, and Youngsoon Um. 2011. Butanol production from thin stillage using Clostridium pasteurianum. *Bioresource technology* 102 (7):4934-4937.

Al-Shorgani, Najeeb Kaid Nasser, Mohd Sahaid Kalil, Wan Mohtar Wan Yusoff, and Aidil Abdul Hamid. 2015. Biobutanol production by a new aerotolerant strain of Clostridium acetobutylicum YM1 under aerobic conditions. *Fuel* 158:855-863.

Allcock, Errol R, Sharon J Reid, David T Jones, and David R Woods. 1981. Autolytic activity and an autolysis-deficient mutant of Clostridium acetobutylicum. *Applied and environmental microbiology* 42 (6):929-935.

Alsaker, Keith V, Carlos Paredes, and Eleftherios T Papoutsakis. 2010. Metabolite stress and tolerance in the production of biofuels and chemicals: gene-expression-based systems analysis of butanol, butyrate, and acetate stresses in the anaerobe Clostridium acetobutylicum. *Biotechnology and bioengineering* 105 (6):1131-1147.

Amiri, Hamid, and Keikhosro Karimi. 2018. Pretreatment and Hydrolysis of Lignocellulosic Wastes for Butanol Production: Challenges and Perspectives. *Bioresource Technology* 270:702-721.

Anes, João, Matthew P McCusker, Séamus Fanning, and Marta Martins. 2015. The ins and outs of RND efflux pumps in Escherichia coli. *Frontiers in microbiology* 6:587.

Bankar, Sandip B, German Jurgens, Shrikant A Survase, Heikki Ojamo, and Tom Granström. 2015. Genetic engineering of Clostridium acetobutylicum to enhance isopropanol-butanol-ethanol production with an integrated DNA-technology approach. *Renewable Energy* 83:1076-1083.

Basler, Georg, Mitchell Thompson, Danielle Tullman-Ercek, and Jay Keasling. 2018. A Pseudomonas putida efflux pump acts on short-chain alcohols. *Biotechnology for biofuels* 11 (1):136.

Bengelsdorf, Frank R, Anja Poehlein, Sonja Linder, Catarina Erz, Tim Hummel, Sabrina Hoffmeister, Rolf Daniel, and Peter Dürre. 2016. Industrial acetogenic biocatalysts: a comparative metabolic and genomic analysis. *Frontiers in microbiology* 7:1036.

Biebl, H. 2001. Fermentation of glycerol by Clostridium pasteurianum—batch and continuous culture studies. *Journal of Industrial Microbiology and Biotechnology* 27 (1):18-26.

Bui, Le Minh, Ju Young Lee, Almando Geraldi, Ziaur Rahman, Jun Hyoung Lee, and Sun Chang Kim. 2015. Improved n-butanol tolerance in Escherichia coli by controlling membrane related functions. *Journal of biotechnology* 204:33-44.

Cañadas, Inés C, Daphne Groothuis, Maria Zygouropoulou, Raquel Rodrigues, and Nigel P Minton. 2019. RiboCas: A Universal CRISPR-Based Editing Tool for Clostridium. *ACS synthetic biology* 8 (6):1379-1390.

Chamkha, Mohamed, Jean-Louis Garcia, and Marc Labat. 2001. Metabolism of cinnamic acids by some Clostridiales and emendation of the descriptions of Clostridium aerotolerans, Clostridium celerecrescens and Clostridium xylanolyticum. *International journal of systematic and evolutionary microbiology* 51 (6):2105-2111.

Chen, Wen-Hsing, and Yan-Ru Zeng. 2018. Mathematical model to appraise the inhibitory effect of phenolic compounds derived from lignin for biobutanol production. *Bioresource technology* 261:44-51.

Chin, Wei-Chih, Kuo-Hsing Lin, Chun-Chi Liu, Kenji Tsuge, and Chieh-Chen Huang. 2017. Improved n-butanol production via co-expression of membrane-targeted tilapia metallothionein and the clostridial metabolic pathway in Escherichia coli. *BMC biotechnology* 17 (1):36.

Cho, Dae Haeng, Yun Jie Lee, Youngsoon Um, Byoung-In Sang, and Yong Hwan Kim. 2009. Detoxification of model phenolic compounds in lignocellulosic hydrolysates with peroxidase for butanol production from Clostridium beijerinckii. *Applied microbiology and biotechnology* 83 (6):1035-1043.

Croux, Christian, Bruno Canard, Gerard Goma, and Philippe Soucaille. 1992. Autolysis of Clostridium acetobutylicum ATCC 824. *Microbiology* 138 (5):861-869.

Dai, Zongjie, Hongjun Dong, Yan Zhu, Yanping Zhang, Yin Li, and Yanhe Ma. 2012. Introducing a single secondary alcohol dehydrogenase into butanol-tolerant Clostridium acetobutylicum Rh8 switches ABE fermentation to high level IBE fermentation. *Biotechnology for biofuels* 5 (1):44.

De Gérando, H Máté, Françoise Fayolle-Guichard, L Rudant, SK Millah, Frédéric Monot, Nicolas Lopes Ferreira, and AM López-Contreras. 2016. Improving isopropanol tolerance and production of Clostridium beijerinckii DSM 6423 by random mutagenesis and genome shuffling. *Applied microbiology and biotechnology* 100 (12):5427-5436.

Dunlop, Mary J, Zain Y Dossani, Heather L Szmidt, Hou Cheng Chu, Taek Soon Lee, Jay D Keasling, Masood Z Hadi, and Aindrila Mukhopadhyay. 2011. Engineering microbial biofuel tolerance and export using efflux pumps. *Molecular systems biology* 7 (1):487.

Fischer, Ralf J, Jan Helms, and P Dürre. 1993. Cloning, sequencing, and molecular analysis of the sol operon of Clostridium acetobutylicum, a chromosomal locus involved in solventogenesis. *Journal of bacteriology* 175 (21):6959-6969.

Fisher, Michael A, Sergey Boyarskiy, Masaki R Yamada, Niwen Kong, Stefan Bauer, and Danielle Tullman-Ercek. 2013. Enhancing tolerance to short-chain alcohols by engineering the Escherichia coli AcrB efflux pump to secrete the non-native substrate n-butanol. *ACS synthetic biology* 3 (1):30-40.

Frank, Claudia, Ulf Schwarz, Carola Matthies, and Harold L Drake. 1998. Metabolism of aromatic aldehydes as cosubstrates by the acetogen Clostridium formicoaceticum. *Archives of microbiology* 170 (6):427-434.

Fu, Y, L Chen, and W Zhang. 2016. Regulatory mechanisms related to biofuel tolerance in producing microbes. *Journal of applied microbiology* 121 (2):320-332.

Gao, Feng, Xiao Z Shen, Feng Jiang, Yongqiang Wu, and Chunyu Han. 2016. DNA-guided genome editing using the Natronobacterium gregoryi Argonaute. *Nature biotechnology* 34 (7):768.

Gößner, Anita S, Flynn Picardal, Ralph S Tanner, and Harold L Drake. 2008. Carbon metabolism of the moderately acid-tolerant acetogen Clostridium drakei isolated from peat. *FEMS microbiology letters* 287 (2):236-242.

Gottumukkala, Lalitha Devi, Kate Haigh, and Johann Görgens. 2017. Trends and advances in conversion of lignocellulosic biomass to biobutanol: Microbes, bioprocesses and industrial viability. *Renewable and Sustainable Energy Reviews* 76:963-973.

Hegge, Jorrit W, Daan C Swarts, Stanley D Chandradoss, Tao Ju Cui, Jeroen Kneppers, Martin Jinek, Chirlmin Joo, and John van der Oost. 2019. DNA-guided DNA cleavage at moderate temperatures by Clostridium butyricum Argonaute. *Nucleic Acid Research* 47 (11):5809–5821.

Higashide, Wendy, Yongchao Li, Yunfeng Yang, and James C Liao. 2011. Metabolic engineering of Clostridium cellulolyticum for production of isobutanol from cellulose. *Appl. Environ. Microbiol.* 77 (8):2727-2733.

Hillmann, Falk, Ralf-Jörg Fischer, and Hubert Bahl. 2006. The rubrerythrin-like protein Hsp21 of Clostridium acetobutylicum is a general stress protein. *Archives of microbiology* 185 (4):270.

Hillmann, Falk, Ralf-Jörg Fischer, Florence Saint-Prix, Laurence Girbal, and Hubert Bahl. 2008. PerR acts as a switch for oxygen tolerance in the strict anaerobe Clostridium acetobutylicum. *Molecular microbiology* 68 (4):848-860.

Horgan, Richard P, and Louise C Kenny. 2011. 'Omic'technologies: genomics, transcriptomics, proteomics and metabolomics. *The Obstetrician & Gynaecologist* 13 (3):189-195.

Horwich, Arthur L, George W Farr, and Wayne A Fenton. 2006. GroEL− GroES-mediated protein folding. *Chemical reviews* 106 (5):1917-1930.

Huffer, Sarah, Melinda E Clark, Jonathan C Ning, Harvey W Blanch, and Douglas S Clark. 2011. The role of alcohols in growth, lipid composition, and membrane fluidity of yeast, bacteria, and archaea. *Applied and environmental microbiology*:AEM. 00694-11.

Jia, Kaizhi, Yanping Zhang, and Yin Li. 2012. Identification and characterization of two functionally unknown genes involved in butanol tolerance of Clostridium acetobutylicum. *PloS one* 7 (6):e38815.

Jiménez-Bonilla, Pablo, and Yi Wang. 2018. In situ biobutanol recovery from clostridial fermentations: a critical review. *Critical reviews in biotechnology* 38 (3):469-482.

Kang, Min-Kyoung, and Jens Nielsen. 2017. Biobased production of alkanes and alkenes through metabolic engineering of microorganisms. *Journal of industrial microbiology & biotechnology* 44 (4-5):613-622.

Kawasaki, Shinji, Yu Sakai, Tohru Takahashi, Ippei Suzuki, and Youichi Niimura. 2009. O2 and reactive oxygen species detoxification complex, composed of O2-responsive NADH: rubredoxin oxidoreductase-flavoprotein A2-desulfoferrodoxin operon enzymes, rubperoxin, and rubredoxin, in Clostridium acetobutylicum. *Applied and environmental microbiology* 75 (4):1021-1029.

Kieboom, Jasper, Jonathan J Dennis, Gerben J Zylstra, and Jan AM De Bont. 1998. Active Efflux of Organic Solvents byPseudomonas putida S12 Is Induced by Solvents. *Journal of bacteriology* 180 (24):6769-6772.

Kim, Daehwan. 2018. Physico-chemical conversion of lignocellulose: Inhibitor effects and detoxification strategies: A mini review. *Molecules* 23 (2):309.

Kolek, Jan, Petra Patáková, Karel Melzoch, Karel Sigler, and Tomáš Řezanka. 2015. Changes in membrane plasmalogens of Clostridium pasteurianum during butanol fermentation as determined by lipidomic analysis. *PLoS One* 10 (3):e0122058.

La Russa, Marie F, and Lei S Qi. 2015. The new state of the art: Cas9 for gene activation and repression. *Molecular and cellular biology* 35 (22):3800-3809.

Lan, Ethan I, and James C Liao. 2012. ATP drives direct photosynthetic production of 1-butanol in cyanobacteria. *Proceedings of the National Academy of Sciences* 109 (16):6018-6023.

Lee, Jeong Wook, Dokyun Na, Jong Myoung Park, Joungmin Lee, Sol Choi, and Sang Yup Lee. 2012. Systems metabolic engineering of microorganisms for natural and non-natural chemicals. *Nature chemical biology* 8 (6):536.

Lee, Joungmin, Yu-Sin Jang, Sung Jun Choi, Jung Ae Im, Hyohak Song, Jung Hee Cho, E Terry Papoutsakis, George N Bennett, and Sang Yup Lee. 2012. Metabolic engineering of Clostridium acetobutylicum ATCC 824 for isopropanol-butanol-ethanol fermentation. *Applied and environmental microbiology* 78 (5):1416-1423.

Lee, Sang Yup, Jin Hwan Park, Seh Hee Jang, Lars K Nielsen, Jaehyun Kim, and Kwang S Jung. 2008. Fermentative butanol production by Clostridia. *Biotechnology and bioengineering* 101 (2):209-228.

Li, Qi, François M Seys, Nigel P Minton, Junjie Yang, Yu Jiang, Weihong Jiang, and Sheng Yang. 2019. CRISPR-Cas9D10A nickase-assisted base editing in solvent producer Clostridium beijerinckii. *Biotechnology and Bioengineering* 113:1475-1483.

Li, Tinggang, Chen Zhang, Kun-Lin Yang, and Jianzhong He. 2018. Unique genetic cassettes in a Thermoanaerobacterium contribute to simultaneous conversion of cellulose and monosugars into butanol. *Science advances* 4 (3):e1701475.

Liao, Chen, Seung-Oh Seo, Venhar Celik, Huaiwei Liu, Wentao Kong, Yi Wang, Hans Blaschek, Yong-Su Jin, and Ting Lu. 2015. Integrated, systems metabolic picture of acetone-butanol-ethanol fermentation by Clostridium acetobutylicum. *Proceedings of the National Academy of Sciences*:201423143.

Liao, Zhengping, Xiaolong Guo, Jialei Hu, Yukai Suo, Hongxin Fu, and Jufang Wang. 2019. The significance of proline on lignocellulose-derived inhibitors tolerance in Clostridium acetobutylicum ATCC 824. *Bioresource technology* 272:561-569.

Liao, Zhengping, Yanan Zhang, Sheng Luo, Yukai Suo, Shaozhi Zhang, and Jufang Wang. 2017. Improving cellular robustness and butanol titers of Clostridium acetobutylicum ATCC824 by introducing heat shock proteins from an extremophilic bacterium. *Journal of biotechnology* 252:1-10.

Lin, Paul P, Luo Mi, Amy H Morioka, Kouki M Yoshino, Sawako Konishi, Sharon C Xu, Beth A Papanek, Lauren A Riley, Adam M Guss, and James C Liao. 2015. Consolidated bioprocessing of cellulose to isobutanol using Clostridium thermocellum. *Metabolic engineering* 31:44-52.

Lin, Zhangnan, Hongjuan Liu, Xiang Yan, Yujie Zhou, Keke Cheng, and Jian'an Zhang. 2017. High-efficiency acetone-butanol-ethanol production and recovery in non-strict anaerobic gas-stripping fed-batch fermentation. *Applied microbiology and biotechnology* 101 (21):8029-8039.

Liu, Dong, Yong Chen, Feng-Ying Ding, Ting Zhao, Jing-Lan Wu, Ting Guo, Heng-Fei Ren, Bing-Bing Li, Huan-Qing Niu, and Zhi Cao. 2014. Biobutanol production in a Clostridium acetobutylicum biofilm reactor integrated with simultaneous product recovery by adsorption. *Biotechnology for biofuels* 7 (1):5.

Liu, Dong, Zhengjiao Yang, Yong Chen, Wei Zhuang, Huanqing Niu, Jinglan Wu, and Hanjie Ying. 2018. Clostridium acetobutylicum grows vegetatively in a biofilm rich in heteropolysaccharides and cytoplasmic proteins. *Biotechnology for biofuels* 11 (1):315.

Liu, Dong, Zhengjiao Yang, Ping Wang, Huanqing Niu, Wei Zhuang, Yong Chen, Jinglan Wu, Chenjie Zhu, Hanjie Ying, and Pingkai Ouyang. 2018. Towards acetone-uncoupled

biofuels production in solventogenic Clostridium through reducing power conservation. *Metabolic engineering* 47:102-112.

Liu, Jun, Qinlu Lin, Xueying Chai, Yunchuan Luo, and Ting Guo. 2018. Enhanced phenolic compounds tolerance response of Clostridium beijerinckii NCIMB 8052 by inactivation of Cbei_3304. *Microbial cell factories* 17 (1):35.

Liu, Jun, Zuojun Liu, Xueying Chai, Yunchuan Luo, Ting Guo, and Hanjie Ying. 2018. Regulation of ρ-coumaric acid tolerance in Clostridium beijerinckii by disturbing the intracellular electron transport chain. *Process Biochemistry* 68:43-52.

Liu, Siqing, Nasib Qureshi, and Stephen R. Hughes. 2017. Progress and perspectives on improving butanol tolerance. *World Journal of Microbiology and Biotechnology* 33 (3):51.

Liu, Wenjin, Xiao-Zhou Zhang, Zuoming Zhang, and Y-H Percival Zhang. 2010. Engineering of Clostridium phytofermentans endoglucanase Cel5A for improved thermostability. *Applied and environmental microbiology* 76 (14):4914-4917.

Liu, Xue, Clement Gallay, Morten Kjos, Arnau Domenech, Jelle Slager, Sebastiaan P van Kessel, Kèvin Knoops, Robin A Sorg, Jing-Ren Zhang, and Jan-Willem Veening. 2017. High-throughput CRISPRi phenotyping identifies new essential genes in Streptococcus pneumoniae. *Molecular systems biology* 13 (5):931.

Liu, Zhen, Kai Qiao, Lei Tian, Quan Zhang, Zi-Yong Liu, and Fu-Li Li. 2015. Spontaneous large-scale autolysis in Clostridium acetobutylicum contributes to generation of more spores. *Frontiers in microbiology* 6:950.

Liu, Zi-Yong, Xiu-Qing Yao, Quan Zhang, Zhen Liu, Ze-Jie Wang, Yong-Yu Zhang, and Fu-Li Li. 2017. Modulation of the acetone/butanol ratio during fermentation of corn stover-derived hydrolysate by Clostridium beijerinckii strain NCIMB 8052. *Appl. Environ. Microbiol.* 83 (7):e03386-16.

Luan, Guodong, Hongjun Dong, Tianrui Zhang, Zhao Lin, Yanping Zhang, Yin Li, and Zhen Cai. 2014. Engineering cellular robustness of microbes by introducing the GroESL chaperonins from extremophilic bacteria. *Journal of biotechnology* 178:38-40.

Luo, Hongzhen, Laibing Ge, Jingshu Zhang, Yanli Zhao, Jian Ding, Zhigang Li, Zhenni He, Rui Chen, and Zhongping Shi. 2015. Enhancing butanol production under the stress environments of co-culturing Clostridium acetobutylicum/Saccharomyces cerevisiae integrated with exogenous butyrate addition. *PloS one* 10 (10):e0141160.

Maddox, IS, E Steiner, S Hirsch, S Wessner, NA Gutierrez, JR Gapes, and KC Schuster. 2000. The Cause of" Acid Crash" and" Acidogenic Fermentations" During the Batch Acetone-Butanol-Ethanol(ABE-) Fermentation Process. *Journal of molecular microbiology and biotechnology* 2 (1):95-100.

Mai, Shuai, Genyu Wang, Pengfei Wu, Chunkai Gu, Hongjuan Liu, Jianan Zhang, and Gehua Wang. 2017. Interactions between Bacillus cereus CGMCC 1.895 and Clostridium

beijerinckii NCIMB 8052 in coculture for butanol production under nonanaerobic conditions. *Biotechnology and applied biochemistry* 64 (5):719-726.

Mann, Miriam S, Zdravko Dragovic, Georg Schirrmacher, and Tina Lütke-Eversloh. 2012. Over-expression of stress protein-encoding genes helps Clostridium acetobutylicum to rapidly adapt to butanol stress. *Biotechnology letters* 34 (9):1643-1649.

Mermelstein, Lee D, Neil E Welker, George N Bennett, and Eleftherios T Papoutsakis. 1992. Expression of cloned homologous fermentative genes in Clostridium acetobutylicum ATCC 824. *Nature biotechnology* 10 (2):190.

Moon, Hyeon Gi, Yu-Sin Jang, Changhee Cho, Joungmin Lee, Robert Binkley, and Sang Yup Lee. 2016. One hundred years of clostridial butanol fermentation. *FEMS microbiology letters* 363 (3).

Nikaido, Hiroshi. 2018. RND transporters in the living world. *Research in microbiology* 169 (7-8):363-371.

Nikaido, Hiroshi, and Yumiko Takatsuka. 2009. Mechanisms of RND multidrug efflux pumps. *Biochimica et Biophysica Acta (BBA)-Proteins and Proteomics* 1794 (5):769-781.

Ogata, S, and M Hongo. 1974. Lysis induced by sodium ion and its relation to lytic enzyme systems in Clostridium saccharoperbutylacetonicum. *Microbiology* 81 (2):315-323.

Patakova, Petra, Jan Kolek, Karel Sedlar, Pavlina Koscova, Barbora Branska, Kristyna Kupkova, Leona Paulova, and Ivo Provaznik. 2018. Comparative analysis of high butanol tolerance and production in clostridia. *Biotechnology Advances* 36 (3):721-738.

Patankar, Siddhi, Amol Dudhane, AD Paradh, and Sanjay Patil. 2018. Improved bioethanol production using genome-shuffled Clostridium ragsdalei (DSM 15248) strains through syngas fermentation. *Biofuels*:1-9.

Peabody, George L, and Katy C Kao. 2016. Recent progress in biobutanol tolerance in microbial systems with an emphasis on Clostridium. *FEMS microbiology letters* 363 (5).

Pyne, Michael E, Mark R Bruder, Murray Moo-Young, Duane A Chung, and C Perry Chou. 2016. Harnessing heterologous and endogenous CRISPR-Cas machineries for efficient markerless genome editing in Clostridium. *Scientific reports* 6:25666.

Qureshi, Nasib, Patrick Karcher, Michael Cotta, and Hans P Blaschek. 2004. High-productivity continuous biofilm reactor for butanol production. *Applied biochemistry and biotechnology* 114 (1-3):713-721.

Raganati, Francesca, Alessandra Procentese, Giuseppe Olivieri, Maria Elena Russo, P Gotz, P Salatino, and A Marzocchella. 2016. Butanol production by Clostridium acetobutylicum in a series of packed bed biofilm reactors. *Chemical Engineering Science* 152:678-688.

Ramos, Juan-Luis, Maria Sol Cuenca, Carlos Molina-Santiago, Ana Segura, Estrella Duque, María R Gómez-García, Zulema Udaondo, and Amalia Roca. 2015. Mechanisms of solvent resistance mediated by interplay of cellular factors in Pseudomonas putida. *FEMS microbiology reviews* 39 (4):555-566.

Reed, WM, FA Keller, FE Kite, ME Bogdan, and JS Ganoung. 1987. Development of increased acetic acid tolerance in anaerobic homoacetogens through induced mutagenesis and continuous selection. *Enzyme and microbial technology* 9 (2):117-120.

Royce, Liam A, Jong Moon Yoon, Yingxi Chen, Emily Rickenbach, Jacqueline V Shanks, and Laura R Jarboe. 2015. Evolution for exogenous octanoic acid tolerance improves carboxylic acid production and membrane integrity. *Metabolic engineering* 29:180-188.

Ruttkay-Nedecky, Branislav, Lukas Nejdl, Jaromir Gumulec, Ondrej Zitka, Michal Masarik, Tomas Eckschlager, Marie Stiborova, Vojtech Adam, and Rene Kizek. 2013. The role of metallothionein in oxidative stress. *International journal of molecular sciences* 14 (3):6044-6066.

Sandoval-Espinola, Walter J, Satya T Makwana, Mari S Chinn, Michael R Thon, M Andrea Azcárate-Peril, and Jose M Bruno-Barcena. 2013. Comparative phenotypic analysis and genome sequence of Clostridium beijerinckii SA-1, an offspring of NCIMB 8052. *Microbiology* 159 (12):2558-2570.

Sandoval, Nicholas R, and Eleftherios T Papoutsakis. 2016. Engineering membrane and cell-wall programs for tolerance to toxic chemicals: Beyond solo genes. *Current opinion in microbiology* 33:56-66.

Schmid, RD., and C. Schmidt-Dannert. 2016. *Biotechnollogy. An ilustrated primer*: Wiley-VCH.

Schwartz, Robert D, and Frederick A Keller. 1982. Acetic acid production by Clostridium thermoaceticum in pH-controlled batch fermentations at acidic pH. *Applied and environmental microbiology* 43 (6):1385-1392.

Suo, Yukai, Sheng Luo, Yanan Zhang, Zhengping Liao, and Jufang Wang. 2017. Enhanced butyric acid tolerance and production by Class I heat shock protein-overproducing Clostridium tyrobutyricum ATCC 25755. *Journal of industrial microbiology & biotechnology* 44 (8):1145-1156.

Tan, Zaigao, Jong Moon Yoon, David R Nielsen, Jacqueline V Shanks, and Laura R Jarboe. 2016. Membrane engineering via trans unsaturated fatty acids production improves Escherichia coli robustness and production of biorenewables. *Metabolic engineering* 35:105-113.

Tao, Wenwen, Hongjun Dong, Yanping Zhang, Zhen Cai, and Yin Li. 2015. Introducing transglutaminase with its precursor region into Clostridium acetobutylicum improves its tolerance to oxidative stress and solvent production. *Process Biochemistry* 50 (1):111-118.

Tian, Bing, Ziqiang Guan, and Howard Goldfine. 2013. An ethanolamine-phosphate modified glycolipid in Clostridium acetobutylicum that responds to membrane stress. *Biochimica et Biophysica Acta (BBA)-Molecular and Cell Biology of Lipids* 1831 (6):1185-1190.

Timmons, Michael D, Barbara L Knutson, Sue E Nokes, Herbert J Strobel, and Bert C Lynn. 2009. Analysis of composition and structure of Clostridium thermocellum membranes from wild-type and ethanol-adapted strains. *Applied microbiology and biotechnology* 82 (5):929-939.

Tolonen, Andrew C, Trevor R Zuroff, Ramya Mohandass, Magali Boutard, Tristan Cerisy, and Wayne R Curtis. 2015. Physiology, genomics, and pathway engineering of an ethanol-tolerant strain of Clostridium phytofermentans. *Applied and environmental microbiology*:AEM. 00619-15.

Turner, William J, and Mary J Dunlop. 2014. Trade-offs in improving biofuel tolerance using combinations of efflux pumps. *ACS synthetic biology* 4 (10):1056-1063.

Van Der Westhuizen, Andre, David T Jones, and David R Woods. 1982. Autolytic activity and butanol tolerance of Clostridium acetobutylicum. *Applied and environmental microbiology* 44 (6):1277-1281.

Virunanon, Chompunuch, Sam Chantaroopamai, Jessada Denduangbaripant, and Warawut Chulalaksananukul. 2008. Solventogenic-cellulolytic clostridia from 4-step-screening process in agricultural waste and cow intestinal tract. *Anaerobe* 14 (2):109-117.

Wang, Chao, Fengxue Xin, Xiangping Kong, Jie Zhao, Weiliang Dong, Wenming Zhang, Jiangfeng Ma, Hao Wu, and Min Jiang. 2018. Enhanced isopropanol–butanol–ethanol mixture production through manipulation of intracellular NAD (P) H level in the recombinant Clostridium acetobutylicum XY16. *Biotechnology for biofuels* 11 (1):12.

Wang, Pixiang. 2018. Engineering Clostridium saccharoperbutylacetonicum for enhanced isopropanol-butanolethanol (IBE) production from lignocellulosic biomass through acetic acid pretreatment, Biosystems Engineering, Auburn University.

Wang, Qinghua, Keerthi Prasad Venkataramanan, Hongzhan Huang, Eleftherios T Papoutsakis, and Cathy H Wu. 2013. Transcription factors and genetic circuits orchestrating the complex, multilayered response of Clostridium acetobutylicum to butanol and butyrate stress. *BMC systems biology* 7 (1):120.

Wang, Shizeng, Xinxiao Sun, and Qipeng Yuan. 2018. Strategies for enhancing microbial tolerance to inhibitors for biofuel production: A review. *Bioresource technology* 258:302-309.

Wang, Yi, Zhong-Tian Zhang, Seung-Oh Seo, Patrick Lynn, Ting Lu, Yong-Su Jin, and Hans P Blaschek. 2016. Bacterial genome editing with CRISPR-Cas9: deletion, integration, single nucleotide modification, and desirable "clean" mutant selection in Clostridium beijerinckii as an example. *ACS synthetic biology* 5 (7):721-732.

Wang, Yi, Zhong-Tian Zhang, Seung-Oh Seo, Patrick Lynn, Ting Lu, Yong-Su Jin, and Hans P Blaschek. 2016. Gene transcription repression in Clostridium beijerinckii using CRISPR-dCas9. *Biotechnology and bioengineering* 113 (12):2739-2743.

Webster, Jocelyn R, Sharon J Reid, David T Jones, and David R Woods. 1981. Purification and characterization of an autolysin from Clostridium acetobutylicum. *Applied and environmental microbiology* 41 (2):371-374.

Wen, Zhiqiang, Rodrigo Ledesma-Amaro, Jianping Lin, Yu Jiang, and Sheng Yang. 2019. Improved n-butanol production from Clostridium cellulovorans by integrated metabolic and evolutionary engineering. *Appl. Environ. Microbiol.*:AEM. 02560-18.

Woolston, Benjamin M, David F Emerson, Devin H Currie, and Gregory Stephanopoulos. 2018. Rediverting carbon flux in Clostridium ljungdahlii using CRISPR interference (CRISPRi). *Metabolic engineering* 48:243-253.

Wu, Pengfei, Genyu Wang, Gehua Wang, Børre Tore Børresen, Hongjuan Liu, and Jianan Zhang. 2016. Butanol production under microaerobic conditions with a symbiotic system of Clostridium acetobutylicum and Bacillus cereus. *Microbial cell factories* 15 (1):8.

Wu, Qian, Liying Zhu, Qing Xu, He Huang, Ling Jiang, and Shang-Tian Yang. 2017. Tailoring the Oxidative Stress Tolerance of Clostridium tyrobutyricum CCTCC W428 by Introducing Trehalose Biosynthetic Capability. *Journal of agricultural and food chemistry* 65 (40):8892-8901.

Wu, You-Duo, Chuang Xue, Li-Jie Chen, Wen-Jie Yuan, and Feng-Wu Bai. 2016. Improvements of metabolites tolerance in Clostridium acetobutylicum by micronutrient zinc supplementation. *Biotechnology and bioprocess engineering* 21 (1):60-67.

Xu, Mengmeng, Jingbo Zhao, Le Yu, I-Ching Tang, Chuang Xue, and Shang-Tian Yang. 2015. Engineering Clostridium acetobutylicum with a histidine kinase knockout for enhanced n-butanol tolerance and production. *Applied microbiology and biotechnology* 99 (2):1011-1022.

Xu, Tao, Yongchao Li, Zhou Shi, Christopher L Hemme, Yuan Li, Yonghua Zhu, Joy D Van Nostrand, Zhili He, and Jizhong Zhou. 2015. Efficient genome editing in Clostridium cellulolyticum via CRISPR-Cas9 nickase. *Appl. Environ. Microbiol.* 81 (13):4423-4431.

Yang, Liejian, Guanhui Bao, Yan Zhu, Hongjun Dong, Yanping Zhang, and Yin Li. 2013. Discovery of a novel gene involved in autolysis of Clostridium cells. *Protein & cell* 4 (6):467-474.

Yang, Shang-Tian, and Jingbo Zhao. 2013. Adaptive engineering of Clostridium for increased butanol production. Ohio State University.

Yang, Shihui, Richard J Giannone, Lezlee Dice, Zamin K Yang, Nancy L Engle, Timothy J Tschaplinski, Robert L Hettich, and Steven D Brown. 2012. Clostridium thermocellum

ATCC27405 transcriptomic, metabolomic and proteomic profiles after ethanol stress. *Bmc Genomics* 13 (1):336.

Yao, Dunfan, Sheng Dong, Pixiang Wang, Tianhu Chen, Jin Wang, Zheng-Bo Yue, and Yi Wang. 2017. Robustness of Clostridium saccharoperbutylacetonicum for acetone-butanol-ethanol production: Effects of lignocellulosic sugars and inhibitors. *Fuel* 208:549-557.

Yoshino, Sadazo, Seiya Ogata, and Shinsaku Hayashida. 1982. Some properties of autolysin of Clostridium saccharoperbutylacetonicum. *Agricultural and Biological Chemistry* 46 (5):1243-1248.

Youn, Sung Hun, Kyung Min Lee, Ki-Yeon Kim, Sun-Mi Lee, Han Min Woo, and Youngsoon Um. 2016. Effective isopropanol–butanol (IB) fermentation with high butanol content using a newly isolated Clostridium sp. A1424. *Biotechnology for biofuels* 9 (1):230.

Zhang, Jie, Wei Hong, Wenming Zong, Pixiang Wang, and Yi Wang. 2018. Markerless genome editing in Clostridium beijerinckii using the CRISPR-Cpf1 system. *Journal of biotechnology* 284:27-30.

Zhang, Jie, Wenming Zong, Wei Hong, Zhong-Tian Zhang, and Yi Wang. 2018. Exploiting endogenous CRISPR-Cas system for multiplex genome editing in Clostridium tyrobutyricum and engineer the strain for high-level butanol production. *Metabolic engineering* 47:49-59.

Zhang, Lei, Xiaoqun Nie, Dmitry A Ravcheev, Dmitry A Rodionov, Jia Sheng, Yang Gu, Sheng Yang, Weihong Jiang, and Chen Yang. 2014. Redox-responsive repressor Rex modulates alcohol production and oxidative stress tolerance in Clostridium acetobutylicum. *Journal of bacteriology*:JB. 02037-14.

Zhang, Yan. 2013. Detoxification of Lignocellulose-derived Microbial Inhibitory Compounds by Clostridium beijerinckii NCIMB 8052 during Acetone-Butanol-Ethanol Fermentation, Animal Sciences, The Ohio State University.

Zhou, Wencan, Jingyun Liu, Senqing Fan, Zeyi Xiao, Boya Qiu, Yuyang Wang, Jianfeng Li, and Yicai Liu. 2018. Biofilm immobilization of Clostridium acetobutylicum on particulate carriers for acetone-butanol-ethanol (ABE) production. *Bioresource Technology Reports* 3:211-217.

Zhu, Linjiang, Hongjun Dong, Yanping Zhang, and Yin Li. 2011. Engineering the robustness of Clostridium acetobutylicum by introducing glutathione biosynthetic capability. *Metabolic engineering* 13 (4):426-434.

Zhu, Ying, and Shang-Tian Yang. 2003. Adaptation of Clostridiumtyrobutyricum for Enhanced Tolerance to Butyric Acid in a Fibrous-Bed Bioreactor. *Biotechnology progress* 19 (2):365-372.

Zhuang, Wei, Xiaojing Liu, Jing Yang, Jinglan Wu, Jingwei Zhou, Yong Chen, Dong Liu, and Hanjie Ying. 2017. Immobilization of Clostridium acetobutylicum onto natural textiles and its fermentation properties. *Microbial biotechnology* 10 (2):502-512.

Zhuang, Wei, Jing Yang, Jinglan Wu, Dong Liu, Jingwei Zhou, Yong Chen, and Hanjie Ying. 2016. Extracellular polymer substances and the heterogeneity of Clostridium acetobutylicum biofilm induced tolerance to acetic acid and butanol. *RSC Advances* 6 (40):33695-33704.

Żwirowski, Szymon, Agnieszka Kłosowska, Igor Obuchowski, Nadinath B Nillegoda, Artur Piróg, Szymon Ziętkiewicz, Bernd Bukau, Axel Mogk, and Krzysztof Liberek. 2017. Hsp70 displaces small heat shock proteins from aggregates to initiate protein refolding. *The EMBO journal* 36 (6):783-796.

Chapter II. Literature Review.

In situ biobutanol recovery from clostridial fermentations: a critical review

This manuscript has been published in: *Critical Reviews in Biotechnology* 38(3):1-14 (2017). doi: 10.1080/07388551.2017.1376308

Supplementary material can be found in appendix II.

Pablo Jiménez-Bonilla[a,b] & Yi Wang[a,c]

[a]Department of Biosystems Engineering, Auburn University, Auburn, AL, USA; [b]Laboratory of Natural Products and Biological Assays (LAPRONEB), Chemistry Department, National University (UNA), Heredia, Costa Rica; [c]Center for Bioenergy and Bioproducts, Auburn University, Auburn, AL, USA

Abstract

Butanol is a precursor of many industrial chemicals, and a fuel that is more energetic, safer and easier to handle than ethanol. Fermentative biobutanol can be produced using renewable carbon sources such as agro-industrial residues and lignocellulosic biomass. Solventogenic clostridia are known as the most preeminent biobutanol producers. However, until now, solvent production through the fermentative routes is still not economically competitive compared to the petrochemical approaches, because the butanol is toxic to their own producer bacteria, and thus, the production capability is limited by the butanol tolerance of producing cells. In order to relieve butanol toxicity to the cells and improve the butanol production, many recovery strategies (either *in situ* or downstream of the fermentation) have been attempted by many researchers and varied success has been achieved. In this article, we summarize in situ recovery techniques that have been

applied to butanol production through *Clostridium* fermentation, including liquid–liquid extraction, perstraction, reactive extraction, adsorption, pervaporation, vacuum fermentation, flash fermentation and gas stripping. We offer a prospective and an opinion about the past, present and the future of these techniques, such as the application of advanced membrane technology and use of recent extractants, including polymer solutions and ionic liquids, as well as the application of these techniques to assist the *in situ* synthesis of butanol derivatives.

Keywords: Solventogenic clostridia; butanol recovery; liquid–liquid extraction; perstraction; reactive extraction; adsorption; pervaporation; vacuum fermentation; flash fermentation; gas stripping

2.1 Introduction

Butanol (1-butanol or n-butanol; simply butanol hereafter) is an interesting industrial chemical that has recently attracted remarkable public attention. It can be used as a fuel source, fuel additive or a chemical feedstock. Butanol has about the same energy content as that of gasoline (one-third higher than ethanol) (Patakova et al. 2013; Xue, Zhao, Liu, Chen, et al. 2013) and is less corrosive and hazardous to handle. As a chemical feedstock, butanol has been used as a precursor for methacrylate esters, butyl acrylate, butyl glycol ether, butyl acetate, butyl butyrate, amino resins and n-butylamines (Zheng et al. 2015). Butanol and its derivatives can also be used for latex surface coatings, enamels and lacquers, flotation agents, cleaners and floor polishers, cosmetics, as a diluent for brake fluid production, as a solvent for hormone and vitamin synthesis, and a swelling agent for textile production (Patakova et al. 2013; Zheng et al. 2015).

Currently, industrial production of butanol named “oxo-process”, is mainly based on catalytic hydroformylation of fossil-obtained propylene to butyraldehyde followed by

hydrogenation (Villadsen et al. 2016). The oxo-process is economically competitive but not renewable. The intrinsic finite nature of petroleum, the geopolitical concerns and associated environmental problems have driven people to focus their eyes on the biological production of butanol from renewable resources.

The butanol fermentation (called acetone–butanol–ethanol (ABE) fermentation) has two metabolic phases: the acidogenesis corresponding to the exponential growth of cells when the cells produce acetic and butyric acids, and the solventogenesis phase when cellular growth becomes slower and the bacteria re-assimilate the acids produced and meanwhile produce acetone, butanol and ethanol. Butanol usually accounts for no less than 60% (w/w) in the total mixture of ABE in the fermentation. Fermentative butanol production is always limited by the solvent toxicity to the cells, and its usual titer does not exceed 20 g/L in a regular batch fermentation, and the productivity is hard to exceed 0.5 g/L-h (Ezeji, Qureshi, and Blaschek 2004).

The main mechanism by which Clostridia exerts its self-intoxication has generally been taken to be the chaotropic effect of butanol on the integrity of the cell's membrane. Various efforts, including conventional mutagenesis and metabolic engineering approaches, were reported for enhancing the butanol tolerance of various solventogenic strains, and indeed, acceptable successes have been achieved (Artış 2008; Dai et al. 2012; Liu et al. 2012). However, in spite of those improvements, the general butanol production of the regular fermentation process is still far from being economically competitive.

The downstream processing (separation and purification) for butanol fermentation is more complex and expensive than classic ethanol recovery from a yeast fermentation broth, due to three main reasons: (1) the butanol concentration in the broth is much lower (about 2% of butanol

compared to ~15% ethanol); (2) the boiling point of butanol/water azeotrope (93 ºC) and that of water (100 ºC) are very close (compared with 78.2 ºC for the ethanol/water azeotrope); and (3) the final distilled butanol concentration in the aqueous azeotrope is only 55.5% compared to 95.5% for the ethanol analog (Abdehagh, Tezel, and Thibault 2014; Dürre 2011; Huang, Ramaswamy, and Liu 2014). Therefore, efficient and inexpensive separation or recovery techniques are highly desirable for biobutanol production in order to enhance its economic efficiency.

To mitigate the butanol toxicity during fermentation, process engineering efforts including various recovery strategies have been employed. In this study, we summarized various in situ recovery techniques in the butanol fermentation process and meanwhile presented our own prospective with this discussion of the future direction in this area. The intent is to provide relevant references to the research community and meanwhile open discussions. These recovery techniques are experiencing evolution, involving the new tendency of green and clean production and using newly developed advanced chemicals and materials; those integrated with the fermentation process for simultaneous production and removal of solvents that can reduce cell poisoning, increase substrate utilization and improve fermentation productivity and solvent yield (Ezeji, Qureshi, and Blaschek 2004).

2.2 Extraction-based techniques

2.2.1 Liquid–liquid extraction

The *in situ* extraction of butanol is a strategy to reduce the concentration of the toxic butanol in the broth and therefore maintaining the cell culture alive and active longer (Huang, Ramaswamy, and Liu 2014). Liquid–liquid extraction is performed using a second layer of extractant with or without mixing (Figure 2.1(a)). The extractant is usually introduced into the process after the

acidogenesis phase, because if it is introduced in the earlier stage, it can potentially extract acetic and butyric acids and negatively influence the solventogenesis (Yen and Wang 2013). The extraction can be continuous or discontinuous. A pseudocontinuous extraction in a batch or fed-batch fermentation can be set up by pumping out the extractant, evaporating the butanol from the extractant and recycling the extractant back into the bioreactor. Such a system can yield a pseudosteady state, whereas the concentration of butanol in the broth remains constant and low, and it reduces the volume of the extractant used inside the bioreactor (Huang, Ramaswamy, and Liu 2014).

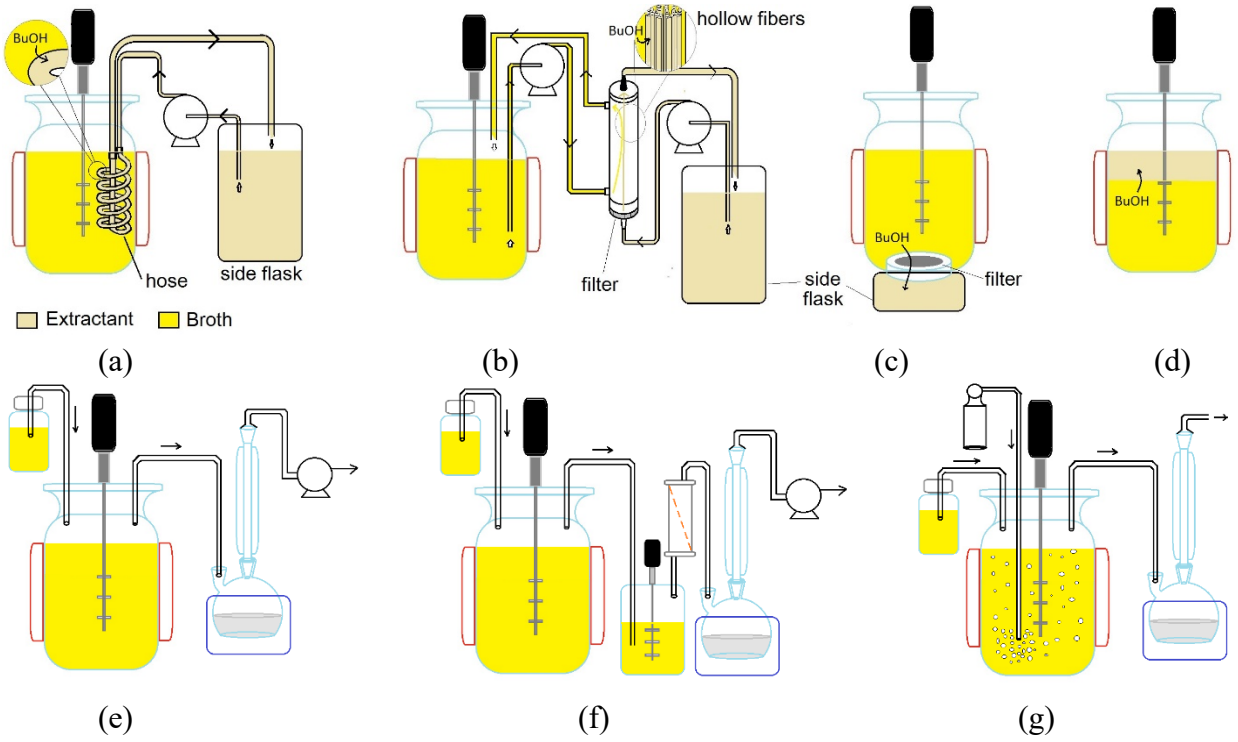

Figure 2.1 Schematic of various recovery systems (a) Regular solvent extraction through direct contact between the extractant and the broth; (b) "Tube"-type perstraction: extractant is pumped through the fermentation flask without direct contact with the broth; butanol migrates from the broth (in contact with the external of the hose) to the extractant (inside of the hose); (c) Fiber filter perstraction: broth is pumped through the shell and returned back to the bioreactor; the

extractant is driven inside of the hollow; (d) Membrane filter perstraction: a circular filter separates the compartment of the broth and the extractant; butanol exchange takes place through the filter; (e) vacuum evaporation; (f) flash fermentation; and (g) gas stripping.

The primary characteristics for the extractant to be used in liquid–liquid extraction includes: no or low inhibition to the cell culture growth, high selectivity, high distribution coefficient, no emulsion formation, high stability and low solubility in aqueous solution. Additional desirable characteristics include low/no harmfulness to the environment, density significantly different from the broth for easy phase separation, low viscosity for less energy consumption during extraction, autoclavability, suitable volatility and commercial availability at low cost (Huang, Ramaswamy, and Liu 2014).

For all these processes, the most extensively studied wild-type bacterial strain is *C. acetobutylicum* ATCC 824. Detailed attention has also been paid to: *C. beijerinckii* NCIMB 8052, *C. pasteurianum* DSM 525 and *C. saccharoperbutylacetonicum* N1–4. In addition, a variety of butanol-tolerant mutants have been developed through traditional evolutionary engineering or metabolic engineering approaches (Baer, Blaschek, and Smith 1987; Tomas, Welker, and Papoutsakis 2003; Xue et al. 2012).

Table 2.1 and supplementary Tables S1, S2 contains a summary of various chemicals tested as butanol extractants in ABE fermentation systems reported in the literature. Partition coefficient (K_D) and selectivity (S) are used to determine the suitability of an extractant for butanol extraction. K_D for butanol ($K_{D\text{-}BuOH}$ hereafter) is the molar ratio between the organic (b) and aqueous phases (a) (Equation (2.1a)). S is defined as the $K_{D\text{-}BuOH}$ over the $K_{D\text{-}H2O}$ (K_D of water) (Equation (2.1b)).

$$K_{D\text{-}BuOH} = \frac{n^{\beta}_{BuOH}}{n^{\alpha}_{BuOH}} \quad (a) \qquad S = \frac{n^{\beta}_{BuOH}/n^{\beta}_{H_2O}}{n^{\alpha}_{BuOH}/n^{\alpha}_{H_2O}} \quad (b) \qquad \text{(Eq. 2.1)}$$

Both values are dependent on temperature. A summary of $K_{D\text{-}BuOH}$ and selectivities of different extractants for liquid–liquid extraction of butanol is shown in Tables 2.1 and S2. 35–37 ºC is the typical temperature used during *Clostridium* fermentations, and thus, the values reported here are mostly for that temperature range.

Table 2.1 The butanol partition coefficient and selectivity of selected extractants during liquid-liquid extraction with ABE fermentation broth or model solutions.

Extractant	Fermentative strain	Toxicity	K_D	Selectivity	T (ºC)	Reference
1-octanol	*C. beijerinckii* LMD27.6	T	10	130	37	(Groot et al. 1990)
2-ethyl-1-hexanol	*C. acetobutylicum* ATCC 824	NT	7.95	311.1	36	(Gonzalez-Penas et al. 2014)
1-decanol	*C. acetobutylicum* ATCC 4259	T	6.2	ND	34	(Evans and Wang 1988)
	C. beijerinckii LMD27.6	T	8	200	37	(Groot et al. 1990)
2-Ethyl-1,3-hexanediol	*C. acetobutylicum* ATCC 824	T	8.1	ND	37	(Barton and Daugulis 1992)
3-Methyl-2,4-heptanediol	*C. acetobutylicum* ATCC 824	T	7.9	ND	37	(Barton and Daugulis 1992)
$[Dec_4N][1\text{-MeCHC}]$	Aqueous model	ND	8.49	130	25	(Garcia-Chavez et al. 2012)
$[Hex_4N][DHSS]$	*C.acetobutylicum* KCTC 1790, *C. beijerinckii* KCTC5579	T	7.99	ND	25	(Cascon et al. 2011)
$[MeOct_3N][Oct]$	Aqueous model	ND	11.29	49	25	(Garcia-Chavez et al. 2012)
$[MeOct_3N][Cl]$	*C. acetobutylicum* ATCC 824	ND	8.86	41.7	36	(Gonzalez-Penas et al. 2014)
$[Oct_4N][2\text{-MNaph}]$	Aqueous model	ND	21	274	25	(Garcia-Chavez et al. 2012)
$[Ph_3t][(^iC_8)_2PO_2]$	Aqueous model	ND	9.21	55	25	(Garcia-Chavez et al. 2012)
	Aqueous model	ND	19-59	80-305	25	(Rabari and Banerjee 2013)
$[Ph_3t][DCN]$	*C.acetobutylicum* KCTC 1790, *C. beijerinckii* KCTC5579	T	7.49	ND	25	(Cascon et al. 2011)
$[Ph_3t][Cl]$	*C. acetobutylicum* ATCC 824	ND	11.55	83	36	(Gonzalez-Penas et al. 2014)

Abbreviations: Ionic liquid cations: $[Dec_4N]$: tetra(decyl)ammonium, $[Hex_4N]$: Tetrahexylammonium, $[Ph_3t]$: Trihexyl(tetradecyl)phosphonium, $[MeOct_3N]$: Methyltrioctylammonium, $[Oct_4N]$: tetraoctylammonium, Ionic liquid anions: $[(^iC_8)_2PO_2]$: bis-2,4,4-(trimethylpentyl) phosphinate, [Cl]: Chloride, [DCN]: dicyanamide, [DHSS]: dihexylsulfosuccinate, [2-MNaph]: 2-methyl-1-naphthoate, [1-MeCHC]: 1-methylcyclohexecarboxylate, [Oct]: octoate. Symbology: T (Toxic), NT (Non-Toxic), ND (No data, non-reported). A extractant is considered toxic or inhibitory when its presence reduces the cell growth response (OD_{600}; or sugar consumption, or gas generation) in more than 10% comparing to the control.

Oleyl alcohol is the model extractant in butanol and ABE *in situ* extraction. It is nontoxic and has a relatively good $K_{D\text{-}BuOH}$ (3–4) and good selectivity (200–300), although it is nonvolatile (Cascon et al. 2011; Gonzalez-Penas et al. 2014).

Alkanes are just slightly toxic and highly selective, but their $K_{D\text{-}BuOH}$ is generally low. The more lipophilic the extractant, the lower the extractant concentration in the aqueous phase. It results in a low interaction of the extractant with cell membrane, low dispersion in growth media, low toxicity, low water uptake but also low butanol extraction capability (Gonzalez-Penas et al. 2014). Aromatic hydrocarbons demonstrate a better $K_{D\text{-}BuOH}$, especially at high temperatures, but most of them are toxic to cells (Kraemer et al. 2010).

Various natural oils and triglycerides have been tested as extractants for butanol fermentation. They are expected to be innocuous against bacterial cultures, but some of them show inhibitory effects. Also, some oils can be consumed by bacteria as a carbon source (Gonzalez-Penas et al. 2014). Ethanol and butanol can be extracted by triglycerides and perform an in situ transesterification reaction in order to produce biodiesel (Zhang et al. 2014). Silicon oil is not metabolizable and has good selectivity, but its $K_{D\text{-}BuOH}$ is low (Gonzalez-Penas et al. 2014).

Esters show a wide scale of values of $K_{D\text{-}BuOH}$ and selectivity. Short chain monoesters are poorly selective but their $K_{D\text{-}BuOH}$ are high. Di- and tri-esters show a very high $K_{D\text{-}BuOH}$, high selectivity and high boiling points (Barton and Daugulis 1992). However, the less lipophilic extractant, the more toxic it is to bacterial cells. Short-chain alcohols show high $K_{D\text{-}BuOH}$ due to their structural similarity to butanol but also exhibit the same toxicity mechanism. Branched medium-chain alcohols are less toxic than their linear analogs but are expensive for industrial extraction purposes.

The toxicity of alcohols as extractants decreases with the increase in alkyl chains size as well as $K_{D\text{-}BuOH}$ (Kim, Iannotti, and Bajpai 1999). Some fatty acids are reported as extractants with acceptable their KD-BuOH. When mixed with oleic alcohol, fatty acids increase $K_{D\text{-}BuOH}$ (Zhang et al. 2017); however, they show undesirable tensioactive behavior.

Polyethylene glycol (PEG) is partially soluble in water and can be used to promote the formation of two aqueous phases, whereas butanol is extracted into the PEG rich phase. The $K_{D\text{-}BuOH}$ of PEG was reported as 3–4.8, decreasing with an increase in molecular weight above 1200 Da. The laborious water removal from the PEG-rich phase and the high polymer price are both disadvantages (Kim, Iannotti, and Bajpai 1999; Wu et al. 2015). However, the study of new polymer solutions opens an area to explore for extracting reagents. In future, smart extractants could be developed by functionalizing polymeric solutions with, for example, supramolecular

hosts or a reversible system of chain extenders that permits modification of the affinity against butanol when they are under a controllable characteristic such as pH, temperature, stress or others.

Recent publications tested the performance of water-insoluble ionic liquid (IL) as an extractant for

butanol extraction. Quaternary ammonium compounds (Figure S1) such as $[Dec_4N][1\text{-}MeCHC]$, $[Hex_4N][DHSS]$, $[MeOct_3N][Oct]$ and $[MeOct_3N]Cl$, and trihexyl(tetradecyl) phosphonium compounds such as $[Ph_3t][(^iC_8)_2PO_2]$, $[Ph_3t][DCN]$ and $[Ph_3t][Cl]$ showed $K_{D\text{-}BuOH}$ values considerably higher than previously reported (7.99–21 and 7.49–59, respectively) and meanwhile

demonstrated high selectivity. In both groups, the conjugation with the anion bis(trifluoromethylsulfonyl) imide is disadvantageous. In spite of the high butanol recovery capacity, several IL are toxic or inhibitory (Cascon et al. 2011; Ha, Mai, and Koo 2010).

Due to the ionic nature, the $K_{D\text{-}BuOH}$ of IL increases with their lipophilicity, which is an opposite trend toother solvents. This means that the more capable the IL is for butanol extraction it is less toxic. The 1-alkyl-3-butylimidazolium-based IL increase $K_{D\text{-}BuOH}$ with the size of the side chain, that is [Bmim]<[Hmim]<[Omim]<[Dmim]. The general order of the $K_{D\text{-}BuOH}$ values of various cations is: imidazole-based<quaternary ammonium-based<tetralkyl phosphonium-based. For the IL in the last two groups discussed above, the $K_{D\text{-}BuOH}$ increases with alkyl chain size in a similar manner.

In general, the highest $K_{D\text{-}BuOH}$ has been reported for organic carboxylates, phosphates or sulfonates anions due to their lipophilicity. There are no reports so far to use IL for in situ butanol extraction. Researchers have reported such studies with ABE model solutions or downstream extraction (Gao, Orr, and Rehmann 2016; Kubiczek and Kamiński 2013). This is a relatively new research area.

2.2.2 Perstraction

In the extraction assisted with membranes, termed as perstraction, a semipermeable membrane (which the extractant cannot go across while butanol can) is used. This approach can avoid emulsions and toxicity problems. Extractants with excellent properties (high $K_{D\text{-}BuOH}$ and selectivity) but are very toxic to bacteria, cannot be applied in a regular extractive fermentation. They can be used in membrane-assisted processes instead, since they are not in direct contact with fermentation broth. The main disadvantage for perstraction, however, is that the membrane builds

an additional barrier which results in slower diffusion (Huang, Ramaswamy, and Liu 2014; Abdehagh, Tezel, and Thibault 2014).

Table 2.2 Summary of performance of perstraction for butanol recovery in various batch fermentations for butanol production.

Membrane			**Strain**[a]	**Solvent**	**Productivity**					**References**
M	*t*	*A*			*Butanol*		*ABE*		*Increase*	
	mm	m^2			*g/Lh*	g/Lhm^2	*g/Lh*	g/Lhm^2	*Δ(g/Lh)*	
PTFE	0.075	0.00502	*C. saccharoperbutylaceticum* N1-4	nC_{12}-OH	0.394	78.6	ND	ND	ND	(Tanaka et al. 2012)
PTFE	0.075	0.00502	*C. saccharoperbutylaceticum* N1-4	OA	0.32	63.7	ND	ND	ND	(Tanaka et al. 2012)
PDMS	0.8	0.227	*C. acetycobutylicum* ATCC 824	OA	0.705	3.07	1.02	4.49	0.54[a]	(Jeon and Lee 1987)
PDMS	0.8	0.227	*C. acetycobutylicum* ATCC 824	PPG	0.538	2.34	0.81	3.57	0.33[a]	(Jeon and Lee 1987)
PDMS	0.8	0.227	*C. acetycobutylicum* ATCC 824	TBA	0.407	1.77	0.68	3.00	0.2[a]	(Jeon and Lee 1987)
PDMS	0.4	0.215	*C. acetycobutylicum* P262	OA	0.16	0.74	0.24	1.12	ND	(Groot et al. 1990)
PDMS	ND	0.113	*C. acetycobutylicum* P262	OA	0.1	0.88	0.21	1.86	0.07[b]	(Qureshi and Maddox 2005)
PDMS	0.8	0.0714	*C. acetycobutylicum* ATCC 824	OA	ND	ND	2.27	31.79	1.19[a]	(Jeon 1989)
PP fibers	ND	0.1	*C. acetycobutylicum* DSM 1731	OA+ dec (50/50)	ND	ND	1.02	10.20	0.39[a]	(Grobben et al. 1993)

Abbreviations: M: material, t: thickness, A: area, PDMS: silicone (Poly(dimethylsiloxane)), PP: polypropylene, PTFE: polytetrafluoroethylene, ABE: acetone-butanol-ethanol, nC12-OH: 1-dodecanol, OA: oleyl alcohol, ND: no data, dec: decane

[a] Productivity increment compared with non-extractive fermentation under same conditions.

[b] Productivity increment compared with *in situ* liquid-liquid extraction under same conditions.

Perstraction becomes especially important in continuous extraction, either in batch or in continuous fermentation processes. The primary benefit is the increase in fermentation productivity over time. Table 2.2 summarizes the performance of perstraction for fermentative butanol recovery with the membranes of various materials as reported in the literature. Traditional butanol fermentation experiments have been conducted with silicone membranes, also named as poly(dimethylsiloxane) (PDMS) (Jeon 1989). The system uses a peristaltic

pump to drive the broth through a hose or tube immersed in the extracting solvent as shown in Figure 2.1(b). In Jeon and Lee's study (Jeon 1989), this system generated an increase in total ABE productivity rate by 0.2–1.19 g/L-h compared with a regular batch fermentation and by 0.07 g/L-h compared with the batch fermentation with direct solvent extraction. Although these values do not represent significant improvement, the length of time that the fermentation can be maintained as active was increased up to 481% of the nonextractive fermentation (Jeon and Lee 1987) and 143% of the fermentation with regular liquid–liquid extraction (Qureshi and Maddox 2005). This means that the final total amount of butanol or ABE generated from this fermentation has been significantly improved, which is very significant because this would dramatically save the time and efforts that are required for medium preparation, inoculation and

reactor setup. The efficiency of silicon hose per unit area is lower compared to other materials such as poly(tetrafluoroethylene) (PTFE).

Polypropylene (PP) fibers with 0.2 mm pores have also been used in a hollow fiber membrane module for butanol recovery as shown in Figure 2.1(c). This system is able to provide a large contact area in a relatively simple apparatus (Grobben et al. 1993). It is composed of several porous PP hoses with a small diameter (just a few millimeters) in a plastic shell, whereas the broth is driven through the shell side and the extractant is inside the fibers.

Filters of PTFE with a pore size of 1 mm are relatively highly selective, and butanol recovery per unit area is very efficient (Tanaka et al. 2012). Such a perstraction system (as shown in Figure 2.1(d), with a PTFE filter disc dividing the flasks of the extractant and the broth) has been tested at temperatures from 303 to 315 K in the solvent container. The extraction capacity increased with temperature. For example, the butanol flux permeate was 0.034 kg/h-m^2 at 28 ºC, 0.039–0.042

kg/h-m^2 at 35 ºC and 0.049 kg/h-m^2 at 42 ºC, when the initial concentration of butanol in the model solution was 12.4 kg/m^3 (Núñez-Gómez et al. 2014). Disadvantages include the complicated and laborious setting up and operation, the requirement for specific equipment, the possibility of clogging and cell or biofilm absorption.

2.2.3 Reactive extraction

Butanol is a short-chain alcohol and its distribution coefficient in organic solvents is not as high as desired. But as we mentioned above, some butanol derivatives are very valuable chemicals. Reactive extraction is a chemical reaction occurring at the same time as the extraction. Since some important derivatives are more lipophilic than butanol itself, especially long-chain esters, the reactive extraction can alter the partition equilibrium and thus reduce the butanol concentration in the broth. Supplementary Figure S3 shows some industrially important derivatives that can be obtained from butanol.

Reactive extraction is not easy to perform since most chemicals used to react with butanol are toxic to the cell culture. Additionally, many reactions need to be performed at temperatures higher than the optimal for fermentation. Therefore, there are not many reports in the literature concerning the reactive extraction within butanol fermentation. Nonetheless, two kinds of such processes are feasible, using either biocatalytic enzymes or chemical heterogeneous catalysts (e.g. active sites in the surface of a silicate particle).

Reactive esterification extractions are well studied in lactic acid and many other fermentations (Wasewar 2012). Esterification reactions along with extraction were also reported in *Clostridium* fermentations, using biocatalysts in the organic phase (van den Berg et al. 2013). Lipase catalyzed butyl butyrate production is an easy-to-achieve in situ derivatization because the

same ABE fermentation can produce both butyric acid and butanol. Ethyl butyrate can be synthesized as coproduct of butyl butyrate, but the yield is very low because ethanol production is usually low in ABE fermentation and ethanol is poorly soluble in the organic phase. Most common extractants for this application are long-chain inert hydrocarbons. Fatty acid butyl esters (applicable as biodiesel) with acyl chain length between 12–20 carbons can also be produced by biocatalysis, from in situ butanol extraction with vegetable oils in the presence of a lipase (van den Berg et al. 2013). All of these esters are poorly soluble in the broth and thus favorable for the reaction in the extractant (Figure S2) (van den Berg et al. 2013). Oleyl alcohol, long-chain secondary alcohols, esters and long-chain hydrocarbons can be used as extractants for reactive extraction, but some secondary products would be expected.

A combination of chemical reaction with fermentation is a promising area to study in future to increase productivity and the economic viability of a bioprocess. Derivatives might be less soluble and less toxic, keeping the fermentation actively running for a longer time. Heterogeneous chemical catalysis, such as a metallic redox system, could be used to synthesize in situ chemical derivatives of butanol without introducing harmful chemicals to the broth. On the other hand, biocatalysts have increasing importance in the industry. Lipases, nitrilases, amidases, lyases, acylases, hydroxylases and many other enzymes are essential to various industrial processes (Schmid et al. 2001; Choi, Han, and Kim 2015). The discovery, isolation and immobilization of new stable enzymes will facilitate the attempt of chemical reactive extraction during butanol fermentation.

Additionally, the attempt of in situ recovery of butanol or ABE, followed by a chemical catalysis process to convert the solvent to long-chain hydrocarbons, has achieved great success. In one study, the ABE mixture was recovered through in situ extraction with glyceryl tributyrate and

was then efficiently converted into ketones by a palladium-catalyzed alkylation (Anbarasan et al. 2012). In a recent report, hydrolysates generated from corn stover was fermented with C. beijerinckii CC101, followed by recovery using gas stripping and pervaporation, and the ABE mixture was then used to synthesize 5–15 carbon ketones as a substitute for jet fuel (Xue et al. 2017). High conversion efficiency and stable conversion rates were demonstrated in such a process.

2.3 Adsorption-based techniques

There are different models explaining adsorption phenomena, depending on the nature of the material, types of interaction with adsorbates, pore size, surface area, concentration of adsorbates and the presence of other adsorbates. During ABE fermentation, the concentration of the substrate, organic acids, acetone, ethanol and butanol are all changing during the process, and any of these substances can be adsorbed. Therefore, from the literature, researchers used different models to study the adsorption of butanol. Here, a critical comparison among them is attempted. When the adsorbate concentration is well below saturation, some adsorbents behave close to linearity while others do not. Some researchers determined a partition coefficient as an approximation (assuming linear behavior) for preliminary screening of the best adsorbents. Adsorption at saturation is another approach used for the same purpose. Supplementary Table S3 summarizes various adsorbents reported for biobutanol recovery for some of which the solid/liquid partition coefficients ($K_{s/w}$) and the saturation loading capacity for butanol (L_{BuOH}) have been determined. By comparing L_{BuOH} in mg of butanol per gram of adsorbent from various literatures (Huang, Ramaswamy, and Liu 2014; Abdehagh, Tezel, and Thibault 2014), we define it as 0< “very low” <25≤ “low” <50≤ “medium” <75≤ “high” <150≤ “very high”.

Activated carbon is the most employed adsorbent. L_{BuOH} of active carbon has been reported as 68–300 mg/g (commonly very high values) in a single or binary component. L_{BuOH} decreases dramatically when the solution composition becomes complicated for some forms of carbon such as Witco 517 or Nuchar WV-G (Giusti, Conway, and Lawson 1974). The second group of adsorbents is composed of silicates and aluminosilicates. Silicalite is an aluminum-free zeolite analog with the same crystal structure of the zeolite ZSM-5. Silicalite is a selective adsorbent, and L_{BuOH} is reported to be 64–100 mg/g even in complex media. The selectivity of silicalite for alcohols increases with an alkyl chain from 1 to 5 carbons (Qureshi, Meagher, and Hutkins 1999). Polymer resins with micro or macropores are used as synthetic adsorbents. Aromatic resins are common because aromatic groups have a large surface area for nonpolar interactions. Polystyrene, crosslinked with divinylbenzene P(S-co-DVB), is the most common polymer-based adsorbent. Commercial resins of P(S-co-DVB) are manufactured by Dowex, Donopore, Amberlite (Fluka), Diaion, Hytrel and Reillex are reported with L_{BuOH} from low to high (1.7–97.5 mg/g), though some of them are already discontinued. These resins are relatively highly selective, because they are nonpolar, and the interactions with cells, glucose and small alcohols are minor. Crosslinked polystyrene resins can be also functionalized with side groups to increase their polarity. Optipore SD-2 and M43 are functionalized with a tertiary amine, and Diaion HP-20 with a sulfonic acid (Nielsen and Prather 2009). Functionalization can promote hydrogen bond interactions with butanol, increasing the affinity but reduce the affinity when functional groups significantly increase the polarity. KA-I resin is a complex adsorbent of the polystyrene framework, functionalized with ester groups developed by the National Engineering Technique Research Center for Biotechnology (Nanjing, China) (Lin et al. 2012). KA-I was well studied and it showed L_{BuOH} (84–93 mg/g) and good selectivity even in complex mixtures (Lin et al. 2012).

Polyvinylpyridine is another aromatic resin reported with an acceptable Ks/w (Yang, Tsai, and Tsao 1994). Mild polar resins have also been reported in literature (Saint Remi, Baron, and Denayer 2012; Yang, Tsai, and Tsao 1994; Nielsen and Prather 2009). Acrylate and methacrylate polymers and ester derivatives are used and have low-to-medium values of L_{BuOH}. Metal-organic framework (MOF) is a modern type of adsorbent with an ordered porous 3D structure composed by a metal interaction with an organic structure. ZIF-8 is a MOF containing zinc, it shows very high L_{BuOH} and selectivity for butanol recovery (Saint Remi, Baron, and Denayer 2012).

Generally, two models are widely used to study adsorption phenomena: Langmuir isotherm and Freundlich isotherm. The Langmuir model (Equation (2.3)) is applicable for samples approximating the following: solution behavior is ideal; just a monolayer is adsorbed; adsorption sites have the same affinity; adsorbed molecules are localized; there is no lateral interactions and adsorbed molecules are in dynamic equilibrium (Benson 2009). In addition, Langmuir model studies the enthalpy of adsorption and is the most extensively used adsorption model reported in the literature as shown in supplementary Table S4 for many adsorbents.

$$q=\frac{q_{max}BC_{eq}}{1+BC_{eq}} \quad (\text{Eq.2.3})$$

where q is the adsorption capacity, q_{max} is the maximum adsorption capacity, B is the Langmuir constant, C_{eq} is the solute concentration at equilibrium in liquid phase (Farzaneh et al. 2015). The physical meaning of q_{max} (for butanol hereafter) is an analog to L_{BuOH} when saturation is reached, and the Langmuir constant (B) is similar as $K_{s/w}$. B describes the affinity of the adsorbent and the adsorbate, or the relation between empty and occupied sorption spots. B and q_{max} can be obtained from the mathematic linearization of Langmuir model. B and q_{max} values mentioned hereafter correspond to butanol adsorption.

A recent study demonstrated very high qmax in active carbon Norit ROW 0.8 even in a complex solution (Xue, Liu, Xu, Tang, et al. 2016). The authors also demonstrated the applicability of this material in a real in situ fermentation process and achieved up to 54.6 g/L butanol (Xue, Liu, Xu, Tang, et al. 2016). The q_{max} of zeolites, silicalite and polystyrene adsorbents show the same trend as L_{BuOH} as discussed above. Silicalite, compared to regular zeolites, is more selective for butanol than water (Farzaneh et al. 2015). Polystyrene resins show Langmuir constant values between 0.2 and 0.4 for single components and some multicomponents solutions, and they remain at an acceptable value until the concentration of a second component is very high as shown in a binary model by Jiao et al. (Jiao et al. 2015). Zeolites show the highest affinities (B), behavior concordant with oxophilicity of aluminum, though a very high value can be counterproductive during the desorption stage.

The Freundlich isotherm empirical model usually fits the adsorption behavior better than Langmuir without complex calculations. The model is expressed in Equation (2.4).

$$q = K_f C_{eq}^{1/n} \qquad \text{(Eq.2.4)}$$

where K_f and n are Freundlich constants (values for butanol hereafter). The equation does not indicate a finite uptake capacity, and thus, it is functional in the low-to-medium concentration ranges (Volesky 2003). If n=1, the expression becomes linear since K_f=$K_{w/s}$. So, n is related to the deviation from this ideal behavior caused by the heterogeneity of the surface adsorption sites. When 1/n is close to zero, the surface is highly heterogeneous (Ali et al. 2013). Therefore, K_f is an improved $K_{w/s}$ and represents the quantity of adsorbate in the solid required to maintain at one unit for the concentration in the solution (i.e. mmol/L). Consequently, K_f is also related to the adsorption capacity (Ali et al. 2013). Researchers have used Freundlich models to describe the

butanol adsorption with various adsorbents (supplementary Table S5). According to analysis of Freundlich model, activated carbon showed the highest K_f, followed by other adsorbents, such as KA-I, and finally, the Optipore L493 and SD2. Diaion HP20, HP2MG and Hytrel 8206 demonstrated relatively low K_f (Nielsen, Amarasiriwardena, and Prather 2010).

Other adsorption models like Brunauer, Emmett and Teller (BET) isotherm, or Lagergren's equation for pseudoorders are also used and can usually fit better for the experimental data (Thompson et al. 2011). However, they are not widely used due to their complexity, and because the physical meaning of their constants is hard to represent. In one example, the BET model was employed when SiO_2 functionalization with calixarene was used as an adsorbent for butanol (Thompson et al. 2011), which demonstrated that butanol adsorption is dependent on the calixarene content on the supramolecular conjugate.

It needs to be pointed out that some adsorbents can be inhibitors for cell growth. For example, resins Diaion HP-20 and Dowex M43 demonstrated severe inhibition on cell growth in the clostridial fermentation, reducing butanol production by 87–99% (Nielsen and Prather 2009). Nontoxic adsorbents are preferable when they need to be in direct contact with the cell culture. Another approach to mitigate the adsorbent inhibition is to pump the culture through a cell filter followed by a cartridge with the adsorbent (Qureshi et al. 2005). This is usually a common procedure when adsorption is used for butanol recovery, and therefore, the toxicity of adsorbents to the fermentation culture is not often studied.

Desorption process is also very important for overall butanol recovery. A good adsorbent should have low affinity at high temperature. The heat required for desorption is highly decisive for the cost of the whole process. For example, zeolites CBV28014 and CBV901 require 275 J/g

and 355 J/g for the desorption of butanol, respectively (Oudshoorn, Van der Wielen, and Straathof 2012), while Norit Row 0.8 requires up to 14,127 J/g (Xue, Liu, Xu, Tang, et al. 2016). Competitive adsorption (e.g. pressurized CO_2), gas stripping, elution and other techniques can be considered as alternatives for desorption, but they are not necessarily less expensive (Oudshoorn, Van der Wielen, and Straathof 2012).

Future adsorption development is dependent on the discovery of new materials. Some of the MOFs are catalysts of chemical reactions with butanol and they exhibit high adsorption and selectivity for butanol as shown above. Therefore, this characteristic can be used to explore possible *in situ* or *ex situ* chemical transformation of the adsorbed butanol. Future intelligent adsorbents should have programmable adsorptivity: strong under fermentation conditions and weak during desorption. Such behavior could be achieved if the structure of the adsorption sites change when conditions are changed. They should also be easy to recover and reuse. Materials with supramolecular structures are one of the most feasible candidates as smart adsorbents.

2.4 Evaporation-based techniques

2.4.1 Pervaporation

Pervaporation is a separation process that combines permeation through a membrane and vacuum evaporation. This traditional technique is considered to be one of the most energetic and timely efficient approaches for butanol recovery, especially in the context of recent advances that the novel membranes can allow the permeation of high flux of butanol with high selectivity (Xue et al. 2015; Hu et al. 2017). Temperature, membrane thickness, vacuum pressure, the concentration and presence of other components are slightly related with the pervaporation performance. Drawbacks for this approach include the chance of membrane contamination and clogging, the

price of highly specific membranes and the accumulation of non-condensable gases on vacuum pumps (Lin et al. 2013; Heitmann et al. 2012). Therefore, we propose to critically discuss and compare the efficiency of pervaporation during real fermentation conditions.

Most studies, employing pervaporation for butanol recovery have been conducted using a silicon membrane (PDMS, polydimethylsiloxane), PDMS blend or PDMS derivative. Qureshi and Blaschek evaluated a PDMS perstraction membrane for ABE recovery in a batch fermentation with C. beijerinckii BA101 (Qureshi and Blaschek 2000). The total solvent productivity was increased from 0.35 g/L-h in a regular batch fermentation to 0.98 g/L-h in the pervaporation integrated fermentation, and a final solvent titer of 165.1 g/L was achieved. Kong *et al.* (Kong et al. 2016) achieved a solvent productivity of 0.98 g/L-h, with a butanol and ABE titers of 93.49 and 150.06 g/L, respectively, (which was 7.13 and 7.98 times, respectively, higher than in a regular batch fermentation) when they applied pervaporation coupled with a batch fermentation using the mutant BT14 of *C. beijerinckii NCIMB 8052*.

Some reinforcements or fillers can be used in PDMS matrix for increasing the efficiency of the membranes. Filler permeability is related with the parameters mentioned above such as $K_{w/s}$, L_{BuOH} and isotherms constants (Kong et al. 2016). Fillers with high L_{BuOH} improve butanol permeability and fillers with good selectivity increase the butanol concentration of the permeate. PDMS/zeolite composites show a lower total flux permeate yet higher butanol flux when zeolite concentration is increased from 0% to 80% (Wang et al. 2016; Xue et al. 2015). PDMS/ceramic composites were reported for in situ pervaporation during fermentation with *C. acetobutylicum* XY16 and showed a total flow of 661 g/m^2-h, a butanol flux of 3.5 g/m^2-h, and an increase in productivity from 0.20 g/L-h in the control fermentation to 0.410 g/L-h in the pervaporative

fermentation (Liu, Gan, et al. 2014). Model of PDMS/silicalite-1 showed a total flow of 1233 g/m^2-h, with a butanol flux of 611 g/m^2-h (Hu et al. 2017).

Polymeric blends containing PDMS and its composites were also tested for butanol recovery through pervaporation. Polyvinylidene fluoride inclusion (PDMS/PVDF) increases the permeation of butanol from 4.1–4.6 to 20.0 g/m^2-h and the total flux from 38.8–45.6 to 120 g/m^2-h (Xue, Du, et al. 2014). Composites of PDMS/PVDF containing metal complexes of Co and Fe increased the total flux up to 331 g/m^2-h in model solutions (Jee, Kim, and Lee 2016). Polyacrylonitrile blend (PDMS/PAN) achieved a flow of 557 g/m^2-h and generated a high butanol concentration of 122.4 g/L in the permeate solution (Li et al. 2014). When PDMS membranes were replaced by triblock copolymer of styrene-silicone-styrene (SDS) in a *C. acetobutylicum* fermentation, the butanol flow was increased from 110 to 220 g/m^2-h, and butanol selectivity from 14 to 21, due to the solvent passing through non-crosslinked joint between the rigid polystyrene and the crosslinked PDMS (Shin et al. 2015). A butanol flow of 12–27 g/m^2-h could be reached with polyimide-silicon (PDMS/PI) (Van Hecke et al. 2012), and a butanol flow of 4–12 g/m^2-h was reported with polyethylene, silicon and metal particle system (PDMS/PE/metal) used for the pervaporation (Li, Srivastava, and Parnas 2011).

Polypropylene hollow fibers are used for pervaporation membranes with low flux (7.1 g/m^2-h), and they are used on high surface area devices (Friedl, Qureshi, and Maddox 1991). Polyether-blockamide (PEBA) can be also used as a membrane, alone or combined with carbon nanotubes (CNT). PEBA/CNT has lower permeate flow than PEBA alone (147 g/m^{2}h and 167 g/m^{2}h, respectively) and higher butanol flux (0.58 and 0.45 g/m^{2}h, respectively). Other materials, such as the polymers of intrinsic microporosity PIM-1, PEBA/ceramic hollow fiber, stainless steel/silicalite, Hyflon AD/PVDF (poly(2,2,4-trifluoro-5-trifluoromethoxy-1,3-dioxole-co-

tetrafloroethylene)/poly(vinylidene fluoride)), poly(octhylmethyl siloxane) (POMS), poly(1-trimethylsilyl-1-propyne) (PTMSP), PDMS/silicalite, have also been used for pervaporation membranes for butanol recovery (Žák et al. 2015; Li et al. 2016; Lin et al. 2015; Jalal et al. 2015; Qureshi et al. 2001; Rom A. 2013).

Membranes swelled in a water-insoluble liquid and coated, can be used to improve pervaporation selectivity (Mai et al. 2013). Similar as extraction, liquids with high L_{BuOH} and selectivity are good candidates for these "liquid membranes". A liquid membrane composed of oleyl alcohol with polypropylene support produced 3.3 g/m^2-h of butanol flux and a total permeate flux of 14.3 g/m^2-h (Mai et al. 2013). A preliminary screening of IL immobilized in Nylon/PDMS showed the best results for [Dmim][B(CN)$_4$]>[Ph$_3$t][B(CN)$_4$]>[Dmim][FAP], and the total flux for [Dmim][B(CN)$_4$] was up to 550 g/m^2-h (Heitmann et al. 2012). PDMS/[Omim][Tf$_2$N] produced a butanol flux of 6.2 g/m^2-h compared with 1.75 g/m^2-h with PDMS alone (Mai et al. 2013), and PDMS/[Pr$_4$N][B(CN)$_4$] generated a butanol flux of up to 15 g/m^2-h (Izák et al. 2008). B(CN)$_4$ anion shows the best performance which are demonstrated when membranes are very thin and there were no significant differences among various IL under those conditions (Izák et al. 2008).

2.4.2 Vacuum and flash fermentation

Vacuum fermentation (Figure 2.1(e)) and flash fermentation (Figure 2.1(f)) are well known methods, which are especially suitable for continuous fermentation. Butanol and other products are removed from a bioreactor under vacuum at normal temperatures during vacuum fermentation. The flash fermentation is carried out using a bioreactor at normal pressure, while the broth is driven through a vacuum chamber, where distillation occurs (Abdehagh N 2012). Broth is filtered in front of the vacuum chamber in order to retain the cells in the reaction vessel.

Vacuum fermentation for butanol production using *C. beijerinckii* NCIMB 8052 or *C. beijerinckii* P260 has been reported (Mariano, Qureshi, et al. 2011). Butanol and water generate an azeotrope mixture, with a boiling point of 92.4 ºC. Vacuum distillation of butanol generated a more concentrated product. Fermentations were conducted under a vacuum of 711–737mm Hg at 35 ºC, starting with a constant or a cyclic vacuum 18 h after fermentation. The total production in a 7-L batch reactor was increased from 80.6 to 106.0 g of butanol and from 110.1 to 132.4 g of total ABE, respectively. When continuous vacuum is used, the production rose to 120.1 g of butanol and 141.2 g of total ABE for cyclic vacuum (Mariano, Qureshi, et al. 2011; Mariano, Maciel Filho, and Ezeji 2012; Mariano et al. 2012).

Optimization of flash vacuum parameters was conducted for continuous fermentation and distillation purification of butanol. Computer simulations assisted the increase in butanol productivity from 4.51 to 7.70 g/L h in a flash vacuum fermentation (Mariano et al. 2010). Flash fermentation could permit a feed of substrate up to 100–300 g/L (sugars or others). The disadvantage was the decrease in sugar conversion efficiency from 98.5% to 92.9% (Mariano et al. 2012; Mariano, Keshtkar, et al. 2011).

2.4.3 Gas stripping

Gas stripping is a simple, inexpensive and nontoxic recovery process. Gas stripping is conducted by bubbling a gas (or gas mixture) into the fermentation broth to promote the evaporation of volatile compounds in the gas stream (Figure 2.1(g)). Gas stripping can be carried out in the bioreactor or in a side chamber. Then, the evaporated stream is condensed in a cold trap and/or a condenser (heat exchanger). A low-cost inert gas like nitrogen (N_2) or the gas(s) (CO_2 and H_2) generated from the ABE fermentation process is typically used. Gas stripping allows the usage

of high concentration of substrate stock, reducing the volume needed for fermentation (Ezeji, Qureshi, and Blaschek 2003; Merlet et al. 2017). Total butanol production was increased from 11.9 g/L in the control to 16.4–46.4 g/L (Ezeji, Qureshi, and Blaschek 2003) and from 16.2 g/L to 19.8 g/L (Xue, Zhao, Liu, Lu, et al. 2013) with gas stripping coupled with batch or fed-batch fermentations. High butanol titer was also demonstrated by Xue, *et al.*(Xue et al. 2012), using intermittent stripping cycles in a fed-batch reactor. In their fermentation, 113.3 g/L butanol was obtained from 474.9 g/L glucose within 326 h.

2.5 Comparison of performance and energy requirement

Butanol has an energy content of 36.2 MJ/kg, and the direct distillation from 2% in broth consumes about the same energy. Lowest values for energy consumption during recovery were reported for pervaporation and adsorption, but the range of energy consumption for these techniques is wide as shown in Figure 2.2(b) (Xue, Zhao, Liu, Chen, et al. 2013; Qureshi et al. 2005). The energy consumption in gas stripping, pervaporation and vacuum flash is significantly associated with the energy used and the condensate purified product. A very low temperature in the condenser can reduce the loss of butanol but increase the cost (Xue, Zhao, et al. 2014). In vacuum-based techniques, intermittent vacuum fermentation was energetic superior to the continuous one because distillation occurs when butanol is more concentrated and the low butanol concentration after each vacuum cycle keeps the bacteria culture at an active growth phase for longer (Mariano, Maciel Filho, and Ezeji 2012). The energetic consumption in adsorption is highly linked to the desorption process as well.

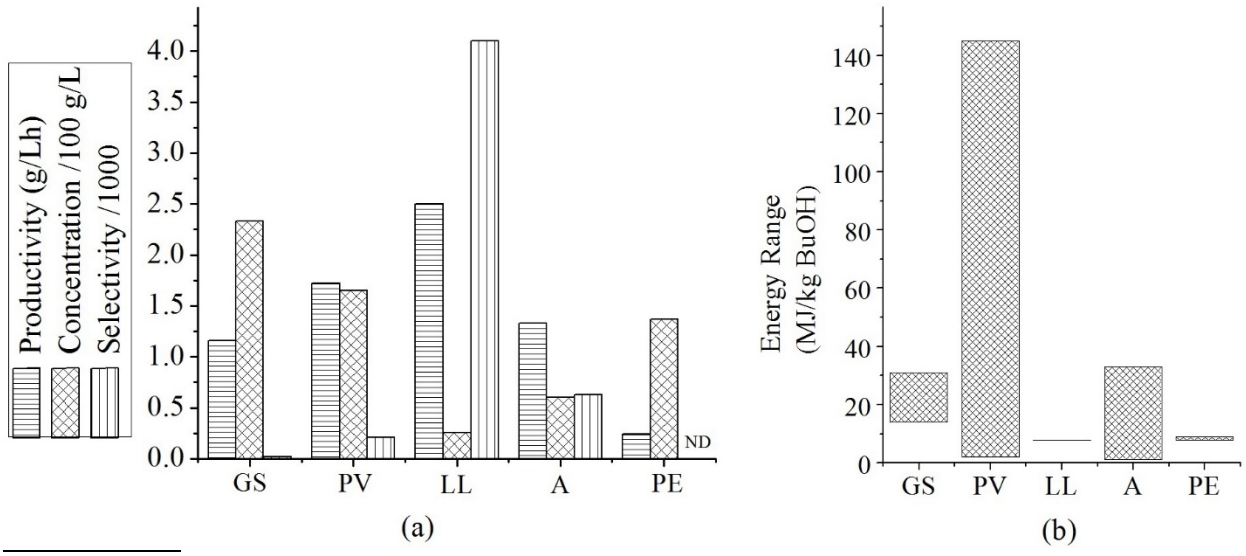

Figure 2.2 Comparison of several primary recovery techniques. (a) highest productivity, concentration and selectivity (PE selectivity not reported) (b) estimated energy consumption range. GS: Gas stripping, PV: Pervaporation, LL: liquid-liquid extraction with oleyl alcohol, A: adsorption, PE: perstraction. ND: No data.

Figure 2.2(a) illustrates the comparative best performance and energy consumption for various butanol recovery techniques. Gas stripping, pervaporation and perstraction can generate higher titers. Pervaporation and adsorption consume the lowest or highest amount of energy, depending on the conditions. The overall costs of the adsorption and extraction processes are also highly dependent on the prices of the used adsorbents and extractants. Gas stripping is particularly interesting when it is used combined with other techniques because of its simplicity. It has been reported that a double gas stripping system required less than 5 MJ/kg of energy to generate about 500 g/L butanol in anintegrated ABE fermentation process (Xue, Zhao, Liu, Lu, et al. 2013). A combination of some of the recovery techniques can make the process more efficient and cost effective. For example, high butanol concentrations from 400 to 550 g/L have been obtained with hybrid gas stripping/pervaporation (Xue, Liu, Xu, Zhao, et al. 2016), double gas stripping (Xue, Zhao, Liu, Lu, et al. 2013) and double pervaporation (Cai et al. 2017) in a single integrated process.

In addition, fermentation with *in situ* extraction and distillation has also been reported (Jin et al. 2017).

2.6 Conclusions and prospects

Intrinsic advantages of butanol as a fuel or fuel additive are extensively noticed, but butanol production through the biological fermentation route is still not economically viable. The simple rule is that the produced butanol should possess more energy than that required to produce and purify itself. A regular distillation process from a dilute solution of butanol requires about the same amount of energy as the heat energy that can be generated through theoretical combustion of the same amount of butanol (Abdehagh, Tezel, and Thibault 2014). *In situ* recovery techniques have a significant effect on the whole process and must be taken seriously into account.

Vacuum distillation, flash fermentation and gas stripping do not show significant progress and current research in this areas applied to butanol fermentation is generally related to process optimization and industrialization studies. However, these techniques (besides pervaporation) are the current best candidates for potential commercial-scale production.

Membrane-associated technologies (pervaporation and perstraction) enjoy coevolution with the development of new materials. The discovery and development of advanced materials can change the general performance of these techniques. Recently, developed membrane materials, including the MOF and liquid membranes, are suitable for butanol recovery (Liu, Chen, et al. 2014).

Liquid–liquid extraction and relevant methods have been proved to be the highest selective techniques, but they are also the most expensive. Polymer solutions, such as poly(ethylene glycol) and IL, are the best current available options. The future development in liquid–liquid extraction

should reside in their application for the production of butanol derivatives such as high-value fine chemicals.

Reactive extraction and a hypothetical reactive pervaporation could constitute a one pot, tandem or multicomponent biotechnological/chemical reaction. Functionalized silicate heterogeneous catalysts are candidates for *in situ* synthesis of butanol derivatives. Reactions catalyzed by enzymes (immobilized or in the free form) are also promising. The discovery, development and isolation of new enzymes are going to widen the spectrum of these chemical derivatives.

2.7 Disclosure statement

The authors report no declarations of interest.

2.8 ORCID

Pablo Jimenez-Bonilla http://orcid.org/0000-0002-5786-9845,

Yi Wang http://orcid.org/0000-0002-0192-3195

References

Abdehagh N, Sharif A, Tezel H, et al. 2012. In situ removal of biobutanol from fermentation broth. In *XXVI Congr Interam Ing Quim.* Montevideo, Uruguay.

Abdehagh, Niloofar, F Handan Tezel, and Jules Thibault. 2014. Separation techniques in butanol production: challenges and developments. *biomass and bioenergy* 60:222-246.

Ali, Wajid, Muhammad Hussain, Mujahid Ali, Muhammad Mubushar, Muhammad Ahmad Raza Tabassam, Muhammad Mohsin, and Hafiz Ashar Abbas Nasir. 2013. Evaluation of Freundlich and Langmuir isotherm for potassium adsorption phenomena. *International Journal of Agriculture and Crop Sciences* 6 (15):1048.

Anbarasan, Pazhamalai, Zachary C Baer, Sanil Sreekumar, Elad Gross, Joseph B Binder, Harvey W Blanch, Douglas S Clark, and F Dean Toste. 2012. Integration of chemical catalysis with extractive fermentation to produce fuels. *Nature* 491 (7423):235.

Artış, Üretiminde. 2008. Enhanced butanol production by mutant strains of Clostridium acetobutylicum in molasses medium. *Türk Biyokimya Dergisi (Turkish Journal of Biochemistry–Turk J Biochem)* 33 (1):25-30.

Baer, Shirley H, Hans P Blaschek, and Terrance L Smith. 1987. Effect of butanol challenge and temperature on lipid composition and membrane fluidity of butanol-tolerant Clostridium acetobutylicum. *Applied and environmental microbiology* 53 (12):2854-2861.

Barton, W Edward, and Andrew J Daugulis. 1992. Evaluation of solvents for extractive butanol fermentation with Clostridium acetobutylicum and the use of poly (propylene glycol) 1200. *Applied microbiology and biotechnology* 36 (5):632-639.

Benson, C. 2009. *Physical chemistry*: Global Media.

Cai, Di, Song Hu, Qi Miao, Changjing Chen, Huidong Chen, Changwei Zhang, Ping Li, Peiyong Qin, and Tianwei Tan. 2017. Two-stage pervaporation process for effective in situ removal acetone-butanol-ethanol from fermentation broth. *Bioresource technology* 224:380-388.

Cascon, Hercules R, Santosh K Choudhari, Grace M Nisola, Eleazer L Vivas, Dong-Ju Lee, and Wook-Jin Chung. 2011. Partitioning of butanol and other fermentation broth components in phosphonium and ammonium-based ionic liquids and their toxicity to solventogenic clostridia. *Separation and Purification Technology* 78 (2):164-174.

Choi, Jung-Min, Sang-Soo Han, and Hak-Sung Kim. 2015. Industrial applications of enzyme biocatalysis: current status and future aspects. *Biotechnology advances* 33 (7):1443-1454.

Dai, Zongjie, Hongjun Dong, Yan Zhu, Yanping Zhang, Yin Li, and Yanhe Ma. 2012. Introducing a single secondary alcohol dehydrogenase into butanol-tolerant Clostridium acetobutylicum Rh8 switches ABE fermentation to high level IBE fermentation. *Biotechnology for biofuels* 5 (1):44.

Dürre, Peter. 2011. Fermentative production of butanol—the academic perspective. *Current opinion in biotechnology* 22 (3):331-336.

Evans, Patrick J, and Henry Y Wang. 1988. Enhancement of butanol formation by Clostridium acetobutylicum in the presence of decanol-oleyl alcohol mixed extractants. *Applied and environmental microbiology* 54 (7):1662-1667.

Ezeji, TC, N Qureshi, and HP Blaschek. 2003. Production of acetone, butanol and ethanol by Clostridium beijerinckii BA101 and in situ recovery by gas stripping. *World Journal of Microbiology and Biotechnology* 19 (6):595-603.

Ezeji, Thaddeus C, Nasib Qureshi, and Hans P Blaschek. 2004. Butanol fermentation research: upstream and downstream manipulations. *The chemical record* 4 (5):305-314.

Farzaneh, Amirfarrokh, Ming Zhou, Elisaveta Potapova, Zoltán Bacsik, Lindsay Ohlin, Allan Holmgren, Jonas Hedlund, and Mattias Grahn. 2015. Adsorption of water and butanol in silicalite-1 film studied with in situ attenuated total reflectance–Fourier transform infrared spectroscopy. *Langmuir* 31 (17):4887-4894.

Friedl, Anton, N Qureshi, and Ian S Maddox. 1991. Continuous acetone-butanol-ethanol (ABE) fermentation using immobilized cells of Clostridium acetobutylicum in a packed bed reactor and integration with product removal by pervaporation. *Biotechnology and bioengineering* 38 (5):518-527.

Gao, Kai, Valerie Orr, and Lars Rehmann. 2016. Butanol fermentation from microalgae-derived carbohydrates after ionic liquid extraction. *Bioresource technology* 206:77-85.

Garcia-Chavez, Lesly Y, Christian M Garsia, Boelo Schuur, and André B de Haan. 2012. Biobutanol recovery using nonfluorinated task-specific ionic liquids. *Industrial & Engineering Chemistry Research* 51 (24):8293-8301.

Giusti, DM, RA Conway, and CT Lawson. 1974. Activated carbon adsorption of petrochemicals. *Journal (Water Pollution Control Federation)*:947-965.

Gonzalez-Penas, Helena, TA Lu-Chau, MT Moreira, and JM Lema. 2014. Solvent screening methodology for in situ ABE extractive fermentation. *Applied microbiology and biotechnology* 98 (13):5915-5924.

Grobben, Nicole G, Gerrit Eggink, F Petrus Cuperus, and Henk J Huizing. 1993. Production of acetone, butanol and ethanol (ABE) from potato wastes: fermentation with integrated membrane extraction. *Applied Microbiology and Biotechnology* 39 (4-5):494-498.

Groot, WJ, HS Soedjak, PB Donck, RGJM Van der Lans, K Ch AM Luyben, and JMK Timmer. 1990. Butanol recovery from fermentations by liquid-liquid extraction and membrane solvent extraction. *Bioprocess Engineering* 5 (5):203-216.

Ha, Sung Ho, Ngoc Lan Mai, and Yoon-Mo Koo. 2010. Butanol recovery from aqueous solution into ionic liquids by liquid–liquid extraction. *Process Biochemistry* 45 (12):1899-1903.

Heitmann, S, J Krings, P Kreis, A Lennert, WR Pitner, A Górak, and MM Schulte. 2012. Recovery of n-butanol using ionic liquid-based pervaporation membranes. *Separation and purification technology* 97:108-114.

Hu, Song, Wenqiang Ren, Di Cai, Timothy C Hughes, Peiyong Qin, and Tianwei Tan. 2017. A mixed matrix membrane for butanol pervaporation based on micron-sized silicalite-1 as macro-crosslinkers. *Journal of Membrane Science* 533:270-278.

Huang, Hua-Jiang, Shri Ramaswamy, and Youyan Liu. 2014. Separation and purification of biobutanol during bioconversion of biomass. *Separation and Purification Technology* 132:513-540.

Izák, Pavel, Katrin Schwarz, Wolfgang Ruth, Hubert Bahl, and Udo Kragl. 2008. Increased productivity of Clostridium acetobutylicum fermentation of acetone, butanol, and ethanol by pervaporation through supported ionic liquid membrane. *Applied microbiology and biotechnology* 78 (4):597-602.

Jalal, Taghreed A, NM Srivatsa Bettahalli, Ngoc Lieu Le, and Suzana P Nunes. 2015. Hydrophobic Hyflon AD/Poly (vinylidene fluoride) membranes for butanol dehydration via pervaporation. *Industrial & Engineering Chemistry Research* 54 (44):11180-11187.

Jee, Ki Yong, Nowon Kim, and Yong Taek Lee. 2016. The effect of metal complex on pervaporation performance of composite membrane for separation of n-butanol/water mixture. *Journal of Industrial and Engineering Chemistry* 44:155-163.

Jeon, YJ, and YY Lee. 1987. Membrane-assisted extractive butanol fermentation. *Annals of the New York Academy of Sciences* 506 (1):536-542.

Jeon, YJ; Lee, YY. 1989. In situ product separation in butanol fermentation by membrane-assisted extraction. *Enzyme and microbial technology* 11 (9):575-582.

Jiao, Pengfei, Jinglan Wu, Yingchun Ji, Xu Ke, Fengxia Zou, Jingwei Zhou, Wei Zhuang, and Hanjie Ying. 2015. Desorption of 1-butanol from polymeric resin: experimental studies and mathematical modeling. *RSC Advances* 5 (127):105464-105474.

Jin, Fuqiang, Xiaodong Zhang, Dongliang Hua, Haipeng Xu, Yan Li, and Hui Mu. 2017. Study on the in-situ coupling process of fermentation, extraction and distillation for biobutanol production: process analysis. Paper read at IOP Conference Series: Earth and Environmental Science.

Kim, Joong Kyun, Eugene L Iannotti, and Rakesh Bajpai. 1999. Extractive recovery of products from fermentation broths. *Biotechnology and bioprocess engineering* 4 (1):1.

Kong, Xiangping, Aiyong He, Jie Zhao, Hao Wu, Jiangfeng Ma, Ce Wei, Wanqin Jin, and Min Jiang. 2016. Efficient acetone–butanol–ethanol (ABE) production by a butanol-tolerant mutant of Clostridium beijerinckii in a fermentation–pervaporation coupled process. *Biochemical engineering journal* 105:90-96.

Kraemer, Korbinian, Andreas Harwardt, Rob Bronneberg, and Wolfgang Marquardt. 2010. Separation of butanol from acetone-butanol-ethanol fermentation by a hybrid extraction-distillation process. In *Computer Aided Chemical Engineering*: Elsevier.

Kubiczek, Artur, and Władysław Kamiński. 2013. Ionic liquids for the extraction of n-butanol from aqueous solutions. *Ecological Chemistry and Engineering. A* 20 (1):77-87.

Li, Jing, Xiangrong Chen, Benkun Qi, Jianquan Luo, Yuming Zhang, Yi Su, and Yinhua Wan. 2014. Efficient production of acetone–butanol–ethanol (ABE) from cassava by a fermentation–pervaporation coupled process. *Bioresource technology* 169:251-257.

Li, Si-Yu, Ranjan Srivastava, and Richard S Parnas. 2011. Study of in situ 1-butanol pervaporation from A-B-E fermentation using a PDMS composite membrane: Validity of solution-diffusion model for pervaporative A-B-E fermentation. *Biotechnology progress* 27 (1):111-120.

Li, Yukai, Jie Shen, Kecheng Guan, Gongping Liu, Haoli Zhou, and Wanqin Jin. 2016. PEBA/ceramic hollow fiber composite membrane for high-efficiency recovery of bio-butanol via pervaporation. *Journal of Membrane Science* 510:338-347.

Lin, De-Shun, Hong-Wei Yen, Wei-Chen Kao, Chieh-Lun Cheng, Wen-Ming Chen, Chieh-Chen Huang, and Jo-Shu Chang. 2015. Bio-butanol production from glycerol with Clostridium pasteurianum CH4: the effects of butyrate addition and in situ butanol removal via membrane distillation. *Biotechnology for biofuels* 8 (1):168.

Lin, Xiaoqing, Renjie Li, Qingshi Wen, Jinglan Wu, Jiansheng Fan, Xiaohong Jin, Wenbin Qian, Dong Liu, Xiaochun Chen, and Yong Chen. 2013. Experimental and modeling studies on the sorption breakthrough behaviors of butanol from aqueous solution in a fixed-bed of KA-I resin. *Biotechnology and bioprocess engineering* 18 (2):223-233.

Lin, Xiaoqing, Jinglan Wu, Xiaohong Jin, Jiansheng Fan, Renjie Li, Qingshi Wen, Wenbin Qian, Dong Liu, Xiaochun Chen, and Yong Chen. 2012. Selective separation of biobutanol from acetone–butanol–ethanol fermentation broth by means of sorption methodology based on a novel macroporous resin. *Biotechnology progress* 28 (4):962-972.

Liu, Gongping, Lin Gan, Sainan Liu, Haoli Zhou, Wang Wei, and Wanqin Jin. 2014. PDMS/ceramic composite membrane for pervaporation separation of acetone–butanol–ethanol (ABE) aqueous solutions and its application in intensification of ABE fermentation process. *Chemical Engineering and Processing: Process Intensification* 86:162-172.

Liu, Jiewei, Lianfen Chen, Hao Cui, Jianyong Zhang, Li Zhang, and Cheng-Yong Su. 2014. Applications of metal–organic frameworks in heterogeneous supramolecular catalysis. *Chemical Society Reviews* 43 (16):6011-6061.

Liu, Xiao-Bo, Qiu-Ya Gu, Xiao-Bin Yu, and Wei Luo. 2012. Enhancement of butanol tolerance and butanol yield in Clostridium acetobutylicum mutant NT642 obtained by nitrogen ion beam implantation. *Journal of microbiology* 50 (6):1024-1028.

Mai, Ngoc Lan, Sung Hoon Kim, Sung Ho Ha, Hwa Sung Shin, and Yoon-Mo Koo. 2013. Selective recovery of acetone-butanol-ethanol from aqueous mixture by pervaporation using immobilized ionic liquid polydimethylsiloxane membrane. *Korean Journal of Chemical Engineering* 30 (9):1804-1809.

Mariano, Adriano P, Mohammad J Keshtkar, Daniel IP Atala, Francisco Maugeri Filho, Maria Regina Wolf Maciel, Rubens Maciel Filho, and Paul Stuart. 2011. Energy requirements for butanol recovery using the flash fermentation technology. *Energy & Fuels* 25 (5):2347-2355.

Mariano, Adriano Pinto, Caliane Bastos Borba Costa, Dejanira de Franceschi De Angelis, Francisco Maugeri Filho, Daniel Ibraim Pires Atala, Maria Regina Wolf Maciel, and Rubens Maciel Filho. 2010. Optimisation of a continuous flash fermentation for butanol production using the response surface methodology. *Chemical engineering research and design* 88 (5-6):562-571.

Mariano, Adriano Pinto, Rubens Maciel Filho, and Thaddeus Chukwuemeka Ezeji. 2012. Energy requirements during butanol production and in situ recovery by cyclic vacuum. *Renewable energy* 47:183-187.

Mariano, Adriano Pinto, Nasib Qureshi, Rubens Maciel Filho, and Thaddeus Chukwuemeka Ezeji. 2011. Bioproduction of butanol in bioreactors: new insights from simultaneous in situ butanol recovery to eliminate product toxicity. *Biotechnology and bioengineering* 108 (8):1757-1765.

Mariano, Adriano Pinto, Nasib Qureshi, Rubens Maciel Filho, and Thaddeus Chukwuemeka Ezeji. 2012. Assessment of in situ butanol recovery by vacuum during acetone butanol ethanol (ABE) fermentation. *Journal of Chemical Technology & Biotechnology* 87 (3):334-340.

Merlet, G, F Uribe, C Aravena, M Rodríguez, R Cabezas, E Quijada-Maldonado, and J Romero. 2017. Separation of fermentation products from ABE mixtures by perstraction using hydrophobic ionic liquids as extractants. *Journal of Membrane Science* 537:337-343.

Nielsen, David R, Gihan S Amarasiriwardena, and Kristala LJ Prather. 2010. Predicting the adsorption of second generation biofuels by polymeric resins with applications for in situ product recovery (ISPR). *Bioresource technology* 101 (8):2762-2769.

Nielsen, David R, and Kristala Jones Prather. 2009. In situ product recovery of n-butanol using polymeric resins. *Biotechnology and bioengineering* 102 (3):811-821.

Núñez-Gómez, Karen-Stephanie, Liliana-Carolina López-Mendoza, Luis-Javier López-Giraldo, and Carlos-Jesús Muvdi-Nova. 2014. Study of acetone, butanol and ethanol liquid extraction from prepared aqueous solutions using membrane contactor technique. *CT&F-Ciencia, Tecnología y Futuro* 5 (4):97-112.

Oudshoorn, A, LAM Van der Wielen, and AJJ Straathof. 2012. Desorption of butanol from zeolite material. *Biochemical engineering journal* 67:167-172.

Patakova, Petra, Michaela Linhova, Mojmir Rychtera, Leona Paulova, and Karel Melzoch. 2013. Novel and neglected issues of acetone–butanol–ethanol (ABE) fermentation by clostridia: Clostridium metabolic diversity, tools for process mapping and continuous fermentation systems. *Biotechnology advances* 31 (1):58-67.

Qureshi, N, and HP Blaschek. 2000. Butanol production using Clostridium beijerinckii BA101 hyper-butanol producing mutant strain and recovery by pervaporation. Paper read at Twenty-First Symposium on Biotechnology for Fuels and Chemicals.

Qureshi, N, MM Meagher, Jicai Huang, and RW Hutkins. 2001. Acetone butanol ethanol (ABE) recovery by pervaporation using silicalite–silicone composite membrane from fed-batch reactor of Clostridium acetobutylicum. *Journal of Membrane Science* 187 (1-2):93-102.

Qureshi, N, MM Meagher, and RW Hutkins. 1999. Recovery of butanol from model solutions and fermentation broth using a silicalite/silicone membrane1. *Journal of Membrane Science* 158 (1-2):115-125.

Qureshi, Nasib, Stephen Hughes, IS Maddox, and MA Cotta. 2005. Energy-efficient recovery of butanol from model solutions and fermentation broth by adsorption. *Bioprocess and biosystems engineering* 27 (4):215-222.

Qureshi, Nasib, and IS Maddox. 2005. Reduction in butanol inhibition by perstraction: utilization of concentrated lactose/whey permeate by Clostridium acetobutylicum to enhance butanol fermentation economics. *Food and Bioproducts Processing* 83 (1):43-52.

Rabari, Dharamashi, and Tamal Banerjee. 2013. Biobutanol and n-propanol recovery using a low density phosphonium based ionic liquid at T= 298.15 K and p= 1atm. *Fluid Phase Equilibria* 355:26-33.

Rom A., Esteve D., Friedl A. 2013. Organophilic Pervaporation of Butanol from an Aqueous Solution with POMS. *Chemical Engineering Transactions* 35:1315-1320.

Saint Remi, J Cousin, G Baron, and J Denayer. 2012. Adsorptive separations for the recovery and purification of biobutanol. *Adsorption* 18 (5-6):367-373.

Schmid, A, JS Dordick, B Hauer, Al Kiener, M Wubbolts, and B Witholt. 2001. Industrial biocatalysis today and tomorrow. *nature* 409 (6817):258.

Shin, Chaeyoung, Zachary C Baer, X Chelsea Chen, A Evren Ozcam, Douglas S Clark, and Nitash P Balsara. 2015. Block copolymer pervaporation membrane for in situ product removal during acetone–butanol–ethanol fermentation. *Journal of Membrane Science* 484:57-63.

Tanaka, Shigemitsu, Yukihiro Tashiro, Genta Kobayashi, Toru Ikegami, Hideyuki Negishi, and Keiji Sakaki. 2012. Membrane-assisted extractive butanol fermentation by Clostridium saccharoperbutylacetonicum N1-4 with 1-dodecanol as the extractant. *Bioresource technology* 116:448-452.

Thompson, Anthony B, Sydney J Cope, T Dallas Swift, and Justin M Notestein. 2011. Adsorption of n-butanol from dilute aqueous solution with grafted calixarenes. *Langmuir* 27 (19):11990-11998.

Tomas, Christopher A, Neil E Welker, and Eleftherios T Papoutsakis. 2003. Overexpression of groESL in Clostridium acetobutylicum results in increased solvent production and tolerance, prolonged metabolism, and changes in the cell's transcriptional program. *Applied and Environmental Microbiology* 69 (8):4951-4965.

van den Berg, Corjan, Arjan S Heeres, Luuk AM van der Wielen, and Adrie JJ Straathof. 2013. Simultaneous clostridial fermentation, lipase-catalyzed esterification, and ester extraction to enrich diesel with butyl butyrate. *Biotechnology and bioengineering* 110 (1):137-142.

Van Hecke, Wouter, Pieter Vandezande, Stan Claes, Silvia Vangeel, Herman Beckers, Ludo Diels, and Heleen De Wever. 2012. Integrated bioprocess for long-term continuous cultivation of Clostridium acetobutylicum coupled to pervaporation with PDMS composite membranes. *Bioresource technology* 111:368-377.

Villadsen, John, Sang Yup Lee, Jens Nielsen, and Gregory Stephanopoulos. 2016. *Fundamental bioengineering*. Vol. 1: John Wiley & Sons.

Volesky, B. 2003. *Sorption and biosorption*. Montreal, Canada: BV-Sorbex, Inc.

Wang, Xiaolu, Jinxun Chen, Manquan Fang, Tao Wang, Lixin Yu, and Jiding Li. 2016. ZIF-7/PDMS mixed matrix membranes for pervaporation recovery of butanol from aqueous solution. *Separation and Purification Technology* 163:39-47.

Wasewar, Kailas L. 2012. Reactive extraction: an intensifying approach for carboxylic acid separation. *International Journal of Chemical Engineering and Applications* 3 (4):249.

Wu, Xiangting, Guoxing Li, Hailong Yang, and Huabin Zhou. 2015. Study on extraction and separation of butyric acid from clostridium tyrobutyricum fermentation broth in PEG/Na2SO4 aqueous two-phase system. *Fluid Phase Equilibria* 403:36-42.

Xue, Chuang, Guang-Qing Du, Li-Jie Chen, Jian-Gang Ren, and Feng-Wu Bai. 2014. Evaluation of asymmetric polydimethylsiloxane-polyvinylidene fluoride composite membrane and incorporated with acetone-butanol-ethanol fermentation for butanol recovery. *Journal of biotechnology* 188:158-165.

Xue, Chuang, Fangfang Liu, Mengmeng Xu, I-Ching Tang, Jingbo Zhao, Fengwu Bai, and Shang-Tian Yang. 2016. Butanol production in acetone-butanol-ethanol fermentation with in situ product recovery by adsorption. *Bioresource technology* 219:158-168.

Xue, Chuang, Fangfang Liu, Mengmeng Xu, Jingbo Zhao, Lijie Chen, Jiangang Ren, Fengwu Bai, and Shang-Tian Yang. 2016. A novel in situ gas stripping-pervaporation process integrated with acetone-butanol-ethanol fermentation for hyper n-butanol production. *Biotechnology and bioengineering* 113 (1):120-129.

Xue, Chuang, Min Liu, Xinwen Guo, Elton P Hudson, Lijie Chen, Fengwu Bai, Fangfang Liu, and Shang-Tian Yang. 2017. Bridging chemical-and bio-catalysis: high-value liquid transportation fuel production from renewable agricultural residues. *Green Chemistry* 19 (3):660-669.

Xue, Chuang, Decai Yang, Guangqing Du, Lijie Chen, Jiangang Ren, and Fengwu Bai. 2015. Evaluation of hydrophobic micro-zeolite-mixed matrix membrane and integrated with acetone–butanol–ethanol fermentation for enhanced butanol production. *Biotechnology for biofuels* 8 (1):105.

Xue, Chuang, Jing-Bo Zhao, Li-Jie Chen, Feng-Wu Bai, Shang-Tian Yang, and Jian-Xin Sun. 2014. Integrated butanol recovery for an advanced biofuel: current state and prospects. *Applied microbiology and biotechnology* 98 (8):3463-3474.

Xue, Chuang, Jingbo Zhao, Fangfang Liu, Congcong Lu, Shang-Tian Yang, and Feng-Wu Bai. 2013. Two-stage in situ gas stripping for enhanced butanol fermentation and energy-saving product recovery. *Bioresource technology* 135:396-402.

Xue, Chuang, Jingbo Zhao, Congcong Lu, Shang-Tian Yang, Fengwu Bai, and I-Ching Tang. 2012. High-titer n-butanol production by clostridium acetobutylicum JB200 in fed-batch fermentation with intermittent gas stripping. *Biotechnology and bioengineering* 109 (11):2746-2756.

Xue, Chuang, Xin-Qing Zhao, Chen-Guang Liu, Li-Jie Chen, and Feng-Wu Bai. 2013. Prospective and development of butanol as an advanced biofuel. *Biotechnology advances* 31 (8):1575-1584.

Yang, Xiaoping, Gow-Jen Tsai, and George T Tsao. 1994. Enhancement of in situ adsorption on the acetone-butanol fermentation by Clostridium acetobutylicum. *Separations Technology* 4 (2):81-92.

Yen, Hong-Wei, and Yi-Cheng Wang. 2013. The enhancement of butanol production by in situ butanol removal using biodiesel extraction in the fermentation of ABE (acetone–butanol–ethanol). *Bioresource technology* 145:224-228.

Žák, Michal, Martina Klepic, Lucie Červenková Šťastná, Zuzana Sedláková, Hana Vychodilová, Štěpán Hovorka, Karel Friess, Alena Randová, Libuše Brožová, and Johannes Carolus Jansen. 2015. Selective removal of butanol from aqueous solution by pervaporation with a

PIM-1 membrane and membrane aging. *Separation and Purification Technology* 151:108-114.

Zhang, Jie, Mintian Gao, Dongliang Hua, Yan Li, Haipeng Xu, Xiaohui Liang, Yuxiao Zhao, Fuqiang Jin, Lei Chen, and Guangfan Meng. 2014. Butanol production of Clostridium pasteurianum SE-5 from transesterification reaction solution using fermentation and extraction coupling system. Paper read at International Conference on Materials for Renewable Energy and Environment (ICMREE), 2013

Zhang, Shaozhi, Xiaoyan Huang, Chunyun Qu, Yukai Suo, Zhengping Liao, and Jufang Wang. 2017. Extractive fermentation for enhanced isopropanol and n-butanol production with mixtures of water insoluble aliphatic acids and oleyl alcohol. *Biochemical engineering journal* 117:112-120.

Zheng, Jin, Yukihiro Tashiro, Qunhui Wang, and Kenji Sonomoto. 2015. Recent advances to improve fermentative butanol production: genetic engineering and fermentation technology. *Journal of bioscience and bioengineering* 119 (1):1-9.

Chapter III.

Tolerance enhancement of *Clostridium saccharoperbutylacetonicum* N1-4 against lignocellulosic-biomass-derived inhibitors by overexpressing of efflux pumps genes from *Pseudomonas putida*.

Supplementary information is available in appendix III.

Abstract

Lignocellulosic biomass is abundant and inexpensive feedstock for biofuel production through microbial fermentation. However, furan aldehydes and phenolic compounds could be generated as byproducts during biomass pretreatment process which can inhibit microbial metabolism and lead to inefficient fermentation. Efflux pumps are membrane proteins that actively transport out of the cell small molecules, such as short chain alcohols, thus sustaining the normal metabolism of the microorganism. *Pseudomonas putida* has outstanding tolerance to butanol and other small molecular compounds, and thus we hypothesize that its efflux pump system could play essential role for enabling such robustness. In this study, in order to enhance the tolerance of the hyper-butanol producing *Clostridium saccharoperbutylacetonicum* N1-4 to fermentation inhibitors, we overexpressed the efflux pump genes from *P. putida*. Interestingly, the overexpression of the whole efflux pump unit (*srpABC*) actually resulted in decreased tolerance of the strain to butanol and fermentation inhibitors, while the overexpression of the subunit (*srpB*) only exerted significant enhanced robustness of the strain against inhibitors based on preliminary cell growth testing. Further characterization through fermentation demonstrated that, compared to the control strain, the engineered strain has enhanced capability to grow in media containing 17%

more furfural or 50% more ferulic acid, and produce around 14 g/L butanol (which was comparable to the fermentation under regular conditions without inhibitors) under such inhibitory conditions. This study provided valuable reference for boosting microbial robustness for efficient biofuel production through fermentation from low-value lignocellulosic materials.

Keywords: Biomass hydrolysates, tolerance, butanol, fermentation inhibitors, efflux pump, *Clostridium saccharoperbutylacetonicum*, *Pseudomonas putida*

3.1 Introduction

Biofuel produced through microbial fermentation is considered as a solution for the exhaustion of fossil fuel and the associated environmental problems. Recently, interests have been revitalized in biobutanol production through acetone-butanol-ethanol (ABE) fermentation with solventogenic clostridia, because butanol can not only be used as a biofuel with various advantages over ethanol, but also be employed as a chemical feedstock for various industries (Moon et al. 2016). The ABE process for butanol production could be dated back from 1916, and has been a prominent industrial process in the history. However, since 1950s, it started to be replaced by petrochemical process for butanol production due to the quick development of petrochemical refineries (Moon et al. 2016). In order to make biobutanol production through the ABE process be economically viable again, various issues still need to be resolved, such as the low butanol production titer due to the limited tolerance of the microorganism as well as the high cost of the feedstock materials.

When the ABE solvents reach high levels, they can disrupt cell envelope, or deactivate protein functions and make the cells die. Butanol is more lipophilic than either acetone or ethanol, then it has a higher interaction with the cell envelope, and thus is the most toxic one in the ABE

mixture (Jiménez-Bonilla and Wang 2018). Thus, the improvement of butanol tolerance of the microorganism has remarkable benefits to enhance butanol production and thus brings about great significance for the economics of the ABE process. Interestingly, some non-solventogenic bacteria have shown natural high tolerance to aromatic and aliphatic solvents including small alcohols such as butanol. For example, *Lactobacillus buchneri,* and *L. brevis* can survive in 3% butanol, *L. amylovorus* in 4% (Liu et al. 2012), and *Pseudomonas putida* in 6% (Rühl, Schmid, and Blank 2009). The exceptional tolerance of *P. putida* to butanol and other organic substances has been explained, besides other reasons, by its active membrane transport systems (Dunlop et al. 2011).

srp efflux pump belongs to the Resistance-Nodulation-Division (RND) family of transporters, and consists of three components: an inner membrane protein which is the extrusion element, an outer pore, and an accessory lipoprotein for stabilization attached to the peptidoglycan (Ramos et al. 2015; Nikaido and Takatsuka 2009). Efflux pumps are complex systems, which can extrude various toxic compounds from the cytoplasm out of the cell. The expression level of the *srp* system increased remarkably when organic solvents (including aromatic, aliphatic and alcohols) are present. Particularly, the expression level of the *srp* system was increased by 6.6 times when 3mM of butanol was added into the medium (Kieboom et al. 1998). While the overexpression of efflux pump *srpABC* or the *srpB* subunit alone in *E. coli* could enhance the butanol tolerance of the host strain by 20-35% (Bui et al. 2015).

On the other hand, lignocellulosic biomass is an ideal feedstock for fermentative butanol (as well as other biofuels) production since it is abundant, inexpensive, and does not compete with the food or feed supplies. In order to convert the biomass feedstock to monomer sugars that microorganism can directly utilize during the fermentation process, physical/chemical pretreatment step, and chemical/enzymatic hydrolysis is needed. During these processes,

excepting the enzymatic, various fermentation inhibitors including furan aldehyde and phenolic compounds will be generated due to the degradation of sugars, lignin and extractives under the harsh conditions for pretreatment or conversion. Such inhibitors can be detrimental to the cell growth and lead to low yield and productivity of the products and even unsuccessful fermentation.

Various strategies have been investigated to enhance the cell tolerance to hydrolysates inhibitors, including the overexpression of stress proteins and heat-shock proteins (Patakova et al. 2018). As described above, efflux pumps are membrane proteins that can actively transport small molecules, such as aromatics or small alcohols or aldehydes out of the cell, thus maintaining the regular metabolism of the microorganism. Therefore, the overexpression of efflux pump genes in solventogenic clostridia could help enhance the tolerance of the cells to hydrolysates inhibitors besides the tolerance to butanol.

3.2 Materials and methods

3.2.1 Reagents, bacterial strains and cultivation

Butanol, furfural and *trans*-ferulic acid were purchased from Alfa Aesar (Haverhill, MA), Merck chemicals (Burlington, MA), and Sigma-Aldrich (St. Louis, MO), respectively. Sterile polyester sealing film was purchased from VWR (Radnor, PA). PCR reagents (Q5 and Phusion Hi-Fi master mix for DNA cloning, Taq and LongAmp for colony PCR (cPCR) for mutation verification) were all purchased from NEB (New England Biolabs Inc., Ipswich, MA). *E. coli* NEB express (New England BioLabs) was used for the plasmid propagation. It was cultivated in Luria-Bertani (LB) broth or LB agar plates, supplemented with 100 μg/mL of ampicillin when needed. *C. saccharoperbutylacetonicum* N1-4 (HMT) (DSM 14923) was routinely cultivated in Tryptone/Glucose/Yeast extract (TGY) medium containing 30 g/L tryptone, 20 g/L glucose, 10

g/L of yeast extract, and 1 g/L of L-cysteine, or with TGY + 1.5% agar plates at 35ºC. All manipulations of the anaerobes were performed in an anaerobic chamber (N_2-CO_2-H_2 with a volume ratio of 85:10:5), and supplemented with 30μg/mL clarithromycin when needed. All strains were preserved in glycerol stock (20% v/v final glycerol concentration) at -80ºC.

3.2.2 Genetic manipulation

The genomic DNA of *P. putida* S12 (ATCC 700801) was kindly provided by Dr. Nick Wierckx from the RWTH Aachen University, Germany. DNA fragments corresponding to the efflux pump subunit *srp*B and the whole cluster *srp*ABC from *P. putida* S12 were PCR-amplified, using the pair of primers YW2197 & YW2198 (for *srp*B); and, YW2199 & YW2202 (for *srp*ABC). Then the two DNA fragments were individually inserted between the *thiolase* promoter (P*thl*) and terminator (T*thl*) in pJZ100 (Zhang, Wang, et al. 2018) with NEB Gibson Assembly approach (Gibson et al. 2010), generating pPJB3 and pPJB5, respectively.

Table 3.1 List of primers, plasmids and strains used in this study

Primers	**Sequence of oligonucleotides**	
YW32	5'-GTTTTCCCAGTCACGACGTT-3'	
YW33	5'-TTGCTGCTCATGCAGATGAT-3'	
YW2197	5'-AGAATTTTAGGAGGTCAAAC**ATGTCTCGTTTCTTTATCGACAGG-3'**	
YW2198	5'-GTTGCGAATGTGAACTTGTATA**TTAAACTTCATGAGTCACCTCCTTG-3'**	
YW2199	5'-AGAATTTTAGGAGGTCAAAC**GTGAGACAGATACGATCCCCG-3'**	
YW2202	5'-GTTGCGAATGTGAACTTGTATA**TTAGTTTTGACTCACGCTCCAG-3'**	
Plasmids	**Description and general characteristics**	**References**
pJZ100	pTJ1 derivative; for gene overexpression under the control of the thiolase promoter (Pthl) from *C.saccharoperbutylacetonicum* N1-4	(Zhang, Wang, et al. 2018)
pPJB3	pJZ100 derivative; for overexpression of *srp*B	This work
pPJB5	pJZ100 derivative; for overexpression of *srp*ABC	This work
Strains		**Sources**
E. coli NEB express	Propagation vector	
C. saccharoperbutylacetonicum		NEB labs
N1-4	Used for electroporation of different plasmids used in this study	DSM
Control	N1-4 harboring pJZ100 (empty plasmid)	This work
PJB3	N1-4 harboring pPJB3, for overexpression of *srp*B	This work
PJB5	N1-4 harboring pPJB5, for overexpression of *srp*ABC	This work

3.2.3 DNA transformation

DNA transformation of *C. saccharoperbutylacetonicum* was carried out with electroporation following our previous protocol with minor modifications (Zhang, Jiménez-Bonilla, et al. 2018).

C. saccharoperbutylacetonicum N1-4 was cultivated in TGY at 35°C, until the culture reach the early exponential phase (OD_{600}~ 0.6-0.8). The cells were harvested through centrifugation at 4,200 × g at room temperature for 10 min. The cell pellets were resuspended and washed once with the same volume (as the original cell culture) of Clostridial SMP buffer (270 mM sucrose, 1mM $MgCl_2$ and 7mM Na_2HPO_3/NaH_2PO_3, adjusted to pH 6.5 and filter sterilized). Then it is centrifuged again and then resuspended in 1/20 volume of SMP buffer. Afterwards, 400 µl of these competent cells were transferred into an ice cold 0.2-cm electroporation cuvette in which 1.0 µg of plasmid DNA was pre-loaded, and cooled down in ice for 20-30 min. Electroporation was carried out at a voltage of 1 kV, a capacitance of 25 µF, and a resistance of 300 Ω using a Gene Pulser Xcell electroporation system (Bio-Rad Laboratories, Hercules, CA) which was connected to the anaerobic chamber. Subsequently, the cells were transferred into 1.6 ml of TGY medium and recovered at 35°C until growth becomes evident (generally for 4-6 h). The recovered cells were centrifuged, resuspended in 100 µL, and then spread onto TGYC (TGY supplemented with 30µg/mL clarithromycin) agar plates. The plates were incubated at 35 °C for about 24-48 h until colonies appeared. Then cPCR was performed to verify the mutants, using primers YW32 & YW33.

3.2.4 Effects of the overexpression of efflux pump genes on the strain tolerance to butanol and lignocellulosic inhibitors

For each strain, 200 mL of culture at OD_{600} of 0.8 was split up into 10 tubes (5 mL each). Then inhibitors were added to make the final concentration as follows in different tubes: butanol of 0.8, 1, or 1.2%, furfural of 4.0, 4.5, or 5.0 g/L, or ferulic acid of 0.2, 0.5, or 0.8 g/L. Then, the cultures were loaded into a 96-well plate, with 8 replicates of 150 µL from each tube. The plate was sealed with a plastic film to keep the anaerobic environment and incubated at 35 ºC in an

infinite M1000 Pro microplate reader (Tecan, Männedorf, Switzerland) with orbital shaking. The OD_{600} of the culture was quantified automatically with the microplate reader every 15 min during a 9-12 h period. The relative growth of each culture compared to the control was calculated based on Equation 3.1, whereas $OD_{600,[x]}$ is the OD_{600} of the culture with the inhibitor concentration of x (either in % or g/L as described above), and $OD_{600,[0]}$ is the OD_{600} of the culture with no inhibitor added (as the control). The relative growths had been used instead of the absolute values in order to demonstrate the effect of genes overexpression on tolerance excluding other possible effects. Similar approach has been employed before by Xu (2015).

$$\%\ relative\ growth = \frac{OD_{600,[x]}}{OD_{600,[0]}} \times 100 \quad \text{(Equation 3.1)}$$

More detailed procedure can be found in the supplementary information

3.2.5 Fermentation procedures

Batch fermentation was carried out in 2.5 L BioFlo benchtop bioreactors (New Brunswick Scientific Co., Enfield, CT) with a 1.5 L working volume using 80 g/L glucose, 6 g/L tryptone, 2 g/L yeast extract, and P2-medium: 0.5 g/L KH_2PO_4, 0.5 g/L K_2HPO_4, 2.2 g/L CH_3COONH_4, 0.2 g/L $MgSO_4 \cdot 7H_2O$, 0.01 g/L $MnSO_4 \cdot H_2O$, 0.01 g/L $FeSO_4 \cdot 7H_2O$, 0.01 g/L NaCl, 0.001 g/L p-aminobenzoic acid, 0.001 g/L thiamine-HCl, and 0.00001 g/L biotin. When the inhibitors were supplemented, 3.0, 3.5 or 4.0 g/L of furfural (after the fermentation medium was autoclaved), or 0.8, 1.0, 1.2 or 1.4 g/L of ferulic (before the fermentation medium was autoclaved) were added. To create an anaerobic condition, after the fermentation broth was sterilized through autoclaving, highly pure nitrogen gas was flushed through before inoculation until the fermentation started and the culture produced its own gases. To prepare the preculture, the glycerol stock of *C. saccharoperbutylacetonicum* wild type and mutant strains were inoculated into TGY medium and

incubate in the anaerobic chamber for 12-16 h until OD_{600} reached ~0.8. The preculture was then inoculated into the bioreactor at a ratio of 5% (v/v). Fermentations were conducted under following conditions: 50 rpm, 30 ºC, with pH controlled ≥5.0 (with 4M NaOH). 30 µg/mL of clarithromycin was supplemented when needed. All fermentations were performed in duplicate.

3.2.6 Analytic procedures

Concentrations of glucose butanol, acetone and ethanol concentration were determined on a High Performance Liquid Chromatographer (Agilent 1260 series, Agilent Technologies, Santa Clara, CA, USA) with a refraction index detector and Varian MetaCarb 87H column (set at 25 ºC). Aqueous 5mM H_2SO_4 at a flow rate of 0.6 mL/min was used as the mobile phase. Cell optical density (OD_{600}) was quantified with a cell density meter (Ultrospec 10, Biochrom Ltd., Cambridge, England).

3.3 Results and discussion

3.3.1 Tolerance test

The tolerance test showed the capability of the strains to grow in media containing different concentrations of inhibitors. Profiles of relative growth were constructed in order to exclude the effects other than gene overexpression on the cell tolerance. As shown in Fig. 3.1, the results showed a similar trend for the same strain for all the three inhibitors tested (butanol, furfural and ferulic acid). In all cases, the cell growth profiles experienced a decline in the first two hours after the culture is challenged with the inhibitor. Afterwards, the microorganism overcame such inhibition exerted by the inhibitor, and started to recover for active growth. For PJB3 strain (the top row in Fig. 3.1), although the cell growth in the initial stage was slower than the control strain, it outgrew to much higher level than the control (by 12 h). By 12 h, the relative growth of PJB3 is

around 20-30% higher than the control. This means that the strain is more tolerant to butanol, ferulic acid or furfural than the control strain. For PJB3 (the bottom row in Fig. 3.1), on the opposite, the cell growth of the mutant was generally similar or lower than that of the control during the time period for the tolerance test (by 12 h), which means that the mutant strain was less tolerant to the inhibitors than the control strain. Based on this result, PJB3 was chosen for the following fermentation experiments.

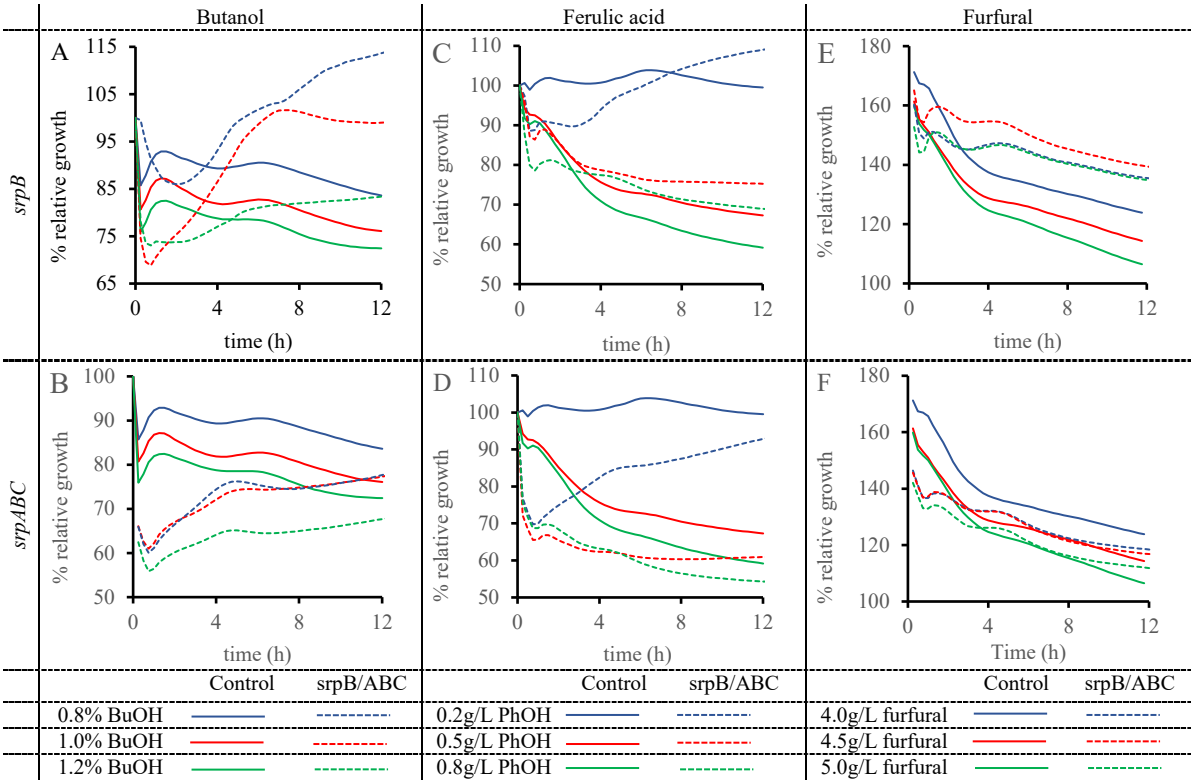

Figure 3.1 Relative growth of PJB3 (A,C and E) and PJB5 (B,D and E), compared to the control strain (*C. saccharoperbutylacetonicum* N1-4 containing pJZ100) when these strains were challenged with butanol (A, B), furfural (C, D) and ferulic acid (E,F).

Most known efflux pumps related with solvent extrusion, including *acr*AB-*tol*C from *E. coli*, *ttg*ABC and *srp*ABC from *P. putida* belong to hydrophobic-amphiphilic efflux (HAE-1) subfamily from RND superfamily, which only present in Gram-negative bacteria (Anes et al. 2015; Nikaido

2018). It is known that all the three subunits (Subunit A, B and C) are necessary for the functionality of the whole system (Anes et al. 2015); but when some of the components is missing, the corresponding function can be made up by some other transporters (Tal and Schuldiner 2009). Previously, Bui et al. (Bui et al. 2015) reported that the effect of the expression of *srp*B or *srp*ABC in *E. coli* are very similar, which could be explained by the above mechanism.

A typical structure of HAE-1 efflux pumps is shown in Fig. 2 (a). The extruder element (*srp*B, in this case) is expressed in the inner membrane, while the element C in the outer membrane and the subunit A within the intermembrane space. In Gram-positive bacteria, such as *C. saccharoperbutylacetonicum*, there is no outer membrane, with a peptidoglycan cell wall as the counterpart instead (Fig. 2b).

HAE-2 family of efflux pumps is closely related to HAE-1. HAE-2 are all expressed in Gram-positive bacteria, such as Mmpl proteins in *Mycobacterium tuberculosis* (Nikaido 2018). The mechanism is not very clear but the crystallized domains of Mmpl11 shown similar pattern to HAE-1 pumps (Nikaido 2018). Based on NCBI Blast tool (supplementary table S3.2): CSPA_RS22990, CSPA_RS18355, CSPA_RS19385, and CSPA_RS10815 encodes four putative transporters in *C. saccharoperbutylacetonicum* N1-4 with an important homology to *srp*B of *P. putida* S12, and the first three are homologous to acrB from *E. coli,* as well. All four genes are annotated as efflux RND transporter permease subunits. CSPA_RS22990 is located in a single operon with CSPA_RS22995, an efflux RND transporter periplasmic adaptor subunit, and CSPA_RS22985, a *tolC* family protein complement. This means that both: the endogenous systems and the HAE-1 efflux pumps are very similar in structure, and also considering the high homology of the native transporters with *srpB* and *acrB*. CSPA_RS18355 is also in an operon of three subunits, among which the other two annotated as a biotin/lypoyl binding protein

(CSPA_RS18360), and an amidohydrolase complement (CSPA_RS18350). CSPA_RS19385 and CSPA_RS10815 are located in an operon with CSPA_RS19380 and CSPA_RS10810, respectively. Both CSPA_RS19380 and CSPA_RS10810, are annotated as efflux RND transporter periplasmic adaptor subunits. This level of homology suggest that *srpB* can works in coordinated overlap with the native transporters, in a similar way as it happens with other RND transporters of Gram-negative bacteria.

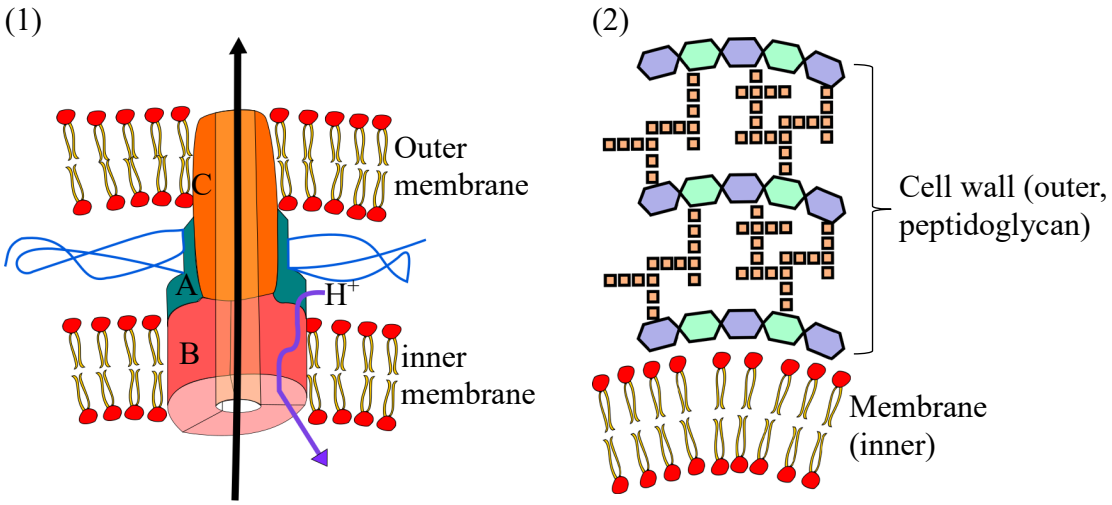

Figure 3.2 (1) HAE-1 efflux pumps in Gram-negative bacteria, and (2) cell member of Gram-positive bacteria

3.3.2 Effects of the overexpression of efflux pump genes on the strain tolerance to furan aldehyde inhibitors

Furan aldehydes are significant inhibitors that can be generated during the lignocellulosic biomass conversion into fermentable sugars. Here, we used furfural as a model compound to evaluate the effects of *srp*B overexpression on the strain tolerance to furan aldehydes inhibitors. As shown in Fig. 3.3, when there is no furfural added to the fermentation, PJB3 strain consumed similar amount of glucose at the similar rate (Fig. 3.3E), but generated higher cell biomass (by

19%, Fig. 3.3A). However, interestingly, the butanol production in PJB3 was lower (14.2 g/L vs. 17.5 g/L in the control) than that in the control (Fig. 3.3I). Similarly, the total solvent production in PJB3 was also lower than that in the control strain. At 3 g/L furfural, there was a lag phase of about 24 h before the cell (for both PJB3 and the control) can grow. However, PJB3 generally demonstrated very similar dynamics as the control strain for glucose consumption; the cell growth of PJB3 was slightly faster than the control strain in the exponential phase, but finally reached the similar maximum OD as the control. PJB3 also produced slightly higher butanol (14.8 g/L vs. 14.0 g/L) and total solvent (23.6 g/L vs. 22.9 g/L) than the control. When furfural was further increased to 3.5 g/L, the control strain cannot grow any more, while PJB3 can still grow to the similar maximum OD_{600} as when 3.0 g/L was supplemented, although a longer lag phase (about 36 h) was observed before the cell started to grow. Correspondingly, PJB3 can still consume 52.2 g/L glucose within 96 h, and produced 12.8 g/L butanol and 19.8 g/L total ABE. When 4.0 g/L furfural was added into the fermentation, neither PJB3 nor the control strain could grow.

We previously reported that *C. saccharoperbutylacetonicum* N1-4 can tolerate up to 3.0 g/L furfural (Yao et al. 2017), which is consistent as shown in Fig. 3.3 for the control strain. Meanwhile, the results here demonstrated that overexpression of *srp*B could enhance the tolerance of the strain to furfural up to 3.5 g/L. However, interestingly, when there was no furfural present, the *srp*B strain produced less butanol or total solvent than the control strain (Fig. 3.3I&M).

High levels of expression of efflux pump genes can lead to a toxic effect on cells, as reported previously (Patakova et al. 2018), probably because the efflux pump can occupy a big fraction of the space on the membrane, limiting the expression of other membrane functions or because of the change in membrane composition due to more protein content. Therefore, the expression level of efflux pumps is critical in order to obtain optimum results.

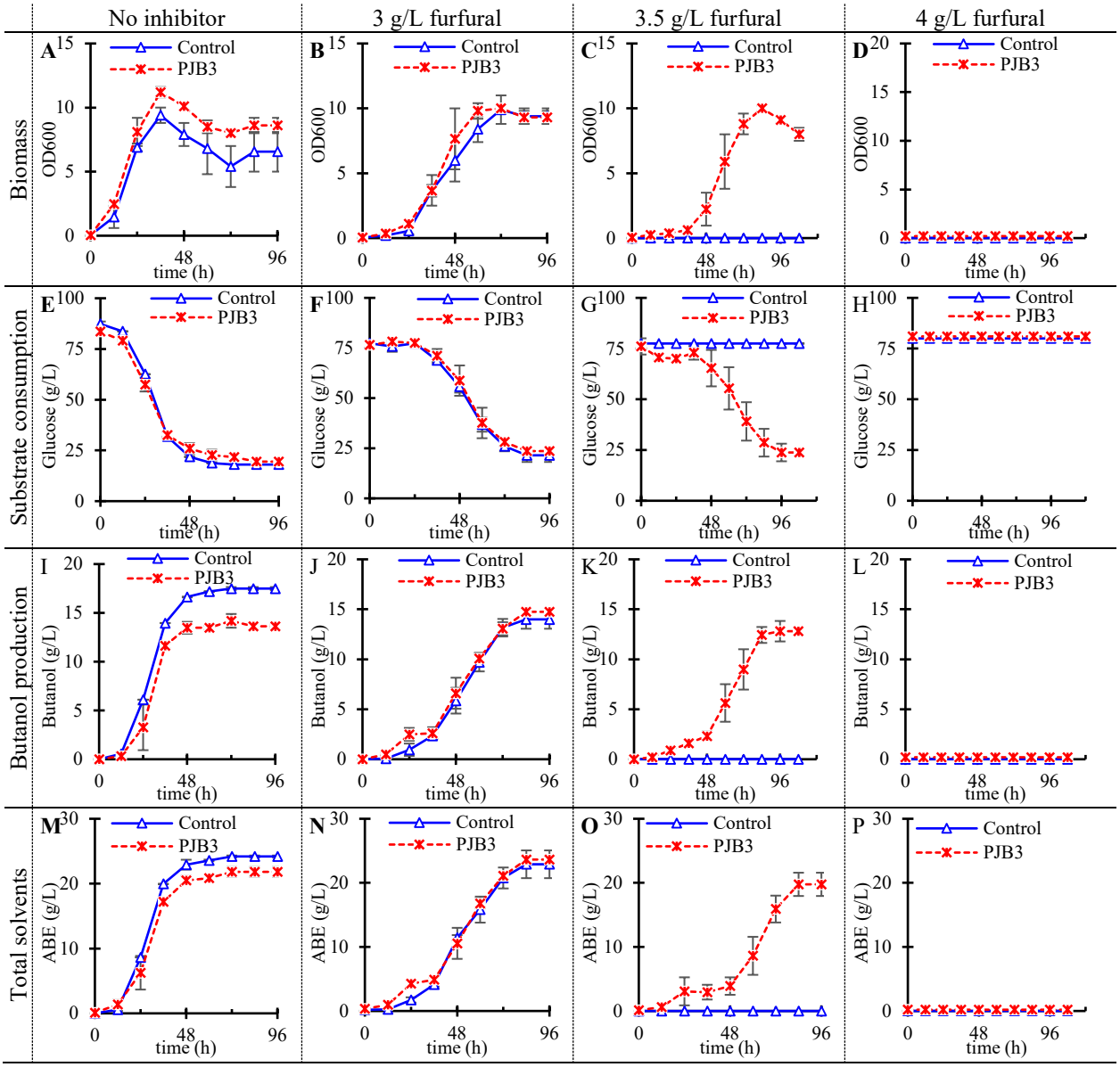

Figure 3.3 Fermentation profile comparison of strain expressing *srp*B (pPJB3) and control strain (pJZ100) with 0 g/L, 3 g/L, 3.5 g/L and 4 g/L of furfural.

Efflux pumps genes from *P. putida* such as *srp*ABC and *ttg*ABC (another pump also related to butanol tolerance) (Basler et al. 2018), contain complex regulation systems. The *ttg*ABC gene is expressed constitutively, but is also assumed to be induced by butanol by another regulator, in combination with efflux systems *ttg*DEF and *ttg*GHI (Basler et al. 2018). *ttg*GHI is the most similar

to *srp*ABC from the transporters mentioned above, in terms of their function and the repression-related clusters (Basler et al. 2018). *ttg*GHI is locally regulated by the repressor *ttg*V. The genes *ttg*V and *ttg*W (an inactive pseudogene) are located upstream from the structural genes *ttg*GHI and are transcribed divergently from this operon; *ttg*V is a repressor for the promoter of *ttg*GHI and *ttg*VW (itself), derepressed by small alcohols and other compounds (Sun et al. 2011). The genes *srp*SR are homologous to *ttg*VW, whereas *srp*S is a repressor of *srp*A, but *srp*R has been identified as an antirepressor regulated by solvents (Sun et al. 2011). Therefore, it is not trivial to optimize the expression level of efflux pumps; such regulation systems as descried above need to be carefully investigated and manipulated. Manipulation of this repression/antirepression systems is not reported, but, they are have a great potential, because they can dynamically control the expression level to respond to different inhibitor concentration over the time, minimizing the toxicity. This is not possible, using the regulators reported before: plasmids of different copy number (Bui et al. 2015), general inducible promoters (Dunlop et al. 2011), stress induced promoters (Boyarskiy et al. 2016), or a combination of the above mentioned.

3.3.3 Effects of the overexpression of efflux pump genes on the strain tolerance to phenolic inhibitors

Phenolic compounds are another group of inhibitors for the fermentation that could be generated during the biomass pretreatment from the lignin degradation. Ferulic acid has been reported previously as a model compound for phenolic biomass inhibitors (Winkler and Kao 2011), and thus we selected it as a representative to evaluate the effects of *srp*B overexpression on the strain tolerate to phenolic inhibitors. As shown in Fig. 3.4, at 0.8 g/L ferulic acid, the dynamics in terms of the glucose consumption, cell growth, and solvent production for PJB3 were all slightly faster than that of control strain. Also, PJB3 produced slightly higher butanol and total solvent

(Fig. 3.4I&M). When the concentration of ferulic acid was further increased to 1.0 g/L, the control could not grow any more, while PJB3 could still grow to about the similar OD_{600}, and produced the similar level of butanol (14.1 g/L vs 14.5 g/L at 0.8 g/L ferulic acid) and slightly lower total solvent (18.0 g/L vs 23.0 g/L at 0.8 g/L ferulic acid) as the fermentation at 0.8 g/L ferulic acid.

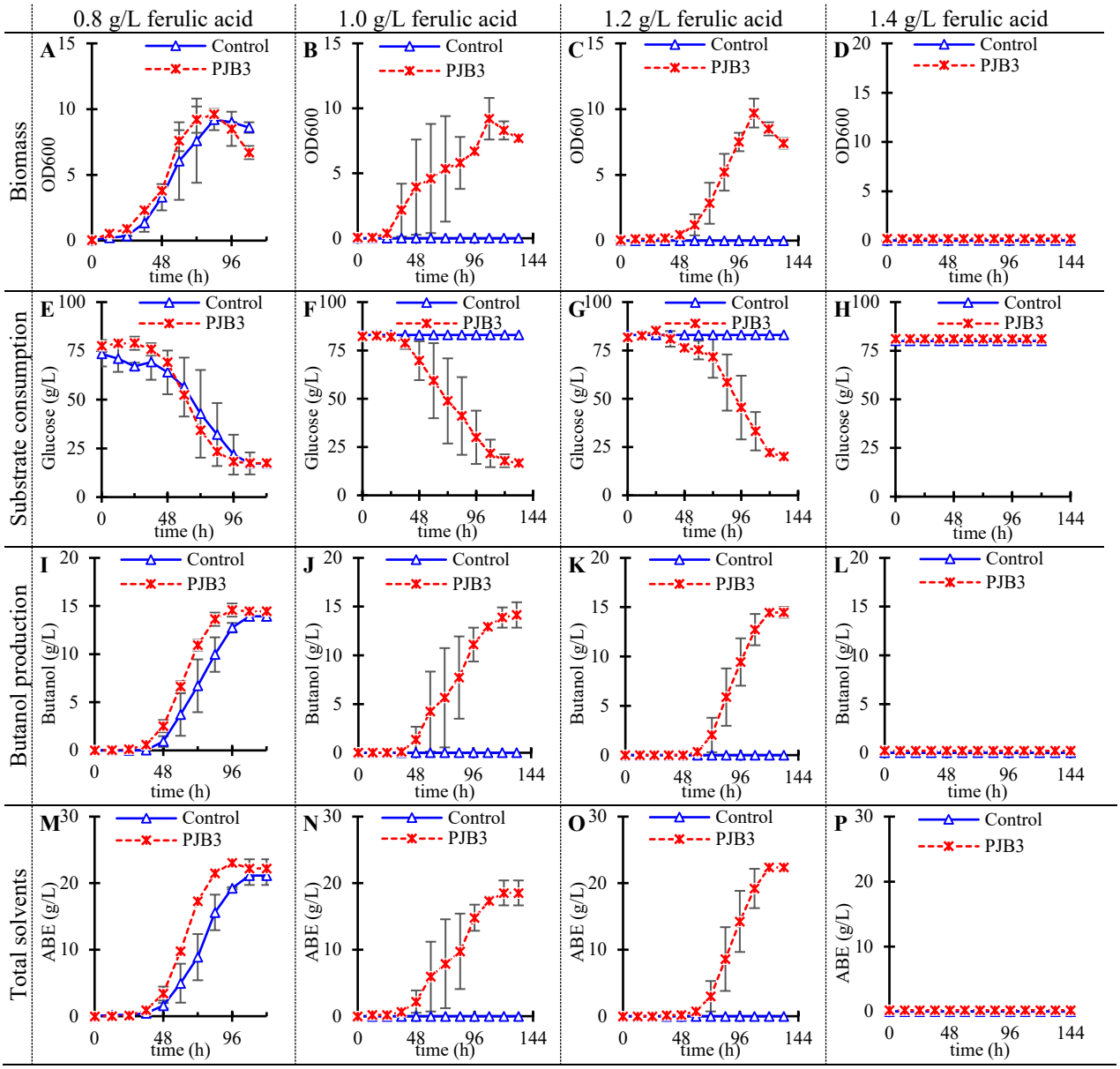

Figure 3.4 Comparison of fermentation profiles of strain expressing *srp*B (pPJB3) and control strain (pJZ100) with 0.8 g/L, 1.0 g/L, 1.2 g/L, and 1.4 g/L ferulic acid.

Further, when the concentration of ferulic acid increased to 1.2 g/L, PJB3 could still grow to the similar of OD_{600}, and produced about the same amount butanol and solvent as the fermentation at 0.8 g/L ferulic acid, although the lag phase is slightly longer (65.6 h vs. 56.6 h at 1.0 g/L ferulic acid). When 1.4 g/L ferulic acid, neither PJB3 nor the control strain could grow. Overall, the results are consistent with our previous report that *C. saccharoperbutylacetonicum* N1-4 can tolerate up to 0.8 g/L furfural. While the overexpression of *srp*B could enhance the strain to tolerate up to 1.2 g/L ferulic acid.

It has been reported that the inhibition severity of the phenolic inhibitors on *C. saccharoperbutylacetonicum* N1-4 is in the order of *p*-coumaric acid > syringaldehyde > ferulic acid (Cho et al. 2009). In addition, it has been deduced that the cellular detoxification mechanism for phenolic inhibitors probably involves a biotransformation process; however, the corresponding bioproducts have not been identified yet. In the real biomass hydrolysates, phenolic compounds with various chemical natures are generated, and thus the inhibition mechanism could be much more complicated and warrant more systematic investigation.

3.3.4 Model fit of the profile of fermentation with inhibitors

In order to make a better description and understanding of the inhibition phenomena, we proceed to fit our data into some models. Inhibition is sometimes described as a percent of improvement at fixed conditions, but different condition chosen can generate very different results, for example, butanol production of PJB3 at 0.8 g/L is 64% higher at 72h, but about the same at 120 h (figure 3.4(I)). Some researchers use the growth rate or the production rate to analyze the inhibition, but in some cases, the inhibition affect the lag time, or the maximum value instead.

Models have applied to fit the fermentation profiles of the mutant strain vs. the control when various levels of inhibitors were added, following a procedure as described previously (Chen and Zeng 2018). We decided to model butanol production instead of growth, because *Clostridium* growth does not fit the models very well, since models do not consider autolytic activity. Values of the parameters λ (lag time (h)), $\mu(t)$ (cumulative butanol production (g L^{-1}) at time t), B (maximum titer(g L^{-1})) and μ_{max} (maximum butanol production rate (g L^{-1} h^{-1})) were determined and adjusted with a good fit to either the Gompertz (Eq.3.1) or logistic (Eq. 3.2) model.

$$\mu(t) = Be^{-e^{\frac{\mu_{max}\times e}{B}(\lambda-t)+1}} \quad (Ec.3.1)$$

$$\mu(t) = \frac{B}{1+e^{\frac{4\times\mu_{max}\times e}{B}(\lambda-t)+2}} \quad (Ec.3.2)$$

Meanwhile, the inhibition of B was modelled using Eq.3.3, whereas $\mu_{max,i}$ is the maximum production rate with inhibitors, $\mu_{max,0}$ is the maximum rate without inhibitor; I is the inhibitor concentration (g L^{-1}); I_{lethal} is the lethal inhibitor concentration (g L^{-1}); n is a constant, related to the severity of inhibition. Eq.3.4 is used for the modeling of B, which is same as Eq. 3.3, just replacing parameters related to μ with parameters related to B.

$$\mu_{max,i} = \mu_{max,0}\left[1-\left(\frac{I}{I_{lethal}}\right)^{n}\right] \text{ (Ec.3.3)}$$

$$B_i = B_0\left[1-\left(\frac{I}{I_{lethal}}\right)^{n}\right] \text{ (Ec.3.4)}$$

Finally, lag time was approximated to the Ec. 3.5.

$$\lambda_i = -\lambda_0\left[\left(\frac{-k}{I-I_{lethal}}+\frac{1}{I_{lethal}}\right)-1\right] \text{ (Ec.3.5)}$$

Fig. 3.5 shows the trend of these parameters with the increase of inhibitor concentrations based on the fermentation results vs. the values of the same parameters obtained based on the model simulation, while table 3.2 summarize parameter values. The experimental data generally fit the model well except for μ_{max} of pPJB3. The μ_{max} value for the *srpB* strain decreased significantly from the fermentation with 0 g/L furfural to the fermentation with 3 g/L furfural. Similar trend was observed for the fermentation with ferulic acid (that is, the μ_{max} value for the *srpB* strain decreased significantly from the fermentation with 0 g/L ferulic acid to the fermentation with 1.2 g/L ferulic acid). This indicated that the efflux pumps could play a more significant role in the fermentation with high concentrations of inhibitors present. Thus, the engineered strain with efflux pump gene overexpressed could be employed for efficient fermentation of lignocellulosic biomass hydrolysates with high levels of inhibitors.

Table 3.2 Summary of parameter values in the simulation models based on the fermentation results at different concentrations of inhibitors

	strain	Cn (g/L)	μ_{max} (g/L-h)	λ (h)	B (g/L)	n (μ)	n (B)
Furfural	Control	0.0	0.6541	14.66	17.49	4.39	10.4
		3.0	0.3215	29.77	13.99		
		3.5	0.0000	∞	0.00		
	PJB3	0.0	0.6970	19.3	14.18	2.28	15.7
		3.0	0.3330	28.15	14.75		
		3.5	0.2873	40.71	12.43		
		4.0	0.0000	∞	0.00		
***trans*-ferulic acid**	Control	0.0	0.6541	14.66	17.49	2.39	3.82
		0.8	0.2701	47.13	13.93		
		1.0	0.0000	∞	0.00		
	PJB3	0.0	0.6970	19.3	14.18	1.85	90.1
		0.8	0.3579	41.46	14.58		
		1.0	0.2821	56.64	14.14		
		1.2	0.3202	65.62	14.45		
		1.4	0.0000	∞	0.00		

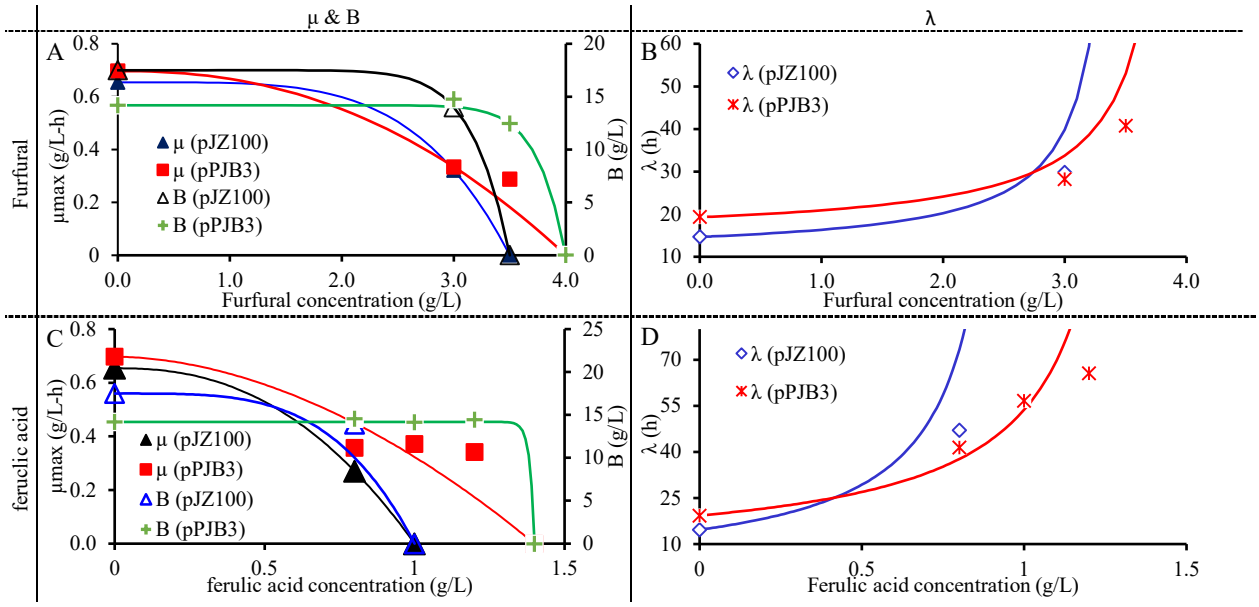

Figure 3.5 Trends of modeling variables against inhibition concentration, for butanol fermentations. Continuous lines represent the models simulation, and the individual points represent the experimental data.

The lag time shows an increasing trend with the increase of the inhibitor concentrations. It is worthwhile to mention that, lag time during the fermentation with inhibition is also influenced by the initial inoculum volume for the fermentation (Pereira, Verheijen, and Straathof 2016). This means that the microorganism could survive at higher concentrations of inhibitors if it is allowed to reach a higher cell density before the inhibition challenge is applied. Such a strategy, although does not represent the actual case for the fermentation with hydrolysates, could help explain why some studies can make the strain tolerate to higher concentrations of inhibitors (Chen and Zeng 2018). In addition, this indicates that, during the fermentation with inhibitory conditions, it is critical to make the culture survive at the beginning of the fermentation, in order to let the

microorganism thrive and produce the products. Thus, for future studies, it would be interesting to elucidate the cell metabolism and inhibitory mechanism at the beginning of the fermentation. A possible explanation about why the lag phase generate a greater change than B or μ is that the main cellular detoxification mechanism for many of these compounds is the transformation into the corresponding alcohol, as reported before (Yao et al. 2017). Furan alcohols are significant less toxic than the analogue aldehydes. This process occurs during the beginning of the fermentation.

3.4 Conclusions

The overexpression of efflux pump gene *srpB* from *P. putida* in *C. saccharoperbutylacetonicum* enhanced the tolerance of the strain against butanol, furfural and ferulic acid. Compared to the control strain, although the mutant produced slightly decreased butanol under regular fermentation conditions with no inhibitors, the mutant strain was capable to grow in media containing up to 3.5 g/L furfural (the control can only tolerate to 3.0 g/L) or 1.2 g/L ferulic acid (the control can only tolerate to 0.8 g/L), and was still able to produce 14 g/L butanol.

3.5 Acknowledgments

This work was supported by supported by the USDA-NIFA Southeastern Sun Grant, the Auburn University Intramural Grants Program (IGP), the USDA-NIFA Hatch project (ALA014-1017025), and the Alabama Agricultural Experiment Station. We thank Dr. Nick Wierckx and M.Sc. Maike Otto from RWTH Aachen University, Germany for generously providing the genomic DNA of *P. putida* S12

References

Anes, João, Matthew P McCusker, Séamus Fanning, and Marta Martins. 2015. The ins and outs of RND efflux pumps in Escherichia coli. *Frontiers in microbiology* 6:587.

Basler, Georg, Mitchell Thompson, Danielle Tullman-Ercek, and Jay Keasling. 2018. A Pseudomonas putida efflux pump acts on short-chain alcohols. *Biotechnology for biofuels* 11 (1):136.

Boyarskiy, Sergey, Stephanie Davis López, Niwen Kong, and Danielle Tullman-Ercek. 2016. Transcriptional feedback regulation of efflux protein expression for increased tolerance to and production of n-butanol. *Metabolic engineering* 33:130-137.

Bui, Le Minh, Ju Young Lee, Almando Geraldi, Ziaur Rahman, Jun Hyoung Lee, and Sun Chang Kim. 2015. Improved n-butanol tolerance in Escherichia coli by controlling membrane related functions. *Journal of biotechnology* 204:33-44.

Chen, Wen-Hsing, and Yan-Ru Zeng. 2018. Mathematical model to appraise the inhibitory effect of phenolic compounds derived from lignin for biobutanol production. *Bioresource technology* 261:44-51.

Cho, Dae Haeng, Yun Jie Lee, Youngsoon Um, Byoung-In Sang, and Yong Hwan Kim. 2009. Detoxification of model phenolic compounds in lignocellulosic hydrolysates with peroxidase for butanol production from Clostridium beijerinckii. *Applied microbiology and biotechnology* 83 (6):1035-1043.

Dunlop, Mary J, Zain Y Dossani, Heather L Szmidt, Hou Cheng Chu, Taek Soon Lee, Jay D Keasling, Masood Z Hadi, and Aindrila Mukhopadhyay. 2011. Engineering microbial biofuel tolerance and export using efflux pumps. *Molecular systems biology* 7 (1):487.

Gibson, Daniel G, Hamilton O Smith, Clyde A Hutchison III, J Craig Venter, and Chuck Merryman. 2010. Chemical synthesis of the mouse mitochondrial genome. *Nature methods* 7 (11):901.

Jiménez-Bonilla, Pablo, and Yi Wang. 2018. In situ biobutanol recovery from clostridial fermentations: a critical review. *Critical reviews in biotechnology* 38 (3):469-482.

Kieboom, Jasper, Jonathan J Dennis, Gerben J Zylstra, and Jan AM De Bont. 1998. Active Efflux of Organic Solvents byPseudomonas putida S12 Is Induced by Solvents. *Journal of bacteriology* 180 (24):6769-6772.

Liu, Siqing, Kenneth M Bischoff, Timothy D Leathers, Nasib Qureshi, Joseph O Rich, and Stephen R Hughes. 2012. Adaptation of lactic acid bacteria to butanol. *Biocatalysis and Agricultural Biotechnology* 1 (1):57-61.

Moon, Hyeon Gi, Yu-Sin Jang, Changhee Cho, Joungmin Lee, Robert Binkley, and Sang Yup Lee. 2016. One hundred years of clostridial butanol fermentation. *FEMS microbiology letters* 363 (3).

Nikaido, Hiroshi. 2018. RND transporters in the living world. *Research in microbiology* 169 (7-8):363-371.

Nikaido, Hiroshi, and Yumiko Takatsuka. 2009. Mechanisms of RND multidrug efflux pumps. *Biochimica et Biophysica Acta (BBA)-Proteins and Proteomics* 1794 (5):769-781.

Patakova, Petra, Jan Kolek, Karel Sedlar, Pavlina Koscova, Barbora Branska, Kristyna Kupkova, Leona Paulova, and Ivo Provaznik. 2018. Comparative analysis of high butanol tolerance and production in clostridia. *Biotechnology Advances* 36 (3):721-738.

Pereira, Joana PC, Peter JT Verheijen, and Adrie JJ Straathof. 2016. Growth inhibition of S. cerevisiae, B. subtilis, and E. coli by lignocellulosic and fermentation products. *Applied microbiology and biotechnology* 100 (21):9069-9080.

Ramos, Juan-Luis, Maria Sol Cuenca, Carlos Molina-Santiago, Ana Segura, Estrella Duque, María R Gómez-García, Zulema Udaondo, and Amalia Roca. 2015. Mechanisms of solvent resistance mediated by interplay of cellular factors in Pseudomonas putida. *FEMS microbiology reviews* 39 (4):555-566.

Rühl, Jana, Andreas Schmid, and Lars Mathias Blank. 2009. Selected Pseudomonas putida strains able to grow in the presence of high butanol concentrations. *Applied and environmental microbiology* 75 (13):4653-4656.

Sun, Xu, Zileena Zahir, Karlene H Lynch, and Jonathan J Dennis. 2011. An anti-repressor, SrpR, is involved in transcriptional regulation of the SrpABC solvent tolerance efflux pump of Pseudomonas putida S12. *Journal of bacteriology* 193 (11):2717-2725.

Tal, Nir, and Shimon Schuldiner. 2009. A coordinated network of transporters with overlapping specificities provides a robust survival strategy. *Proceedings of the National Academy of Sciences* 106 (22):9051-9056.

Winkler, James, and Katy C Kao. 2011. Transcriptional analysis of Lactobacillus brevis to N-butanol and ferulic acid stress responses. *PloS one* 6 (8):e21438.

Xu, Mengmeng, Jingbo Zhao, Le Yu, I-Ching Tang, Chuang Xue, and Shang-Tian Yang. 2015. Engineering Clostridium acetobutylicum with a histidine kinase knockout for enhanced n-butanol tolerance and production. *Applied microbiology and biotechnology* 99 (2):1011-1022.

Yao, Dunfan, Sheng Dong, Pixiang Wang, Tianhu Chen, Jin Wang, Zheng-Bo Yue, and Yi Wang. 2017. Robustness of Clostridium saccharoperbutylacetonicum for acetone-butanol-ethanol production: Effects of lignocellulosic sugars and inhibitors. *Fuel* 208:549-557.

Zhang, Jie, Pixiang Wang, Xiaofei Wang, Jun Feng, Hardev S Sandhu, and Yi Wang. 2018. Enhancement of sucrose metabolism in Clostridium saccharoperbutylacetonicum N1-4 through metabolic engineering for improved acetone–butanol–ethanol (ABE) fermentation. *Bioresource Technology* 270:430-438.

Zhang, Zhong-Tian, Pablo Jiménez-Bonilla, Seung-Oh Seo, Ting Lu, Yong-Su Jin, Hans P Blaschek, and Yi Wang. 2018. Bacterial Genome Editing with CRISPR-Cas9: Taking Clostridium beijerinckii as an Example. In *Synthetic Biology*, edited by B. J. New York, NY: Humana Press.

Chapter IV.

Identification and deletion of the autolysin genes in *Clostridium saccharoperbutylacetonicum* N1-4

Supplementary material is available in appendix IV.

Abstract

Biobutanol is a valuable biochemical and one of the most promising biofuels. *Clostridium saccharoperbutylacetonicum* N1-4 is a hyper-butanol producing strain. However, its applicability at industrial scale is limited by its strong autolytic behavior, which leads to poor stability especially under continuous fermentation processes. Autolysis is the process of cell self-lysis, and thus it reduces the number of active cells, with a negative impact on the butanol production. Also, the autolysis makes it unstable and difficult for the long-term continuous fermentation. In this study, we have identified four significant autolysin encoding genes and deleted them from the genome of *C. saccharoperbutylacetonicum* N1-4, in order to increase the strain stability, and enhanced butanol production. Firstly, putative autolysin encoding genes were identified based on the comparison of amino acid sequence homologous with related strains of which the autolysin encoding genes are well characterized. Then, these putative genes were overexpressed and cell growth curves of the recombinant strains were compared with that of the control. Those genes which demonstrated elevated autolytic effects were deleted using our customized CRISPR-Cas9 gene-editing tool. Fermentation characterization demonstrated enhanced performance of the mutants during fermentation.

***Keywords*:** Autolysis, fermentation, biobutanol, *Clostridium*, CRISPR-Cas9

4.1 Introduction

Biobutanol production from low-value renewable resources attracts great interests as a potential biofuel source and biochemical feedstock with various applications. However, currently there are still various limitations on butanol production in an economically competitive manner including the low yield, low productivity and low final concentration.

Clostridium saccharoperbutylacetonicum N1-4 is a hyper-butanol producing strain, which can produce around 17 g/L of butanol in a regular batch fermentation (Wang et al. 2017). This is significantly higher than other prominent butanol producing strains, such as *C. beijerinckii* (10 g/L) (Wang, Li, and Blaschek 2013) and *C. acetobutylicum* (8 g/L) (Al-Shorgani et al. 2018). However, *C. saccharoperbutylacetonicum* N1-4 is known for its instability for a long term fermentation (such as the continuous fermentation process), which limits its potential industrial applications for butanol production.

Autolysis activity is known in many *Clostridium* genus. Autolysins are responsible for the hydrolysis of different components of cell wall (Figure 4.1). They also play roles in processes such as motility, cell separation, cell elongation, peptidoglycan maturation, cell wall turnover, germination, sporulation and induced lysis (Smith, Blackman, and Foster 2000). Spontaneous autolysis leads to significant loss of cell biomass, and an obvious stationary phase could be missing in the growth curve of most butanol-producing clostridia (Liu et al. 2015), including *C. saccharoperbutylacetonicum* N1-4. Induced autolysis (accompanied by sporulation) also occurs during chemical induced-stress, such as butyrate, acetate, oxygen and butanol stresses (Branska et al. 2018).

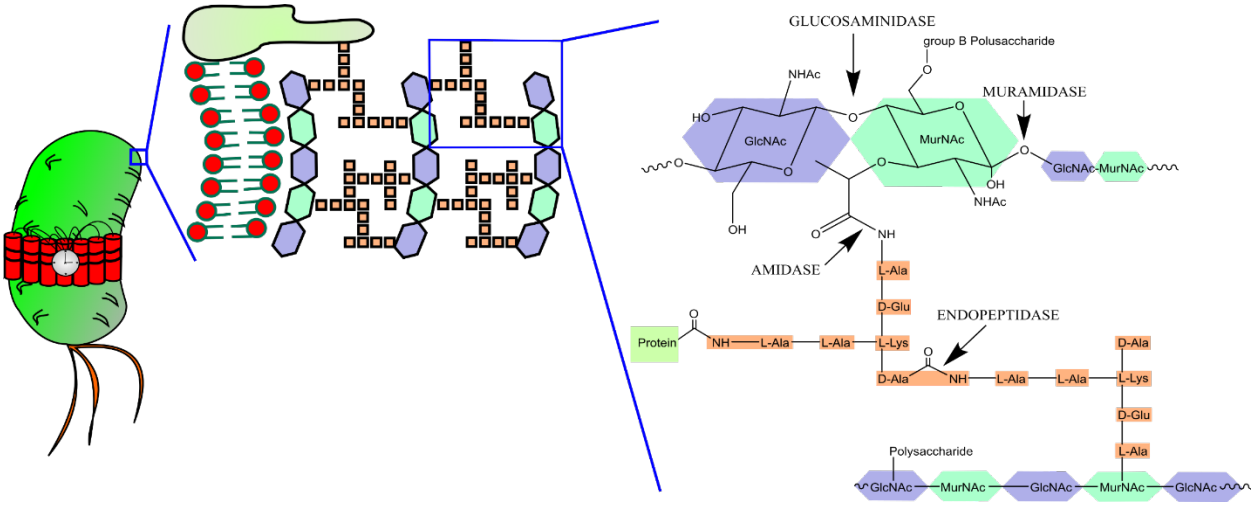

Figure 4.1 Autolysin groups by hydrolytic activity

Some autolysins have been reported in solventogenic clostridia, such as *lyt*-1 (from *C. acetobutylicum* P262), CA_C0554, SMB_G3117, (from *C. acetobutylicum* ATCC824) (Croux and García 1991; Croux et al. 1992), SMB_G2359, and SMB_G3117 (from *C. acetobutylicum* DSM 1731) (Yang et al. 2013). CA_C0554 is known to play an important role in sporulation (Liu et al. 2015), and the disruption of SMB_G3117 generated an significant increase in the cell biomass (Yang et al. 2013). Some *N*-acetylmuramidases have also been isolated from extracellular components of *C. saccharoperbutylacetonicum* (ATCC 13564) (Yoshino, Ogata, and Hayashida 1982).

Identification and deletion of autolysin genes can not only help to keep the level of cell biomass and increase the butanol titer, but also increase the stability of the strain, the cell recyclability, and the performance during long term continuous fermentations.

In this study, we identified the autolysin genes in *C. saccharoperbutylacetonicum* N1-4 based on the homologous analysis using BLAST, and then further confirmed by comparing the growth curves of the strains overexpressing 16 putative autolysins individually to a control strain.

We further deleted those genes the overexpression of which led to significant reduction of cell biomass using customized CRISPR-Cas9 system. Further characterization of the mutants was performed through fermentation.

4.2 Materials and methods

4.2.1 Reagents and strains

Phanta HS Super-Fidelity DNA Polymerase and ClonExpress MultiS One Step Cloning Kit from Vazyme Biotech (Nanjing, China) were used for PCR cloning purposes, and plasmid construction through DNA assembly, respectively. Taq DNA polymerase (Green Mountains Biosystems, Ann Arbor, MI) and LongAmp Taq from (New England BioLabs Inc., Ipswich, MA) were used for colony PCR (cPCR) to confirm the mutation. *Btg*ZI and *Not*I restriction enzymes were obtained from New England BioLabs Inc. (Ipswich, MA). All polymerases and restriction enzymes were used following manufacturer's protocol. *E. coli* NEB express (New England BioLabs Inc., Ipswich, MA) was used for plasmid propagation. *E. coli* was cultivated in Luria-Bertani (LB) broth or LB agar plates, supplemented with 100 μg/mL of carbenicillin when needed. *C. saccharoperbutylacetonicum* N1-4 (HMT) (DSM 14923) obtained from DSMZ (Braunschweig, Germany), was routinely cultivated in Tryptone/Glucose/Yeast extract (TGY) broth containing 30 g/L of tryptone, 20 g/L of sucrose, 10 g/L of yeast extract, and 1 g/L of L-cysteine, or in TGY agar solid plates, in an anaerobic chamber at 35 ºC. 30μg/mL clarithromycin (Cla^+) and/or 40mM lactose were supplemented when necessary. Phage deficient strains *C. saccharoperbutylacetonicum* Δ1234 and Δ12345 were generated by Dr. Jun Feng, and cultivated in same conditions as wild type. SMP buffer used for electrotransformation is composed of 270 mM sucrose, 1mM $MgCl_2$, and 7mM Na_2HPO_3/NaH_2PO_3 (pH adjusted to 6.5 and filter sterilized).

Clostridium strains were stored at -80 °C in glycerol stocks (20-30%). The stock was inoculated into TGY at 5% inoculum, and the culture was incubated at 35 °C for overnight.

4.2.2 Overexpression of putative autolysin

pJZ100 (Zhang, Wang, et al. 2018), a derivative from pTJ1, was used as the mother vector to construct the mother vector pPJB14. The pPJB14 plasmid was constructed by inserting the lactose inducible promoter (P_{lac}) from *C. perfringens*, the *Btg*ZI restriction site, the thiolase terminator from *C. saccharoperbutylacetonicum* N1-4 (T*thl*) between the *Apa*I and *Bam*HI restriction sites. Digestion on *Apa*1 and *Btg*ZI sites of pJZ100 were done in order to replace P_{thl} with P_{lac}. Primers YW2583, and YW2584 (Table S4.1) were used to clone P_{lac} from plasmid pYW51 (Table S4.2).

15 putative autolysin encoding genes (CSPA_RS26630, CSPA_RS03200, CSPA_RS08050, CSPA_RS01160, CSPA_RS21780, CSPA_RS09105, CSPA_RS06245, CSPA_RS00240, CSPA_RS18890, CSPA_RS13245, CSPA_C38900, CSPA_RS11880, CSPA_RS15280, CSPA_RS03880, CSPA_135p00690, CSPA_RS24880) from *C. saccharoperbutylacetonicum* N1-4 were identified using NCBI Blast tool based on the homologous amino acid sequences from previously identified autolysin encoding genes in related strains (Yang et al. 2013).

pPJB14 was digested using *Btg*ZI. DNA fragments of putative autolysin genes were cloned individually by PCR, using the particular set of primers (Table S4.1) with genomic DNA as the template. Then, the fragment was ligated into the corresponding overexpression plasmid (pPJB15 to pPJB30, Table 4.1), propagated in *E. coli* NEB express, and electroporated into *C. saccharoperbutylacetonicum* N1-4.

Procedure for electroporation of *Clostridium* cells is modified from our previous published protocol (Zhang, Jiménez-Bonilla, et al. 2018). Approximately 20 mL of culture was prepared for per each transformation (TGY media, 35ºC, 5% inoculum, under anaerobic conditions). The cells were grown to the early exponential phase (OD_{600}=0.8), and collected by centrifugation (4,000 rpm, for 10 minutes, at room temperature). The supernatant was dumped and cells were re-suspended in SMP buffer (at the same original volume). Cells were harvested by centrifugation again, the cell pellet was re-suspended into 1/20 volume of SMP buffer, and chilled in ice for 20 min. 400 µl of this suspension was immediately mixed with 1 µg of plasmid DNA in an ice-cold 0.2 mm electroporation cuvette, and electroporation was delivered using a BioRad Gene Pulser (2.0 kV (1kV/mm), 25 µf, and 300 Ω). After electroporation, cells were mixed with 1.6 mL TGY (35 °C) and placed into the incubator until visible sign of cell growth was evident (light bubbling, usually takes around two hours). After that, cells were centrifuged again, suspended into 100 µL of TGY, plated onto TGY-Cla^+ agar plates, and incubated for 24-48 hours at 35 ºC under anaerobic conditions, until colonies appear.

4.2.3 Autolysin gene identification

The strain harboring the plasmid for overexpression of the autolysin gene (pPJB15 to pPJB30, as shown in Table 4.1) was grown in P2-TYL fermentation media containing 80 g/L of glucose, 13.7 g/L lactose, 6 g/L tryptone, 2 g/L yeast extract, 1 mg/L parabenzoic acid, 1 mg/L thiamine hydrochloride and 10 µg/L of biotin, 0.5 g/L of KH_2PO_4, 0.5 g/L of K_2HPO_4 and 2.20 g/L ammonium acetate, 200 mg/L $MgSO_4x7H_2O$, 10 mg/L $MnSO_4xH_2O$, 10 mg/L $FeSO_4x7H_2O$, and 10 mg/L NaCl, and supplemented with 30 mg/L clarithromycin. Fermentations were carried out in 500 mL bioreactors (GS-MFC, Shanghai Gu Xin Biological Technology Co., Shanghai, China) under anaerobic conditions. The fermentation was started with 5% inoculum from

preculture. The pH was started at 6.4, and controlled > 5.0 using 4 M of NaOH. The temperature for the fermentation was kept at 30 ºC. Samples were taken every 12 hours during a total fermentation time of 72 hours. At least two replicated were carried out for each fermentation. Cell biomass was determined as optical density at 600 nm, and the strain containing the empty plasmid (pPJB14) was used as the control. The data analysis was conducted by means of repeated ANOVA analysis.

4.2.4 Gene deletion

Genes are named from 15-30, and the plasmids were named correspondingly (that is, pPJBN indicates the plasmid carrying gene 'N' for overexpression; Table 4.1). Genes 26 and 30 (those corresponding to plasmids pPJB26 and pPJB30) were selected for deletion in *C. saccharoperbutylacetonicum* N1-4, Δ1234 and Δ12345 using our customized CRISPR-Cas9 genome editing system (Zhang, Jiménez-Bonilla, et al. 2018). Plasmid pYW51 was the mother vector used to construct the plasmid for gene deletion (Table S4.2). It is consisted of two homologous arms (1kb upstream and 1 kb downstream of the gene) cloned into *Btg*ZI site, the erythromycin selection marker, the Cas9 gene from *Streptococcus pyogenes* under the lactose inducible promoter, and the gRNA sequence. For the gRNA to bind to the target gene, small RNA promoter (P_{sRNA}) of *C. beijerinckii,* and a target sequence for Cas9 ds breakage ("20-NT") were cloned into the *Not*I restriction site. Plasmids pPJB31 and pPJB32, for the deletion of Genes 26 and 30 respectively, were constructed by cloning the recombination arms through overlap PCR of the fragments. Also, P_{sRNA} was cloned from *C. beijerinckii* genomic DNA, fused with the "20NT" designed in the primer. Refer supplementary Table S4.1 for detailed information about the primers used. Both fragments were ligated into the respective restriction sites of pYW51 as mentioned above.

Plasmids were transformed into the cells, and the culture was cultivated on TYG-Cla^+ agar plates. Antibiotic marker is used for the selection of transformants. A single colony from transformants was re-cultured into 2 mL of TGYL liquid and then 50 µL of it was plated into TGYL-Cla^+ agar plates, to induce the Cas9 activity for mutant selection. Mutation was confirmed by means of cPCR, using primers flanking the upstream and downstream of the targeted homologous recombination region (Table S4.1). Clean mutants were cultured in liquid TGY, plated onto TGY agar plate, and replicated-plating into TGY-Cla^+, in order to cure the plasmid. Some colonies from the TGY-Cla^- plate are unable to grow, when they were replicated plated on the TGY-Cla^+ Clean mutant with plasmid cured is confirm by being cultured in liquid TGY (Cla^+ and Cla^-; there should be no growth on TGY (Cla^+)), and by cPCR.

4.2.5 Serum bottle fermentation

Small scale fermentations were carried out in 250 mL serum bottles with a working volume of 100 mL for each fermentation for the 9 strains of *C. saccharoperbutylacetonicum*: N1-4, Δ26, Δ30, Δ1234, Δ1234Δ26, Δ1234Δ30, Δ12345, Δ12345Δ26, and Δ12345Δ30. The P2-TY medium for the fermentation contains 80 g/L glucose, 6 g/L tryptone, 2 g/L yeast extract, 1 mg/L parabenzoic acid, 1 mg/L thiamine hydrochloride, 10 µg/L of biotin, 0.5 g/L of KH_2PO_4, 0.5 g/L of K_2HPO_4, 2.20 g/L ammonium acetate, 200 mg/L $MgSO_4x7H_2O$, 10 mg/L $MnSO_4xH_2O$, 10 mg/L $FeSO_4x7H_2O$, and 10 mg/L NaCl. 5% inoculum was used, and the bottles were placed in an orbital shaker at 150 rpm and 30 ºC. Samples were taken every 24 hours for analysis.

4.2.6 Bioreactor fermentation

Batch fermentation of wild type, Δ1234 and Δ1234Δ26 strains were carried-out with replicates in Eppendorf New Brunswick BioFlo/Celligen 115 bioreactors with a working volume

of 1.5 L of P2-TY. The fermentation was carried out at 50 rpm, 30 ºC, and pH control > 5.0 (adjusted with 4M NaOH). Bioreactors were inoculated with a 5% preculture in TGY at early exponential stage (OD_{600}=0.8). Samples were taken every 12 hours for analysis.

4.3 Results

4.3.1 Identification of autolysin genes

Table 4.1 contains the analysis of homologous genes, with the putative autolysin genes grouped into families, the corresponding plasmids, the known gene from other strains and the % of identity. In our results, most significant activity was found for the muramidase encoding genes.

Figure 4.2 shows the growth curve of the 16 strains containing the putative autolysin genes. In all of them, the cell showed decreased growth than the control strain, suggesting that all of them are possibly related to the autolytic activity, although not such difference for all of them were found to be significant. The gray area represents this difference of cell growth (Figure 4.2). The data were analyzed by means of multiple Tukey test analysis. For this purpose, the curves were split at 36h, finding no significance difference during the exponential phase (up to 36 h) but significance (at 90% confidence level, $\alpha < 0.1$) in four samples (24, 26, 29, and 30) during the steady and death phase (after 36 h). The p-value is shown at the top of each profile in Figure 4.2. From these four genes 24, 26, 29 and 30 (corresponding to the plasmid number), two (24, 29) of them have already been deleted in two bacteriophage-deficient strain (N1-4Δ1234 and N1-4Δ12345) provided by Dr. Jun Feng (unpublished data). For this reason, we decided to delete the other two genes (26 and 30) in all the three strains of N1-4 wild type, Δ1234 and Δ12345.

Table 4.1 Fifteen putative autolysin genes in *C. saccharoperbutylacetonicum* N1-4

Family	Plasmid	Homolog gene (N1-4)	Mother gene	% query	% identity	Organism
Endopeptidases	pPJB15	CSPA_RS26630	ydilL (BSU06010)	37%	33%	*B. subtilus* 168
	pPJB16	CSPA_RS03200	ydilL (BSU06010)	56%	26%	*B. subtilus* 168
		no significant similarities	ypbD (BSU23010)			*B. subtilus* 168
		no significant similarities	yyaK (BSU40830)			*B. subtilus* 168
Glucosaminidases	pPJB17	CSPA_RS08050	lytD (BSU35780)	3%	48%	*B. subtilus* 168
		no significant similarities	lytD (SMB_G2359)			*C. acetobutylicum* DSM 1731
N-acetyl-alanine amidases		no significant similarities	cwlJ (BSU02600)			*B. subtilus* 168
	pPJB18	CSPA_RS01160	ykvT (BSU13820)	85%	41%	*B. subtilus* 168
			sleB (BSU22930)	68%	56	*B. subtilus* 168
			sleB (SMB_G3117)	36%	44%	*C. acetobutylicum* DSM 1731
	pPJB19	CSPA_RS21780	sleB (SMB_G3117)	16%	37%	*C. acetobutylicum* DSM 1731
	pPJB20	CSPA_RS09105	sleB (SMB_G3117)	20%	28%	*C. acetobutylicum* DSM 1731
	pPJB21	CSPA_RS06245	sleB (SMB_G3117)		52%	*C. acetobutylicum* DSM 1731
Muramidases	pPJB22	CSPA_RS00240	ykuG (BSU14071)	5%	41%	*B. subtilus* 168
	pPJB23	CSPA_RS18890	lyc (CA_C0554)	56%	41%	*C. acetobutylicum* ATCC 824
	pPJB24	CSPA_RS13245	lyc (CA_C0554)	67%	36%	*C. acetobutylicum* ATCC 824
	pPJB25	Cspa_c38900	lyc (CA_C0554)	56%	41%	*C. acetobutylicum* ATCC 824
	pPJB26	CSPA_RS11880	lyc (CA_C0554)	56%	37%	*C. acetobutylicum* ATCC 824
	pPJB27	CSPA_RS15280	lyc (CA_C0554)	58%	38%	*C. acetobutylicum* ATCC 824
	pPJB28	CSPA_RS03880	lyc (CA_C0554)	60%	34%	*C. acetobutylicum* ATCC 824
	pPJB29	Cspa_135p00690	lyc (CA_C0554)	57%	34%	*C. acetobutylicum* ATCC 824
	pPJB30	CSPA_RS24880	lyc (CA_C0554)	53%	26%	*C. acetobutylicum* ATCC 824

The recently published strain N1-4-C (Gu et al. 2019) is the parental strain of Δ1234 and Δ12345. N1-4-C was prepared by curing the endogenous megaplasmid, and this deletion lead to a small increase in solvent production. The authors explain the solvent increase is because of the possible presence of a temperate bacteriophage, but fail to verify that hypothesis. Autolysin 29

(Cspa_135p00690), which generates significant autolysin activity (Figure 4.2), is located on the megaplasmid. This is a possible explanation on the increase of the solvent production on N1-4-C strain versus the parental wild type strain, whether the autolysin gene belongs to a temperate bacteriophage or not. Autolysin 24 is contained in a putative bacteriophage and is probably used by the phage to enter into lytic cycle.

4.3.2 Phenotype of the autolysin deficient mutants

Clean single deletion of Genes 26 and 30 based on the three strains (N1-4 wild type, Δ1234 and Δ12345) were obtained. Primers YW5195 & YW5196 were used for the detection of mutant 26, and YW5203 & YW5204 for mutant 30 using cPCR. Figure 4.3 showed the confirmation of the mutation: Gene 26 has a size of 1,980 bp and Gene 30 has a size of 942 bp. Figure 4.3 G also showed the scheme for the gene editing in these strains.

We were unable to obtain the double mutant (Δ26Δ30) in any of these strains, despite many attempts. We concluded that it might not be feasible to obtain such a mutant. Although the reason behind this is not very clear, autolysin genes are related to important biological processes such as the cell division and the sporulation.

We run small scale batch fermentations in serum bottles in order to study the phenotype of the single mutant. Figure 4.4 showed the cell biomass and metabolites profiles of the fermentations. Deletion of Gene 30 did not produce a detectable effect on fermentation performance, except for Δ30, which suffered acid crash. Deletion of gene 26 did generate an increase in the cell biomass with higher maximum optical density in wild type (16.8 vs 14.6) and Δ12345 (18.8 vs 17.6), and a similar maximum but with slower decrease in Δ1234. Strain

Δ1234Δ26 produced the highest cell biomass (OD_{600} of 19), and produced the highest level of butanol.

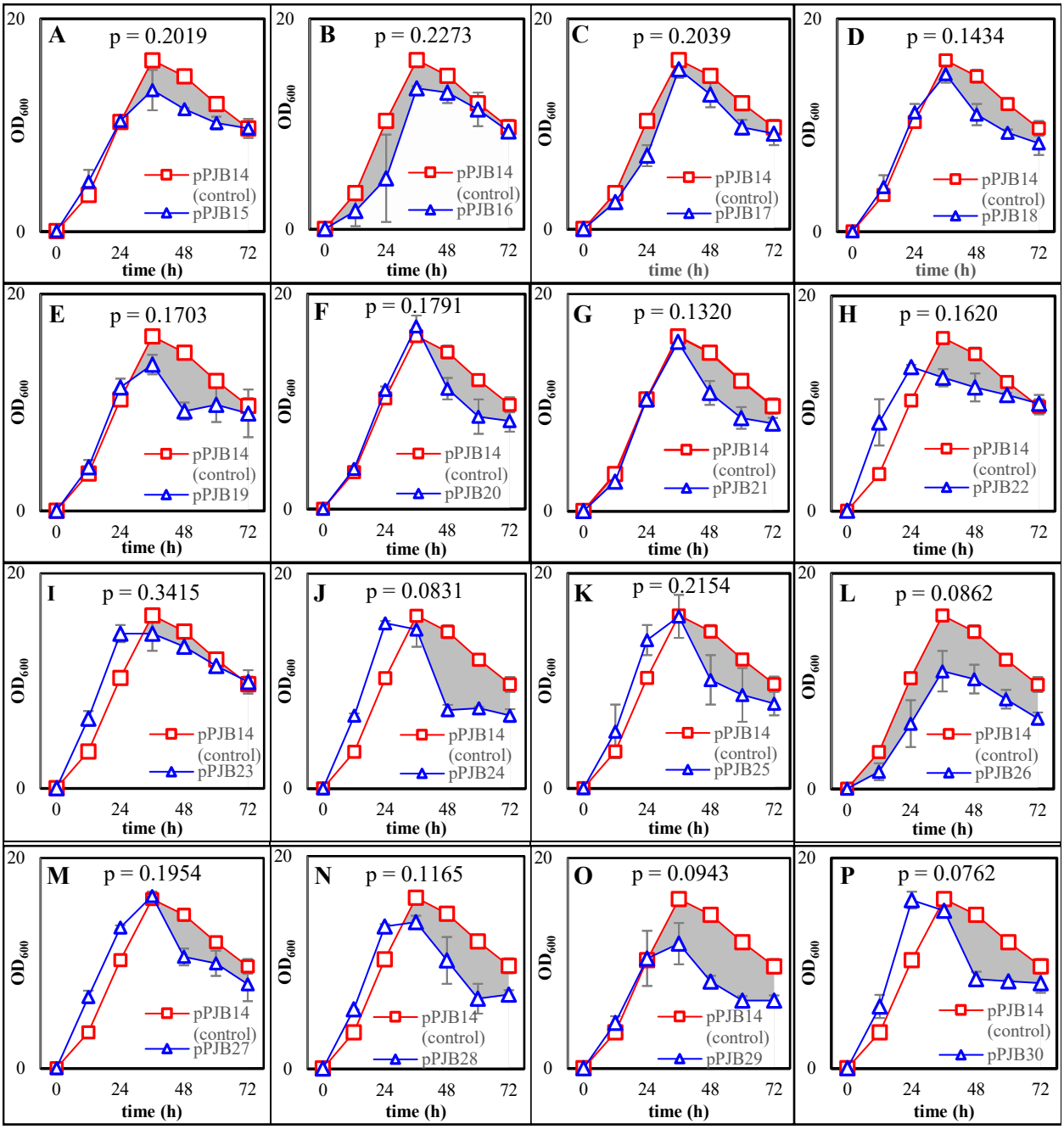

Figure 4.2 Growth curves of six strains overexpressing the putative autolysin gene. P-value for repeated measures ANOVA comparison during stationary/death phase (36 h-72 h) is included on the top of each profile. The error bars represents the standard error at 95% interval of confidence.

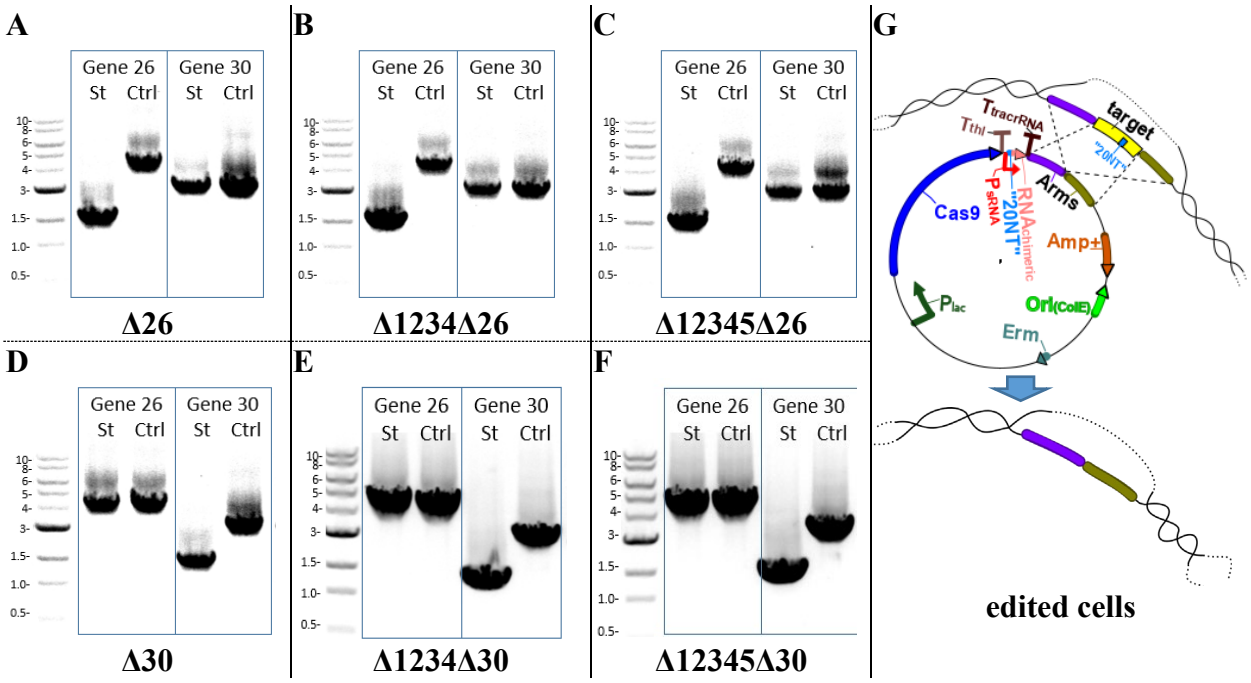

Figure 4.3 A)-F): Agarose gel electropherogram showed the PCR results confirming the gene deletion in the mutant strain (St) versus control (Ctrl), which are 4166 vs 2186, and 3070 vs 2125 for genes 26 and 30, respectively. Length of genes 1980 (gene 26) and 945 bp (gene 30). G) Scheme of gene deletion using the CRISPR-Cas9 system.

Deletion of Gene 26 did not result in a big impact on the solvent production of the strain. In Δ26, there is a small increase in butanol production, and in the other strains (Δ1234Δ26 and Δ12345Δ26), solvent production and glucose utilization are virtually the same as the mother strain. Main difference is in the cell biomass profile. Highest OD values at late stages of fermentation are proof of less cells lysed and also consistent with overexpression experiment that showed the effect during steady-death phase and not during exponential phase. In Δ1234Δ26, this effect is less significant because it already reached a very high value.

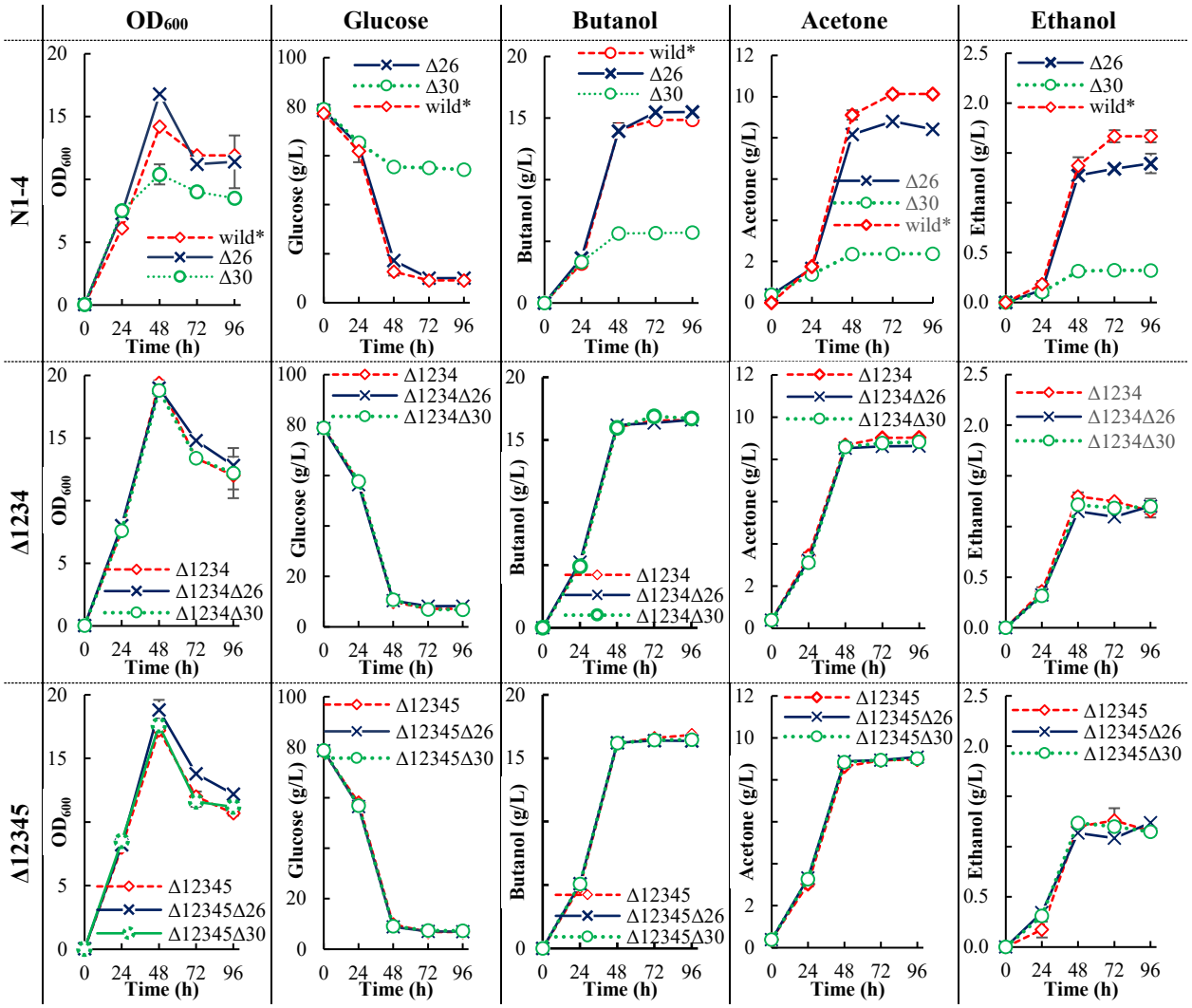

Figure 4.4 Profiles of serum bottle fermentation of the single deletion mutant of Gene 26 and Gene 30 compared to the mother strains (*C. saccharoperbutylacetonicum* N1-4, Δ1234, and Δ12345). The error bar represents the standard error at 95% interval of confidence.

Further characterization with batch fermentations in bioreactors with pH control was performed for *C. saccharoperbutylacetonicum* N1-4, Δ1234, and Δ1234Δ26. As shown in Figure 4.5, profiles showed a small difference in butanol production between either Δ1234 or Δ1234Δ26 vs. wild type. The Δ1234 and Δ1234Δ26 showed very similar fermentation profiles. It took slightly

longer for Δ1234 and Δ1234Δ26 to reach the maximum levels for solvent production and cell growth with slightly higher glucose utilization, than the wild type.

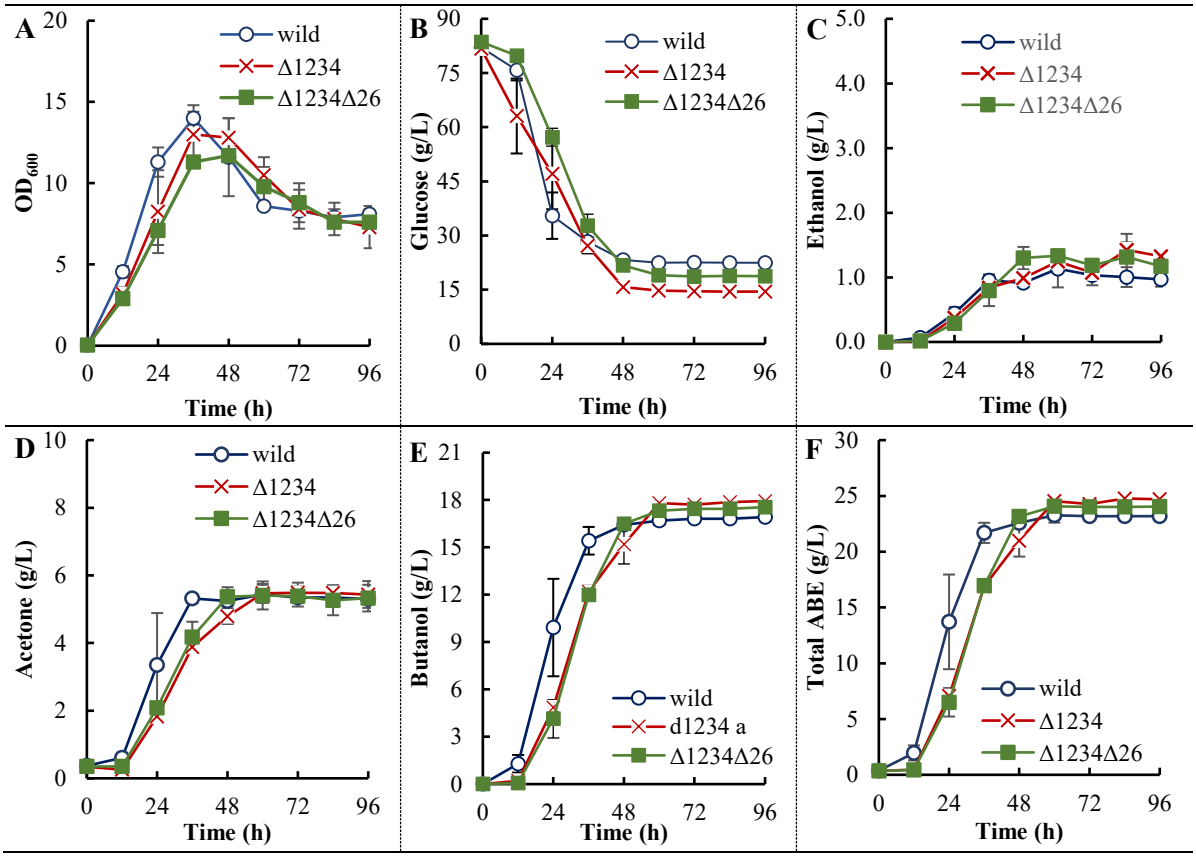

Figure 4.5 Profiles of batch fermentation in bioreactors with pH controlled for Δ1234Δ26 compared to Δ1234 and wild type. The error bar represents the standard error at 95% interval of confidence.

According to Tukey's test (supplementary Table S4.3), only wild type and Δ26 have a significantly different titer from the others, and not significant between them, during bottle fermentations, while Δ30 is very different from all the others because of the acid crash. For pH-controlled fermentations in bioreactors, wild type and Δ1234 are significantly different, while Δ1234Δ26 are not significantly different from either wild type or Δ1234.

4.3.3 Transformation efficiency

The development of the CRISPR-Cas9 system in *Clostridium* have opened a broad range of possibilities in the utilization of these strains as biochemical production platforms. In our system, Cas9 expression is controlled using an inducible promoter, to let the recombination events occurs without Cas9 expression, and then use Cas9 (with induction of expression) as a selection tool. Usually, the transformation of the CRISPR-Cas9 plasmid is not successful (no transformants could be obtained) when Cas9 is expressed using a strong constitutive promoter. The expression of Cas9 under an inducible promoter is a feasible strategy but generally lower transformation efficiency is still observed (compared to the control plasmid does not contain Cas9) due to the leakage of the inducible promoter and thus toxicity of Cas9 to the cells. Alternatively, other researchers have proposed the utilization of nickase-Cas9, which makes single strained breakages, and induce lower toxicity, but sacrificing the selection efficiency (Xu et al. 2015). The Cas12a protein (Cpf1) makes double breakage but 5bp distal, reducing some toxicity as well, and keeping most of the activity. A more complex expression system, such as riboswitches has also being used to reduce Cas9 toxicity during transformation, and increased expression during selection (Cañadas et al. 2019). Unfortunately, riboswitches occupy more loci, which also generate problems for transformation.

Transformation efficiency is a common problem in *Clostridium*. Although in N1-4 strain, this problem is not as severe as in other strains, but it is still an issue in some processes, such as for the insertion of large genes with the CRISPR-Cas9 system. Also, in other strains, the transformation efficiency really limits the applicability of the CRISPR tools. In all cases, an improvement in the transformation is something desired.

Table 4.2 Transformation efficiency

Plasmid	Wild	Δ1234	Δ12345
	(cfu/μg)	(cfu/μg)	(cfu/μg)
pPJB31	200	192	1300
pPJB32	101	271	1500
pPJB31 (Δ30)	236	329	771

During our experiments, we noticed an exceptionally high transformation efficiency of the Δ12345 strain. Table 4.2 show 6.5-15 fold increased in transformation efficiency of Δ12345 compared to the wild type and Δ1234. This is a significant increase, and also means that deletion of autolysin genes in other *Clostridium* strains may enhance DNA transformation efficiency as well.

4.4 Conclusions

Four autolysin genes were identified in *C. saccharoperbutylacetonicum* N1-4 based on the results that the overexpression of these genes would decreased the cell growth levels. The deletion of the four significant genes shown higher cell biomass levels in batch fermentations. The fermentations strains N1-4-C, Δ1234 and Δ12345, which contains the deletion of Cspa_135p00690 and CSPA_RS13245, confirms the autolytic activity of both genes. CSPA_RS24880 deletion does not show a big impact on the profiles, and CSPA_RS11880 deletion led to a slight increase in the cell biomass as well as butanol production.

4.5 Acknowledgements

I want to thank Dr. Jun Feng for providing the phage deficient strains, and Xeline Xia, Yu Gu and Dr. Philippe Gaillard for their assistance with the statistical analysis.

References

Al-Shorgani, Najeeb Kaid Nasser, Hafiza Shukor, Peyman Abdeshahian, Mohd Sahaid Kalil, Wan Mohtar Wan Yusoff, and Aidil Abdul Hamid. 2018. Enhanced butanol production by optimization of medium parameters using Clostridium acetobutylicum YM1. *Saudi Journal of Biological Sciences* 25 (7):1308-1321.

Branska, Barbora, Zora Pechacova, Jan Kolek, Maryna Vasylkivska, and Petra Patakova. 2018. Flow cytometry analysis of Clostridium beijerinckii NRRL B-598 populations exhibiting different phenotypes induced by changes in cultivation conditions. *Biotechnology for biofuels* 11 (1):99.

Cañadas, Inés C, Daphne Groothuis, Maria Zygouropoulou, Raquel Rodrigues, and Nigel P Minton. 2019. RiboCas: A Universal CRISPR-Based Editing Tool for Clostridium. *ACS synthetic biology* 8 (6):1379-1390.

Croux, Christian, Bruno Canard, Gerard Goma, and Philippe Soucaille. 1992. Purification and characterization of an extracellular muramidase of Clostridium acetobutylicum ATCC 824 that acts on non-N-acetylated peptidoglycan. *Applied and environmental microbiology* 58 (4):1075-1081.

Croux, Christian, and JoséL García. 1991. Sequence of the lye gene encoding the autolytic lysozyme of Clostridium acetobutylicum ATCC824: comparison with other lytic enzymes. *Gene* 104 (1):25-31.

Gu, Yanyan, Jun Feng, Zhong-Tian Zhang, Shaohua Wang, Liang Guo, Yifen Wang, and Yi Wang. 2019. Curing the endogenous megaplasmid in Clostridium saccharoperbutylacetonicum N1-4 (HMT) using CRISPR-Cas9 and preliminary investigation of the role of the plasmid for the strain metabolism. *Fuel* 236:1559-1566.

Liu, Zhen, Kai Qiao, Lei Tian, Quan Zhang, Zi-Yong Liu, and Fu-Li Li. 2015. Spontaneous large-scale autolysis in Clostridium acetobutylicum contributes to generation of more spores. *Frontiers in microbiology* 6:950.

Smith, Thomas J, Steve A Blackman, and Simon J Foster. 2000. Autolysins of Bacillus subtilis: multiple enzymes with multiple functions. *Microbiology* 146 (2):249-262.

Wang, Shaohua, Sheng Dong, Pixiang Wang, Yong Tao, and Yi Wang. 2017. Genome editing in Clostridium saccharoperbutylacetonicum N1-4 with the CRISPR-Cas9 system. *Appl. Environ. Microbiol.* 83 (10):e00233-17.

Wang, Yi, Xiangzhen Li, and Hans P Blaschek. 2013. Effects of supplementary butyrate on butanol production and the metabolic switch in Clostridium beijerinckii NCIMB 8052: genome-wide transcriptional analysis with RNA-Seq. *Biotechnology for biofuels* 6 (1):138.

Xu, Tao, Yongchao Li, Zhou Shi, Christopher L Hemme, Yuan Li, Yonghua Zhu, Joy D Van Nostrand, Zhili He, and Jizhong Zhou. 2015. Efficient genome editing in Clostridium cellulolyticum via CRISPR-Cas9 nickase. *Appl. Environ. Microbiol.* 81 (13):4423-4431.

Yang, Liejian, Guanhui Bao, Yan Zhu, Hongjun Dong, Yanping Zhang, and Yin Li. 2013. Discovery of a novel gene involved in autolysis of Clostridium cells. *Protein & cell* 4 (6):467-474.

Yoshino, Sadazo, Seiya Ogata, and Shinsaku Hayashida. 1982. Some properties of autolysin of Clostridium saccharoperbutylacetonicum. *Agricultural and Biological Chemistry* 46 (5):1243-1248.

Zhang, Jie, Pixiang Wang, Xiaofei Wang, Jun Feng, Hardev S Sandhu, and Yi Wang. 2018. Enhancement of sucrose metabolism in Clostridium saccharoperbutylacetonicum N1-4 through metabolic engineering for improved acetone–butanol–ethanol (ABE) fermentation. *Bioresource technology* 270:430-438

Zhang, Zhong-Tian, Pablo Jiménez-Bonilla, Seung-Oh Seo, Ting Lu, Yong-Su Jin, Hans P Blaschek, and Yi Wang. 2018. Bacterial Genome Editing with CRISPR-Cas9: Taking Clostridium beijerinckii as an Example. In *Synthetic Biology*, edited by B. J. New York, NY: Humana Press.

Chapter V.

Polycationic surfaces promote whole cell immobilization and induce micro-granulation of *C. saccharoperbutylacetonicum* N1-4 for enhanced biobutanol productivity

Supplementary material can be found in appendix V.

Abstract

Some *Clostridium* strains are prominent workhorses for the production of many interesting bioproducts, including bio-butanol. Butanol is a desirable biofuel with better properties than ethanol, but its toxicity on the host strain prevents the production to high levels with high productivity. Immobilization is a strategy used to protect bacterium cells in order to improve the performance during fermentations. In this work, we demonstrated that the utilization of chitosan powder as immobilization carrier improves the butanol productivity by 97% in a fermentation with *Clostridium saccharoperbutylacetonicum* N1-4, and improves the butanol titer by 21% in a fermentation with *C. beijerinckii* NCIMB 8052. We also demonstrated that the interaction between the cell and the material occurs by a double mechanism involving adsorption immobilization and induced aggregation. Additionally, we have prepared some analogue derivatives using cellulose cationized on the surface with 3-chloro-2-hydroxypropyltrymethylammonium (CHPTA) and 2-chloro-N,N-diethylaminoethane (CDEAE). The CHPTA derivatives of cotton and microcrystalline cellulose (MCC) showed a slightly increased production of butanol and total solvent with *C. saccharoperbutylacetonicum*. This work also provides information about the relationship between the fermentation performance and some chemical properties of the carrier

materials such as the cation density, surface area and others, for a better understanding of the interaction between the bacterial cells and the cationic materials.

Keywords: *Clostridium*, butanol, adsorption immobilization, granulation, ABE fermentation.

5.1 Introduction

Clostridium strains contain the native pathways for the production of different chemicals, including butanol, which is a valuable biochemical and biofuel. *C. saccharoperbutylacetonicum* N1-4 can produce 17 g/L of butanol in batch fermentation, which is among the highest levels for butanol production with natural solventogenic clostridia. However, this process is still not very competitive compared with the production of butanol through the petrochemical route. Various strategies have been evaluated in order to improve the performance of biobutanol fermentation, such as the *in situ* solvent recovery and the cell immobilization. Cells can be immobilized using entrapment, adsorption, encapsulation, chemical bonding or cell aggregation. The adsorption of cells is used to improve cell density, achieve cell recycling and protect cells from toxins and inhibitors. The attachment of bacterial cells to the material surface develops biofilm, which can enhance the robustness of the cell culture for butanol production or the resistance to fermentation inhibitors. Different materials have been tested for cell immobilization in clostridial fermentations such as lignocellulosic biomass, organic and synthetic fibers, synthetic polymers metals, ceramics, clays and zeolites. A summary about these previous studies are illustrated in Table 5.1.

Fibrous cellulosic and lignocellulosic materials are commonly used as adsorption carriers, because they are cheap, widely available, and easy to prepare. Recent studies showed that the cationization of lignocelluloses with polyethylenimide (PEI) improved the cell adsorption for *Clostridium* immobilization (Chen et al. 2013; Zhuang et al. 2017; Kong et al. 2015). In such cases, PEI has been proposed as a modifier of linen, cotton, and sugarcane bagasse (Zhuang et al. 2017).

Contradictory, PEI and other polycations are well known for being antibacterial. The antibacterial behavior is related to a strong interaction between the negatively-charged bacterial surface and the positive polymer. Although this same interaction apparently can be modulated to favor the cell attachment without hurting the cells, this has not been very well described in the literature.

Table 5.1 Materials for adsorption of *Clostridium*

		Titer batch						Productivity continuous			Reference
		Butanol			Total titer						
Material	Strain	Free	Immob	%	Free	Immob	%	Free	Immob	%	
	Fabrics										
Linen	*C. acetobutylicum* CGMCC 5234	-	9.56	-	-	15.7	-				(Zhuang et al. 2017)
Linen-PEI	*C. acetobutylicum* CGMCC 5234	-	10.34	-	-	17.0	-				(Zhuang et al. 2017)
Linen-SA	*C. acetobutylicum* CGMCC 5234	-	10.21	-	-	16.6	-				(Zhuang et al. 2017)
Cotton-PEI	*C acetobutylicum* CGMCC 5234	9.6	12.3	28.4	13.0	19.8	52.3				(Chen et al. 2013)
Cotton-PEI	*C acetobutylicum* CGMCC 5234	8.5	10.02	18.2	11.7	14.3	22.8				(Chen et al. 2013)
Belting strips	*C. acetobutylicum* IMB B-7407	6	7	16.7							(Tigunova et al. 2017)
Cotton towels	*C. acetobutylicum* CGMCC 5234	8.9	11.386	28.3				0.148	0.201	35.8	(Zhuang et al. 2016)
Wound fibrous matrix	*C. acetobutylicum* ATCC 55025								7.6		(Huang, Ramey, and Yang 2004)
	Raw lignocellulosic										
Beachwood shavings	*C acetobutylicum* ATCC 824							16.3	36.6	125	(Förberg and Häggström 1985)
empty fruit bunch fiber	*C. saccharoperbutyl-acetonicum* N1-4	7.5	12	60	10	17	70				(Shamsudin, Kalil, and Yusoff 2006)
coconut fibers	*C. acetobutylicum* ATCC 824	5.3	11.58	119	9.4	20.3	116				(Tripathi et al. 2010)
wood pulp	*Clostridium* DSM 792								13.7		(Survase, van Heiningen, and Granström 2012)
Corn stalk	*C. beijerinckii* ATCC 55025								5.1		(Zhang et al. 2009)
sugarcane bagasse with PEI	*C. acetobutylicum* XY16	11.7	12.19	4.4	18.8	19.5	3.51	0.4	11.3	2730	(Kong et al. 2015)
	Charcoal										
Bonechar	*C. acetobutylicum* P262								6.5		(Qureshi and Maddox 1988)
coal	*C. acetobutylicum* ATCC 824	5.3	11.59	120	9.4	19.9	112				(Tripathi et al. 2010)

Table 5.1 (continued) Materials for adsorption of Clostridium

	Synthetic polymer										
nylon scrubber	*C. saccharoperbutyl-acetonicum* N1-4	7.5	2.5	-66.7	10	4.5	-55				(Shamsudin, Kalil, and Yusoff 2006)
polyurethane pore 4	*C. saccharoperbutyl-acetonicum* N1-4	7.5	7.5	0	10	12	20				(Shamsudin, Kalil, and Yusoff 2006)
polyurethane pore 5	*C. saccharoperbutyl-acetonicum* N1-4	7.5	20	167	10	27.5	175				(Shamsudin, Kalil, and Yusoff 2006)
	Metallic										
ferrite rings	*C. acetobutylicum* IMB B-7407	6	0	-100							(Tigunova et al. 2017)
stainless steel scrubber	*C. saccharoperbutyl-acetonicum* N1-4	7.5	12	60	10	16	60				(Shamsudin, Kalil, and Yusoff 2006)
	Biopolymer hydrogel										
Agarose-alginate cryogel	*C. acetobutylicum* ATCC 824	5.4	10.79	101	9.4	21.6	131				(Tripathi et al. 2010)
Alginate hydrogel bead	*C. acetobutylicum* ATCC 824	5.3	12.7	141	9.4	23.1	146				(Tripathi et al. 2010)
	Other inorganic										
zeolite 13X	*C. beijerinckii* TISTR 1461	5.2	8.58	63.7							(Vichuviwat et al. 2014)
Bricks	*C. beijerinckii* TISTR 1461	5.2	5.8	9.6							(Vichuviwat et al. 2014)
Clay brick	C. beijerinckii BA101								16.2		(Lienhardt et al. 2002)
Clay brick	*C. beijerinckii* BA101								15.8		(Qureshi et al. 2000)
Clay brick	C. acetobutylicum ATCC 824	5.3	13.71	160	9.4	24.4	160				(Tripathi et al. 2010)
ceramic D-21 beads	*C acetobutylicum* P262	4.2	5.52	31.1	5.9	7.3	24.7	0.12	1	733	(Badr, Toledo, and Hamdy 2001)
Raschig rings	*C. acetobutylicum* IMB B-7407	6	10.5	75							(Tigunova et al. 2017)

The proposed antibacterial mechanism was related to the disruption of the cell membrane due to the electrostatic interaction (Hassanpour et al. 2018); long cationic polymers can penetrate cells disrupting the membrane like a needle bursting a balloon (Murata et al. 2007). Other hypothesis include the blocking of the membrane functions by the interaction with the cationic surface, or the ion exchange of calcium and others divalent cations, in some of the membrane functions. Antibacterial behavior in cationic polymers is related with degree of substitution and other factors such as long aliphatic chain lengths and bulky groups on the chemical structure (Grace et al. 2016). Maybe one of the most important aspects is the accessible charge density. At

very low charge density, no inhibition is observed. When charge density is increasing, the inhibition grows, and after a critical concentration the inhibition seem to be constant (Murata et al. 2007; Rauytanapanit et al. 2018).

Also, the immobilization by self-aggregation or "granulation" has been recently explored to be used in the fermentative production of biochemicals (Carvajal-Arroyo et al. 2019). This technique is commonly used for wastewater treatment, and it is related to the interaction between different microorganisms and the Extracellular Polymeric Substances (EPS) produced by them (Szabó et al. 2017). Aggregation can also being induced by autoagglutinins (Trunk, Salah Khalil, and Leo 2018), or by some chemicals. Chitosan solutions, and other polycationic compounds have been commonly applied to promote bacterial flocculation, either in wastewater treatment (Yang et al. 2014), or bacterial pure cultures (Hughes, Ramsden, and Symes 1990), but with the sole purpose of removing cells from solution. The application of granulation in fermentative production of chemicals can be a powerful technique with many advantages over other immobilization strategies, such as the cheaper price and the no need of volume to be occupied by cell carriers.

In this work, we explored the utilization of insoluble chitosan for immobilization to improve cell density and butanol productivity. We also investigated the relationship between the fermentation performance and some chemical properties of the carrier materials. This article provides evidence of double mechanism of chitosan as carrier based on "cell adsorption immobilization" and "induced cell self-aggregation", which is reported for the first time in clostridial fermentations. Additionally, we studied two cationization on cellulosic supports (cotton and Microcrystalline Cellulose (MCC)), in order to better understand how the chemical properties affect the cell adsorption and the fermentation performance. This chemical modification strategy can be applied in many others cellulosic or lignocellulosic materials for various purposes.

5.2 Materials and methods

For details about the following procedures, refer to the supplementary materials

5.2.1 Strain cultivation

C. saccharoperbutylacetonicum N1-4 (HMT) (DSM 14923) from DSMZ (Braunschweig, Germany) is stored in glycerol stock at -80°C, and routinely cultivated in Tryptone/Glucose/Yeast extract (TGY) broth containing 30 g/L of tryptone, 20 g/L of sucrose, 10 g/L of yeast extract, and 1 g/L of L-cysteine, or in TGY agar solid plates, in an anaerobic chamber at 35ºC. *C. beijerinckii* NCIMB 8052 spores were stored in sterile water at 4°C. Spores were heat-shocked at 80°C for 10 min, followed by cooling on ice for 5 min. The heat-shocked spores were inoculated at a 1% inoculum in TGY medium at 37°C, and recultured using 5% inoculum in fresh TGY.

5.2.2 Preparation and characterization of carrier material for immobilization

Powdered chitosan 85% deacetylated J64143 and microcrystalline cellulose A17730 were obtained from Alfa Aesar (Massachusetts, USA). Commercial cotton prepping balls were obtained from Covidien, plc (Dublin, Ireland). Cotton and microcrystalline cellulose were modified with two cationizing agents: 3-chloro-2-hydroxypropyltrymethylammonium (CHPTA) and 2-chloro-N,N-diethylaminoethane (CDEAE) from VWR (Radnor, PA) as a modification of previously reported methods (Song et al. 2008; Rousseau, Ferrell, and Reardon 1984; Liesiene and Kazlauske 2013; Song, Zhou, and Chen 2012). The chemical reaction is shown in Figure 5.1.

14 bottles containing 4g (2%) of cotton in 200 mL sodium hydroxide (NaOH; 2 mol/L) were used to prepare two cationizations on the material surface. Samples 1-7 were modified with different amounts of CHPTA, and 8-14 with DEAEC, at molar ratios of 4.5, 2.7, 1.8, 0.9, 0.675, 0.45 and 0.225 (cationizing agent/matrix), respectively. After all the components were mixed up,

the solutions were placed in an orbital shaker at 50 rpm and 25 °C four 24 hours. The modified cotton was washed up with distilled water for several times until the pH become neutral and does not change after 12 h. Same experiments were carry with commercial microcrystalline cellulose (MCC). The CHTPA-MCC derivatives were labeled as 15-21 and the DEAEC-MCC as 22-28. The modified cellulose was collected by filtration, then washed with distilled water and collected until water become neutral. Finally, the samples were dried at 60 °C and used for the adsorption purposes. Degree of substitution (DS) was calculated based on n/m ratio (Figure 5.1, and supplementary information for details) using nitrogen content. Nitrogen Content was determined for duplicates samples using a Vario Micro Cube CHNS elementar analyzer from Elementar, Germany.

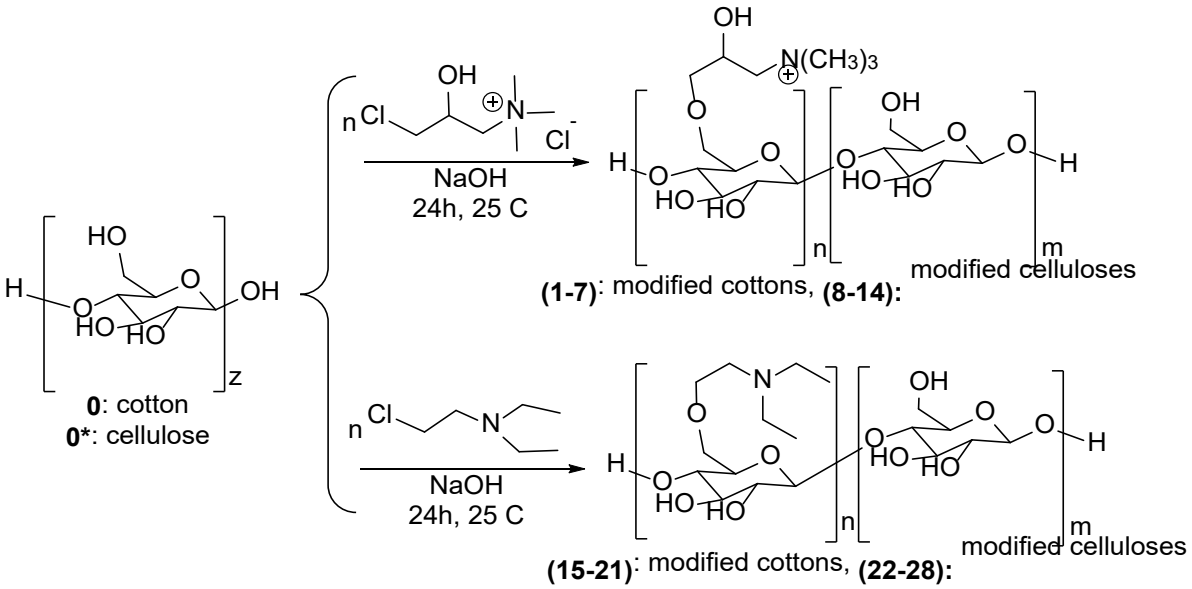

Figure 5.1 Reaction of cellulosic materials (cotton and microcrystalline cellulose) with CHTPA (top) and DEAEC (bottom) for partial cationization of the surface

5.2.3 Investigation of Maillard reaction's effects

4 g of chitosan (insoluble powder) was placed in 250 mL serum bottles with 100 mL of 90 g/L glucose solutions, sparged with N_2 and the bottle was sealed. The bottles were autoclaved for 15, 20, 30 min exposure time respectively, for a total time of 45, 60, 85 min (respectively). The samples were identified as R45, R60, R85 (corresponding to the autoclave time), and R0 (autoclaved in water). All the experiments were done in duplicate. After the autoclaving was done, samples were cooled down to room temperature and the glucose solution was replaced with 95 mL of TGY medium, in the anaerobic chamber. Bottles containing the prepared medium as descried above were inoculated with *C. saccharoperbutylacetonicum* culture at 5% inoculum ratio in the early exponential stage (OD_{600}= 0.8), and samples were taken at 6, 12 and 18 h.

5.2.4 Serum bottle fermentations

A frozen glycerol stock (-80°C) of the strain was used to prepare the pre-culture, by culturing it overnight in TGY medium and then transferring once to a fresh medium. 5 mL of an active pre-culture was added to 95 mL of P2-TY medium in 250 mL serum bottles. Fermentation were run in an orbital shaker at 150 rpm and 30ºC. Samples were taken every 12 h. Materials were autoclaved together with fermentation media when needed.

5.2.5 Analysis of metabolites

Glucose, butanol, acetone and ethanol concentration were determined using an Agilent 1260 series High Performance Liquid Chromatography (Agilent Technologies, Santa Clara, CA, USA) equipped with a refraction index detector, using 5mM H_2SO_4 in water as mobile phase at a flow rate of 0.6 mL/min. The Varian MetaCarb 87H (with the temperature set at 25 ºC) was used for sample separation.

5.2.6 Biomass analysis

Cell optical density (OD_{600}) was quantified during free cell fermentation with a cell density meter (Ultrospec 10, Biochrom Ltd., Cambridge, England).

The cell biomass in fermentations containing powders of materials for immobilization was analyzed using a method reported by Munir, *et al*. with modifications (2014). This method is based on Bradford's colorimetric protein quantification, estimating the biomass based on the protein content. The solid fraction was collected and washed with water and frozen dried in a FreeZone 2.5 (Labconco, Kansas, Missouri, USA). 100 µL of 0.2 M sodium hydroxide were added into 100 mg of solid. Samples were incubated at 90 ºC for 10 mins. The protein solution was diluted by 40 times, and then 20 µL of it was mixed with 200 µL of Bradford reagent (VWR, Radnor, PA). Samples were analyzed by absorbance at 595 nm in a microplate reader (Tecan infinite M1000 Pro, Tecan Trading AG, Switzerland) against Bovine Serum Albumin (VWR, Radnor, PA) standards. For planktonic cells, 1 mL of culture was centrifuged at 10,000 g for 10 min to separate the pellet from the supernatant. Then the pellet was washed with water and centrifuged for 10 min. The supernatant was discarded and the pellet was re-suspended in 1 mL of 0.2 M sodium hydroxide. 100 µL of the alkaline cell suspension was incubated at 90 ºC for 10 min, and the supernatant was collected, diluted between 15-250 times (as needed) and used as described above.

In order to compare the biomass results obtained from OD_{600} and protein, 500 mL of TGY was inoculated with 5% of an active culture of *C. saccharoperbutylacetonicum* N1-4, and grew for overnight. Cells were collected by centrifugation (at 4000 rpm for 10 min), suspended into 100 mL water, centrifuged, and resuspended into 50 mL of water. Then, it was diluted into 7 different solutions with OD_{600} between 0.5 – 22. OD_{600} and protein were determined for each solution (in duplicates), and the plot of OD_{600} vs mg/mL albumin equivalents (supplementary Figure S5.5), resulting in the relationship between them were stablished by Eq. 5.1.

$$OD_{600} = 3.4774 \times (mg/mL)_{albumin\ eq} - 0.1369 \quad \text{(Eq 5.1)}$$

5.2.7 Surface area analysis

Methylene blue adsorption method was used to calculate the surface area of the different samples of cotton, microcrystalline cellulose and chitosan. This method was adapted from the previously reported (Kaewprasit et al. 1998), and it is based on the adsorption of a monolayer of dye into the surface of the material. Methylene blue was purchased from Merck chemicals (Darmstadt, Germany). 20-80 mg of each sample (in duplicates) weas immersed into 1 mL of methylene blue solutions in the range of 0.004 to 0.18 x 10^{-3} kg L^{-1} (1x10^{-6}–0.00048 mol L^{-1}) and concentration of the dye was measured by spectrophotometric analysis at 660 nm against a calibration curve. Langmuir isotherms were used to calculate the moles of methylene blue adsorbed in the monolayer. Then, the specific surface area (*S*) in $10^{-3}$$km^2$ kg^{-1} is calculated using Eq. 5.2.

$$S = N_m \times a_{MB} \times N \times 10^{-20} \text{(Eq. 5.2)}$$

Where a_{MB} is the occupied surface area of one molecule of methylene blue =197.2 $Å^2$; *N* is Avogadro's number, 6.02 x 10^{23} mol^{-1}.

5.2.8 Cationic charge density determination

The method used for cationic charge density determination is modified from the fluorescein stained method reported by Roest (2015). 20 mg of each sample (triplicates) immersed in 1.5 ml 1 m/v% fluorescein disodium salt (from solid fluorescein purchased from VWR) solution in demineralized water for 10 min, washed 6 times with 2 ml water. Fluorescein bind cationic groups present. Next, the samples were placed in 1 ml of a 0.1 wt.% cetyltrimethylammonium chloride solution (a cationic surfactant) in demineralized water to desorb complexed fluorescein dye.

Samples were diluted by 1/500. Subsequently, 100 µL of sample were mixed with 20 µL of 100 mM phosphate buffer (pH 8), and analyzed using fluorescence at 520 nm (emission), and 485 (excitation) in a microplate reader against a calibration curve.

$$\text{Charge density} = [\text{Dye}] \times V \times N/S \quad \text{(Eq. 5.3)}$$

Cation surface density is calculated using Eq. 5.3, in which V is the volume of the extraction solution (1.0 mL), N is Avogadro's number (6.023×10^{23}) and S is the surface area of the samples.

5.2.9 Cell zeta potential

A fresh culture of *C. saccharoperbutylacetonicum* N1-4 in TGY (same conditions as mentioned above) in the exponential phase (OD_{600} is ~3.0) was harvested by centrifugation at 10,000 rpm for 10 min. The supernatant was discarded, and the cells were washed for two times in water and finally re-suspended into P2 buffer (0.5 g/L KH_2PO_4, 0.5 g/L K_2HPO_4, and 2,2 g/L $NH_4(CH_3COO)$, pH 7). The cells were suspended to reach a final OD_{600} of about 0.1. Finally, the pH was adjusted to approximate 3, 5, 6, 7, and 10, with acetic acid or NaOH. Electrophoretic motility of the suspensions was measured in a Zetasizer nano series NanoZS (Malvern Instruments, Malvern, United Kingdom).

5.2.10 Bacterial potentiometric titration

A culture of *C. saccharoperbutylacetonicum* N1-4 in TGY (same conditions as mentioned above) in the exponential phase (OD_{600} is ~3.0) was harvested by centrifugation at 10,000 rpm for 10 min. The supernatant was discarded, and the cells were washed for two times with water and suspended in water to reach the OD_{600} of 7.6. 100 mL of the suspension was titrated against NaOH 0.02M, and HCl 0.01M, standardized against Potassium hydrogen phthalate. pH was recorded

using a pH-meter symphony BIOP, from VWR. First and second derivatives were calculated from the curves (d(pH)/d(mol) & d^2(pH)/d(mol)^2), and used to estimate the buffer regions.

5.2.11 Microscopy

Scanning Electronic Microscopy (SEM) was conducted using a Zeiss EVO50 Microscope (Oberkochen, Germany). Samples containing bacteria cells were fixed using a 5% glutaraldehyde solution in 1 M 4-(-2 hydroxyethyl) piperazine-1-ethanesulfonic acid (HEPES) buffer at pH 7.2. The samples was left stand for 12 hours, and then were dehydrated with increasing ethanol concentrations, during at least 10 min in 25%, 30 min in 50%, 10 h in 70%, and 1h in 100%. All the procedures were carried out at 4°C. Then samples were placed in an aluminum mount, using double sided conductive carbon tape, coated with gold, and examined under the microscope.

Optical microscopy was conducted in an Olympus DP73. Fresh samples were stained with 0.5% crystal violet and then inspected directly.

5.3 Results and analysis

5.3.1 Performance of the fermentation containing chitosan (insoluble) as the carrier material

Chitosan is derived from chitin: the second most abundant polysaccharide on earth. It is biocompatible and biodegradable. Although it is soluble under acidic conditions, it remains primarily insoluble at regular butanol fermentation conditions (pH 5-7), making it possible to be applied as a solid carrier for cell adsorption and fermentation. It is one of the cheapest and most abundant bio-based polycationic compounds available for such purposes.

Table 5.2 and supplementary Figure S5.6 illustrate the results for pH-uncontrolled batch fermentations with *C. saccharoperbutylacetonicum* or *C. beijerinckii*. In the fermentation with

C. saccharoperbutylacetonicum, the cell biomass in the liquid fraction is 31% higher when chitosan is present than in the control fermentation (without chitosan). Additionally, the cell growth profile shows a straight stationary phase, which is rarely observed for this strain due to its strong autolytic behavior. This means, the protection provided by the immobilization system reduced the autolysis activity. The butanol yield in both immobilized and control fermentations is about the same value (0.214 vs. 0.215), and this confirms that the higher cell biomass in immobilized fermentation is not because of a re-route on the metabolic flow, but because of a lower cell lysis. Butanol and acetone titers are very similar in the immobilized fermentation as that in the control, although the productivity is increased by about one fold. The immobilization system did not improve the butanol titer, which is consistent with what we generally seen for the N1-4 strain; the butanol titer in the batch fermentation with the wild type strain is already very high, and it is very hard to further improve with either genetic engineering or other strategies. We noticed similar results when we carried out numerous genetic manipulations in this strain in our group, although similar genetic manipulations could lead to significant improvement in butanol titer in other *Clostridium* (data not shown).

Table 5.2 Serum bottle fermentation performance of *C. saccharoperbutylacetonicum* N1-4 and *C. beijerinckii* NCIMB 8052 immobilized with chitosan as the carrier material

	***C. saccharoperbutylacetonicum* N1-4**			***C. beijerinckii* NCIMB 8052**		
	Control	Chitosan	Difference	Control	Chitosan	Difference
Max BuOH (g/L)	14.9±0.0	14.7±0.6	≈ 0	10.0±0.2	12.1±0.4	+21%
BuOH productivity (g/Lh)	0.21±0.00	0.41±0.02	+97%	0.14±0.00	0.25±0.01	+81%
Max Acetone (g/L)	10.1±0.1	10.0±0.4	≈ 0	7.6±0.2	9.8±0.2	+30%
Max EtOH (g/L)	1.7±0.1	0.7±0.0	-55%	0.4±0.1	0.5±0.1	+25%
Butanol yield (g/g)	0.214±0.003	0.215±009	≈ 0	0.16±0.01	0.22±0.01	+37.5%
Growth rate (exponential)	0.167	0.177	+6%	0.145	0.243	+68%
Max OD_{600} (liquid)	14.2±0.7	18.6±0.6	+31%	12.6±1.0	14±0.8	+11%

As shown in Table 5.2, *C. beijerinckii* NCIMB 8052 showed much higher improvement when chitosan is supplemented as carrier compared to the control. Not only the cell biomass and butanol productivity have been improved, but also the production of butanol (by 21%), acetone (by 30%) and ethanol (by 25%) all has been elevated. This confirmed that our immobilization system simply with chitosan as the carrier material had a positive effect for the butanol fermentation. Another thing worthwhile to be pointed out is that the regular fermentation with *C. beijerinckii* NCIMB 8052 does not reach a very high level of butanol (~10 g/L) and solvent production, and thus the improvement is remarkable when chitosan was supplemented, which is different from the fermentation with *C. saccharoperbutylacetonicum* N1-4 as we discussed above.

There is no previous report of insoluble chitosan used as a carrier for cell adsorption in butanol fermentation, although ionomeric gelation of chitosan acetate with sodium triphosphate has been evaluated for entrapment immobilization (Frick and Schügerl 1986), the results of which was not very promising. We have also tried to immobilize cells and spores by entrapment into polyelectrolyte complexes of chitosan and anionic polysaccharides such as alginate and carboxymethylcellulose, but the strain was not able to grow, or could merely generate very weak growth (data not shown). We finally concluded that entrapment immobilization underwent many disadvantages over the adsorption immobilization, when the carrier material was generated from chitosan solution (at regular working concentrations: 0.5-3%). Some of these disadvantages are: high acetate concentration (or another counter-anion, such as sulfate, chlorine, butyrate, etc.) inhibits the cell growth (Wang 2018), high cationic density generates a strong antimicrobial behavior (Kong et al. 2010), pH lower than 4 is needed to dissolve chitosan but it is incompatible with cells, and salts generated as subproduct are hard to clean. Solid chitosan has been used before

for adsorption immobilization of *Bacillus*, for enhanced production of surfactants (Khondee et al. 2015).

5.3.2 Effect of the Maillard reaction on surface of chitosan-glucose carrier

Maillard reaction occurs by heating the glucose solution together with chitosan at 100 ºC for1-8 h (Phisut and Jiraporn 2013). Maillard adducts increase mechanical properties (Umemura, Mihara, and Kawai 2010) and antioxidant activity (Phisut and Jiraporn 2013), decrease the antibacterial behavior (Tanaka et al. 1993), and at same time keep polycationic feature of chitosan. Maillard reaction occurs when we autoclave the culture media with the chitosan present inside. This reaction can be avoided if separate sterilization is carried out, although we found that Maillard reaction actually resulted in the advantage of modulating some of the chitosan properties, such as the surface area, and the cation density. Also, the sterilization of two components (medium and chitosan) together in a single step is apparently simpler and more convenient.

In our fermentation, we noticed that the starting concentration of glucose was decreased after autoclave. Maillard reaction can be estimated by means of three strategies: UV absorption at 294/420 nm (where 294 nm represents an intermediate and 420 the browning product) (Wu et al. 2014), glucose loss (by HPLC quantification) (Song et al. 2016), or a new peak presented on the HPLC profile. In our experiment, the preliminary test with three methods showed similar results. For simplicity, we estimated the degree of substitution based on the glucose lost in the following steps.

Figure 5.2 shows the results for the first 18 hours of the fermentation containing chitosan. R0 represents the fermentation with samples autoclaved in water. R45, R60, and R85 represent chitosan autoclaved in the medium containing 90 g/L glucose for 45, 60 and 85 minutes

respectively (total autoclave time). After the autoclave treatment, the liquid was replaced with TGY medium. As shown in Figure 5.2, the autoclave with longer reaction times generally generates the higher substitution degree, although the substitution degrees from the autoclave for 60 and 85 min are very similar. In addition, with longer reaction time, the surface area of the material is decreased while the cation density is increased.

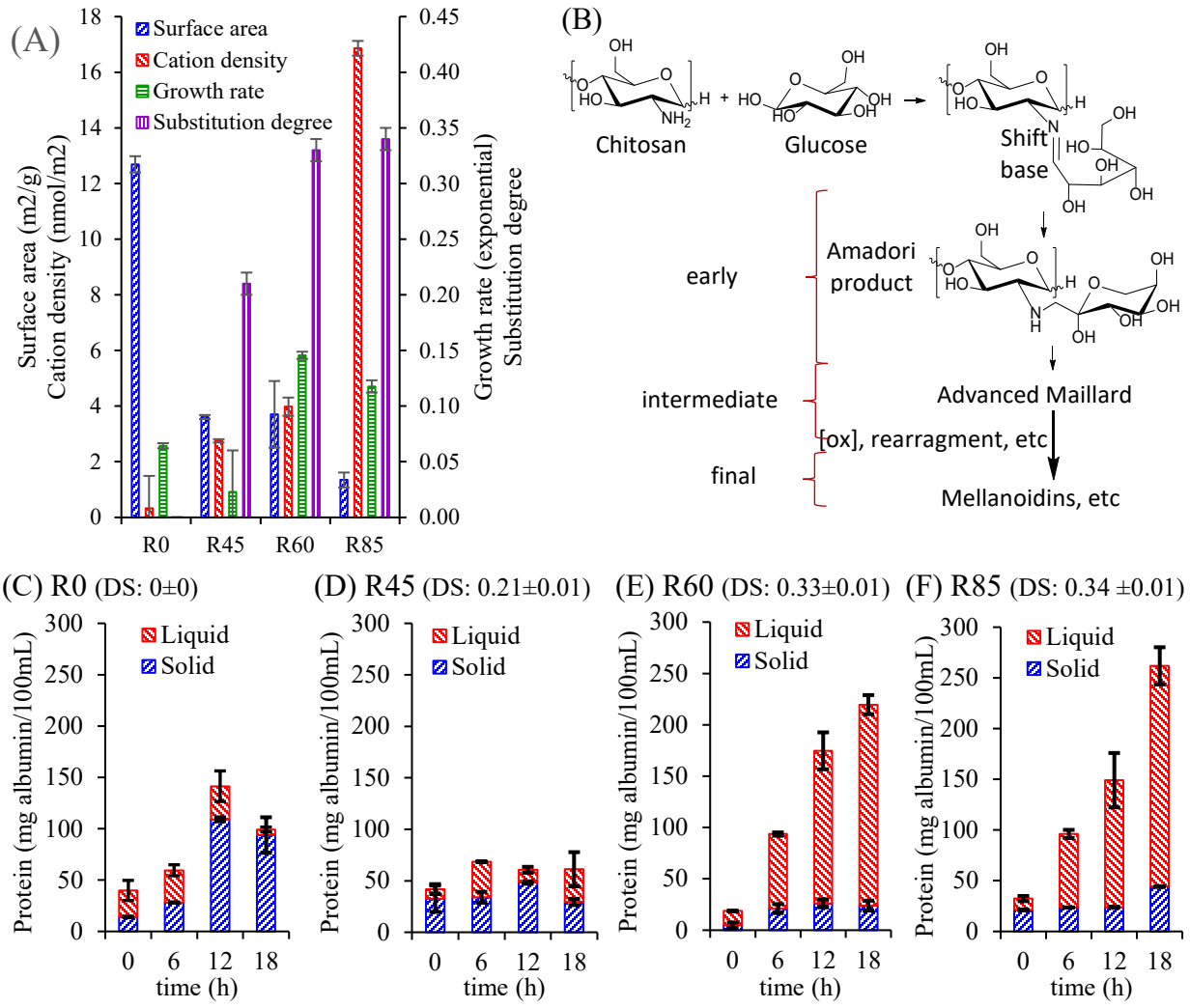

Figure 5.2 Chitosan Millard reaction effects on the fermentations with immobilized *C. saccharoperbutylacetonicum* N1-4, containing Chitosan-Maillard adducts with different reaction times: R0 = 0 min, R45 = 45 min, R60 = 60 min, and R85 = 85 min. (A) Effects of Maillard reaction on different properties of the material: surface area, cation density, growth rate, and

estimated substitution degree. (B) Maillard – Amadori reaction scheme. (C), (D), (E), and (F) illustrate the immobilized cell biomass (expressed as protein concentration) in R0, R45, R60 and R85, respectively.

Longer reaction times make the immobilized biomass decrease, although, the total biomass is higher. Figure 5.2(C) shows the higher biomass values on the solid (absorbed) during all times for R0 sample, compared with R45 (D), R60 (E), and R85 (F); although after 18 hours either solid, liquid and total biomass start decreasing. Figures (E), and (F) show the higher total biomass values, corresponding to reaction times of 60 and 85 minutes. The trend of the biomass of R60 and R85 in both solid and liquid fractions is to increase, although the immobilized biomass is smaller than in R0, and R45. Cell adsorption is stronger in R0 and 45. With the increase in Maillard reaction time, the interaction of cell-material is weakened by the decrease in the surface area, and intensified by the increase in the cation density. The surface area effect, and the protection made by the bulky group attached on the surface are the predominant effects. As mentioned above, a very strong interaction can be inhibitory, explaining the reduction on biomass production at 18 h in R0 and R45. R60 showed the highest total growth rate, and thus was selected as the preferred condition.

In R60, only about 10% of cell biomass is attached to the material, and the 90% rest is in the liquid medium. Fermentation results (Table 5.2 and supplementary Figure S5.6) show that the bacterial cells grow faster and reach higher biomass levels when the chitosan is present compared to the control, when we just consider the liquid fraction. This means that the material helps to populate the liquid medium. Otherwise, we could conclude that the higher biomass in the liquid fraction in Figure 5.2(E), is just because of a poor adsorption of cells in the carrier, which is not the case. Because in that situation we would not expect an increase in the growth rate and

maximum cell biomass. Moreover, this means that the mechanism of interaction between the chitosan and the bacterium is not just a simple adsorption immobilization. In next section, we describe the additional interaction between the carrier and the cells, as a combination of adsorption immobilization and “induced microgranulation”.

5.3.3 Adsorption, microgranulation, and proposed mechanism

Chitosan used for this study is powder with flake-type micro-morphology. The surface is flat but some layers are visible in the SEM micrographs (Figure 5.3(A) and 5.3(E)). As we discussed above, the fermentation containing chitosan does not show a high cell density on the carrier material, but the biomass in liquid fraction is significantly higher than the free cell fermentation. The chitosan enhances the cell density.

SEM microscopies in Figure 5.3(A-H) show how this process happened. At time zero (Figures 5.3 (A) & (E)), the chitosan surface looks flat and just a few cells are on the surface. The speed of the starting adsorption is modulated by the properties of the material, as discussed above. At 24 h (Figures 5.3B & F), biofilm structures are visible on the chitosan surface, as well as many cells. These structures start pulling the outer layers of the chitosan surface, detaching from it, and forming micro-granules. At 48 and 72 h (Figures 5.3 (C) & (G), and (D) & (H), respectively), small amount of biofilm and cells are observed. Detachment process could be mechanical, but maybe is influenced by partial neutralization of the chitosan charge with the extracellular polymeric substances (EPS), which is negatively charged. However, there is no evident reduction in the amount of chitosan carrier.

In Figure 5.3 (N) and (O), we can see some of these particles suspended in the liquid medium, with a size of approximately 25 μm, in which both EPS and cells have been stained with the crystal

violet dye. In Figure 5.3 (N), a small particle of chitosan is still attached to it. Although, there is just a fraction immobilized with still many free cells surrounded it, it is enough to generate some positive effect on the butanol productivity of the fermentation.

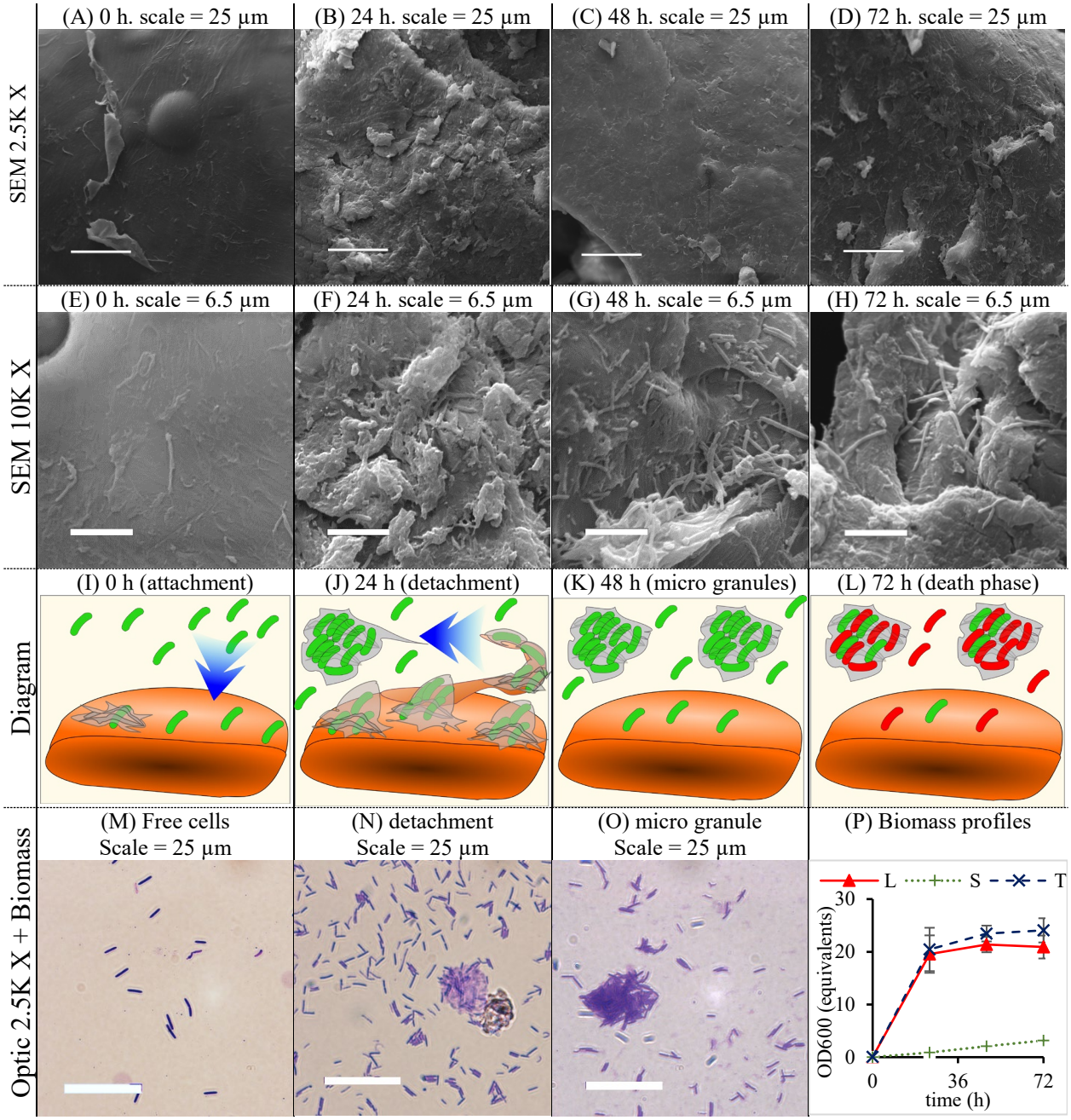

Figure 5.3 Adsorption and induced-microgranulation process of *C. saccharoperbutylacetonicum* N1-4 with chitosan. (A-H) SEM micrographs ((A-D) 2500X, (E-H) 10000X, at different times).

(I-L) scheme of adsorption immobilization and microgranulation process. (M-O) Optical micrograph of cell culture at 24 h stained with crystal violet, for planktonic cells, a small piece of chitosan suspended and attached to a microgranule, and a high cell-density microgranule. (P) The cell biomass profiles, L: liquid, S: solid, T: total

The micrograph of fermentation without chitosan (Figure 5.3(M)) does not show significant aggregation of cells at 24 h. Big granules (macroscopical) have the same disadvantages as big immobilized particles: cell activity decreases with depth in the biofilm, and the internal cells are inaccessible to the nutrients and inactive. Generation of small granulates guarantees the cell activity, and no special conditions are needed to avoid flocculation. Based on the fermentation results (Table 5.2 and supplementary Figure S5.6), small particles do not have a negative influence on the butanol yield (actually, it improved the butanol yield in *C. beijerinckii*), while the OD600 equivalents are higher. This means the metabolic flux is not re-routed into cell biomass, but the cells are protected from autolytic activity instead.

Figure 5.3(P) shows the cell biomass profile of the strain in the liquid medium, adsorbed in the solid chitosan and the total. At 72h, the immobilized cells (OD600 equivalents= 3.1) is only about 13% of the total. As mentioned above, a 31% increase in the biomass suspended in the liquid compared to the control fermentation was observed, and therefore the microgranulation is the main mechanism involved in the fermentation. Petrova et al. (2016) identified three deferent ways in which a microorganism can “escape” from the carrier: desorption, detachment, and dispersion. Detachment mechanisms include erosion and sloughing. The absorption-desorption is highly influenced by the properties of the material such as surface area, and cation density. This is important at the beginning of the fermentation, and also during the exponential phase with an

increased number of free cells are present in the liquid media. Once the EPS are released, the growth rate in the carrier occurs at different rate, depending on how deep the cells from the surface are. The detachment occurs as "sloughing" mechanism, which means, the small fragments are still covered by the EPS, and then protected. Agitation seems to be a very important factor on this process: fermentations using a magnetic stirred bioreactors did not grow or grow weakly in many attempts. Magnetic agitation probably promotes erosion, and thus the whole process becomes harmful to the cells, especially because magnetic agitation needs to be strong enough to avoid the sedimentation of the carrier material.

5.3.4 Effect of cellulosic materials prepared through two different cationization approaches by amination or ammonization

Based on the results obtained with chitosan, we prepared cellulosic materials using two different modification approaches to introduce cationic groups, which are analogue to the amino group of chitosan.

We performed similar procedures with two cationizing agents: DEAEC and CHPTA. These chemicals create a partial functionalization with amino and ammonium groups respectively, on the hydroxyl of the carbon number 6 (of the glucose units). It means that some glucose units from the cellulose chain will remain with the hydroxyl free group and others will contain the tertiary ammine or the quaternary ammonium. The ratio between the cationized and the free groups is known as the substitution degree and is shown in Figures 5.4 (G) & (H). In general, the substitution degree tends to decrease with small molar ratio (cationizing agent/matrix) as expected. The surface area is also changed during this reaction. Differences between degree of substitution are small and do not explain very well the fermentation behavior as other properties such as the cation density.

Cation density is the relationship between the number of cationic centers on the surface, able to adsorb an anionic dye divided by the surface area. In PEI, the cationic density has been identified as the key property related to the antibacterial behavior (Roest et al. 2015).

During the fermentation with *C. saccharoperbutylacetonicum*, acid crash occurred when either raw cotton or raw MCC was employed. The fermentation with the planktonic cells sometimes experiences acid crash, but it is possible to achieve a completed and successful fermentation sometimes. In the Series 1-7 in Figure 5.4, sample number 1 represents the highest molar ratio of cationizing agent (and degree of substitution of the material), and number 7 the smallest. Likewise, in the other Series 8-14, 15-21, and 22-28, the smaller number represents the highest substitution degree. Results with DEAEC (Figure S5.9) showed that the derivatization failed to improve the properties of the material, and most fermentations suffered "acid crash". But even those in which the cells could grow and the fermentation could be completed produced considerably lower butanol than the control.

CHTPA cationization reduces the tendency to 'acid crash' for the fermentation with the increase in the cation density, excepting for sample number 1, in which the cation density decreased again. In most cases the cell growth rate in the fermentation with immobilization is slower than those with free cells. But in some cases, the final cell biomass is more important, when the final solvent production is higher than the control. We did not quantify the immobilized cell biomass here. However, based on the final value of the cell biomass (Figure S5.8), the immobilized cell biomass seems to be less than the fraction presented in the liquid medium.

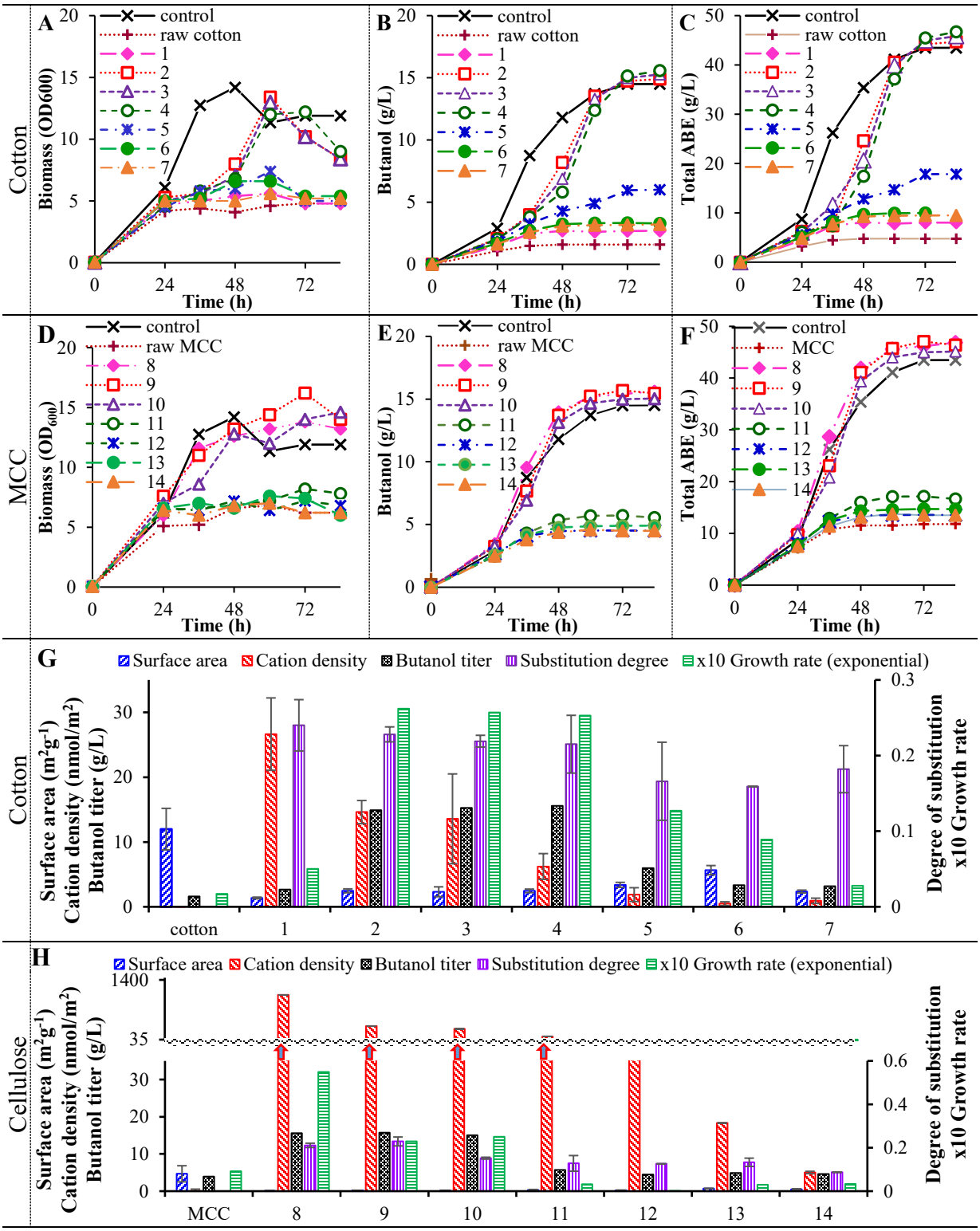

Figure 5.4 Profiles of fermentations with cellulosic materials modified with CHTPA as the immobilization carrier, with the properties of the carrier were illustrated as well. (A) & (D) Cell biomass profiles, (B) & (E) Butanol production profiles, and (C) & (F) total ABE production,

(G) & (H) the properties for cotton and MCC respectively. Increasing numbers from 1-7 and 8-14 represent decreasing molar rates used for the derivatization.

The most significant effect is on the MCC samples. Figure 5.4(D) shows that, samples 8, 9, and 10 have less autolytic behavior, and the biomass continues growing for a prolongated time. This additional growth in biomass is probably the reason for the additional solvent production, as illustrated in Figures 5.4 (E) and (F), where the butanol and total ABE production of samples 8, 9 and 10 are slightly higher than those in the control. In the fermentations of 2, 3, and 4 with Cotton as the carrier, increased maximum butanol titer (Figure 5.4 (B)) and total ABE (Figure 5.4 (C)) were also observed, although the production took longer time.

5.3.5 Effect of electrostatic interactions

When pH >5 during the fermentation, the *Clostridium* cell envelope contains functional groups, but the net charge is negative. The zeta potential (ζ), which is a potential determined by the electrophoretic motility, is negative for *C. saccharoperbutylacetonicum* N1-4 strain (Figure 5.5(A)) as has also been reported for *C. acetobutylicum* CGMCC 5234 (Zhuang et al. 2017). Interestingly, in N1-4, the potential is totally neutralized becoming zero when the pH is around 4.4, at which the cells suffer acid crash. Potentiometric titration shows two buffering regions: one is around 7.7, corresponding to amino groups from the protein, and the other is at pH 5.5 corresponding to a carboxy group.

We can compare the bacteria with a particle negatively charged, because from cell surface (membrane and wall) negative phospholipids are predominant. Covering the cell wall, we have the tight-bonded layer EPS, analogue to a polymer coating layer coating the negative particle. The EPS is complex and contains cationic (such as DNA and Arg, His, or Lys residues), neutral (such

as polysaccharides), and anionic (carboxy from protein or polysaccharides). In *Clostridium*, previous reports identified heteropolysaccharides containing glucuronic and uronic acids, and cytoplasmic proteins (including some chaperons) as major components of biofilm for *C. acetobutylicum* (Liu et al. 2018). In the biofilm, usually negative charge also predominates. Underneath the TB-EPS, there is another layer called the loose-bonded (LB)-EPS, which has a loose structure, low density, and is sensitive to the environment (Pan et al. 2016). Since LB-EPS is more permeable and diffusible, the Stern layer potential is most likely located on the TB-EPS, and the LB-EPS is part of the diffuse layer, as shown in Figures 5.5 (B) & (C).

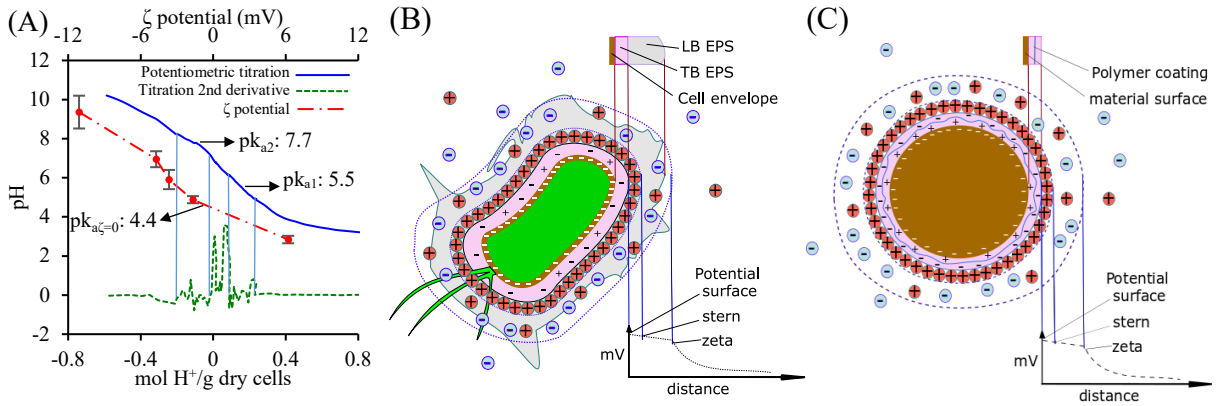

Figure 5.5 Cell envelope, potentiometric titration and electrophoretic motility. (A) ζ potential and potentiometric titration of cell envelope. (B) Cell envelope diagram. (C) Particle analogue. EPS: Extracellular polymeric substances, LB: loose bonded, TB: tight bonded

Mechanisms of synthesis of the different components on the cell envelope are obviously more complex than in a particle, and involve the expression of many genes such as the ones responsible for regulation of EPS, sporulation, cell division and quorum sensing (Liu et al. 2018). However, the electrostatic interactions are still very important. High negative potential has a protective behavior, but also prevents cell aggregation (Liu et al. 2018). The attraction to the different materials we used is improved by the electrostatic attraction between the negatively

charged cells and the cationic material surface. The presence of the amino group is a common element on the previously reported PEI and our chitosan experiments, but we ignored this element as a key factor because the CHPTA functionalization (no amino group) produces a similar effect. Also, we ignored the importance of the affinity between glucose-like residues of the early Maillard reaction, and cell surface receptors because Maillard reaction does not occurs on the quaternized carriers (CHPTA derivatives).

The shape of the curves of potentiometric titration of cells and ζ is very similar (Figure 5.5 (A)). In N1-4 strain, bacteria can grow well at pH 5, but experiment severe acid crash around pH 4.5. At this pH, both buffer regions are fully protonated, making changes in protein configuration, and eventually compromising cell membrane integrity. These events can also happens when bacterial envelope interacts with polycations, and it explains why at relatively low concentration or lo cation density, the effect is positive, but at very high values, they are harmful.

5.3.6 Effects of functional group

Figure 5.6 summarizes the chemical structure of the different carriers used for adsorption immobilization in this study, and PEI, which was previously reported as a modifier of lignocellulosic materials.

Cellulosic and lignocellulosic materials are always good candidates as carriers thanks to their easy availability and cheapness. All these carbohydrate bones are very hydrophilic. The presence of ionic groups increases the water uptake, but also the solubility. In our experiments with cotton and MCC, we just modified some of the C-6 hydroxyl groups from the surface. DEAE group in cellulose is considered a weak ion exchanger, compared with HTPA group, which is considered a strong one. This could suggest that a greater substitution degree can lead to a better result; but on

the other hand, a big substitution degree can make the compound soluble. This is a possible explanation about the failure of this group. Also, pKa of DEAE-cellulose used in this study is higher than 11, which also promotes a very basic behavior.

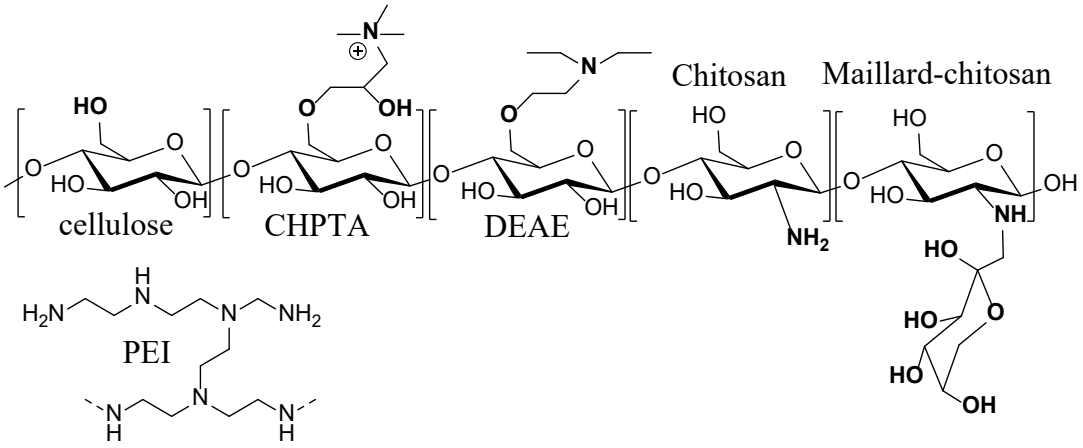

Figure 5.6 Structure of different carriers for adsorption immobilization in this study

The pKa of chitosan is around 6.5 (primary amine), which warrants a partial protonation and some buffering behavior during fermentations. The pKa of PEI is in the range of 7.0-8.5 (primary, secondary and tertiary amines), similar to chitosan. Also, both of these compounds possess many nitrogen atoms. Maillard reaction seems to modulate the chitosan interaction. The bulky group on the surface can reduce the toxic effect of the interaction with the cell envelope, and make it more effective for immobilization, which also explain the reduction of antibacterial behavior as previously reported. These compounds can also absorb anions, such as acetate and butyrate, and make themselves more accessible for the immobilized cells. However since the degree of substitution is small for cellulose derivatives, and the protonated fraction is small for chitosan, either buffering capacity or ion adsorption does not seems to be a significant effect.

5.4 Conclusions

The use of chitosan powder to enhance ABE fermentation of *Clostridium* strains has led to a significant increase in the cell biomass in the liquid medium. Cells adsorbed onto the chitosan surface generate biofilm and detached into the liquid medium by sloughing, inducing the formation of high cell density microgranules, which are surrounded and protected by EPS. The microgranulation resulted in a reduction on the autolysis of the system, with no negative impact on the butanol yield, but with an increase on the butanol productivity in *C. saccharoperbutylacetonicum* N1-4, and increase on the butanol production in *C. beijerinckii*. MCC and cotton cationized with CHTPA showed a greater interaction with cells than the raw materials, and the butanol production was slightly increased with the use of these materials. The derivatization can be applied in most lignocellulosic materials to modulate the properties and enhance the interaction between the cell and the carrier material. Either chitosan, cotton-HPTA, or MCC-HPTA decreased the trend of the fermentation to 'acid crash', because the biofilm protects the cells against acidic conditions.

5.5 Acknowledgements

We thank Dr. Sushil Adhikari from the Biosystems Engineering Department of Auburn University for the access of the elemental analyzer, Dr. Allan David from Chemical Engineering Department of Auburn University for the access of the Zeta potential analyzer, Dr. Brendan Higgins from the Biosystems Engineering Department of Auburn University for the access of the Freeze dryer, Dr. Brian Via from the School of Forestry & Wildlife Sciences at Auburn University for the access of the Zeiss optical microscope, and Dr. Michael Miller from the AU Research Instrumentation Facility for the training and the access of the SEM facility.

References

Badr, HR, R Toledo, and MK Hamdy. 2001. Continuous acetone–ethanol–butanol fermentation by immobilized cells of Clostridium acetobutylicum. *Biomass and Bioenergy* 20 (2):119-132.

Carvajal-Arroyo, José M, Pieter Candry, Stephen J Andersen, Ruben Props, Thomas Seviour, Ramon Ganigué, and Korneel Rabaey. 2019. Granular fermentation enables high rate caproic acid production from solid-free thin stillage. *Green Chemistry* 21 (6):1330-1339.

Chen, Yong, Tao Zhou, Dong Liu, An Li, Songbo Xu, Qingguo Liu, Bingbing Li, and Hanjie Ying. 2013. Production of butanol from glucose and xylose with immobilized cells of Clostridium acetobutylicum. *Biotechnology and bioprocess engineering* 18 (2):234-241.

Förberg, Cecilia, and Lena Häggström. 1985. Control of cell adhesion and activity during continuous production of acetone and butanol with adsorbed cells. *Enzyme and microbial technology* 7 (5):230-234.

Frick, Ch, and K Schügerl. 1986. Continuous acetone-butanol production with free and immobilized Clostridium acetobutylicum. *Applied microbiology and biotechnology* 25 (3):186-193.

Grace, James L, Johnny X Huang, Soon-Ee Cheah, Nghia P Truong, Matthew A Cooper, Jian Li, Thomas P Davis, John F Quinn, Tony Velkov, and Michael R Whittaker. 2016. Antibacterial low molecular weight cationic polymers: dissecting the contribution of hydrophobicity, chain length and charge to activity. *RSC advances* 6 (19):15469-15477.

Hassanpour, Anita, Sakineh Asghari, Moslem Mansour Lakouraj, and Mojtaba Mohseni. 2018. Preparation and characterization of contact active antibacterial surface based on chemically modified nanofibrillated cellulose by phenanthridinium silane salt. *International journal of biological macromolecules* 115:528-539.

Huang, Wei-Cho, David E Ramey, and Shang-Tian Yang. 2004. Continuous production of butanol by Clostridium acetobutylicum immobilized in a fibrous bed bioreactor. Paper read at Proceedings of the Twenty-Fifth Symposium on Biotechnology for Fuels and Chemicals Held May 4–7, 2003, in Breckenridge, CO.

Hughes, J, DK Ramsden, and KC Symes. 1990. The flocculation of bacteria using cationic synthetic flocculants and chitosan. *Biotechnology techniques* 4 (1):55-60.

Kaewprasit, Chongrak, Eric Hequet, Noureddine Abidi, and Jean Paul Gourlot. 1998. Quality measurements. *J. Cotton Sci* 2:164-173.

Khondee, Nichakorn, Sitti Tathong, Onruthai Pinyakong, Rudolf Müller, Suwat Soonglerdsongpha, Chalermchai Ruangchainikom, Chantra Tongcumpou, and Ekawan Luepromchai. 2015. Lipopeptide biosurfactant production by chitosan-immobilized Bacillus sp. GY19 and their recovery by foam fractionation. *Biochemical engineering journal* 93:47-54.

Kong, Ming, Xi Guang Chen, Ke Xing, and Hyun Jin Park. 2010. Antimicrobial properties of chitosan and mode of action: a state of the art review. *International journal of food microbiology* 144 (1):51-63.

Kong, Xiangping, Aiyong He, Jie Zhao, Hao Wu, and Min Jiang. 2015. Efficient acetone–butanol–ethanol production (ABE) by Clostridium acetobutylicum XY16 immobilized on chemically modified sugarcane bagasse. *Bioprocess and biosystems engineering* 38 (7):1365-1372.

Lienhardt, Jason, Justin Schripsema, Nasib Qureshi, and Hans P Blaschek. 2002. Butanol production by Clostridium beijerinckii BA101 in an immobilized cell biofilm reactor. *Applied biochemistry and biotechnology* 98 (1-9):591-598.

Liesiene, Jolanta, and Jurgita Kazlauske. 2013. Functionalization of cellulose: Synthesis of water-soluble cationic cellulose derivatives. *Cellulose Chemistry and Technology* 47 (7-8):515-525.

Liu, Dong, Zhengjiao Yang, Yong Chen, Wei Zhuang, Huanqing Niu, Jinglan Wu, and Hanjie Ying. 2018. Clostridium acetobutylicum grows vegetatively in a biofilm rich in heteropolysaccharides and cytoplasmic proteins. *Biotechnology for biofuels* 11 (1):315.

Munir, Riffat I, John Schellenberg, Bernard Henrissat, Tobin J Verbeke, Richard Sparling, and David B Levin. 2014. Comparative analysis of carbohydrate active enzymes in Clostridium termitidis CT1112 reveals complex carbohydrate degradation ability. *PLoS One* 9 (8):e104260.

Murata, Hironobu, Richard R Koepsel, Krzysztof Matyjaszewski, and Alan J Russell. 2007. Permanent, non-leaching antibacterial surfaces—2: How high density cationic surfaces kill bacterial cells. *Biomaterials* 28 (32):4870-4879.

Pan, Mei, Liang Zhu, Lin Chen, Yunpeng Qiu, and Jun Wang. 2016. Detection techniques for extracellular polymeric substances in biofilms: a review. *BioResources* 11 (3):8092-8115.

Petrova, Olga E, and Karin Sauer. 2016. Escaping the biofilm in more than one way: desorption, detachment or dispersion. *Current opinion in microbiology* 30:67-78.

Phisut, N, and B Jiraporn. 2013. Characteristics and antioxidant activity of Maillard reaction products derived from chitosan-sugar solution. *International Food Research Journal* 20 (3):1077.

Qureshi, N, and IS Maddox. 1988. Reactor design for the ABE fermentation using cells of Clostridium acetobutylicum immobilized by adsorption onto bonechar. *Bioprocess Engineering* 3 (2):69-72.

Qureshi, N, J Schripsema, J Lienhardt, and HP Blaschek. 2000. Continuous solvent production by Clostridium beijerinckii BA101 immobilized by adsorption onto brick. *World Journal of Microbiology and Biotechnology* 16 (4):377-382.

Rauytanapanit, Monrawat, Apiradee Opitakorn, Masahiro Terashima, Rungaroon Waditee-Sirisattha, and Thanit Praneenararat. 2018. Antibacterial cotton fabrics based on hydrophilic amino-containing scaffolds. *Colloids and Surfaces B: Biointerfaces* 164:42-49.

Roest, Steven, Henny C van der Mei, Ton JA Loontjens, and Henk J Busscher. 2015. Charge properties and bacterial contact-killing of hyperbranched polyurea-polyethyleneimine coatings with various degrees of alkylation. *Applied Surface Science* 356:325-332.

Rousseau, Ronald W, James K Ferrell, and Robert F Reardon. 1984. Synthesis of diethylaminoethyl cellulose on cotton fabric. *Industrial & engineering chemistry product research and development* 23 (2):250-252.

Shamsudin, Saleha, Mohd Sahaid Hj Kalil, and WM Wan Yusoff. 2006. Production of acetone, butanol and ethanol (ABE) by Clostridium saccharoperbutylacetonicum N1-4 with different immobilization systems. *Pakistan Journal of Biological Sciences* 9 (10):1923-1928.

Song, Yongbo, Yunxia Sun, Xianzheng Zhang, Jinping Zhou, and Lina Zhang. 2008. Homogeneous quaternization of cellulose in NaOH/urea aqueous solutions as gene carriers. *Biomacromolecules* 9 (8):2259-2264.

Song, Yongbo, Ying Zhou, and Lingyun Chen. 2012. Wood cellulose-based polyelectrolyte complex nanoparticles as protein carriers. *Journal of Materials Chemistry* 22 (6):2512-2519.

Survase, Shrikant A, Adriaan van Heiningen, and Tom Granström. 2012. Continuous bio-catalytic conversion of sugar mixture to acetone–butanol–ethanol by immobilized Clostridium acetobutylicum DSM 792. *Applied microbiology and biotechnology* 93 (6):2309-2316.

Szabó, Enikö, Raquel Liébana, Malte Hermansson, Oskar Modin, Frank Persson, and Britt-Marie Wilén. 2017. Comparison of the bacterial community composition in the granular and the suspended phase of sequencing batch reactors. *AMB Express* 7 (1):168.

Tanaka, Munehiko, Jin Ru Huang, Wen Kuei Chiu, Shoichiro Ishizaki, and Takeshi Taguchi. 1993. Effect of the Maillard Reaction on Functional Properties of Chitosan. *Nippon Suisan Gakkaishi* 59 (11):1915-1921.

Tigunova, OO, HS Andriiash, N Ye Beiko, and SM Shulga. 2017. Biobutanol accumulation using alternative substrates by cultivation of Clostridium acetobutylicum strains. *Biotechnologia Acta* 10 (5).

Tripathi, Anuj, Haider Sami, Seema R Jain, Maria Viloria-Cols, Natalia Zhuravleva, Göran Nilsson, Hans Jungvid, and Ashok Kumar. 2010. Improved bio-catalytic conversion by novel immobilization process using cryogel beads to increase solvent production. *Enzyme and Microbial Technology* 47 (1-2):44-51.

Trunk, Thomas, Hawzeen Salah Khalil, and Jack Christopher Leo. 2018. Bacterial autoaggregation. *Aims Microbiology* 4 (1):140-164.

Umemura, Kenji, Ayako Mihara, and Shuichi Kawai. 2010. Development of new natural polymer-based wood adhesives III: effects of glucose addition on properties of chitosan. *Journal of wood science* 56 (5):387-394.

Vichuviwat, Rapeephat, Akarin Boonsombuti, Apanee Luengnaruemitchai, and Sujitra Wongkasemjit. 2014. Enhanced butanol production by immobilized Clostridium beijerinckii TISTR 1461 using zeolite 13X as a carrier. *Bioresource technology* 172:76-82.

Wang, Pixiang. 2018. Engineering Clostridium saccharoperbutylacetonicum for enhanced isopropanol-butanolethanol (IBE) production from lignocellulosic biomass through acetic acid pretreatment, Biosystems Engineering, Auburn University.

Yang, Zhen, Jean-Regis Degorce-Dumas, Hu Yang, Eric Guibal, Aimin Li, and Rongshi Cheng. 2014. Flocculation of Escherichia coli using a quaternary ammonium salt grafted carboxymethyl chitosan flocculant. *Environmental science & technology* 48 (12):6867-6873.

Zhang, Yuedong, Yujiu Ma, Fangxiao Yang, and Chunhui Zhang. 2009. Continuous acetone–butanol–ethanol production by corn stalk immobilized cells. *Journal of industrial microbiology & biotechnology* 36 (8):1117-1121.

Zhuang, Wei, Xiaojing Liu, Jing Yang, Jinglan Wu, Jingwei Zhou, Yong Chen, Dong Liu, and Hanjie Ying. 2017. Immobilization of Clostridium acetobutylicum onto natural textiles and its fermentation properties. *Microbial biotechnology* 10 (2):502-512.

Zhuang, Wei, Jing Yang, Jinglan Wu, Dong Liu, Jingwei Zhou, Yong Chen, and Hanjie Ying. 2016. Extracellular polymer substances and the heterogeneity of Clostridium acetobutylicum biofilm induced tolerance to acetic acid and butanol. *RSC Advances* 6 (40):33695-33704.

Summary and perspective

The experimental work realized in this dissertation can be summarized in three main findings: the overexpression of efflux pump from *Pseudomonas putida* increase tolerance against biomass-derived inhibitors; the deletion of 4 new identified autolysins increase titer, cell biomass, plasmid stability, and transformation efficiency; and the utilization of chitosan and CHPTA-functionalized cellulosic materials for immobilization improves butanol titer, ABE titer, cell biomass, and productivity.

The overexpression of efflux pump gene *srpB* from *P. putida* S12 in *C. saccharoperbutylacetonicum* N1-4 increase the tolerance to butanol, furfural and ferulic acid, the last two as model compounds for phenolic and furan aldehydes inhibitors. Also, the mutant strain was capable to grow in media containing up to 3.5 g/L furfural (the control can only tolerate to 3.0 g/L) or 1.2 g/L ferulic acid (the control can only tolerate to 0.8 g/L), and was still able to produce 14 g/L butanol. However, the mutant produced slightly decreased butanol compared to the control strain under regular fermentation conditions with no inhibitors. For these reasons, we did not integrate the genes into the chromosome. It would be very valuable to understand why this occurs and eliminate these limitations before making a gene integration of *srp*B.

Efflux pump overexpression can lead to some toxicity, as we mentioned in chapter III (Patakova et al. 2018). Also, the natural regulation of this system is based in a cluster of repressor/antirepressor genes (*srp*SR) (Sun et al. 2011). We do not know whether this system would be active or not if it is expressed in *Clostridium*, but if so, it would probably maximized the

benefits of the system. In our plasmid overexpression of *srp*B, since the gene express from the very beginning of the fermentation, it show advantage on the fermentation containing inhibitors (which are present from the very beginning as well). So, in an ideal system, the expression should be activated by butanol, and the required inhibitors (just as in the natural system), in order to minimize the toxicity produced by the expression of the pump itself. In order to achieve this, we recommend trying the express *srp*SR and *srp*ABC together in *C. saccharoperbutylacetonicum* N1-4. If *srp*SR results active, then *srp*SR can be modeled and mutated in order to increase the specificity to butanol, and biomass inhibitors.

The both genetic strategies (*srp*B integration and autolysin deletion) could be integrated in the same strain, if the limitations described here above are efficiently addressed. The four autolysin genes identified in *C. saccharoperbutylacetonicum* N1-4 decrease the cell biomass when overexpressed. The test for the deletion of the autolysin genes confirm their autolytic activity, although the effect on the phenotype during batch fermentations is almost imperceptible. However, we believe the autolysis of these genes can generate a greater difference on continuous fermentations, because the presence of autolysins make the culture unstable in the long term. We recommend running a continuous fermentation in future to see the effect on the phenotype.

In our results 12 of 16 putative autolysins in which the test did not find significance, still showed a difference respecting the control, suggesting they have autolytic activity. The summative effect of all autolysins could be significant even when the individual effect is not. Therefore, we recommend studying the deletion of all the putative autolysins together or at least those identified as muramidases. Another possibility could be silencing the autolysins in the mid and late stage of growth, instead of the deletion. Silencing could reduce the increasing in the lag phase observed in

our experiments, because autolysin activity is related to some fundamental functions such as cell division, and release of intracellular chaperones.

The chitosan immobilization system can be integrated to the genetic strategies, as well. The chitosan immobilization showed a dual mechanism of adsorption and "induced microgranulation", reported by first time. The utilization of chitosan powder to enhance ABE fermentation of *Clostridium* strains had produce a significant increase in the biomass in the liquid medium. The microgranulation conduct to a reduction on the autolysis of the system, with no negative impact on the yield, but with an increase on the productivity of *C. saccharoperbutylacetonicum* N1-4, and in the production on *C. beijerinckii*. The chitosan immobilization showed some advantages during batch fermentation, but it can also be applied for continuous fermentations. The autolysin deficient strains can be a good candidates to be immobilized for continuous fermentations, since, they probably will show a better performance in the long term.

MCC and cotton cationized with CHTPA had shown a greater interaction than raw materials, and the production is slightly increased by the use of this materials. This derivatization can be applied to most lignocellulosic materials to modulate the properties and enhance the interaction cell-carrier. We also recommend to apply this strategy over cheap lignocellulosic support materials such as agricultural wastes, in order to use them for immobilization.

Additional genetic work can make the strain generate more or better EPS in order to be immobilized or granulated. In *Bacillus subtilis*, several genes have been reported for biosynthesis of different groups of EPS, such as structural neutral polysaccharides, sorptive ionic EPSs, surface active lipopeptides, extracellular enzymes and others (Marvasi, Visscher, and Casillas Martinez 2010). In the same way, some neutral and anionic polysaccharides, and proteins has been identified

in *C. acetobutylicum*, as well as, some related genes (Liu et al. 2018). Overexpression of different genes related with EPSs can help to increase the cell attachment. Finally, some agglutinin and quorum sensing genes are related with the self-aggregation and granulation.

References

Liu, Dong, Zhengjiao Yang, Yong Chen, Wei Zhuang, Huanqing Niu, Jinglan Wu, and Hanjie Ying. 2018. Clostridium acetobutylicum grows vegetatively in a biofilm rich in heteropolysaccharides and cytoplasmic proteins. *Biotechnology for biofuels* 11 (1):315.

Marvasi, Massimiliano, Pieter T Visscher, and Lilliam Casillas Martinez. 2010. Exopolymeric substances (EPS) from Bacillus subtilis: polymers and genes encoding their synthesis. *FEMS microbiology letters* 313 (1):1-9.

Patakova, Petra, Jan Kolek, Karel Sedlar, Pavlina Koscova, Barbora Branska, Kristyna Kupkova, Leona Paulova, and Ivo Provaznik. 2018. Comparative analysis of high butanol tolerance and production in clostridia. *Biotechnology Advances* 36 (3):721-738.

Sun, Xu, Zileena Zahir, Karlene H Lynch, and Jonathan J Dennis. 2011. An anti-repressor, SrpR, is involved in transcriptional regulation of the SrpABC solvent tolerance efflux pump of Pseudomonas putida S12. *Journal of bacteriology*.

Appendix I.

General procedures

General equipment

Anaerobic chamber (Globes box)

General culture management is done in COY Labs anaerobic chamber filled with a gas mixture of 5% hydrogen (H_2), 1% carbon dioxide (CO_2), and 94% nitrogen (N_2). A COY Labs airlock is used to introduce and take out material from the chamber, guarantying anaerobic conditions by 2 cycles of vacuum and purge gas (nitrogen (N_2)) and a last cycle of vacuum and mix gas. COY Labs CAM-12 monitor is used to monitor oxygen and hydrogen concentration, and a heater box with catalyst is used to remove traces of oxygen. COY Labs incubator Model 2000 is used to culture inside of the chamber. A commercial dehumidifier is used to reduce moisture, with the help of a desiccant in a tray when necessary to keep moisture under 40%.

Culture media

Liquid culture media

LB media is composed by 10 g/L tryptone, 10 g/L sodium chloride (NaCl), and 5 g/L yeast extract in water, autoclave sterilized.

TGY media is composed by 30 g/L tryptone, 20 g/L of glucose, 10 g/L of yeast extract, and 1g/L of cysteine hydrochloride in water, autoclave sterilized

P2 stock solutions: P2 vitamins (100X): 0.1 g/L of parabenzoic acid, 0.1 g/L of thiamine hydrochloride and 0.001 g/L of biotin in water and filter sterilized. P2 buffer (100X): 50 g/L of KH_2PO_4, 50 g/L of K_2HPO_4 and 220 g/L ammonium acetate in water, filter sterilized. P2 trace elements (100X): 20 g/L $MgSO_4*7H_2O$, 1g/L $MnSO_4*H2O$, 1g/L $FeSO_4*7H2O$, and 1g/L NaCl dissolved in water and filter sterilized.

P2-TY: variant of P2 containing a supplementation of tryptone and yeast extract, used as fermentation media for *C. saccharoperbutylacetonicum* N1-4. 80 g of glucose as carbon source (or otherwise indicated), 6g of tryptone and 2 g of yeast extract are dissolved in water to complete 920 mL and called P2-TY premedia, which is autoclave sterilized. After autoclave, at room temperature, the P2-TY is completed by addition of 10 mL of each P2 solution stock (P2 vitamins (100X), P2 trace elements (100X) and P2 buffer (100X)), and 50 mL (5%) inoculum.

P2-YE: variant of P2 containing a supplementation of yeast extract, used as fermentation media for *C. beijerinckii*. Preparation is same as P2-TY, just without tryptone supplementation.

Solid culture media

1.5 %m/v of agar is added before autoclave to LB or TGY media. Then, the media is let cool down until around 50 C, placed on petri dishes in a biosafety cabinet, let cool down to room temperature uncovered and then covered. For anaerobes, plates are placed in anaerobic chamber at least 12 hours before use to let deoxygenate.

Antibiotic supplementation

Stock solutions of antibiotic are prepared at 1000X concentration. Clarithromycin stock solutions were prepared in DMF at 30 mg/mL of concentration (working concentration is 30 μg/mL).

***Fermentations*:**

Serum bottles

100 mL serum bottle fermentation: 100 mL of P2-TY are prepared in 250 mL serum bottles as describe hereafter: 92 mL of P2-TY premedia as described before, bubbled with nitrogen, and autoclaved. It is let cool at room temperature, and transferred into an anaerobic chamber whereas 1 mL P2 vitamins, 1 mL P2 buffer and 1 mL P2 trace elements and 5% inoculum, are added. Then, the bottles are transferred to an orbital shaker at 150 rpm and 30ºC. Samples are taken every 12 h.

Analytic determination of glucose, butanol, acetone, ethanol, butyric and acetic acid by HPLC

Agilent 1260 infinity with refraction index detector, 5mM H_2SO_4 in water as mobile phase at 0.6 mL/min flux, and column Varian MetaCarb 87H.

Table S1.1 Glucose and solvents standard curve preparation

standard	g glucose	g/L glucose	ml acetone	g/L acetone	mL butanol	g/L butanol	mL ethanol	g/L ethanol
1	12.732	25.46	3	4.75	3	4.81	1	1.50
2	25.2156	50.43	6	9.50	6	9.62	2.5	3.74
3	37.4652	74.93	9.5	15.05	9.5	15.24	4	5.99
4	49.9937	99.99	12.5	19.80	12.5	20.05	5.5	8.24
5	62.682	125.36	16	25.34	16	25.66	7	10.48
6	74.4089	148.82	19	30.10	19	30.47	8	11.98

A set of two standards were prepared, the first one containing the glucose and the solvents, both of them in 500 mL volumetric flasks. The following chart shows the volumes used to prepare the standards, and the equivalent concentration

The second set of standards contain the acids were prepared in same way.

The corresponding retention time of each metabolite in the refraction index detector is: 10.1 min glucose, 16.4 min acetic acid, 19.7 min ethanol, 22.5 min acetone, 24.1 min butyric acid, and 33.6 min butanol.

Table S1.2 Acid standard curve preparation

standard	mL butyric	g/L butyric	mL acetic	g/L acetic
1	2.5	4.82	2	4.20
2	8	15.42	4.5	9.44
3	13	25.06	7	14.69
4	18	34.70	9.5	19.93
5	23	44.34	12	25.18

Then, the peak area is calculated from the integration of the peaks at the corresponding times. For solvent they correspond to:

Table S1. 3 Glucose and solvents standard curve HPLC measurement

standard	ri	glucose (g/L)	ri	Acetone (g/L)	ri	butanol (g/L)	ri	Ethanol (g/L)
	0	0	0	0	0	0	0	0
1	1666357	25.464	140277.1	4.752	239174.5	4.8114	43203.86	1.49758
2	3520515	50.4312	327712	9.504	479072.9	9.6228	111895.7	3.74395
3	5108967	74.9304	471477.9	15.048	705506.7	15.2361	180917.8	5.99032
4	6669969	99.9874	672158.1	19.8	989521.9	20.0475	245544.4	8.23669
5	8336449	125.364	835840.7	25.344	1228004	25.6608	313037.6	10.48306
6	9469907	148.8178	975389.3	30.096	1431564	30.4722	357542.4	11.98064

Ri: refraction index

And for acids they correspond to:

Table S1.4 Acid standard curve HPLC measurement

standard	ri	butyric (g/L)	ri	acetic (g/L)
	0	0	0	0
1	210788.5	4.82	134166	4.196
2	696357.9	15.424	296569.9	9.441
3	1120319	25.064	474550.2	14.686
4	1523735	34.704	632389.3	19.931
5	1955752	44.344	794021.9	25.176

Then, the calibration curves with the corresponding equations are shown here, whereas y is the concentration and x the peak area.

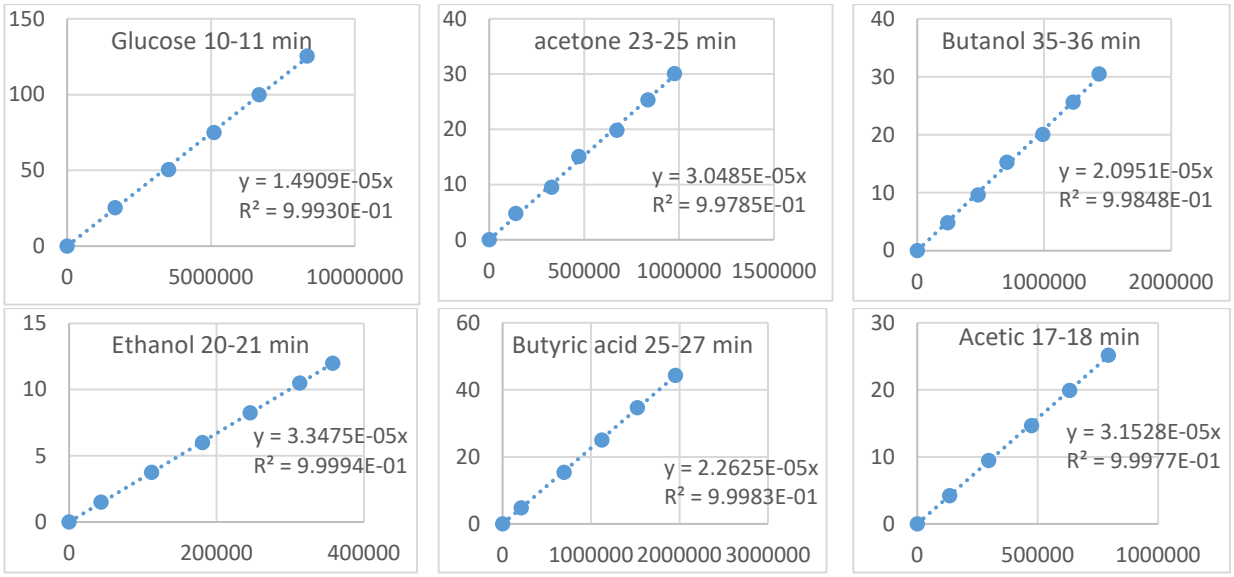

Figure S1.1 Standard curves for ABE metabolites

Electrotransformation on C. saccharoperbutylacetonicum N1-4

Before starting procedure, prepare/chill the following:

- TGY plate (TGY+15g/l agar and 30 ug/ml claritromycin)
- 250 ml TGY media (no antibiotics), store at room temperature
- 300 ml SMP buffer: 270 mM sucrose, 1mM $MgCl_2$ and 7mM Na_2HPO_3, then adjusted to pH 6.5 with HCl.
- 50ml conical tubes (or sterilized 175ml Centrifuge bottles) and autoclaved 1.5ml centrifuge tubes.
- 0.2 cm electroporation cuvette (stored at -20ºC; reusable)

Day 1

a. 250 µL of N1-4 glycerol stock (from -80ºC biofreezer) is activated overnight at 35ºC under in 5 mL TGY under anaerobic conditions.

Day 2 (Transportation of cell culture needs to be done on ice all the time)

b. This overnight culture was used to inoculate 100-200 ml TGY (depends on how much culture you need) at the 5% level. This culture was then grown at 35ºC under anaerobic conditions to an OD_{600} of 0.8. The cells were collected into 50ml conical tubes or 175ml centrifuge bottles, and harvested by centrifugation at 4,000 rpm for 10 minutes at room temperature.

c. The centrifuged culture is transported back into A.C.; Supernatant is dumped and one volume of SMP buffer. Shake briefly to resuspend the cell pellets (you may not need to resuspend the cell pellet all the way), and another centrifugation is conducted as in Step 1.

d. The centrifuged culture is transported back into A.C.; the cell pellet is re-suspended into 1/20 volume of SMP buffer and chilled in ice during 20 min and used immediately for electroporation.

e. An aliquot of 400 µl of electrocompetent N1-4 cells is added to 1 µg of plasmid DNA in an ice cold 0.2 mm electroporation cuvette. (Tip: you can add your DNA into cuvettes outside of the A.C., and then put cuvettes on ice and transfer into A.C. Then, competent cells are added once they are ready).

f. For electroporation, a BioRad Gene Pulser is used with the following parameters: 2.0 kV (1kV/mm) voltage, 25 µf capacitance and Ω (300) resistance.

g. Immediately following electroporation, the cell culture is transferred into a 10ml falcon tube or a 2ml centrifuge tube, and 1.6ml pre-warmed TGY is added. (Tip: you can pipette the pre-warmed TGY into cuvette to mix with the cell culture, and then transfer the whole mixture into a 10ml falcon tube or a 2ml centrifuge tube).

h. The culture is incubated at 35ºC under anaerobic conditions until visible sign of cell growth is evident (usually takes around two hours). Transfer the cell culture into 2ml centrifuge tubes (if it is not already in 2ml tubes), spin down the cell pellet, discard the supernatant, and resuspend using

TGY of appropriate volume (depends on your plating need). ~100µl of the resuspend culture is plated onto TGY agar plates containing 25 ug/ml erythromycin (or other desired antibiotics marker), and incubated at 35ºC under anaerobic conditions.

Day 3-4

i. After 12-48 hours of incubation, antibiotics resistant colonies would appear on plates. Further confirmation is conducted using colony PCR. Or: Colonies are picked and inoculated into TGY supplemented with antibiotics (usually use 2ml centrifuge tubes or large tubes).

j. Glycerol stock (20% v/v final glycerol concentration) can be prepared for the desirable transformants and stored into -80ºC.

k. If further fermentation experiment or longer cell growth is needed using the transformants, selective pressure is maintained by the addition of 30 ug/ml clarithromycinevery 24 hours.

PCR procedures

Protocol for Q5® High-Fidelity 2X Master Mix (according to manufacturer)

Table S1.5. Q5 reaction components

Component	50 µl Reaction	Final Concentration
Q5 High-Fidelity 2X Master Mix	25 µl	1X
10 µM Forward Primer	2.5 µl	0.5 µM
10 µM Reverse Primer	2.5 µl	0.5 µM
Template DNA	variable	< 1,000 ng
Nuclease-Free Water	to 50 µl	

Transfer PCR tubes to a PCR machine and begin thermocycling.

Thermocycling Conditions for a Routine PCR:

Table S1.6 Termocycling conditions for Q5

Step	Temperature	Time
Initial Denaturation	98°C	1 minute
30 Cycles	98°C	10 seconds
	*50–72°C	30 seconds
	72°C	1 minute/kb
Final Extension	72°C	10 minutes
Hold	4–10°C	

*NEB T_m Calculator is highly recommended.

General guidance

1. Template:

   Purified genomic DNA is the preferred source of templates. Amounts of DNA template for a 50 µl reaction are: 1µg for genomic DNA and 1 ng for plasmid

2. Primers:

   Oligonucleotide primers are generally 20–40 nucleotides in length and ideally have a GC content of 40–60%. Computer programs such as Primer3 can be used to design or analyze primers.

3. Annealing:

   Optimal annealing temperatures for Q5 High-Fidelity DNA Polymerase tend to be higher than for other PCR polymerases. The **NEB T_m Calculator** should be used to determine the annealing temperature when using this enzyme. Typically use a 10–30 second annealing step at 3°C above the T_m of the lower T_m primer. A temperature gradient can also be used to optimize the annealing temperature for each primer pair. For high T_m primer pairs, two-step cycling without a separate annealing step can be used (see note 10).

Appendix II.

Supplementary information for Chapter II. *In situ* biobutanol recovery from clostridial fermentation: a critical review

Pablo Jiménez-Bonilla[1,2], Yi Wang[1,3,*]

[1]Department of Biosystems Engineering, Auburn University, Auburn, AL 36849, USA. [2]Laboratory of Natural Products and Biological Assays (LAPRONEB), Chemistry Department, National University (UNA), Costa Rica. [3]Center for Bioenergy and Bioproducts, Auburn University, Auburn, AL 36849, USA

Supplementary Materials

Table S2.1 Toxicity on cells of selected extractant candidates tested in the literature for butanol recovery.

Substance	Strain	Toxic*	References
Alcohols			
1-pentanol	*C. acetycobutylicum* IAM19012	T	(Ishii, Taya, and Kobayashi 1985)
1-hexanol	*C. acetycobutylicum* IAM19012	T	(Ishii, Taya, and Kobayashi 1985)
1-octanol	*C. acetycobutylicum* IAM19012	T	(Ishii, Taya, and Kobayashi 1985)
1-Nonanol	*C. acetycobutylicum* ATCC824	T	(Barton and Daugulis 1992)
1-decanol	*C. acetycobutylicum* IAM19012	T	(Ishii, Taya, and Kobayashi 1985)
1-dodecanol	*C. acetycobutylicum* IAM19012	T	(Ishii, Taya, and Kobayashi 1985)
1-Dodecanol	*C. acetycobutylicum* ATCC824	T	(Barton and Daugulis 1992)
1-tridecanol	*C. acetycobutylicum* IAM19012	T	(Ishii, Taya, and Kobayashi 1985)
1,1-dihydrotridecafluoro-1-heptanol	*C. acetycobutylicum* IAM19012	T	(Ishii, Taya, and Kobayashi 1985)
1,7-Heptanediol	*C. acetycobutylicum* ATCC 824	T	(Barton and Daugulis 1992)
2-octanol	*C. acetycobutylicum* IAM19012	T	(Ishii, Taya, and Kobayashi 1985)
2-decanol	*C. acetycobutylicum* IAM19012	T	(Ishii, Taya, and Kobayashi 1985)
2-ethyl-1-hexanol	*C. acetycobutylicum* IAM19012	T	(Ishii, Taya, and Kobayashi 1985)
2-methyl-1-hexanol	*C. acetycobutylicum* IAM19012	T	(Ishii, Taya, and Kobayashi 1985)
2,4,6,8-tetramethyl-1-nonanol	*C. acetycobutylicum* IAM19012	T	(Ishii, Taya, and Kobayashi 1985)
CO-1214 FA	*C. acetycobutylicum* ATCC824	T	(Barton and Daugulis 1992)
Dobanol	*C. acetycobutylicum* IAM19012	T	(Ishii, Taya, and Kobayashi 1985)
EPAL 1214	*C. acetycobutylicum* ATCC824	T	(Barton and Daugulis 1992)
EPAL 1218	*C. acetycobutylicum* ATCC824	T	(Barton and Daugulis 1992)
Farnesol	*C. acetycobutylicum* ATCC824	T	(Barton and Daugulis 1992)

Geraniol	*C. acetycobutylicum* ATCC824	T	(Barton and Daugulis 1992)
Lauryl alcohol	*C. acetycobutylicum* ATCC824	T	(Barton and Daugulis 1992)
Linalool	*C. acetycobutylicum* ATCC824	T	(Barton and Daugulis 1992)
Neodol 23	*C. acetycobutylicum* ATCC824	T	(Barton and Daugulis 1992)
Neodol 25	*C. acetycobutylicum* ATCC824	T	(Barton and Daugulis 1992)
Neodol 45	*C. acetycobutylicum* ATCC824	NT	(Barton and Daugulis 1992)
Phytol	*C. acetycobutylicum* ATCC824	NT	(Barton and Daugulis 1992)
Polyether			
PPG 400	*C. acetycobutylicum* ATCC824	T	(Barton and Daugulis 1992)
PPG 425	*C. acetycobutylicum* ATCC824	T	(Barton and Daugulis 1992)
PPG 725	*C. acetycobutylicum* ATCC824	T	(Barton and Daugulis 1992)
Esters			
Benzyl benzoate	*C. acetycobutylicum* IAM19012	T	(Ishii, Taya, and Kobayashi 1985)
Dibutyl adipate	*C. acetycobutylicum* ATCC824	NT	(Barton and Daugulis 1992)
Dodecyl Ac	*C. acetycobutylicum* ATCC824	NT	(Barton and Daugulis 1992)
Ethyl caproate	*C. acetycobutylicum* IAM19012	T	(Ishii, Taya, and Kobayashi 1985)
Ethyl salicylate	*C. acetycobutylicum* IAM19012	T	(Ishii, Taya, and Kobayashi 1985)
ϒ-undecalactona	*C. acetycobutylicum* ATCC824	T	(Barton and Daugulis 1992)
Pentyl valerate	*C. acetycobutylicum* ATCC824	T	(Barton and Daugulis 1992)
Fatty acids			
Linoleic acid	*C. acetycobutylicum* ATCC824	NT	(Barton and Daugulis 1992)
Nonanoic acid	*C. acetycobutylicum* ATCC824	T	(Barton and Daugulis 1992)
Ricinoleic acid	*C. acetycobutylicum* IAM19012	T	(Ishii, Taya, and Kobayashi 1985)
Terpenes			
Dipentene	*C. acetycobutylicum* IAM19012	T	(Ishii, Taya, and Kobayashi 1985)
Oils			
Corn oil	*C. acetycobutylicum* ATCC824	NT	(Barton and Daugulis 1992)
Safflower oil	*C. acetycobutylicum* ATCC824	T	(Barton and Daugulis 1992)
Soy oil	*C. acetycobutylicum* ATCC824	NT	(Barton and Daugulis 1992)
Sunflower oil	*C. acetycobutylicum* ATCC824	NT	(Barton and Daugulis 1992)
Tricaprin	*C. acetycobutylicum* ATCC824	T	(Barton and Daugulis 1992)
Tributyrin	*C. beijerinckii* LMD27.30	NT	(Groot et al. 1990)

Abbreviations: CO-1214 FA: Commercial fatty alcohol blend of Lauryl/Myristyl Alcohol, Dobanol: high quality detergent range primary alcohols and primary alcoholethoxylates, EPAL 1214: commercial blend of 12-14 carbon linear saturated fatty alcohol, EPAL 1218: commercial blend of 12-18 carbon linear saturated fatty alcohol, Farnesol: (*2E,6E*)-3,7,11-trimethyldodeca-2,6,10-trien-1-ol, Geraniol: *trans*-3,7-dimethyl-2,6-octadien-1-ol, Neodol 23: commercial blend of C12 and C13 high purity primary alcohols, Neodol 25: commercial blend of C12, C13, C14 and C15 high purity primary alcohol, Neodol 45: commercial blend of C14 and C15 high purity primary alcohols, Phytol: *(2E,7R,11R)*-3,7,11,15-tetramethyl-2-hexadecen-1-ol, PPG: polypropyleneglycol, T: Toxic, NT: Non-Toxic, ND: No data, non-reported.

*A extractant is considered toxic or inhibitory when its presence reduces the cell growing response (gas generation, OD600, sugar consumption) in more than 10% respecting the control

Table S2.2 The butanol partition coefficient and selectivity of various extractants during liquid-liquid extraction for butanol recovery in ABE fermentation broth or model solutions.

Extractant	Fermentative strain	Toxic	K_D	Select	T (ºC)	Reference
Hydrocarbons						
Hexane	Aqueous model	ND	0.126-0.218	ND	25	(Núñez-Gómez et al. 2014)
	C. beijerinckii LMD27.6	NT	0.5	2700	37	(Groot et al. 1990)
Heptane	*C. beijerinckii* LMD27.6	NT	0.5	3300	37	(Groot et al. 1990)
Octane	*C. beijerinckii* LMD27.6	NT	0.3	4100	37	(Groot et al. 1990)
Decane	*C. beijerinckii* LMD27.6	NT	0.3	4300	37	(Groot et al. 1990)
Dodecane	*C. beijerinckii* LMD27.6	NT	0.3	2900	37	(Groot et al. 1990)
Petroleum ether	Aqueous model	ND	0.136-0.207	ND	25	(Núñez-Gómez et al. 2014)
Gasoline	*C. beijerinckii* LMD27.6	NT	0.3	ND	37	(Groot et al. 1990)
Octadecafluorodecalin	*C. acetobutylicum* IAM19012	NT	0.65	ND	37	(Ishii, Taya, and Kobayashi 1985)
Toluene	Aqueous model	ND	0.776-0.956	ND	25	(Núñez-Gómez et al. 2014)
1,3,5-Trimethylbenzene	Aqueous model	T	0.76	1650	25	(Kraemer et al. 2010)
	Aqueous model	T	2.2	1970	80	(Kraemer et al. 2010)
Oils						
Castor oil	*C. acetobutylicum* ATCC 824	ND	2.85	285.7	36	(Gonzalez-Penas et al. 2014)
	C. beijerinckii LMD27.6	NT	2.6	270	37	(Groot et al. 1990)
Cocos oil	*C. beijerinckii* LMD27.6	NT	0.8	440	37	(Groot et al. 1990)
Corn oil	*C. beijerinckii* LMD27.6	NT	0.7	440	37	(Groot et al. 1990)
Olive oil	*C. acetobutylicum* ATCC 824	T	0.68	ND	37	(Barton and Daugulis 1992)
	C. beijerinckii LMD27.6	NT	0.7	470	37	(Groot et al. 1990)
Pomace oil	*C. acetobutylicum* ATCC 824	NT	0.62	577.6	36	(Gonzalez-Penas et al. 2014)
Rapeseed oil	*C. beijerinckii* LMD27.6	NT	0.7	400	37	(Groot et al. 1990)
Sesame oil	*C. beijerinckii* LMD27.6	NT	0.3	220	37	(Groot et al. 1990)
Silicon oil	*C. acetobutylicum* ATCC 824	NT	0.59	3162	36	(Gonzalez-Penas et al. 2014)
Soy oil	*C. beijerinckii* LMD27.6	NT	0.7	440	37	(Groot et al. 1990)
Sunflower oil	*C. acetobutylicum* ATCC 824	NT	0.44	623.4	36	(Gonzalez-Penas et al. 2014)
Triolein	*C. acetobutylicum* ATCC 824	NT	0.75	ND	37	(Barton and Daugulis 1992)
Polyether						
Freon E	*C. acetobutylicum* IAM 19012	NT	0.31	ND	37	(Ishii, Taya, and Kobayashi 1985)
PPG 1000	*C. acetobutylicum* ATCC 824	T	4.8	ND	37	(Barton and Daugulis 1992)
PPG 1200	*C. acetobutylicum* ATCC 824	NT	4.8	ND	37	(Barton and Daugulis 1992)
PPG 2000	*C. acetobutylicum* ATCC 824	NT	3.9	ND	37	(Barton and Daugulis 1992)
PPG 3000	*C. acetobutylicum* ATCC 824	NT	3.5	ND	37	(Barton and Daugulis 1992)
PPG 4000	*C. acetobutylicum* ATCC 824	NT	3	ND	37	(Barton and Daugulis 1992)
Ester						
Butyl acetate	*C. beijerinckii* LMD27.6	T	3	ND	37	(Groot et al. 1990)
Hexyl acetate	*C. beijerinckii* LMD27.6	NT	3.6	5	37	(Groot et al. 1990)
Ethyl heptanoate	*C. beijerinckii* LMD27.6	NT	2	4	37	(Groot et al. 1990)
Methyl laurate	*C. beijerinckii* LMD27.6	NT	1.8	7	37	(Groot et al. 1990)
Ethyl laurate	*C. beijerinckii* LMD27.6	NT	1.7	7	37	(Groot et al. 1990)
Butyl laurate	*C. acetobutylicum* ATCC 824	NT	1.1	ND	37	(Barton and Daugulis 1992)
Ethyl stearate	*C. beijerinckii* LMD27.6	NT	0.8	7	37	(Groot et al. 1990)
Butyl stearate	*C. beijerinckii* LMD27.6	NT	1.2	ND	37	(Groot et al. 1990)
Isopropyl myristate	*C. beijerinckii* LMD27.6	NT	1.4	7	37	(Groot et al. 1990)
Methyl oleate	*C. beijerinckii* LMD27.6	NT	1.3	6	37	(Groot et al. 1990)

Oleyl oleate	*C. acetobutylicum* ATCC 824	NT	0.58	ND	37	(Barton and Daugulis 1992)
Dibutyl maleate	*C. beijerinckii* LMD27.6	T	2	3	37	(Groot et al. 1990)
Dibutyl adipate	*C. beijerinckii* LMD27.6	T	2.5	3	37	(Groot et al. 1990)
Diisobutyladipate	*C. acetobutylicum* ATCC 824	NT	2.6	834.1	36	(Kraemer et al. 2010)
Bis-(2-ethylhexyl) adipate	*C. acetobutylicum* ATCC 824	NT	1.83	668.3	36	(Kraemer et al. 2010)
	C. acetobutylicum ATCC 824	NT	1.6	ND	37	(Barton and Daugulis 1992)
Dibutyl sebacate	*C. acetobutylicum* ATCC 824	ND	1.89	474	36	(Kraemer et al. 2010)
	C. acetobutylicum ATCC 824	NT	1.8	ND	37	(Barton and Daugulis 1992)
Bis-(2-Ethylhexyl) sebacate	*C. acetobutylicum* ATCC 824	NT	1.2	ND	37	(Barton and Daugulis 1992)
Dibutyl phthalate	*C. acetobutylicum* ATCC 824	ND	1.91	36.3	36	(Kraemer et al. 2010)
	C. acetobutylicum ATCC 824	NT	1.8	ND	37	(Barton and Daugulis 1992)
	C. beijerinckii LMD27.6	NT	1.4	3	37	(Groot et al. 1990)
Bis-(methylglycol) phtalate	*C. beijerinckii* LMD27.6	T	2.5	ND	37	(Groot et al. 1990)
Bis-(3,5,5-Trimethylhexyl) phthalate	*C. acetobutylicum* ATCC 824	NT	1.1	ND	37	(Barton and Daugulis 1992)
Ethyleneglycol monosalicylate	*C. acetobutylicum* ATCC 824	T	5.5	ND	37	(Barton and Daugulis 1992)
Ethyl-DL-mandelate	*C. acetobutylicum* ATCC 824	T	5	ND	37	(Barton and Daugulis 1992)
Diisopropyl-L-tartrate	*C. acetobutylicum* ATCC 824	T	4.5	ND	37	(Barton and Daugulis 1992)
Dibutyl-L-tartrate	*C. acetobutylicum* ATCC 824	T	2.3	ND	37	(Barton and Daugulis 1992)
Triethyl citrate	*C. acetobutylicum* ATCC 824	T	3.5	ND	37	(Barton and Daugulis 1992)
Tributylcitrate	*C. acetobutylicum* ATCC 824	ND	1.67	73.7	36	(Kraemer et al. 2010)
	C. beijerinckii LMD27.6	NT	2.4	2	37	(Groot et al. 1990)
Acetyltriethyl Citrate	*C. acetobutylicum* ATCC 824	T	2.3	ND	37	(Barton and Daugulis 1992)
Soybean biodiesel	Aqueous model	ND	0.91	ND	25	(Li et al. 2010)
Biodiesel	*C. acetobutylicum* ATCC 824	ND	1.23	ND	30	(Li et al. 2010)
	C. acetobutylicum BCRC10639	NT	1.43	ND	37	(Yen and Wang 2013)
	C. Pasteurianum SE-5	NT	0.94-1.1	ND	37	(Zhang et al. 2014)
Alcohols						
1-hexanol	*C. beijerinckii* LMD27.6	T	12	160	37	(Groot et al. 1990)
1-heptanol	*C. beijerinckii* LMD27.6	T	11	180	37	(Groot et al. 1990)
1-octanol	*C. beijerinckii* LMD27.6	T	10	130	37	(Groot et al. 1990)
2-ethyl-1-hexanol	*C. acetobutylicum* ATCC 824	NT	7.95	311.1	36	(Kraemer et al. 2010)
1-decanol	*C. acetobutylicum* ATCC 4259	T	6.2	ND	34	(Evans and Wang 1988)
	C. beijerinckii LMD27.6	T	8	200	37	(Groot et al. 1990)
2-butyl-1-octanol	*C. acetobutylicum* ATCC 824	NT	6.76	644.8	36	(Kraemer et al. 2010)
1-dodecanol	*C. acetobutylicum* ATCC 824	NT	5.06	171.5	36	(Kraemer et al. 2010)
	C. saccharoperbutylacetonicum N1-4	ND	5.52	ND	30	(Tanaka et al. 2012)
	C. beijerinckii LMD27.6	T	6	140	37	(Groot et al. 1990)
Isohexadecanol	*C. acetobutylicum* IAM 19012	NT	3	ND	37	(Ishii, Taya, and Kobayashi 1985)
2-hexyl-1-decanol	*C. acetobutylicum* ATCC 824	T	3.41	509.2	36	(Kraemer et al. 2010)
	C. acetobutylicum ATCC 824	NT	3.2	ND	37	(Barton and Daugulis 1992)
	C. acetobutylicum IAM 19012	NT	4.5	ND	37	(Ishii, Taya, and Kobayashi 1985)
Oleyc alcohol	*C.acetobutylicum* KCTC 1790, *C. beijerinckii* KCTC5579	NT	3.32	ND	25	(Cascon et al. 2011)
	Aqueous model	ND	2.8	ND	25	(Li et al. 2010)
	Aqueous model	ND	3.42	194	25	(Garcia-Chavez et al. 2012)
	C. saccharoperbutylacetonicum N1-4	ND	3.67	ND	30	(Tanaka et al. 2012)
	Aqueous model	NT	3.8	180	30	(Matsumura et al. 1988)

	C. acetobutylicum ATCC 4259	NT	3.2	ND	34	(Evans and Wang 1988)
	C. acetobutylicum ATCC 824	NT	4.57	294.7	36	(Kraemer et al. 2010)
	C. acetobutylicum IAM 19012	NT	4.1-4.3	ND	37	(Ishii, Taya, and Kobayashi 1985)
Oleyc alcohol 85%	*C. acetobutylicum* ATCC 824	NT	3.6	ND	37	(Barton and Daugulis 1992)
HD Oleyc alcohol	*C. acetobutylicum* ATCC 824	NT	3.6	ND	37	(Barton and Daugulis 1992)
2-octyldodecanol	*C. acetobutylicum* ATCC 824	NT	2.6	ND	37	(Barton and Daugulis 1992)
	C. acetobutylicum IAM 19012	NT	3.2-3.5	ND	37	(Ishii, Taya, and Kobayashi 1985)
Adol 66	*C. acetobutylicum* ATCC 824	NT	3.5	ND	37	(Barton and Daugulis 1992)
Adol 85 NF	*C. acetobutylicum* ATCC 824	NT	3.7	ND	37	(Barton and Daugulis 1992)
Adol 330	*C. acetobutylicum* ATCC 824	NT	3.8	ND	37	(Barton and Daugulis 1992)
lsophytol	*C. acetobutylicum* ATCC 824	NT	3.2	ND	37	(Barton and Daugulis 1992)
Oxocol 1415	*C. acetobutylicum* IAM 19012	NT	4.7	ND	37	(Ishii, Taya, and Kobayashi 1985)
2-Ethyl-1,3-hexanediol	*C. acetobutylicum* ATCC 824	T	8.1	ND	37	(Barton and Daugulis 1992)
3-Methyl-2,4-heptanediol	*C. acetobutylicum* ATCC 824	T	7.9	ND	37	(Barton and Daugulis 1992)
Fatty acids						
Isostearic acid	*C. acetobutylicum* IAM 19012	NT	2.2	ND	37	(Ishii, Taya, and Kobayashi 1985)
Oleic acid	*C. acetobutylicum* IAM 19012	NT	3	ND	37	(Ishii, Taya, and Kobayashi 1985)
	C. beijerinckii LMD27.6	NT	3.9	6	37	(Groot et al. 1990)
Ionic liquids						
[Bmim][PF_6]	*C. pasteurianum* NRRL B-598	ND	0.828	20.58	50	(Ha, Mai, and Koo 2010)
	C. pasteurianum NRRL B-598	ND	0.742	21.03	25	(Ha, Mai, and Koo 2010)
[Bmim][Tf_2N]	*C. pasteurianum* NRRL B-598	ND	1.025	39.07	25	(Ha, Mai, and Koo 2010)
	C. pasteurianum NRRL B-598	ND	1.103	47.23	50	(Ha, Mai, and Koo 2010)
	Aqueous model	ND	1.243	58.11	10	(Kubiczek and Kamiński 2013)
	Aqueous model	ND	1.558	58.94	30	(Kubiczek and Kamiński 2013)
	Aqueous model	ND	1.964	65.56	50	(Kubiczek and Kamiński 2013)
[Dec_4N][1-MeCHC]	Aqueous model	ND	8.49	130	25	(Garcia-Chavez et al. 2012)
[Dmim][$B(CN)_4$]	Aqueous model	ND	3.2	100	25	(Huang, Ramaswamy, and Liu 2014)
	Aqueous model	ND	3.27	104	25	(Huang, Ramaswamy, and Liu 2014)
[Hex_4N][DHSS]	*C.acetobutylicum* KCTC 1790, *C. beijerinckii* KCTC5579	T	7.99	ND	25	(Cascon et al. 2011)
[Hmim][BF_4]	*C. pasteurianum* NRRL B-598	ND	0.902	3.906	25	(Ha, Mai, and Koo 2010)
	C. pasteurianum NRRL B-598	ND	1.186	4.258	50	(Ha, Mai, and Koo 2010)
[Hmim][PF_6]	Aqueous model	ND	1.263	46.14	30	(Kubiczek and Kamiński 2013)
	Aqueous model	ND	0.963	43.95	10	(Kubiczek and Kamiński 2013)
	Aqueous model	ND	1.616	54.01	50	(Kubiczek and Kamiński 2013)

	C. pasteurianum NRRL B-598	ND	0.967	37.48	25	(Ha, Mai, and Koo 2010)
	C. pasteurianum NRRL B-598	ND	1.411	42.43	50	(Ha, Mai, and Koo 2010)
[Hmim][Tf_2N]	*C. pasteurianum* NRRL B-598	ND	1.253	66.12	25	(Ha, Mai, and Koo 2010)
	C. pasteurianum NRRL B-598	ND	1.545	74.88	50	(Ha, Mai, and Koo 2010)
	Aqueous model	ND	1.11	120	25	(14)
[Hmim][TfO]	*C. pasteurianum* NRRL B-598	ND	0.905	2.619	25	(Ha, Mai, and Koo 2010)
	C. pasteurianum NRRL B-598	ND	1.217	4.011	50	(Ha, Mai, and Koo 2010)
[$MeOct_3N$][Oct]	Aqueous model	ND	11.29	49	25	(Garcia-Chavez et al. 2012)
[$MeOct_3N$][Tf_2N]	*C.acetobutylicum* KCTC 1790, *C. beijerinckii* KCTC5579	T	1.44	ND	25	(Cascon et al. 2011)
[$MeOct_3N$][Cl]	*C. acetobutylicum* ATCC 824	ND	8.86	41.7	36	(Gonzalez-Penas et al. 2014)
[Oct_4N][2-MNaph]	Aqueous model	ND	21	274	25	(Garcia-Chavez et al. 2012)
[Omim][$B(CN)_4$]	Aqueous model	ND	3.7	97	25	(Huang, Ramaswamy, and Liu 2014)
[Omim][BF_4]	*C. pasteurianum* NRRL B-598	ND	2.183	21.24	25	(Ha, Mai, and Koo 2010)
	C. pasteurianum NRRL B-598	ND	2.479	12.97	50	(Ha, Mai, and Koo 2010)
[Omim][PF_6]	*C. pasteurianum* NRRL B-598	ND	1.307	51.41	50	(Ha, Mai, and Koo 2010)
	C. pasteurianum NRRL B-598	ND	1.105	49.23	25	(Ha, Mai, and Koo 2010)
[Omim][Tf_2N]	*C. pasteurianum* NRRL B-598	ND	1.372	78.89	25	(Ha, Mai, and Koo 2010)
	C. pasteurianum NRRL B-598	ND	1.939	132.4	50	(Ha, Mai, and Koo 2010)
[Omim][TfO]	*C. pasteurianum* NRRL B-598	ND	1.028	3.562	25	(Ha, Mai, and Koo 2010)
	C. pasteurianum NRRL B-598	ND	2.343	8.116	50	(Ha, Mai, and Koo 2010)
[Ph_3t][$(^iC_8)_2PO_2$]	Aqueous model	ND	9.21	55	25	(Garcia-Chavez et al. 2012)
	Aqueous model	ND	19-59	80-305	25	(Rabari and Banerjee 2013)
[Ph_3t][$B(CN)_4$]	Aqueous model	ND	2.0	500	25	(Huang, Ramaswamy, and Liu 2014)
[Ph_3t][DCN]	*C.acetobutylicum* KCTC 1790, *C. beijerinckii* KCTC5579	T	7.49	ND	25	(Cascon et al. 2011)
[Ph_3t][Tf_2N]	*C.acetobutylicum* KCTC 1790, *C. beijerinckii* KCTC5579	T	1.1	ND	25	(Cascon et al. 2011)
[Ph_3t][Cl]	*C. acetobutylicum* ATCC 824	ND	11.55	83	36	(Gonzalez-Penas et al. 2014)
[Pmim][TfO]	*C. pasteurianum* NRRL B-598	ND	1.046	4.959	25	(Ha, Mai, and Koo 2010)
[Pmim][TfO]	*C. pasteurianum* NRRL B-598	ND	1.186	6.539	50	(Ha, Mai, and Koo 2010)

Abreviations: T: Toxic, NT: Non-Toxic, ND: No data or non-reported, ADOL 66: isoestearyl alcohol, Adol 85NF: commercial alcohol blend 69% oleyl alcohol, Adol 330: commercial alcohol blend 62% oleyl alcohol, Freon E: 2H-Perfluoro-5,8,11,14,17,20,23-Heptakismethyl-3,6,9,12,15,18,21,24-octaoxoheptacosane, Isophytol: 3,7,11,15-tetramethyl-1-hexadecen-3-ol, Oxocol 1415: commercial C14-C15 alcohol blend, PPG: Poly(propyleneglycol) (number indicates molecular weigth), Ionic liquid cations: [Bmim]: 1-butyl-3-methylimidazolium, [Dmim]: 1-decyl-3-methylimidazolium, [Dec_4N]: tetra(decyl)ammonium, [Hex_4N]: Tetrahexylammonium, [Hmim]: 1-hexyl-3-methylimidazolium, [Ph_3t]: Trihexyl(tetradecyl)phosphonium, [Pmim]: 1-pentyl-3-methylimidazolium, [$MeOct_3N$]: Methyltrioctylammonium, [Oct_4N]: tetraoctylammonium, [Omim]: 1-octyl-3-methylimidazolium, [Pr_4N]: Tetrapropylammonium; Ionic liquid anions: [$B(CN)_4$]: tetracyanoborate, [BF_4]: Boron tetrafluoride, [$(^iC_8)_2PO_2$]: bis-2,4,4-(trimethylpentyl) phosphinate, [Cl]: Chloride, [DCN]: dicyanamide, [DHSS]: dihexylsulfosuccinate, [FAP]: tris(pentafluoroethyl)trifluorophosphate, [2-MNaph]: 2-methyl-1-naphthoate, [1-MeCHC]: 1-methylcyclohexecarboxylate, [Oct]: octoate, [PF_6]: Phosphorous hexafluoride, [Tf_2N]: bis(trifluoromethylsulphonyl)imide, [TfO]: Triflate,

Table S2.3 Summary of partition coefficients and loading capacities of the adsorbants used for biobutanol recovery from the literature.

Type	Name	Media	T (ºC)	$K_{s/w}$	L (mg/g)	References
Active carbon	Chemivron AP3-60	Single component model	25	ND	~300	(Saint Remi, Baron, and Denayer 2012)
Active carbon	Nuchar WV-G	Single component model	25	0.34	68	(Giusti, Conway, and Lawson 1974)
Active carbon	Norit ROW 0.8	Single component model	ND	ND	220	(Groot and Luyben 1986)
Active carbon	Norit ROW 0.8	Single component model	37	0.15	210	(Xue et al. 2016)
Active carbon	Norit W52	Single component model	ND	ND	220	(Groot and Luyben 1986)
Active carbon	Witco Grade 517	Single component model	25	1.05	110	(Giusti, Conway, and Lawson 1974)
Active carbon	Witco Grade 517	Binary component model	25	1.05	116	(Giusti, Conway, and Lawson 1974)
Active carbon	Witco Grade 517	Quaternary component model	25	0.28	31	(Giusti, Conway, and Lawson 1974)
Active carbon	Nuchar WV-G	Quaternary component model	25	0.34	23	(Giusti, Conway, and Lawson 1974)
Zeolite	CBV901	Single component model	37	0.03	150	(Xue et al. 2016)
Zeolite	CBV28014	Single component model	37	0.02	110	(Xue et al. 2016)
Zeolite	Silicalite Silikalit	Single component model	25	ND	~100	(Saint Remi, Baron, and Denayer 2012)
Zeolite	silicalite-1	Ternary component model	25	ND	93-98	(Huang and Meagher 2001)
Zeolite	Silicalite-1	Ternary component model	36	ND	85-90	(Qureshi, Meagher, and Hutkins 1999)
Zeolite	Silicalite-1	Fermentation broth	20	ND	64-85	(Xue et al. 2016)
P(S-co-DVB)	Dowex Optipore SD2	Single component model	37	0.03	140	(Xue et al. 2016)
P(S-co-DVB)	Dowex Optipore SD2	Ternary component model	25	187.5	49.6	(Nielsen and Prather 2009)
P(S-co-DVB)	Dowex Optipore L493	Single component model	37	0.04	140	(Xue et al. 2016)
P(S-co-DVB)	Dowex Optipore L493	Ternary component model	25	9.9	5.4	(Nielsen and Prather 2009)
P(S-co-DVB)	Diaion HP20	Single component model	37	0.02	90	(Xue et al. 2016)
P(S-co-DVB)	Diaion HP20	Ternary component model	25	44.0	44.3	(Nielsen and Prather 2009)
P(S-co-DVB)	Dowex M43	Ternary component model	25	2.2	1.7	(Nielsen and Prather 2009)
P(S-co-DVB)	Bonopore	Single component model	20	ND	74.0	(Nielsen et al. 1988)
P(S-co-DVB)	Bonopore	*C.acetycobutylicum* broth	20	ND	23.0	(Nielsen et al. 1988)
P(S-co-DVB)	Bonopore, nitrated	Single component model	20	ND	55.0	(Nielsen et al. 1988)
P(S-co-DVB)	Bonopore, nitrated	*C.acetycobutylicum* broth	20	ND	13.0	(Nielsen et al. 1988)
P(S-co-DVB)	KA-I resin	ternary component model	37	ND	84-93	(29)(Liu et al. 2014)
P(S-co-DVB)	Amberlite IRA-900	Single component model	37	<0.01	40	(Xue et al. 2016)
P(S-co-DVB)	Amberlite XAD 2	Single component model	20	ND	50	(Groot and Luyben 1986)
P(S-co-DVB)	Amberlite XAD-4	Single component model	37	0.02	90	(Xue et al. 2016)
P(S-co-DVB)	Amberlite XAD-4	Single component model	20	ND	97.5	(Groot and Luyben 1986)
P(S-co-DVB)	Amberlite XAD-4	Single component model	20	ND	83.0	(Nielsen et al. 1988)
P(S-co-DVB)	Amberlite XAD-4	*C.acetycobutylicum* broth	20	ND	27.0	(Nielsen et al. 1988)
P(S-co-DVB)	Amberlite XAD 8	Single component model	20	ND	40	(Groot and Luyben 1986)
PA ester	Amberlite XAD-7	Single component model	20	ND	69.0	(Nielsen et al. 1988)
PA ester	Amberlite XAD-7	*C.acetycobutylicum* broth	20	ND	22.0	(Nielsen et al. 1988)
PMA	Diaion HP-2MG	Single component model	37	0.01	60	(Xue et al. 2016)
PMA	Diaion HP-2MG	Ternary component model	25	3.4	2.7	(Nielsen and Prather 2009)
PBP	Hytrel 8206	Ternary component model	25	0.8	0.7	(Nielsen and Prather 2009)
PVP	Reillex 425	*C.acetycobutylicum* broth	38	4.95	ND	(Yang, Tsai, and Tsao 1994)
MOF Zn-im	ZIF-8	Quaternary component model	25	ND	~300	(Saint Remi, Baron, and Denayer 2012)

Abbreviations: T: Temperature. Ks/w: Partition coefficient of solid-water, L: loading charge (mg butanol/g adsorbent), P(S-co-DVB): Polystyrene-divinylbenzene, PA ester: Polyacrylic ester side, PMA: Polymethacrylate, PBP: Polybutylene phthalate, PVP: Polyvinylpiridine, MOF: Zn-im Metal organic framework Zn-imidazole.

Table S2.4 The parameters and adsorbent characteristics in Langmuir model for butanol adsorption.

Type	Name	Media	Pore (A)	Particle (mesh)	Surface (m^2/g)	T (°C)	q_{imax} (mg/g)	B_i L/g	Reference
Active carbon	Norit ROW 0.8	ABE model	20-500	20-25	ND	37	480	0.581	(Xue et al. 2016)
Active carbon	Norit ROW 0.8	ABE model	20-500	20-25	ND	60	450	0.498	(Xue et al. 2016)
Zeolite	Silicalite-1	single component model	ND	ND	ND	35	133	0.860	(Farzaneh et al. 2015)
Zeolite	Silicalite-1	single component model	ND	ND	ND	50	133	0.267	(Farzaneh et al. 2015)
Zeolite	Silicalite-1	single component model	ND	ND	ND	85	133	0.0156	(Farzaneh et al. 2015)
Zeolite	Silicalite-1	single component model	ND	ND	ND	120	133	0.0026	(Farzaneh et al. 2015)
Zeolite Y	CBV901	single component model	ND	ND	400	25	168	3.14	(Oudshoorn, van der Wielen, and Straathof 2009)
Zeolite Y	CBV901	ABE model	ND	ND	400	37	240	0.556	(Xue et al. 2016)
Zeolite Y	CBV901	ABE model	ND	ND	400	60	210	0.901	(Xue et al. 2016)
Zeolite Beta	CBV811	single component model	ND	ND	620	25	126	1.68	(Oudshoorn, van der Wielen, and Straathof 2009)
Zeolite ZSM-5	CBV28014	single component model	ND	ND	700	25	118	42.8	(Oudshoorn, van der Wielen, and Straathof 2009)
P(S-co-DVB)	Dowex L493	ABE model	46	20-50	1100	37	360	0.249	(Xue et al. 2016)
P(S-co-DVB)	Dowex L493	ABE model	46	20-50	1100	60	330	0.249	(Xue et al. 2016)
P(S-co-DVB)	Dowex SD2	ABE model	50	16-50	800	37	380	0.231	(Xue et al. 2016)
P(S-co-DVB)	Dowex SD2	ABE model	50	16-50	800	60	310	0.203	(Xue et al. 2016)
P(S-co-DVB)	Optipore L493	single component model	23	300-800	ND	37	140.7	0.4	(Lee et al. 2015)
P(S-co-DVB)	Sepabeads SP850	single component model	62	250-600	ND	37	130.2	0.4	(Lee et al. 2015)
P(S-co-DVB)	KA-I resin	single component model	145-155	20-25	850-950	25	49.0	0.30	(Wu et al. 2015)
P(S-co-DVB)	KA-I resin	single component model	145-155	20-25	850-950	25	167	0.40	(Lin, Wu, Jin, et al. 2012)
P(S-co-DVB)	KA-I resin	single component model	145-155	20-25	850-950	10	139.836	0.418	(Lin, Wu, Fan, et al. 2012)
P(S-co-DVB)	KA-I resin	single component model	145-155	20-25	850-950	20	170.744	0.341	(Lin, Wu, Fan, et al. 2012)
P(S-co-DVB)	KA-I resin	single component model	145-155	20-25	850-950	30	231.73	0.265	(Lin, Wu, Fan, et al. 2012)
P(S-co-DVB)	KA-I resin	single component model	145-155	20-25	850-950	37	304.397	0.234	(Lin, Wu, Fan, et al. 2012)
P(S-co-DVB)	KA-I resin	single component model	145-155	20-25	850-950	25	174.5	0.3	(Jiao et al. 2015)
P(S-co-DVB)	KA-I resin	single component model	145-155	20-25	850-950	25	191	0.300	(Lin et al. 2013)
P(S-co-DVB)	KA-I resin	binary model 118 g/L ethanol	145-155	20-25	850-950	25	174.5	0.079	(Jiao et al. 2015)
P(S-co-DVB)	KA-I resin	binary model 197 g/L ethanol	145-155	20-25	850-950	25	174.5	0.02	(Jiao et al. 2015)
P(S-co-DVB)	KA-I resin	binary model 394 g/L ethanol	145-155	20-25	850-950	25	174.5	0.0076	(Jiao et al. 2015)

P(S-co-DVB)	KA-I resin	binary model 591 g/L ethanol	145-155	20-25	850-950	25	174.5	0.0013	(Jiao et al. 2015)
P(S-co-DVB)	KA-I resin	ternary component model	145-155	20-25	850-950	25	48.0	0.30	(Wu et al. 2015)
P(S-co-DVB)	KA-I resin	*C. acetobutylicum* B3 broth	145-155	20-25	850-950	25	48.0	0.30	(Wu et al. 2015)
P(S-co-DVB)	H511	single component model	84-94	35	1000-1100	25	206	0.20	(Lin, Wu, Jin, et al. 2012)
PA-g-ester	XD41	single component model	280-300	25-30	540-620	25	127	0.25	(Lin, Wu, Jin, et al. 2012)

Abbreviations: T: temperature. P(S-co-DVB): Polystyrene-divinylbenzene.

Table S2.5 Freundlich constants for butanol adsorption with different adsorbents

Type	Name	Media	Pore (A)	Particle (mesh)	Surface (m^2/g)	T (°C)	k (mmol/kg)	n	Reference
Active carbon	Witco 517	water model pH 2	ND	12-30	1050	25	1848	2.29	(Giusti, Conway, and Lawson 1974)
Active carbon	Witco 517	water model pH 11	ND	12-30	1050	25	2402	1.98	(Giusti, Conway, and Lawson 1974)
Active carbon	Filtrabsorb 400	water model pH 2	ND	12-40	1050-1200	25	1268	2.25	(Giusti, Conway, and Lawson 1974)
Active carbon	Filtrabsorb 400	water model pH 11	ND	12-40	1050-1200	25	1862	1.68	(Giusti, Conway, and Lawson 1974)
Active carbon	Nuchar WV-G	water model pH 2	ND	12-40	1100	25	1214	2.11	(Giusti, Conway, and Lawson 1974)
Active carbon	Nuchar WV-G	water model pH 11	ND	12-40	1100	25	1525	2.29	(Giusti, Conway, and Lawson 1974)
Active carbon	Nacar G107	water model pH 2	ND	12-30	1000-1100	25	850	1.09	(Giusti, Conway, and Lawson 1974)
Active carbon	Nacar G107	water model pH 11	ND	12-30	1000-1100	25	917	1.07	(Giusti, Conway, and Lawson 1974)
C (P6mm)	FDU-15-800	binary component model	ND	ND	538	37	371	3.65	(Levario et al. 2012)
C (Im3m)	FDU-16-800	binary component model	ND	ND	671	37	708	4.61	(Levario et al. 2012)
C-Si (Im3m)	CS-68-800	binary component model	ND	ND	1287	37	245	1.92	(Levario et al. 2012)
C-Si (Im3m)	CS-81-800	binary component model	ND	ND	1307	37	446	2.39	(Levario et al. 2012)
P(S-co-DVB)	Optipore SD2	single component model	ND	ND	900	37	398	2.17	(Nielsen, Amarasiriwardena, and Prather 2010)
P(S-co-DVB)	Diaion HP20	single component model	ND	ND	500	37	95	1.64	(Nielsen, Amarasiriwardena, and Prather 2010)
P(S-co-DVB)	Dowex M43	single component model	ND	ND	ND	37	17	1.28	(Nielsen, Amarasiriwardena, and Prather 2010)
P(S-co-DVB))	KA-I resin	single component model	145-155	20-25	850-950	10	601.31	2.68	(Lin, Wu, Fan, et al. 2012)
P(S-co-DVB)	KA-I resin	single component model	145-155	20-25	850-950	20	653.05	2.48	(Lin, Wu, Fan, et al. 2012)
P(S-co-DVB)	KA-I resin	single component model	145-155	20-25	850-950	30	722.00	2.19	(Lin, Wu, Fan, et al. 2012)
P(S-co-DVB)	KA-I resin	single component model	145-155	20-25	850-950	37	891.65	1.03	(Lin, Wu, Fan, et al. 2012)

P(S-co-DVB)	Optipore L493	single component model	46	20-50	1100	37	362	2.00	(Wiehn et al. 2014)
P(S-co-DVB)	Optipore L493	single component model	46	ND	1100	37	446	2.22	(Nielsen, Amarasiriwardena, and Prather 2010)
P(S-co-DVB))	Optipore L493	binary component model	ND	ND	>1100	37	446	2.22	(Levario et al. 2012)
P(S-co-DVB)	Optipore L493	tertiaty component model	46	ND	1100	37	328	2.03	(Wiehn et al. 2014)
PMA	Diaion HP2MG	single component model	ND	ND	500	37	18	1.18	(Nielsen, Amarasiriwardena, and Prather 2010)
PBA	Hytrel 8206	single component model	ND	ND	ND	37	0.1	0.65	(Nielsen, Amarasiriwardena, and Prather 2010)

Abbreviations: PMA: Polymethaacrylate. PBA: P(butylene phthalate). C(P6mm): Carbon hexagonally packed cilindrical. C(Im3m): Carbon body centered cubic. C-Si(Im3m): Carbon-silica Im3m (spherical) packed espherical, T: temperature, n and k: Freunlich parameters

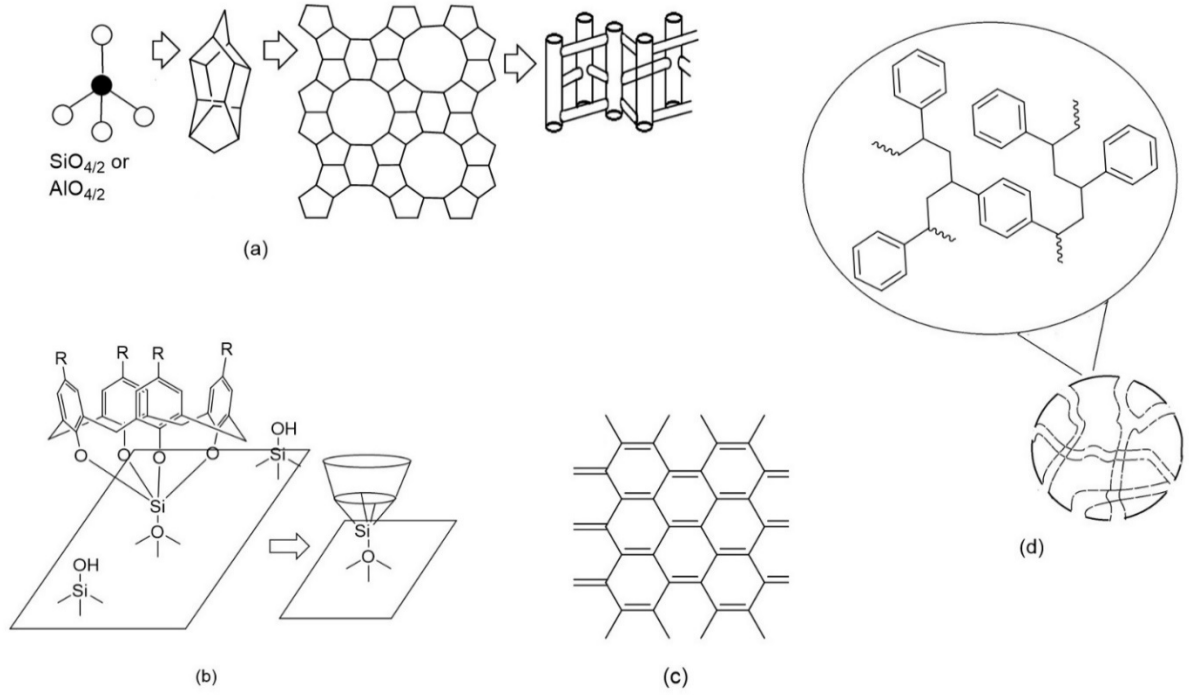

Figure S2.1 Structure and morphology of selected adsorbents for butanol recovery. (a) Silicalite and zeolite ZSM-5, (b) Silicon oxide functionalized with calixarenes, (c) Carbon (graphite), (d) Poly(styrene-co-divinylbenzene).

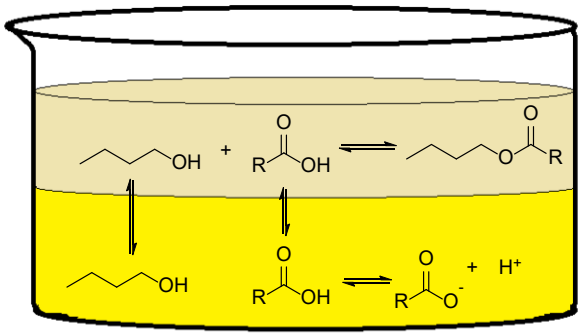

Figure S2.2 Butanol extractive esterification equilibria

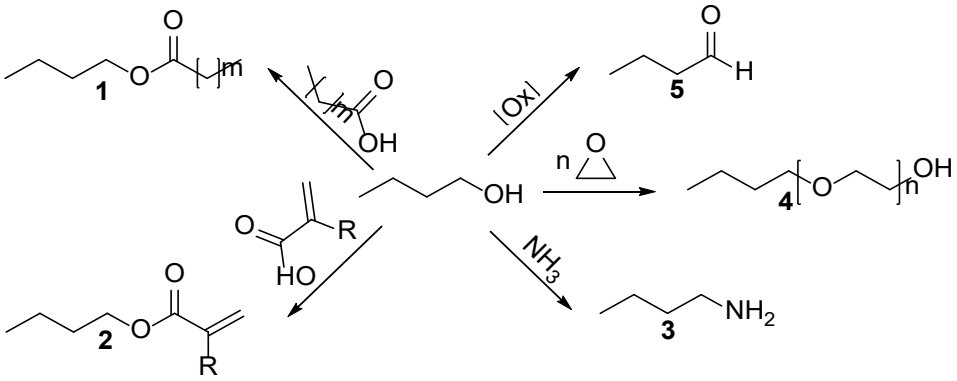

Figure S2.3 Selected butanol derivatives that can be potentially produced by in situ reactive extraction. 1 represents butyl linear esters, m=0, 2 for acetic and butyric and m=0-22 for linear saturated derivatives; 2 represents butyl acrylic esters: butyl acrylate when R=H and butyl methacrylate when R= CH_3; 3 is butylamine; 4 represents butyl glycol ethers: n has typical values 1-3; 5 is butyraldehyde: [Ox] means oxidation. Details about catalysts, coproducts and conditions are not specified.

References

Barton, W Edward, and Andrew J Daugulis. 1992. Evaluation of solvents for extractive butanol fermentation with Clostridium acetobutylicum and the use of poly (propylene glycol) 1200. *Applied microbiology and biotechnology* 36 (5):632-639.

Cascon, Hercules R, Santosh K Choudhari, Grace M Nisola, Eleazer L Vivas, Dong-Ju Lee, and Wook-Jin Chung. 2011. Partitioning of butanol and other fermentation broth components in phosphonium and ammonium-based ionic liquids and their toxicity to solventogenic clostridia. *Separation and Purification Technology* 78 (2):164-174.

Evans, Patrick J, and Henry Y Wang. 1988. Enhancement of butanol formation by Clostridium acetobutylicum in the presence of decanol-oleyl alcohol mixed extractants. *Applied and environmental microbiology* 54 (7):1662-1667.

Farzaneh, Amirfarrokh, Ming Zhou, Elisaveta Potapova, Zoltán Bacsik, Lindsay Ohlin, Allan Holmgren, Jonas Hedlund, and Mattias Grahn. 2015. Adsorption of water and butanol in silicalite-1 film studied with in situ attenuated total reflectance–Fourier transform infrared spectroscopy. *Langmuir* 31 (17):4887-4894.

Garcia-Chavez, Lesly Y, Christian M Garsia, Boelo Schuur, and André B de Haan. 2012. Biobutanol recovery using nonfluorinated task-specific ionic liquids. *Industrial & Engineering Chemistry Research* 51 (24):8293-8301.

Giusti, DM, RA Conway, and CT Lawson. 1974. Activated carbon adsorption of petrochemicals. *Journal (Water Pollution Control Federation)*:947-965.

Gonzalez-Penas, Helena, TA Lu-Chau, MT Moreira, and JM Lema. 2014. Solvent screening methodology for in situ ABE extractive fermentation. *Applied microbiology and biotechnology* 98 (13):5915-5924.

Groot, WJ, and K Ch AM Luyben. 1986. In situ product recovery by adsorption in the butanol/isopropanol batch fermentation. *Applied microbiology and biotechnology* 25 (1):29-31.

Groot, WJ, HS Soedjak, PB Donck, RGJM Van der Lans, K Ch AM Luyben, and JMK Timmer. 1990. Butanol recovery from fermentations by liquid-liquid extraction and membrane solvent extraction. *Bioprocess Engineering* 5 (5):203-216.

Ha, Sung Ho, Ngoc Lan Mai, and Yoon-Mo Koo. 2010. Butanol recovery from aqueous solution into ionic liquids by liquid–liquid extraction. *Process Biochemistry* 45 (12):1899-1903.

Huang, Hua-Jiang, Shri Ramaswamy, and Youyan Liu. 2014. Separation and purification of biobutanol during bioconversion of biomass. *Separation and Purification Technology* 132:513-540.

Huang, Jicai, and MM Meagher. 2001. Pervaporative recovery of n-butanol from aqueous solutions and ABE fermentation broth using thin-film silicalite-filled silicone composite membranes. *Journal of Membrane Science* 192 (1-2):231-242.

Ishii, Shigeo, Masahito Taya, and Takeshi Kobayashi. 1985. Production of butanol by Clostridium acetobutylicum in extractive fermentation system. *Journal of chemical engineering of Japan* 18 (2):125-130.

Jiao, Pengfei, Jinglan Wu, Yingchun Ji, Xu Ke, Fengxia Zou, Jingwei Zhou, Wei Zhuang, and Hanjie Ying. 2015. Desorption of 1-butanol from polymeric resin: experimental studies and mathematical modeling. *RSC Advances* 5 (127):105464-105474.

Kraemer, Korbinian, Andreas Harwardt, Rob Bronneberg, and Wolfgang Marquardt. 2010. Separation of butanol from acetone-butanol-ethanol fermentation by a hybrid extraction-distillation process. In *Computer Aided Chemical Engineering*: Elsevier.

Kubiczek, Artur, and Władysław Kamiński. 2013. Ionic liquids for the extraction of n-butanol from aqueous solutions. *Ecological Chemistry and Engineering. A* 20 (1):77-87.

Lee, Sang-Hyun, Moon-Ho Eom, Sooah Kim, Min-A Kwon, Jungyeon Kim, Yong-An Shin, and Kyoung Heon Kim. 2015. Ex situ product recovery and strain engineering of Clostridium acetobutylicum for enhanced production of butanol. *Process Biochemistry* 50 (11):1683-1691.

Levario, Thomas J, Mingzhi Dai, Wei Yuan, Bryan D Vogt, and David R Nielsen. 2012. Rapid adsorption of alcohol biofuels by high surface area mesoporous carbons. *Microporous and Mesoporous Materials* 148 (1):107-114.

Li, Qing, Hao Cai, Bo Hao, Congling Zhang, Ziniu Yu, Shengde Zhou, and Liu Chenjuan. 2010. Enhancing clostridial acetone-butanol-ethanol (ABE) production and improving fuel properties of ABE-enriched biodiesel by extractive fermentation with biodiesel. *Applied biochemistry and biotechnology* 162 (8):2381-2386.

Lin, Xiaoqing, Renjie Li, Qingshi Wen, Jinglan Wu, Jiansheng Fan, Xiaohong Jin, Wenbin Qian, Dong Liu, Xiaochun Chen, and Yong Chen. 2013. Experimental and modeling studies on the sorption breakthrough behaviors of butanol from aqueous solution in a fixed-bed of KA-I resin. *Biotechnology and bioprocess engineering* 18 (2):223-233.

Lin, Xiaoqing, Jinglan Wu, Jiansheng Fan, Wenbin Qian, Xiqun Zhou, Chen Qian, Xiaohong Jin, Lili Wang, Jianxin Bai, and Hanjie Ying. 2012. Adsorption of butanol from aqueous solution onto a new type of macroporous adsorption resin: studies of adsorption isotherms and kinetics simulation. *Journal of Chemical Technology & Biotechnology* 87 (7):924-931.

Lin, Xiaoqing, Jinglan Wu, Xiaohong Jin, Jiansheng Fan, Renjie Li, Qingshi Wen, Wenbin Qian, Dong Liu, Xiaochun Chen, and Yong Chen. 2012. Selective separation of biobutanol from acetone–butanol–ethanol fermentation broth by means of sorption methodology based on a novel macroporous resin. *Biotechnology progress* 28 (4):962-972.

Liu, Dong, Yong Chen, Feng-Ying Ding, Ting Zhao, Jing-Lan Wu, Ting Guo, Heng-Fei Ren, Bing-Bing Li, Huan-Qing Niu, and Zhi Cao. 2014. Biobutanol production in a Clostridium acetobutylicum biofilm reactor integrated with simultaneous product recovery by adsorption. *Biotechnology for biofuels* 7 (1):5.

Matsumura, M, H Kataoka, M Sueki, and K Araki. 1988. Energy saving effect of pervaporation using oleyl alcohol liquid membrane in butanol purification. *Bioprocess Engineering* 3 (2):93-100.

Nielsen, David R, Gihan S Amarasiriwardena, and Kristala LJ Prather. 2010. Predicting the adsorption of second generation biofuels by polymeric resins with applications for in situ product recovery (ISPR). *Bioresource technology* 101 (8):2762-2769.

Nielsen, David R, and Kristala Jones Prather. 2009. In situ product recovery of n-butanol using polymeric resins. *Biotechnology and bioengineering* 102 (3):811-821.

Nielsen, Lena, Mats Larsson, Olle Holst, and Bo Mattiasson. 1988. Adsorbents for extractive bioconversion applied to the acetone-butanol fermentation. *Applied Microbiology and Biotechnology* 28 (4-5):335-339.

Núñez-Gómez, Karen-Stephanie, Liliana-Carolina López-Mendoza, Luis-Javier López-Giraldo, and Carlos-Jesús Muvdi-Nova. 2014. Study of acetone, butanol and ethanol liquid extraction from prepared aqueous solutions using membrane contactor technique. *CT&F-Ciencia, Tecnología y Futuro* 5 (4):97-112.

Oudshoorn, Arjan, Luuk AM van der Wielen, and Adrie JJ Straathof. 2009. Adsorption equilibria of bio-based butanol solutions using zeolite. *Biochemical engineering journal* 48 (1):99-103.

Qureshi, N, MM Meagher, and RW Hutkins. 1999. Recovery of butanol from model solutions and fermentation broth using a silicalite/silicone membrane1. *Journal of Membrane Science* 158 (1-2):115-125.

Rabari, Dharamashi, and Tamal Banerjee. 2013. Biobutanol and n-propanol recovery using a low density phosphonium based ionic liquid at T= 298.15 K and p= 1atm. *Fluid Phase Equilibria* 355:26-33.

Saint Remi, J Cousin, G Baron, and J Denayer. 2012. Adsorptive separations for the recovery and purification of biobutanol. *Adsorption* 18 (5-6):367-373.

Tanaka, Shigemitsu, Yukihiro Tashiro, Genta Kobayashi, Toru Ikegami, Hideyuki Negishi, and Keiji Sakaki. 2012. Membrane-assisted extractive butanol fermentation by Clostridium saccharoperbutylacetonicum N1-4 with 1-dodecanol as the extractant. *Bioresource technology* 116:448-452.

Wiehn, Michael, Kyle Staggs, Yuchen Wang, and David R Nielsen. 2014. In situ butanol recovery from Clostridium acetobutylicum fermentations by expanded bed adsorption. *Biotechnology progress* 30 (1):68-78.

Wu, Jinglan, Wei Zhuang, Hanjie Ying, Pengfei Jiao, Renjie Li, Qingshi Wen, Lili Wang, Jingwei Zhou, and Pengpeng Yang. 2015. Acetone–butanol–ethanol competitive sorption simulation from single, binary, and ternary systems in a fixed-bed of KA-I resin. *Biotechnology progress* 31 (1):124-134.

Xue, Chuang, Fangfang Liu, Mengmeng Xu, I-Ching Tang, Jingbo Zhao, Fengwu Bai, and Shang-Tian Yang. 2016. Butanol production in acetone-butanol-ethanol fermentation with in situ product recovery by adsorption. *Bioresource technology* 219:158-168.

Yang, Xiaoping, Gow-Jen Tsai, and George T Tsao. 1994. Enhancement of in situ adsorption on the acetone-butanol fermentation by Clostridium acetobutylicum. *Separations Technology* 4 (2):81-92.

Yen, Hong-Wei, and Yi-Cheng Wang. 2013. The enhancement of butanol production by in situ butanol removal using biodiesel extraction in the fermentation of ABE (acetone–butanol–ethanol). *Bioresource technology* 145:224-228.

Zhang, Jie, Mintian Gao, Dongliang Hua, Yan Li, Haipeng Xu, Xiaohui Liang, Yuxiao Zhao, Fuqiang Jin, Lei Chen, and Guangfan Meng. 2014. Butanol production of Clostridium pasteurianum SE-5 from transesterification reaction solution using fermentation and extraction coupling system. Paper read at International Conference on Materials for Renewable Energy and Environment (ICMREE), 2013

Appendix III.

Supplementary information for chapter III. Tolerance improvement of *Clostridium saccharoperbutylacetonicum* N1-4 against biomass-derived phenolics and furan aldehydes inhibitors by overexpression of efflux pumps srpABC from *Pseudomonas putida* S12.

Methods

Tolerance test

For each strain, 200 mL of culture OD 0.8 was spitted out into 10 different tubes (5 mL each), and mixed with butanol, furfural, or a 100 g/L solution on *trans*-ferulic acid in DMF, as describe in the following table:

Table S3.1 Ammounts of inhibitors used in tolerance tests

Tube	Culture	Butanol (µL)	*trans*-ferulic acid (µL)	Furfural (µL)
Control	5 mL	-	-	-
0.8 % butanol	5 mL	40	-	-
1 % butanol	5 mL	50	-	-
1.2 % butanol	5 mL	60	-	-
0.2 g/L ferulic acid	5 mL	-	10	-
0.5 g/L ferulic acid	5 mL	-	25	-
0.8 g/L ferulic acid	5 mL	-	40	-
4 g/L furfural	5 mL	-	-	17.2
4.5 g/L furfural	5 mL	-	-	19.4
5 g/L furfural	5 mL	-	-	21.6

Conditions for Tecan Infinity

- Temperature 35ºC
- Wait for temperature:
    - minimum 30ºC
    - maximum 38ºC
- Kinetic cyle
    - Number of cycles: 72
        - Shaking
            - Duration: 885 sec
            - Amplitude: 3
            - Mode: orbital
        - Wait (timer)

- Wait time: 00:00:00 (hh:mm:ss)
- No other options marked

▪ Absorbance

- Wavelenght: 600 nm
- Number of flashes: 10
- Settle time: 0 ms

Results

Homology comparison using NCBI Blast

Table S3.2 Homologous of P. putida S12 srpABC efflux pump in *C. saccharoperbutylacetonicum* N1-4

					Homology to srpB *P. putida*			Homology to AcrB *E.coli*		
	Gene N1-4	protein	Name	Subunit	Query cover	E value	Ident	Query cover	E value	Ident
1	CSPA_RS22990	WP_015394794.1	Cation/multidrug efflux pump	ABC	98%	1.00E-106	27%	98%	5.00E-106	27%
2	CSPA_RS18355	WP_015393855.1	Nodulation protein NolG	ABC	98%	1.00E-60	22%	98%	3.00E-49	21%
3	CSPA_RS19385	WP_015394064.1	Cation/multidrug efflux pump	BC	86%	2.00E-60	26%	97%	1.00E-86	24%
4	CSPA_RS10815	WP_015392303.1	Cation/multidrug efflux pump	AB	97%	2.00E-48	23%	nd	nd	nd

srpB Blast

Description	Max score	Total score	Query cover	E value	Ident	Accession
cation/multidrug efflux pump [Clostridium saccharoperbutylacetonicum]	354	354	98%	1e-106	27%	WP_015394794.1
nodulation protein NolG [Clostridium saccharoperbutylacetonicum]	223	223	98%	1e-60	22%	WP_015393855.1
cation/multidrug efflux pump [Clostridium saccharoperbutylacetonicum]	222	341	86%	2e-60	26%	WP_015394064.1
cation/multidrug efflux pump [Clostridium saccharoperbutylacetonicum]	184	184	97%	2e-48	23%	WP_015392303.1
Mg-chelatase subunit ChlD [Clostridium saccharoperbutylacetonicum]	28.9	28.9	3%	3.6	35%	WP_015394505.1

Homology to AcrB from *Escherichia coli* BW25113 (BW25113_RS02385)

cation/multidrug efflux pump [Clostridium saccharoperbutylacetonicum]	353	353	98%	5e-106	27%	WP_015394794.1
cation/multidrug efflux pump [Clostridium saccharoperbutylacetonicum]	299	299	97%	1e-86	24%	WP_015394064.1
nodulation protein NolG [Clostridium saccharoperbutylacetonicum]	187	187	98%	3e-49	21%	WP_015393855.1
cell wall-binding protein [Clostridium saccharoperbutylacetonicum]	32.0	32.0	5%	0.15	33%	WP_035280777.1
hypothetical protein [Clostridium saccharoperbutylacetonicum]	32.0	32.0	5%	0.16	33%	WP_015392622.1
MFS transporter [Clostridium saccharoperbutylacetonicum]	28.1	28.1	4%	4.5	34%	WP_015392406.1

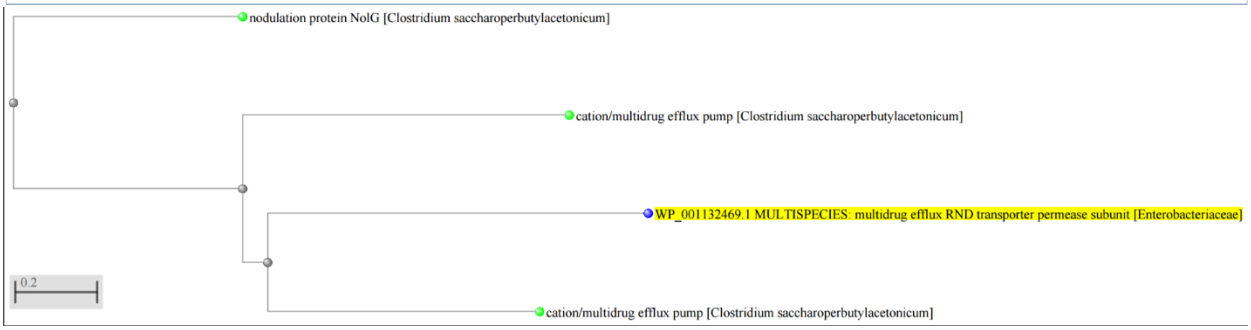

Appendix IV.

Supplementary information chapter IV. Identification, deletion, and study of new autolysins on *Clostridium saccharoperbutylacetonicum* N1-4

Genetic manipulations

Table S4.1 List of primers used in this study

Name	Sequence	Cloning purpose
YW2583	CTAAAACTgaattgattgggcccttatatacttggtttatttacttg	P_{lac} construction (pPJB14)
YW2584	GAATGTGAACTTGTATAttattacagtCATCGCtatatatattcattGCGATGg atatatcatttcagccctcctgtgaaattg	
YW2585	caatttcacaggagggctgaaATGATAAATGATTTTGAAC	CSPA_RS26630 (pPJB15)
YW2586	gcgaatgtgaacttgtataCTAATTATTTAATACTTTCATTAC	
YW2587	caatttcacaggagggctgaaTTGAAGTCTGAAAGCGAATT	CSPA_RS03200 (pPJB16)
YW2588	CTTGTTGCGAATGTGAACTTGTATActatctaaaacttcctt	
YW2589	caatttcacaggagggctgaaATGAAAAAAAGATTATTATC	CSPA_RS08050 (pPJB17)
YW2590	gcgaatgtgaacttgtataTTATTTAATTAATGATCCATC	
YW2591	caatttcacaggagggctgaaATGAAAAAGAAATGTAGTAT	CSPA_RS01160 (pPJB18)
YW2592	gcgaatgtgaacttgtataTTATGCTTTAATTTTGAAAAATG	
YW2593	atttcacaggagggctgaaTTGAAAGGAAGAACTCTAAT	CSPA_RS21780 (pPJB19)
YW2594	gcgaatgtgaacttgtataTTAATCTACCAAAGTAATCC	
YW2595	caatttcacaggagggctgaaATGTTTAAAGTAAAGAAAG	CSPA_RS09105 (pPJB20)
YW2596	gcgaatgtgaacttgtataTTATCCCTCTAAAATTATTTTTC	
YW2597	caatttcacaggagggctgaaGTGGATAATTTTAACATATAC	CSPA_RS06245 (pPJB21)
YW2598	gcgaatgtgaacttgtataTTATAATATTATACAAATCAACC	
YW2599	caatttcacaggagggctgaaATGCCTGAAATAGGTAGT	CSPA_RS00240 (pPJB22)
YW2600	gcgaatgtgaacttgtataTTAGTAATAAAATTTTGGTATTCCTC	
YW2601	caatttcacaggagggctgaaGTGAAAATGAAAAAGAAAAT	CSPA_RS18890 (pPJB23)
YW2602	gcgaatgtgaacttgtataCTATCTTAGAATATCCTGTG	
YW2603	caatttcacaggagggctgaaATGAAAGGTATAGATGTAAG	CSPA_RS13245 (pPJB24)
YW2604	gcgaatgtgaacttgtataTTATTTTGTTTCTATTGAATAGA	
YW2605	caatttcacaggagggctgaaATGAAAAAGAAAATAACTAT	CSPA_C38900 (pPJB25)
YW2606	gcgaatgtgaacttgtataCTATCTTAGAATATCCTGTG	
YW2607	caatttcacaggagggctgaaATGAATATTAAAAAGAAATTTG	CSPA_RS11880 (pPJB26)
YW2608	gcgaatgtgaacttgtataTTAGTTTAAAATGTCTTGAG	
YW2609	caatttcacaggagggctgaaATGAAAGGTTTAGATGTAAG	CSPA_RS15280 (pPJB27)
YW2610	gcgaatgtgaacttgtataTTAACATTTTTCTATAGGTAAGA	
YW2611	caatttcacaggagggctgaaATGAAAAATATAAAAGGAATAG	CSPA_RS03880 (pPJB28)
YW2612	gcgaatgtgaacttgtataCTAAGATAGTTTAGTTGCAAC	
YW2613	caatttcacaggagggctgaaATGTCATTAATTACTGGAATAG	CSPA_135p00690 (pPJB29)
YW2614	gttgcgaatgtgaacttgtataTTATTTTTCTAAAGTATTTTTAGTTGC	
YW2615	atttcacaggagggctgaaATGCAAGACAAGAATCC	CSPA_RS24880 (pPJB30)
YW2616	gttgcgaatgtgaacttgtataTTACAAATTTACTTTTGATCG	

YW484	aaagttaaaagaagaaaatagaaatATAATCTTTAATTTGAAAAGATTTAAG	P_{sRNA}+"20NT" (pPJB31 and pPJB32)
YW5190	TTGCTATTTCTAGCTCTAAAACgactctccattaatagtaatccATGGTGGAATGATAAGGG	P_{sRNA}+"20NT" (pPJB31)
YW5201	TTGCTATTTCTAGCTCTAAAACactggtatcccataacttctATGGTGGAATGATAAGGG	P_{sRNA}+"20NT" (pPJB32)
YW5191	gtgatatgactaataattaCTGATGCGTATGATGCAATG	Arm for deletion of gene 26
YW5247	CCACTATGTTGTAATTAGAATCcatattatttgggaagcatatc	
YW5193	TAAACAGAATTTAATATTAatttttatctccttagtac	Arm for deletion of gene 26
YW5194	cactagtaaccatcacactgATACTTAATTATATTATGAAG	
YW5195	GAGAGATGGGATGGAAGTGG	For cPCR detection of gene 26 deletion
YW5196	CCAAAAATATCCCACCATGG	
YW5197	gtgatatgactaataattaACTACTGTCCCATTTATGG	Arm for deletion of gene 30
YW5249	gcgaatttcttccataatcCATAAATCCAACTGTACCG	
YW5250	cacggtacagttggatttatgGATTATGGAAGAAATTCGC	Arm for deletion of gene 30
YW5200	atccactagtaaccatcacactgCAGGAGTAACTTGTGTTATG	
YW5203	CAACCGTTCTAGGTCCGAC	For cPCR detection of gene 30 deletion
YW5204	CAAATCCAGTTACGCCTCATC	

Table S4.2 List of plasmids used in this study

Strain	Purpose	Source or reference
pJZ100	Derivated from TJ1, used for pPJB14 constriction	(Jinek et al. 2012)
pPJB14	Mother vector for gene overexpression	This study
pPJB15	CSPA_RS26630 overexpression	This study
pPJB16	CSPA_RS03200 overexpression	This study
pPJB17	CSPA_RS08050 overexpression	This study
pPJB18	CSPA_RS01160 overexpression	This study
pPJB19	CSPA_RS21780 overexpression	This study
pPJB20	CSPA_RS09105 overexpression	This study
pPJB21	CSPA_RS06245 overexpression	This study
pPJB22	CSPA_RS00240 overexpression	This study
pPJB23	CSPA_RS18890 overexpression	This study
pPJB24	CSPA_RS13245 overexpression	This study
pPJB25	Cspa_c38900 overexpression	This study
pPJB26	CSPA_RS11880 overexpression	This study
pPJB27	CSPA_RS15280 overexpression	This study
pPJB28	CSPA_RS03880 overexpression	This study
pPJB29	Cspa_135p00690 overexpression	This study
pPJB30	CSPA_RS24880 overexpression	This study
pYW51	CRISPR-Cas9 mother vector	(Zhang et al. 2018)
pPJB31	CSPA_RS11880 deletion	This study
pPJB32	CSPA_RS24880 deletion	This study

Statistics

Table S4.3 Yields, maximum titers and Tukey's HSD analysis

Serum bottle fermentations								
	BuOH yield ± SE		**BuOH titer ± SE**		**ABE yield ± SE**		**ABE titer ± SE**	
	g/g	*	g/L	*	g/g	*	g/L	*
wild*	0.215±0.007	b	14.71±0.38	b	0.386±0.013	a	26.35±0.82	a
Δ26	0.226±0.001	ab	15.50±0.01	b	0.374±0.002	a	25.61±0.18	a
Δ30	0.232±0.002	a	5.71±0.20	c	0.340±0.001	b	8.41±0.37	b
Δ1234	0.231±0.001	a	16.58±0.14	a	0.375±0.001	a	26.85±0.18	a
Δ1234Δ26	0.236±0.003	a	16.60±0.19	a	0.375±0.001	a	26.43±0.06	a
Δ1234Δ30	0.234±0.005	a	16.89±0.19	a	0.373±0.006	a	26.84±018	a
Δ12345	0.236±0.001	a	16.83±0.03	a	0.378±0.001	a	27.00±0.05	a
Δ12345Δ26	0.230±0.001	ab	16.47±0.08	a	0.372±0.002	a	26.68±0.10	a
Δ12345Δ30	0.230±0.002	a	16.47±0.02	a	0.372±0.002	a	26.61±0.01	a
Ph-controlled bioreactors								
	BuOH yield ±SE		**BuOH titer ±SE**		**ABE yield ±SE**		**ABE titer ±SE**	
	g/g	*	**g/L**	*	**g/g**	*	**g/L**	*
wild	0.283±0.008	a	16.91±0.17	b	0.370±0.001	a	25.00±0.23	a
Δ1234	0.267±0.002	a	18.01±0.11	a	0.395±0.008	a	23.57±0.43	a
Δ1234Δ26	0.2700±0.0006	a	17.55±0.15	ab	0.371±0.005	a	24.13±0.55	a

* Groups in Tukey's HSD test α = 0.1, SE: standard error

Table S4.4 Statistical analysis on OD_{600} difference for bottle fermentations

strains	**p-value**	**strains**	**p-value**	**strains**	**p-value**
wild-d26	0.0325	d1234-d1234d26	0.2027	d12345-d12345d26	0.1253
wild-d30	0.1614	d1234-d1234d30	0.6999	d12345-d12345-d30	0.7129
d26-d30	0.0467	d1234d26-d1234d30	0.2332	d12345d26-d12345d30	0.1503
wild-d1234	0.0185	d26-d1234	0.0673	d26-d12345	0.5896
wild-d12345	0.0312	d30-d1234	0.0394	d30-d12345	0.0544
wild-d1234d26	0.0189	d26-d1234d26	0.0574	d26-d12345d26	0.1129
wild-d1234d30	0.0341	d30-d1234d26	0.0372	d30-d12345d26	0.0547
wild-d12345d26	0.0198	d26-d1234d30	0.0752	d26-d12345d30	0.5
wild-d12345d30	0.0319	d30-d1234d30	0.0242	d30-d12345d30	0.0713
d1234-d12345	0.0859	d1234d26-d12345	0.0694	d1234d30-d12345	0.1115
d1234-d12345d26	1	d1234d26-d12345d26	0.2884	d1234d30-d12345d26	0.7978
d1234-d12345d30	0.1301	d1234d26-d12345d30	0.0981	d1234d30-d12345d30	0.1841

References

Jinek, Martin, Krzysztof Chylinski, Ines Fonfara, Michael Hauer, Jennifer A Doudna, and Emmanuelle Charpentier. 2012. A programmable dual-RNA–guided DNA endonuclease in adaptive bacterial immunity. *science* 337 (6096):816-821.

Zhang, Zhong-Tian, Pablo Jiménez-Bonilla, Seung-Oh Seo, Ting Lu, Yong-Su Jin, Hans P Blaschek, and Yi Wang. 2018. Bacterial Genome Editing with CRISPR-Cas9: Taking Clostridium beijerinckii as an Example. In *Synthetic Biology*, edited by B. J. New York, NY: Humana Press.

Appendix V.

Supplementary information chapter V. Polycationic surfaces promote whole cell immobilization and induced micro-granulation on *C. saccharoperbutylacetonicum* N1-4 fermentation, for increased biobutanol productivity.

Methods

Adsorption support preparation and characterization

Specific reagent quantity used to react with 4 g of cotton or cellulose

Table S5.1 Cationization

	ammonization	amination
Molar ratio (agent/matrix)	Volume of CHPTA 65% (mL)	Mass of DEAEC 99% (g)
4.5	26.5	15.3
2.7	15.9	9.19
1.8	10.6	6.13
0.9	5.3	3.06
0.675	4.0	2.30
0.45	2.65	1.53
0.225	1.33	0.766

Surface area determination

Solution preparation

Standard mother solution (MSt)= 2 g/L = 0.2g/100 mL

The mother solution is used to prepare the real standards. For each repetition of each sample, 1 mL is needed, plus an additional one for the standard curve. Next table is for preparation of 250 mL

Table S5.2 Methylene blue calibration curve preparation

Standard	Blank	#1	#2	#3	#4	#5	#6
Conc (g/L)	0	0.005	0.01	0.05	0.1	0.15	0.2
mL MSt	0	0.625	1.25	6.25	12.5	18.75	25

Every solution were filled to 250 mL with water in volumetric flask

Calibration curve

10 µL of each standard solution (blank, #1 … #6) is added into a microplate containing 190 µL of water, pipet mixed and adsorption is measured at 660 nm in a microplate reader TECAN infinity m1000. Dilutions of 10^{-1} and 10^{-2} were done for some cellulose samples, as needed.

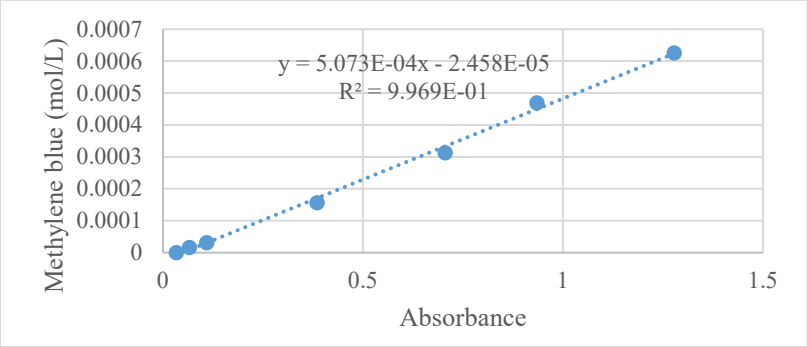

Figure S5.1 Methylene blue calibration curve

Samples

12 samples (6 standards x duplicates) of 20-60 mg of each material treatment are weighted in 2mL tubes. 1 mL of each standard is added into 2 tubes. The tubes are mixed in the vortex and placed in a shaker during at least 24 h at 20ºC for cotton and cellulose, and at least four days for chitosan. After that time, the powders are let to settle down. Then, 10 µL of each sample is added into a microplate containing 190 µL of water and measured at 660 nm against the calibration curve.

Concentration of both standard and samples were recalculated using the calibration curve. The Langmuir isotherm was used to calculate the specific surface area of the cotton fiber.

$$\frac{C}{n} = \frac{C}{n_m} + \frac{1}{Kn_m} \text{ (Ec. S6.1)}$$

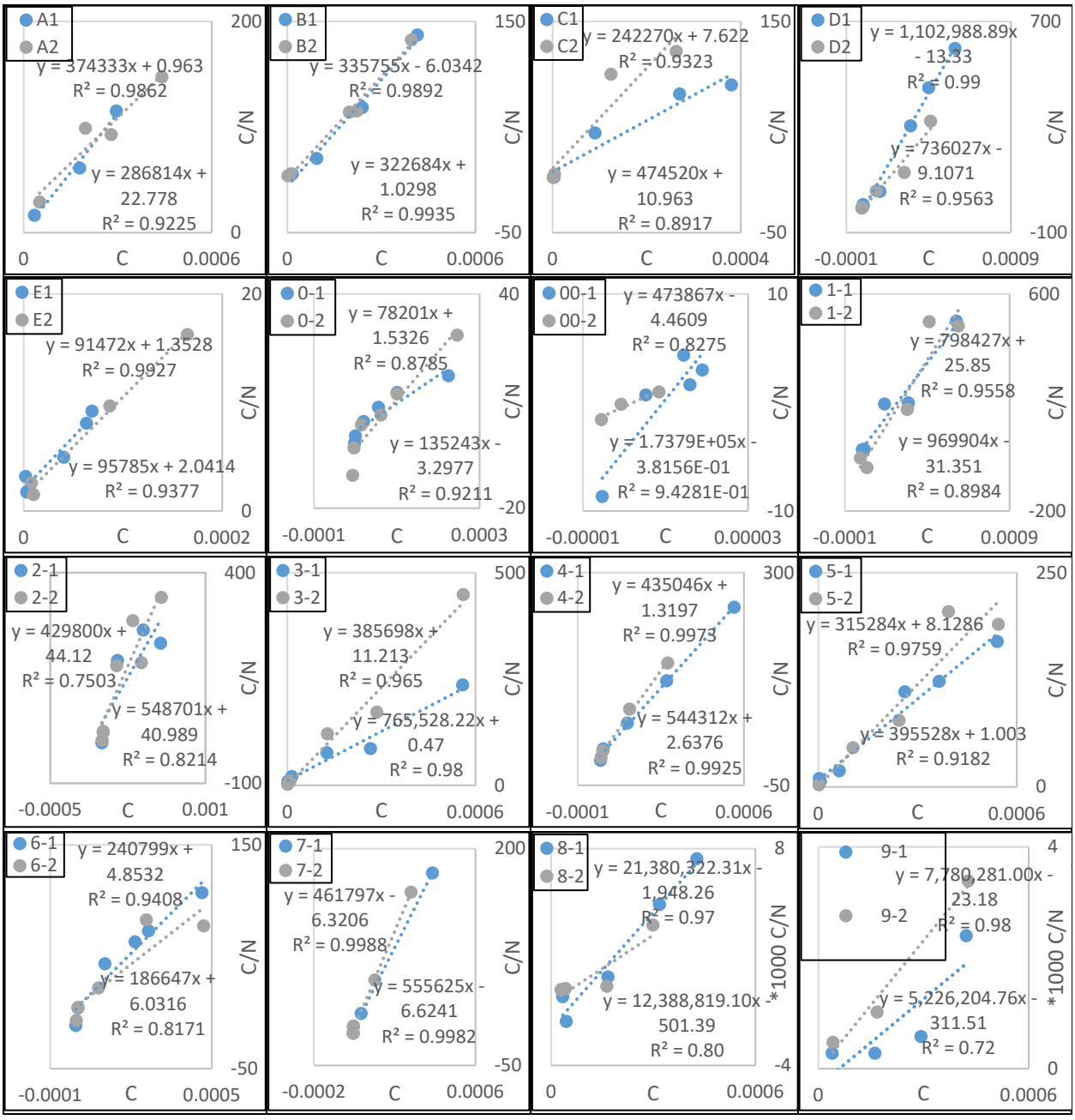

Figure S5.2 Langmuir isotherm linearization for raw and modified samples of chitosan, microcrystalline cellulose and cotton.

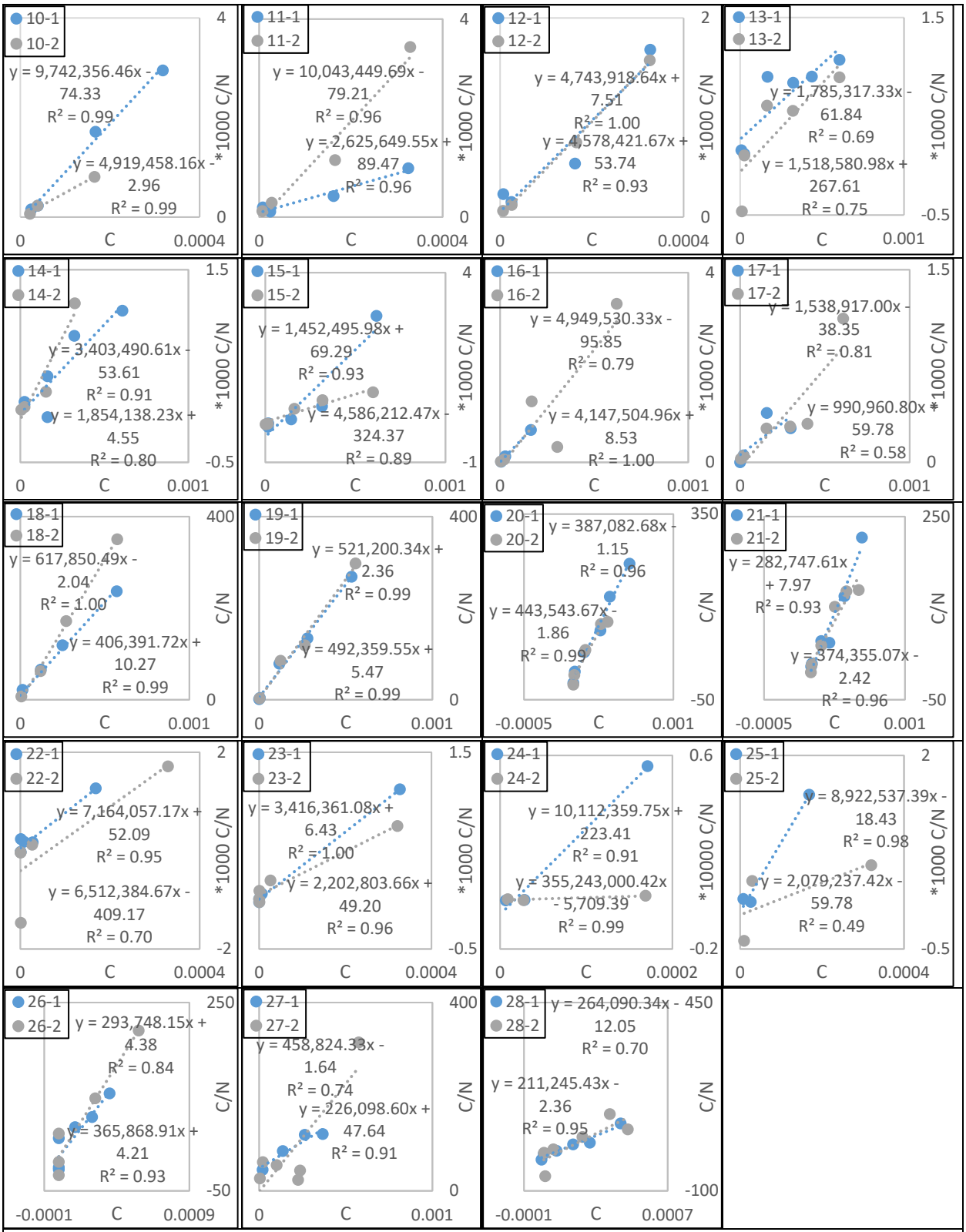

Figure S5.2 Langmuir isotherm linearization for raw and modified samples of chitosan, microcrystalline cellulose and cotton.

Ec 6.1 represent the linearized version of Langmuir equation. *K* is an adsorption constant, and *C* is the equilibrium concentration of methylene blue solution. *n* represents the number of moles of methylene blue adsorbed per gram of cotton at equilibrium concentration, and n_m is the number of moles of methylene blue per gram of cotton required to form a monolayer. We plot of *C/n* vs *C* to get the slope ($1/n_m$), and the intercept ($1/Kn_m$).

$$S = n_m\left(\frac{mol_{MB}}{g_{sample}}\right) \times a_{MB}\left(\frac{\text{Å}^2}{molecule_{MB}}\right) \times N\left(\frac{molecule_{MB}}{mol_{MB}}\right) \times 10^{-20}\left(\frac{m^2}{\text{Å}^2}\right) \quad \text{(Ec. S5.3)}$$

The specific surface area (S) in 10^{-3}km^2 kg^{-1} is calculated using Ec. 6.3. a_{MB} is the occupied surface area of one molecule of methylene blue =197.2 Å²; N is Avogadro's number, 6.02 x 10^{23} mol^{-1}.

Cation density and fluorescein determination

Fluorescein concentration were determined by a method modified from Sigma-Aldrich. Basic Protocol for the SciFlow™1000 System Create Fluorescein Standard Curve Calibration for Flow Tracking Drug Exposure & Monolayer Culture.

Stock solutions

- 250 mL of 0.1 wt.% cetyltrimethylammonium chloride
- 100 mL of 100 mM phosphate buffer pH 8.
- Pre-solution 10 mM Fluorescein: 0.4 g (1 mmol) in 100mL fluorescein sodium salt, and fill with 0.1 wt.% cetyltrimethylammonium chloride. Protect from light
- Standard mother solution (StM) 10 µM Fluorescein: dilute 1/1000 pre-solution and fill with 0.1 wt.% cetyltrimethylammonium chloride. Protect from light.

Standard curve

Table S5.3 Fluoresceine calibration curve preparation

Standard number	blank	#1	#2	#3	#4	#5	#6	#7
Standard concentration (µM)	0	0.01	0.03	0.05	0.1	0.3	1	2
µL of StM	0	1	3	5	10	30	100	200
µL 0.1% cetyltrimethylammonium chloride	1000	999	997	995	990	970	900	800

100 µL of each sample and standard are using in each well of a microplate + 20 µL of phosphate buffer

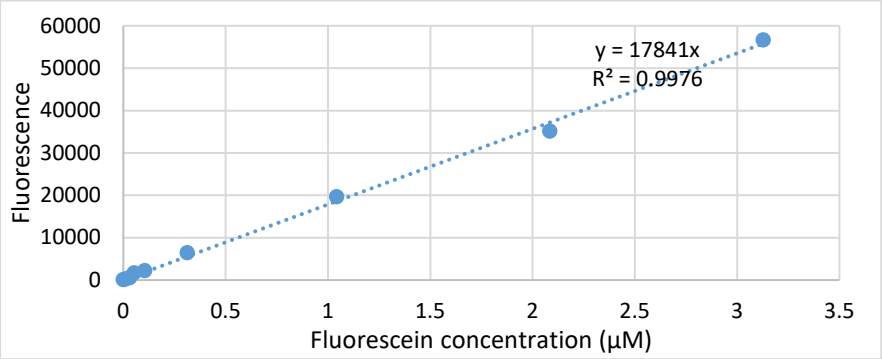

Figure S5.3 Fluorescein calibration curve

Microplate reader conditions

Tecan Infinite M1000 Pro was used to. 100 µL of each dilution was added to all the wells of a single row.

Table S5.4 Conditions for fluorescence analysis

Mode	Fluorescence Top Reading	
Excitation Wavelength	485	
Emission Wavelength	525	
Excitation Bandwidth	5	
Emission Bandwidth	5	
Gain	88	
Number of Flashes	10	
Flash Frequency	400	Hz
Integration Time	20	µs
Lag Time	0	µs
Settle Time	0	ms

Samples

1.5 mL x 108 samples = 162 mL, 250 mL 1% fluoresceine (2.5g/250 mL)

200 mL 0.1 wt.% cetyltrimethylammonium chloride (0.2 g/200 mL)

20 mg of each sample (duplicates) were immersed at RT in 1.5 ml 1 m/v% fluorescein disodium salt (from solid fluorescein purchased from VWR) solution in demineralized water for 10 min, washed 6 times with 2 ml water. Next, the samples were placed in 1 ml of a 0.1 m/v% cetyltrimethylammonium chloride solution in demineralized water and agitated. Subsequently, 2 µL were diluted into 200 µL (first dilution). The wells were filled with 80µL of cetyltrimethylammonium chloride solution, 20 µL of phosphate buffer and 20 µL of sample (second dilution). Total dilution factor is 500. Samples were analyzed by fluorescence at 520 nm (emission), and 485 (excitation) in a microplate reader against a calibration curve.

$$\text{Charge density} = [\text{Dye}] \times V \times N/S \quad \text{(Ec. 6.1)}$$

Cation surface density is calculated from Ec. 6.1, in which V is the volume of the extraction solution (1.0 mL), N is Avogadro's number (6.023×10^{23}) and S is the surface area of the samples.

Protein analysis for biomass analysis

Procedure for Bradford protein analysis is based on the supplier VWR Life Science AMRESCO protocol. The table below contains the preparation of protein standards in triplicate using a 0.5 mg/mL BSA stock solution.

Table S5.5 Bradford standard preparation

Standard Dilution	Volume 0.5 mg/mL BSA (µL)	Volume 0.15 M NaCl (µL)	Volume of Standard to Add Per Well (µL)	BSA Per Well (µg)
Blank	0	50	20	0
S1	2.5	47.5	20	0.5
S2	5	45	20	1
S3	7.5	42.5	20	1.5
S4	10	40	20	2

20 µL of each standard is pipetted into the wells of a 96-well plate. 200 µL Bradford Reagent are added to each standard dilution and mix by pipetting. It is allowed to stand at room temperature for 2 minutes, and absorbance is measured at 595 nm using a plate reader. Sample are measured

using same procedure, using the unknown in place of the BSA. Use the standard curve as a reference to determine the concentration of the unknown.

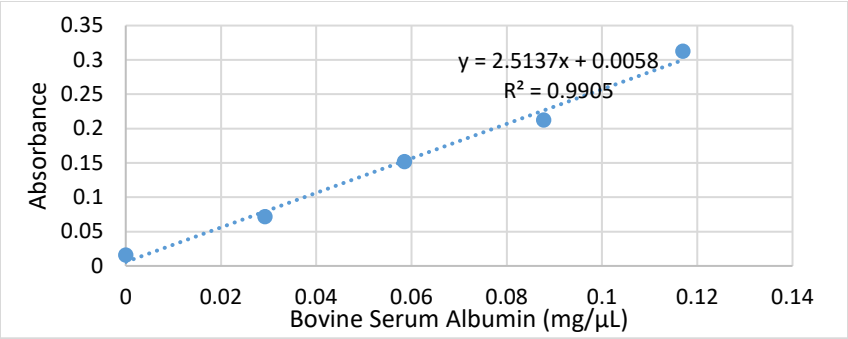

Figure S5.4 Bradford calibration curve

Solid fraction were collected and washed with water and freeze. 100 µL of 0.2 M sodium hydroxide were added into 100 mg of solid. Samples were incubated at 90 ºC for 10 mins. The protein solution were diluted 40 times, and then 20 µL were mixed with 200 µL of Bradford reagent (VWR, Radnor, PA). Samples were analyzed by absorbance at 595 nm in a microplate reader Tecan infinite M1000 Pro, against Bovine Serum Albumin standards. For planktonic cells, 1 mL of cultures were centrifuged at 10,000 g for 10 min to separate the pellets from the supernatants. Then pellets were washed with water and centrifuged for 10 min. The supernatant was discarded and the pellet was re-suspended in 1 mL of 0.2 M sodium hydroxide. 100 µL of the alkaline cell suspension were incubated at 90ºC for 10 min, and the supernatants were collected, diluted between 15-250 times (as needed) and used as described above.

In similar way, we analyzed samples of a washed cell pellet diluted at different concentrations, in order to relate biomass determined by two difference methods (OD600 and protein).

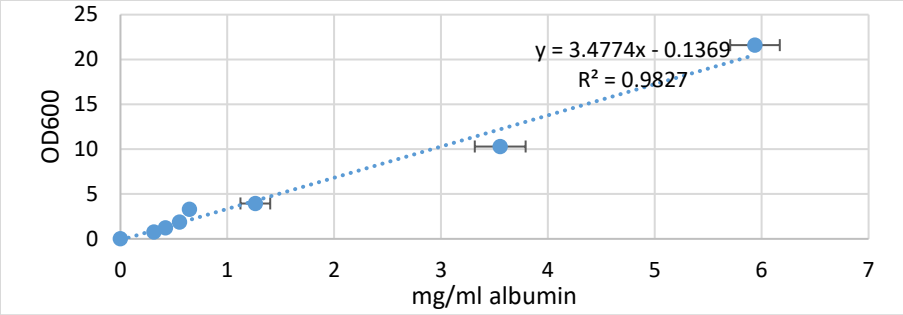

Figure S5.5 Protein vs OD_{600} equivalence

Elemental analysis raw data

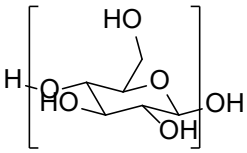 Chemical Formula: $C_6H_{10}O_5$ Exact Mass: 162.05 Molecular Weight: 162.14 m/z: 162.05 (100.0%), 163.06 (6.5%), 164.06 (1.0%) Elemental Analysis: C, 44.45; H, 6.22; O, 49.34	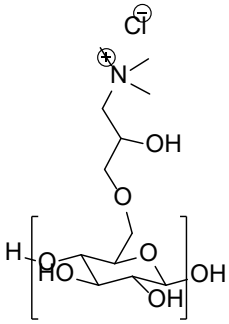 Chemical Formula: $C_{12}H_{24}ClNO_6$ Exact Mass: 313.13 Molecular Weight: 313.78 m/z: 313.13 (100.0%), 315.13 (32.0%), 314.13 (13.0%), 316.13 (4.1%), 315.13 (1.2%) Elemental Analysis: C, 45.93; H, 7.71; Cl, 11.30; N, 4.46; O, 30.59	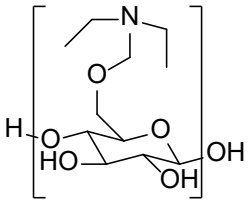 Chemical Formula: $C_{11}H_{21}NO_5$ Exact Mass: 247.14 Molecular Weight: 247.29 m/z: 247.14 (100.0%), 248.15 (11.9%), 249.15 (1.0%) Elemental Analysis: C, 53.43; H, 8.56; N, 5.66; O, 32.35
	Degree of substitution = %N/4.46	Degree of substitution = %N/5.66

Figure S5.6 Elemental percent composition and structure

Table S5.6 Elemental analysis data

sample	%N			Degree of substitution		
	Rep	Avg	SD	Rep	Avg	SD
A1(a)	1.22	1.07	0.15	0.273543	0.23991	0.047563
A1(b)	0.92			0.206278		
A2(a)	1.06	1.015	0.045	0.237668	0.227578	0.014269
A2(b)	0.97			0.217489		
A3(a)	1.01	0.975	0.035	0.226457	0.21861	0.011098
A3(b)	0.94			0.210762		

A4(a)	0.79	0.96	0.17	0.17713	0.215247	0.053905
A4(b)	1.13			0.253363		
A5(a)	0.97	0.74	0.23	0.217489	0.165919	0.07293
A5(b)	0.51			0.11435		
A6(a)	0.71	0.71	0	0.159193	0.159193	0
A6(b)	0.71			0.159193		
A7(a)	0.95	0.81	0.14	0.213004	0.181614	0.044392
A7(b)	0.67			0.150224		
B1(a)	0.9	0.945	0.045	0.201794	0.211883	0.014269
B1(b)	0.99			0.221973		
B2(a)	0.93	1.02	0.09	0.20852	0.2287	0.028538
B2(b)	1.11			0.248879		
B3(a)	0.7	0.68	0.02	0.156951	0.152466	0.006342
B3(b)	0.66			0.147982		
B4(a)	0.41	0.57	0.16	0.091928	0.127803	0.050734
B4(b)	0.73			0.163677		
B5(a)	0.56	0.56	0	0.125561	0.125561	0
B5(b)	0.56			0.125561		
B6(a)	0.68	0.595	0.085	0.152466	0.133408	0.026953
B6(b)	0.51			0.11435		
B7(a)	0.39	0.39	0	0.087444	0.087444	0
B7(b)	0.39			0.087444		
C1(a)	0.74	0.745	0.005	0.130742	0.131625	0.001249
C1(b)	0.75			0.132509		
C2(a)	1.11	1.135	0.025	0.196113	0.20053	0.006247
C2(b)	1.16			0.204947		
C3(a)	0.84	0.905	0.065	0.14841	0.159894	0.016241
C3(b)	0.97			0.171378		
C4(a)	0.84	0.715	0.125	0.14841	0.126325	0.031233
C4(b)	0.59			0.10424		
C5(a)	0.59	0.64	0.05	0.10424	0.113074	0.012493
C5(b)	0.69			0.121908		
C6(a)	0.82	0.78	0.04	0.144876	0.137809	0.009994
C6(b)	0.74			0.130742		
C7(a)	0.76	0.72	0.04	0.134276	0.127208	0.009994
C7(b)	0.68			0.120141		
D1(a)	0.99	0.99	0	0.174912	0.174912	0
D1(b)	0.99			0.174912		
D2(a)	0.7	0.73	0.03	0.123675	0.128975	0.007496
D2(b)	0.76			0.134276		
D3(a)	0.63	0.545	0.085	0.111307	0.09629	0.021238

D3(b)	0.46			0.081272		
D4(a)	0.63	0.6	0.03	0.111307	0.106007	0.007496
D4(b)	0.57			0.100707		
D5(a)	0.56	0.58	0.02	0.09894	0.102473	0.004997
D5(b)	0.6			0.106007		
D6(a)	0.57	0.545	0.025	0.100707	0.09629	0.006247
D6(b)	0.52			0.091873		
D7(a)	0.44	0.23	0.21	0.077739	0.040636	0.052471
D7(b)	0.02			0.003534		

Additional fermentation data

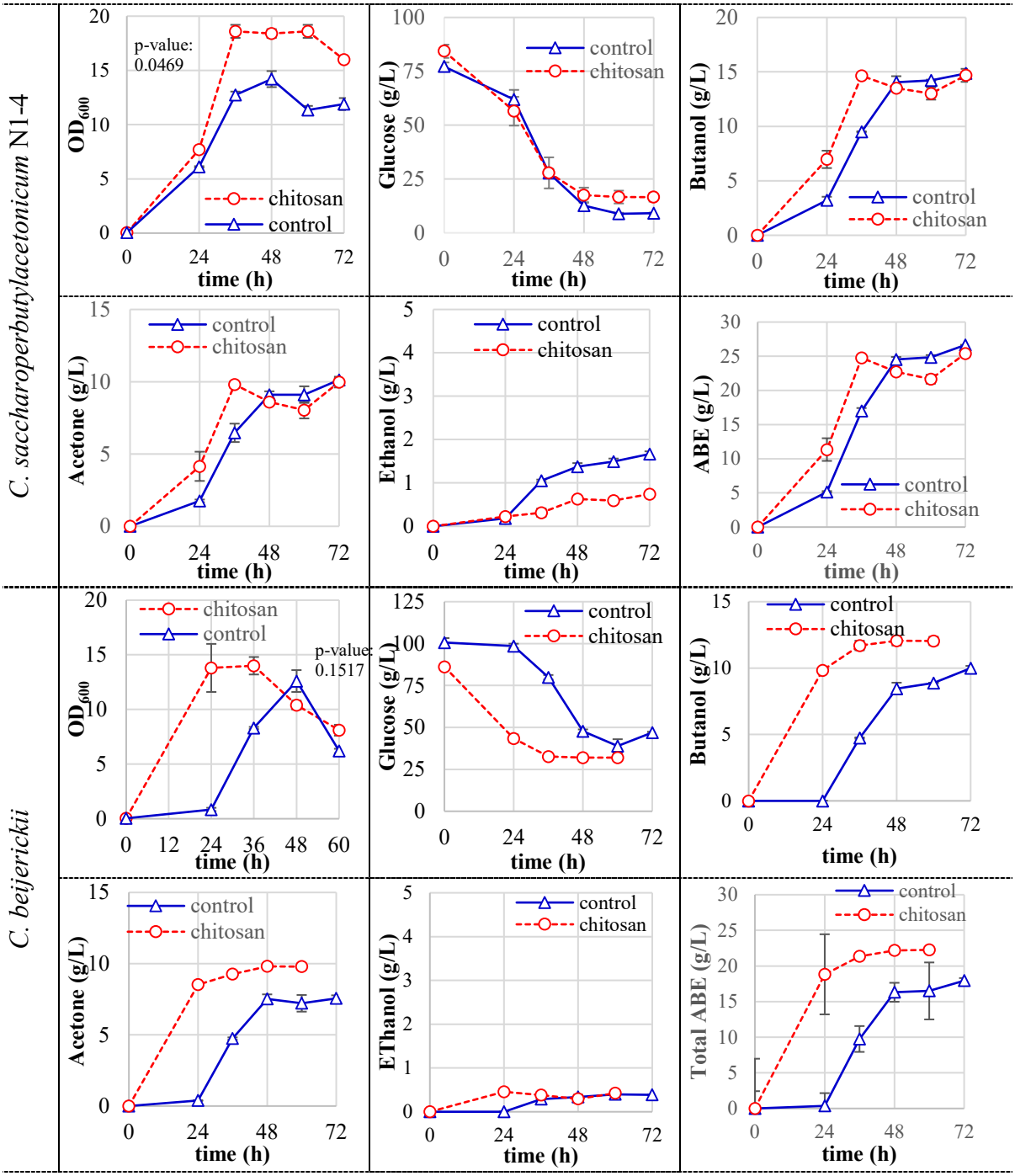

Figure S5.7 Fermentation profiles for bottles fermentation containing chitosan

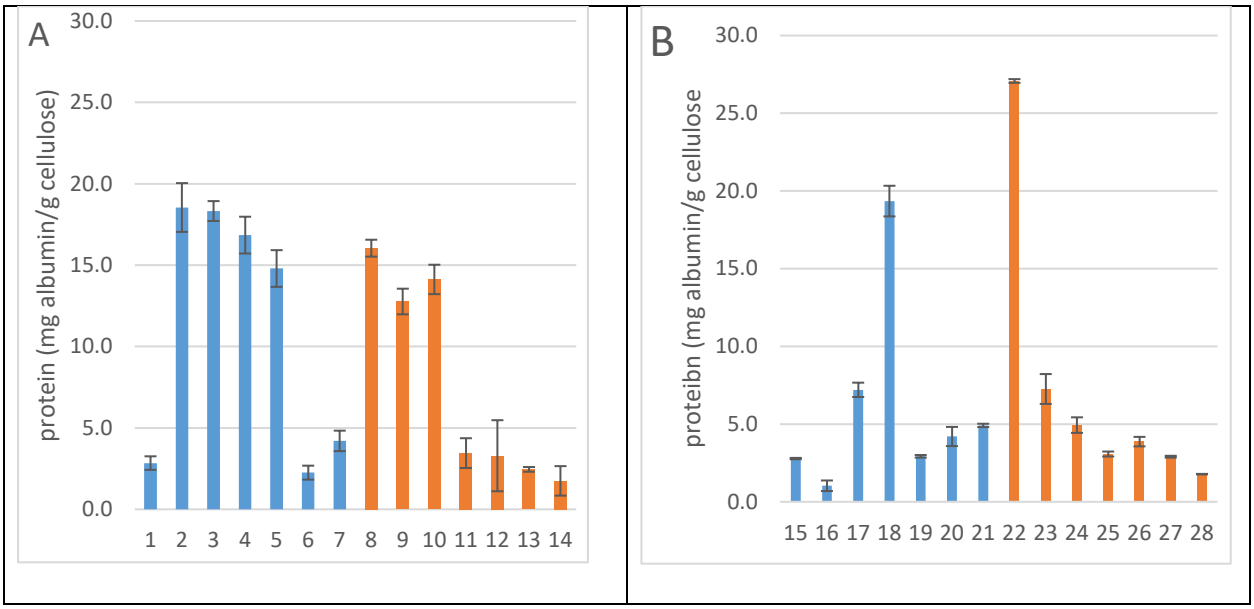

Figure S5.8 Biomass in the carrier at the end of fermentation. (A) CHPTA, (B) DEAE

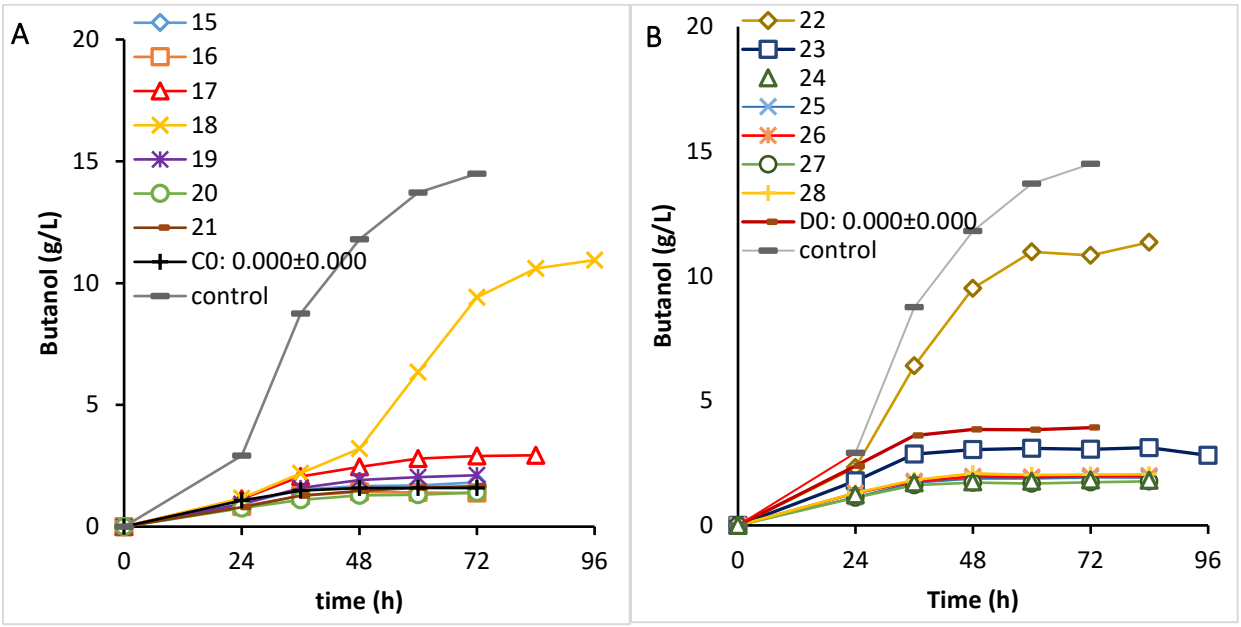

Figure S5.9 Fermentation profiles containing cellulosic materials modified with DEAE as immobilization carrier, as well as the properties of carriers.